National Library
of Canada

Bibliothèque nationale
du Canada

Canadian Theses Service

Services des thèses canadiennes

Ottawa, Canada
K1A 0N4

## CANADIAN THESES

## THÈSES CANADIENNES

### NOTICE

The quality of this microfiche is heavily dependent upon the quality of the original thesis submitted for microfilming. Every effort has been made to ensure the highest quality of reproduction possible.

If pages are missing, contact the university which granted the degree.

Some pages may have indistinct print especially if the original pages were typed with a poor typewriter ribbon or if the university sent us an inferior photocopy.

Previously copyrighted materials (journal articles, published tests, etc.) are not filmed.

Reproduction in full or in part of this film is governed by the Canadian Copyright Act, R.S.C. 1970, c. C-30.

### AVIS

La qualité de cette microfiche dépend grandement de la qualité de la thèse soumise au microfilmage. Nous avons tout fait pour assurer une qualité supérieure de reproduction.

S'il manque des pages, veuillez communiquer avec l'université qui a conféré le grade.

La qualité d'impression de certaines pages peut laisser à désirer, surtout si les pages originales ont été dactylographiées à l'aide d'un ruban usé ou si l'université nous a fait parvenir une photocopie de qualité inférieure.

Les documents qui font déjà l'objet d'un droit d'auteur (articles de revue, examens publiés, etc.) ne sont pas microfilmés.

La reproduction, même partielle, de ce microfilm est soumise à la Loi canadienne sur le droit d'auteur, SRC 1970, c. C-30.

THIS DISSERTATION
HAS BEEN MICROFILMED
EXACTLY AS RECEIVED

LA THÈSE A ÉTÉ
MICROFILMÉE TELLE QUE
NOUS L'AVONS REÇUE

NL-339 (r.86/06)

Canada

THE UNIVERSITY OF ALBERTA

# GEOTECHNICAL CHARACTERISTICS OF GENESEE CLAY

by

© Chan Wen CHAN CHIM YUK

A THESIS

SUBMITTED TO THE FACULTY OF GRADUATE STUDIES AND RESEARCH
IN PARTIAL FULFILMENT OF THE REQUIREMENTS FOR THE DEGREE
OF DOCTOR OF PHILOSOPHY

DEPARTMENT OF CIVIL ENGINEERING

EDMONTON, ALBERTA
Spring 1986

Permission has been granted to the National Library of Canada to microfilm this thesis and to lend or sell copies of the film.

The author (copyright owner) has reserved other publication ~~rights~~, and neither the thesis nor extensive extracts from it may be printed or otherwise reproduced without his/her written permission.

L'autorisation a été accordée à la Bibliothèque nationale du Canada de microfilmer cette thèse et de prêter ou de vendre des exemplaires du film.

L'auteur (titulaire du droit d'auteur) se réserve les autres droits de publication; ni la thèse ni de longs extraits de celle-ci ne doivent être imprimés ou autrement reproduits sans son autorisation écrite.

ISBN 0-315-30262-3

THE UNIVERSITY OF ALBERTA

## RELEASE FORM

NAME OF AUTHOR Chan Wen CHAN CHIM YUK

TITLE OF THESIS GEOTECHNICAL CHARACTERISTICS OF GENESEE CLAY

DEGREE FOR WHICH THESIS WAS PRESENTED DOCTOR OF PHILOSOPHY

YEAR THIS DEGREE GRANTED Spring 1986

Permission is hereby granted to THE UNIVERSITY OF ALBERTA LIBRARY to reproduce single copies of this thesis and to lend or sell such copies for private, scholarly or scientific research purposes only.

The author reserves other publication rights, and neither the thesis nor extensive extracts from it may be printed or otherwise reproduced without the author's written permission.

(SIGNED) ....................

PERMANENT ADDRESS:

11, Magon Street,
Port Louis,
MAURITIUS.

DATED November 6, 1985.

THE UNIVERSITY OF ALBERTA

FACULTY OF GRADUATE STUDIES AND RESEARCH

The undersigned certify that they have read, and recommend to the Faculty of Graduate Studies and Research, for acceptance, a thesis entitled GEOTECHNICAL CHARACTERISTICS OF GENESEE CLAY submitted by Chan Wen CHAN CHIM YUK in partial fulfilment of the requirements for the degree of DOCTOR OF PHILOSOPHY.

..............................
N.R. Morgenstern
Supervisor

J.D. Scott
..............................
J.D. Scott

..............................
R. Gerard

Frank W. Schwartz
..............................
F.W. Schwartz

J. Graham
..............................
J. Graham
External Examiner

Date. November 6, 1985

# ABSTRACT

Geotechnical data is reported from the site of the Genesee Power Project, Alberta. During progress of the project, failures occurred during slope excavation and embankment construction indicating that the design of structures on the class of material encountered cannot be based solely on routine engineering investigation and procedures. The present research was undertaken to improve our understanding of the behaviour of the class of soil found at Genesee.

The material of interest is a lacustrine clay, termed Genesee Clay, which has a thickness varying between 10 and 20 m and which overlies a 2 to 20 m thick layer of ablation till. The clay has an undulating topography resembling that of a hummocky disintegration moraine, suggesting the likelihood of supraglacial deposition on ice-rich debris. Slickensides and fissures constitute the dominant macrostructures and were formed at various stages after deposition including severe shearing due to melting of buried ice. Consolidated undrained triaxial tests have shown that the clay is strain-weakening. This behaviour originates from the presence of numerous randomly oriented slickensides and fissures.

Another important characteristic of the clay deposit is the areal variation in undrained strength. Measurement of the in-situ lateral stresses show that there is a trend between the variation of the undrained strength and that of $K_0$. This investigation shows that stress history effects due

to bottom melt-out processes may dominate those associated with vertical effective stress change alone.

Back analysis of the failures have shown that for this class of material, the total stress analysis based on strengths derived from empirical correlations is not a useful tool for design purposes. On the other hand, effective stress analyses have shown that the operational strength of the Genesee Clay lies between the peak and residual strength envelopes. This behaviour is an indication that a progressive failure mechanism is operational in the cases studied. It was also found that the mobilised strength parameters of c'=0 and $\phi$'=20° for the Genesee Clay could be adequately obtained from the large strain strength envelope determined from consolidated undrained triaxial tests carried to strains of about 15%.

# ACKNOWLEDGEMENTS

This research was proposed and supervised by Professor N.R. Morgenstern. It was a unique and rewarding opportunity to work with a reputable teacher like Professor Morgenstern who, in spite of his authority in geotechnical engineering, encouraged me to express my own ideas and gave expert advice when the need arose. He guided me patiently through the key issues raised in this thesis. While he required high quality work, Professor Morgenstern was also attentive to the non-academic problems. In that respect, he made sure that I got the necessary technical support to complete the thesis within the limited period of study leave granted by my employer. It would be endless to write my appreciation for the help of Professor Morgenstern in my professional development and my vocabulary limits me to just say "thank you".

I am also indebted to Dr. S. Thomson for making valuable comments on the first three chapters of the thesis and to Dr. D. Cruden for his helpful suggestions at various stages of the project.

I was fortunate to share an office with a geologist, Po Tsui, who was always willing to discuss geological matters. Po was also a valuable advisor on some of the field trips.

I am grateful to Mr. G. Cyre and the technical staff in geotechnical engineering for their dedication during the field and laboratory investigations. Mr. R.L. Martin of EBA Engineering Consultants Ltd, Mr. G. Kack and Dr. P.K.

Chatterji of Thurber Consultants Ltd and Dr. J. Crooks of Golder Associates Ltd were most helpful in providing pertinent data on the Genesee Power Project. Messrs M. Clark, R. Hanma and R. Trowsdale of Edmonton Power kindly made necessary arrangements for our access to the construction sites.

The financial support of the National Research Council of Canada is gratefully acknowledged.

I am also thankful to the lecturers in soil mechanics at Imperial College, London, U.K. who provided me with a solid foundation in the subject during my study for the MSc degree at that institution.

I would like to express my appreciation to the University of Mauritius for granting me three years' leave of absence, to Professor G. Mohamedbhai for his support and to other colleagues for shouldering my workload during my absence.

Last but not least, I owe the most gratitude to my parents who sacrificed so much to give me an education and to my brothers and sisters for their precious encouragement and support.

## Table of Contents

Chapter Page

1. INTRODUCTION ....................................1
1.1 SCOPE AND OBJECTIVES OF THESIS ....................1
1.2 THE GENESEE POWER PROJECT ....................5
1.2.1 General description ....................5
1.2.2 Geotechnical problems ....................8
1.3 ORGANIZATION OF THESIS ....................9
2. GEOLOGY OF STUDY AREA ....................10
2.1 GLACIAL HISTORY ....................10
2.2 AIRPHOTO INTERPRETATION AND GEOLOGICAL MAP STUDY ....................14
2.3 STRATIGRAPHY ....................24
2.3.1 Stratigraphy outside bedrock depression ...24
2.3.2 Stratigraphy within bedrock depression ....28
2.4 BEDROCK GEOLOGY ....................31
2.5 TILL GEOLOGY ....................32
2.6 GEOLOGY OF GENESEE CLAY ....................35
2.6.1 Hummocky terrain in lacustrine clay - a literature review ....................37
2.6.1.1 Supraglacial origin ....................40
2.6.1.2 Subglacial origin ....................41
2.6.1.3 Periglacial origin ....................42
2.6.1.4 Differential shrinkage or consolidation ....................43
2.6.2 Hummocky terrain at Genesee ....................43
2.6.3 Characteristics of Genesee Clay ....................45
2.6.3.1 Weathered brown clay ....................45
2.6.3.2 Unweathered grey clay ....................47

2.7 GROUNDWATER CONDITIONS ....................................49

3. MACRO AND MICROSTRUCTURES OF GENESEE CLAY ...........50

3.1 INTRODUCTION ................................................50

3.2 MACROSTRUCTURES ..........................................52

3.2.1 Method of investigation .........................53

3.2.2 Depositional features ..............................53

3.2.2.1 Descriptive scheme ...............54

3.2.3 Examples of depositional features in Genesee Clay ................................................57

3.2.3.1 Sample 2-10 (Plate 3.1) ..........58

3.2.3.2 Sample 4-9 (Plate 3.2) ............58

3.2.3.3 Sample 6-6 (Plate 3.3) ............58

3.2.3.4 Sample 5-3 (Plate 3.4) ............62

3.2.4 Structural features .................................62

3.2.4.1 Descriptive scheme ...............64

3.3 MICROSTRUCTURES ..........................................66

3.3.1 Method of investigation .........................66

3.3.2 Examples of microstructures in Genesee Clay ...........................................................67

3.4 DISCUSSION OF DEPOSITIONAL FEATURES ..............73

3.5 DISCUSSION OF STRUCTURAL FEATURES ..................78

3.5.1 Minor shears formed shortly after deposition .....................................................78

3.5.2 Fissures due to weathering ...............82

3.5.3 Major shears due to basal melt-out processes ..................................................85

3.5.4 Unsheared fissures ...............................86

3.6 SUMMARY .........................................................90

4. FIELD INVESTIGATION ........................................93

4.1 INTRODUCTION ....................................93
4.2 LOCATION OF TEST SITES ............................93
4.3 IN-SITU MEASUREMENT OF LATERAL STRESSES .........95
    4.3.1 General review ..............................95
    4.3.2 Evaluation of test methods ..................97
        4.3.2.1 Self-boring pressuremeter .........97
        4.3.2.2 Push-in stress cell ...............99
        4.3.2.3 Iowa stepped blade ...............101
        4.3.2.4 Marchetti flat plate dilatometer .102
        4.3.2.5 Hydraulic fracture test ..........103
    4.3.3 Methods used at Genesee ....................105
    4.3.4 Test procedures ............................106
        4.3.4.1 Total stress cell (TSC) ..........106
        4.3.4.2 Marchetti flat plate dilatometer (DMT) ............................110
        4.3.4.3 Hydraulic fracture test ..........114
    4.3.5 Discussion of test results .................118
        4.3.5.1 Total stress cell ................118
        4.3.5.2 Marchetti flat plate dilatometer .120
        4.3.5.3 Hydraulic fracture test ..........130
        4.3.5.4 Summary ..........................132
4.4 IN-SITU VANE TEST ................................132
4.5 IN-SITU POREWATER PRESSURE MEASUREMENT .........134
5. LABORATORY INVESTIGATIONS .........................135
5.1 INTRODUCTION .....................................135
5.2 CLASSIFICATION TESTS .............................135
5.3 ONE-DIMENSIONAL CONSOLIDATION TEST ..............136

5.4 DIRECT SHEAR TEST ... 137

5.5 CONSOLIDATED UNDRAINED TRIAXIAL TESTS ... 137

5.6 LABORATORY DETERMINATION OF THE COEFFICIENTS OF EARTH PRESSURES ... 141

    5.6.1 Introduction ... 141

    5.6.2 Determination of the normally consolidated $K_0$ ... 143

    5.6.3 Estimation of the existing in-situ $K_0$ ... 144

5.7 DETERMINATION OF HORIZONTAL PRECONSOLIDATION PRESSURE ... 151

5.8 DETERMINATION OF YIELD ENVELOPE ... 156

    5.8.1 Laboratory procedures ... 157

6. GEOTECHNICAL CHARACTERISTICS OF GENESEE CLAY ... 162

6.1 CLASSIFICATION ... 162

6.2 CONSOLIDATION CHARACTERISTICS ... 169

6.3 VARIATION IN LATERAL STRESSES ... 173

6.4 STRESS - STRAIN BEHAVIOUR ... 180

    6.4.1 Unweathered grey clay ... 180

    6.4.2 Weathered brown clay ... 185

6.5 STRENGTH PARAMETERS ... 188

    6.5.1 Unweathered grey clay ... 188

    6.5.2 Weathered brown clay ... 196

6.6 VARIATION OF $A_f$ WITH OCR AND $K_0$ ... 196

6.7 ANISOTROPY IN GENESEE CLAY ... 200

6.8 VARIATION IN UNDRAINED STRENGTH ... 207

6.9 YIELDING IN GENESEE CLAY ... 212

7. STABILITY ANALYSIS OF SLOPES AND EMBANKMENTS ON GENESEE CLAY ... 213

7.1 INTRODUCTION ... 213

7.2 SLOPE FAILURE AT DIVERSION DITCH ..............213

7.3 BACKANALYSIS OF SR770 EMBANKMENT FAILURE .......220

7.3.1 Total stress analysis ..................225

7.3.2 Effective stress analysis ..............228

7.4 LARGE DEFORMATION AT HIGH DYKE .................231

7.5 DISCUSSION .....................................245

8. CONCLUSIONS ........................................248

8.1 CHARACTERISTICS OF GENESEE CLAY ................248

8.2 FIELD AND LABORATORY INVESTIGATIONS ............249

8.3 FIELD BEHAVIOUR OF GENESEE CLAY ................250

REFERENCES .............................................252

APPENDIX A - CHARACTERISTICS OF TILL ....................282

APPENDIX B - GRAIN SIZE ANALYSIS OF CLAY ................286

APPENDIX C - DETAILED BOREHOLE LOGGING ..................293

APPENDIX D - FIELD INVESTIGATION RESULTS ................312

APPENDIX E - LABORATORY INVESTIGATION RESULTS ...........330

APPENDIX F - AUTOMATIC CONTROLLER FOR THE BISHOP AND WESLEY TRIAXIAL CELL ...............................371

# List of Tables

Table Page

3.1 Structural discontinuities in unweathered clay. ....91

4.1 List of in-situ tests performed. ....94

5.1 Consolidation test results on vertical and horizontal samples. ....155

C.1 Detailed borehole log for UA1. ....295

C.2 Detailed borehole log for UA1 (continued). ....296

C.3 Detailed borehole log for UA1 (continued). ....297

C.4 Detailed borehole log for UA2. ....298

C.5 Detailed borehole log for UA2 (continued). ....299

C.6 Detailed borehole log for UA2 (continued). ....300

C.7 Detailed borehole log for UA5. ....301

C.8 Detailed borehole log for UA5 (continued). ....302

C.9 Detailed borehole log for UA5 (continued). ....303

C.10 Detailed borehole log for UA3. ....304

C.11 Detailed borehole log for UA3 (continued). ....305

C.12 Detailed borehole log for UA3 (continued). ....306

C.13 Detailed borehole log for UA4. ....307

C.14 Detailed borehole log for UA4 (continued). ....308

C.15 Detailed borehole log for UA4 (continued). ....309

C.16 Detailed borehole log for UA6. ....310

Table Page

C.17 Detailed borehole log for UA6 (continued). ....................311

E.1 Summary of consolidation test data. ...............331

E.2 Summary of consolidation test data (continued). ....................332

E.3 Summary of direct shear tests on clay samples. ....................333

E.4 Summary of triaxial tests on UA1 grey clay samples. ....................334

E.5 Summary of triaxial tests on UA2 grey clay samples. ....................335

E.6 Summary of triaxial tests on UA5 grey clay samples. ....................336

E.7 Summary of triaxial tests on UA3 grey clay samples. ....................337

E.8 Summary of triaxial tests on UA4 grey clay samples. ....................338

E.9 Summary of CIU tests on weathered brown clay. ....................339

E.10 Summary of CIU tests on grey clay block samples - vertical specimens. ....................340

E.11 Summary of CIU tests on grey clay block samples - horizontal specimens. ....................341

E.12 Summary of data on samples for yield tests. ....................342

# List of Figures

Figure Page

1.1 Location of study area, Genesee. ....................6

2.1 Sequence of glacial lakes in north-central Alberta (modified after Quigley,1980). ..............11

2.2 Simplified surficial geology map, Genesee and vicinity (modified after Andriashek et al,1979). ...12

2.3 Map of the bedrock topography (modified after Carlson,1970). .................................18

2.4 Preglacial valleys in the Genesee area (modified after Andriashek et al,1979). .............19

2.5 Typical topography within study area. ..............21

2.6 Cross-section X-X (refer to Plate 2.2 for location). ........................................25

2.7 Stratigraphy at Hugget. ............................29

2.8 Cross-section Y-Y (refer to Plate 2.2 for location). ........................................38

2.9 Cross-section Z-Z (refer to Plate 2.2 for location). ........................................39

2.10 Plasticity characteristics of weathered brown clay. ......................................46

2.11 Plasticity characteristics of unweathered grey clay. .......................................48

3.1 Variation of OCR with depth at (a) UA2 (b) plant site. ...................................76

4.1 Example of dissipation of TSC pressure with time. .......................................109

4.2 Example of DMT results (test location UA1). ..............................................113

4.3 Determination of closure pressure from hydraulic fracture. ..............................117

4.4 TSC one-minute pressure against equilibrium pressure. ..................................119

4.5 Measurement of $K_0$ at (a) UA1 (b) UA2. .............121

Figure Page

4.6 Measurement of $K_0$ at UA5. ........................ 122

4.7 Measurement of $K_0$ at (a) UA3 (b) UA4. ............ 123

4.8 DMT test results at UA2. ........................ 125

4.9 TSC $K_0$ against DMT $K_D$ . ........................ 126

4.10 Laboratory OCR against DMT $K_D$ . .................... 128

4.11 Normalised field vane strength against DMT $K_D$ . ........................................ 129

5.1 Corrected stress-strain curve for brittle failure. ........................................ 142

5.2 Determination of normally consolidated $K_0$. ........................................ 145

5.3 Variation of $K_0$ with OCR. ........................ 146

5.4 Volume change against isotropic consolidation pressure. ........................ 149

5.5 Determination of lateral yield point by Poulos and Davis method. ........................ 152

5.6 Stress path followed in Davis and Poulos method. ........................................ 153

5.7 Example of determination of yield point. .......... 160

5.8 Yield envelope for Genesee Clay. .................. 161

6.1 Summary of test results for UA1. .................. 163

6.2 Summary of test results for UA2. .................. 164

6.3 Summary of test results for UA5. .................. 165

6.4 Summary of test results for UA3. .................. 166

6.5 Summary of test results for UA4. .................. 167

6.6 Summary of test results for UA6. .................. 168

6.7 Variation of $c_v$ with pressure. .................... 171

6.8 Variation of $m_v$ with pressure. .................... 171

Figure Page

6.9 e-log $\sigma_v$ relationship for vert. and hor. specimen..172

6.10 Comparison of $m_v$ for vertical and horizontal specimen. ................................172

6.11 Variation of OCR and $K_0$ with depth at cooling pond. ................................175

6.12 Variation of OCR and $K_0$ with depth at plant site. ................................176

6.13 $K_0$ against OCR for Genesee Clay. ..................179

6.14 Example of CIU test results for intact unweathered clay. ................................181

6.15 CIU test results on unweathered clay with discontinuities. ................................182

6.16 Stress paths for CIU tests in Fig. 6.14 and 6.15. ................................183

6.17 CIU test results on weathered brown clay. .........186

6.18 Stress paths of tests shown in Fig. 6.17. .........187

6.19 Peak strength envelope of grey clay at cooling pond. ................................189

6.20 Peak strength envelope of grey clay at plant site. ................................190

6.21 Bilinear peak strength envelope of grey clay. ................................191

6.22 Strength parameters from direct shear test on grey clay. ................................194

6.23 Large strain strength envelope of grey clay. ................................195

6.24 Strength parameters from direct shear tests on brown clay. ................................197

6.25 Variation of $A_f$ with OCR. ........................199

6.26 Variation of $A_f$ with $K_0$. ........................199

6.27 CIU test results on vertical and horizontal samples. ................................203

Figure Page

6.28 Stress paths of tests shown in Fig. 6.27. .........204

6.29 Drained direct shear test results on dark grey clay. ....................................205

6.30 $c_u/\sigma_{vo}$ against $K_o$ for cooling pond area. ..........210

6.31 $c_u/\sigma_{vo}$ against $K_o$ for plant site area. ............211

7.1 Assumed failure surface at diversion ditch. ...........................................215

7.2 Soil properties at location close to diversion ditch. ...............................216

7.3 Total stress analysis of slope at diversion ditch. ...............................218

7.4 Construction history of SR770 embankment fill. ............................................221

7.5 Plan view of SR770 embankment failure. ............222

7.6 Cross section of SR770 embankment. ................223

7.7 Critical failure surfaces for SR770 embankment. ......................................226

7.8 Total stress analysis results of SR770 embankment. ......................................227

7.9 Effective stress analysis of SR770 embankment. ......................................230

7.10 Stages in construction of high dyke. ..............232

7.11 Pore pressure response with construction activities under centreline of dyke. ..............233

7.12 Movement registered by Thurber SI5 slope indicator. .........................................234

7.13 Variation of movement of slope indicator SI5 with time. .........................................236

7.14 Cross section of high dyke for stability analysis. ..........................................237

7.15 Pore pressure response of piezometer Thurber HDP29 ..................................238

Figure Page

7.16 Total stress analysis results of high dyke. ....................240

7.17 Effective stress analysis of high dyke. ...........241

7.18 Observed excess pore pressure against applied surface pressure. ........................242

7.19 Stress paths at piezometer HDP23. ................243

A.1 Grain size analysis of till. .......................283

A.2 Plasticity characteristics of till. ...............284

B.1 Grain size analysis of UA1 clay samples. ..........287

B.2 Grain size analysis of UA2 clay samples. ..........288

B.3 Grain size analysis of UA3 clay samples. ..........289

B.4 Grain size analysis of UA4 clay samples. ..........290

B.5 Grain size analysis of UA5 clay samples. ..........291

B.6 Grain size analysis of UA6 clay samples. ..........292

D.1 TSC results at UA1 with cell in North-South direction. ............................313

D.2 TSC results at UA1 with cell in East-West direction. .......................................313

D.3 TSC results at UA2 with cell in North-South direction. ............................314

D.4 TSC results at UA2 with cell in East-West direction. .......................................314

D.5 TSC results at UA5 with cell in North-South direction. ............................315

D.6 TSC results at UA5 with cell in East-West direction. .......................................315

D.7 TSC results at UA3 with cell in North-South direction. ............................316

D.8 TSC results at UA4 with cell in North-South direction. ............................316

Figure Page

D.9 TSC results at UA6 with cell in North-South direction. ....................317

D.10 Dilatometer test results at UA3. ..................318

D.11 Dilatometer test results at UA4. ..................319

D.12 Hydraulic fracture at UA1 at depth of 8.4 m. ..........................................320

D.13 Hydraulic fracture at UA1 at depth of 11.4 m. ......................................321

D.14 Hydraulic fracture at UA1 at depth of 16.0 m. ......................................322

D.15 Hydraulic fracture at UA2 at depth of 10.8 m. ......................................323

D.16 Hydraulic fracture at UA2 at depth of 13.8 m. ......................................324

D.17 Hydraulic fracture at UA3 at depth of 8.3 m. ..........................................325

D.18 Hydraulic fracture at UA3 at depth of 10.3 m. ......................................326

D.19 Hydraulic fracture at UA4 at depth of 9.7 m. ..........................................327

D.20 Hydraulic fracture at UA4 at depth of 11.7 m. ......................................328

E.1 Direct shear test on grey clay - sample DST.B3.1. ....................................343

E.2 Direct shear test on grey clay - sample DST.B3.2. ....................................344

E.3 Direct shear test on grey clay - sample DST.B3.3. ....................................345

E.4 Direct shear test on grey clay - sample DST.B3.4. ....................................346

E.5 Direct shear test on brown clay - sample DST.4.1. ......................................347

Figure Page

E.6 Direct shear test on brown clay - sample DST.4.2. ....................348

E.7 Direct shear test on brown clay - sample DST.4.3. ....................349

E.8 Direct shear test on brown clay - sample DST.4.4. ....................350

E.9 Direct shear test strength parameters for brown clay. ....................351

E.10 Triaxial test results on UA1 grey clay. ....................352

E.11 Triaxial stress paths for UA1 grey clay. ....................353

E.12 Triaxial test results on UA2 grey clay. ....................354

E.13 Triaxial test stress paths for UA2 grey clay. ....................355

E.14 Triaxial test results on UA5 grey clay. ....................356

E.15 Triaxial test stress paths for UA5 grey clay. ....................357

E.16 Triaxial test results on UA3 grey clay. ....................358

E.17 Triaxial test stress paths for UA3 grey clay. ....................359

E.18 Triaxial test results on UA4 grey clay. ....................360

E.19 Triaxial test stress paths for UA4 grey clay. ....................361

E.20 Triaxial test results on grey clay block samples(V). ....................362

E.21 Triaxial test stress path for grey clay block samples(V). ....................363

E.22 Triaxial test results on grey clay block samples(H). ....................364

E.23 Triaxial test stress path for grey clay block samples(H). ....................365

Figure Page

E.24 Yielding in Genesee Clay with $\sigma_3'/\sigma_1'=0.6$. ....366

E.25 Yielding in Genesee Clay with $\sigma_3'/\sigma_1'=0.7$. ....367

E.26 Yielding in Genesee Clay with $\sigma_3'/\sigma_1'=1.0$. ....368

E.27 Yielding in Genesee Clay with $\sigma_3'/\sigma_1'=1.2$. ....369

E.28 Yielding in Genesee Clay with $\sigma_3'/\sigma_1'=1.8$. ....370

F.1 Diagrammatic layout of Bishop and Wesley cell. ....373

# List of Plates

Plate Page

1.1 Layout of Genesee Power Project. ....................7

2.1 Ice-thrusted bedrock on sand. ......................15

2.2 Airphotograph showing topographic features and test locations. ........................16

2.3 General view of hummocky terrain at Genesee. ..........................................22

2.4 (a) South face of exposure (b) Till between ice thrusted bedrock. ......................27

2.5 Depositional features of top 1 m of till. ..........36

3.1 Lenticular laminae of silt within clay matrix-sample 2-10. ..............................59

3.2 Depositional sequences in bottom 1 m of clay - sample 4-9. ...............................60

3.3 Depositional sequences in unweathered clay - sample 6-6. ...............................61

3.4 Mottled appearance of top of unweathered clay - sample 5-3. ...............................63

3.5 (a) Open flocculated structure-light grey clay
(b) Dispersed structure-dark grey clay
(c) Magnification of (b) (d) Honeycomb structure. ..68

3.6 (a) Compact arrangement of silty clay
(b) Micronodule in weathered clay
(c) Clay particles wrapping micronodule. ...........71

3.7 Shearing along bedding with intrastratal flow structure. ..................................80

3.8 Minor coherent slump (sample 1-2). ................80

3.9 Shearing due to lateral compression (sample 1-3). ...........................................81

3.10 Slickenside with (a) no striation (b) slight striations ...............................83

3.11 High angle major sheared fissure (sample 6-2). ...............................................84

3.12 Subhorizontal and subvertical major sheared fissures(sample 2-5). ......................84

Plate Page

3.13 Highly striated high angle slickenside (sample 1-6). ....................................87

3.14 Smooth vertical fissures (block sample). ...........88

3.15 Randomly oriented fissures (sample 6-3). ...........88

4.1 Total stress cell and protective casing. ...........107

4.2 Marchetti flat plate dilatometer. .................111

4.3 (a) Piezometer (b) Pressure system and volume change device. ..............................115

4.4 Example of field vane shear test chart. ...........133

7.1 Slope failure at diversion ditch. .................215

A.1 Homogeneous structure of till. ....................285

D.1 Calibration chamber for total stress cell. ..............................................329

F.1 Bishop and Wesley cell. ...........................374

F.2 Automatic controller. .............................374

# 1. INTRODUCTION

## 1.1 SCOPE AND OBJECTIVES OF THESIS

This research originated from geotechnical problems encountered during the construction of the Genesee Power Generation Station. These problems indicate that the design of structures on the class of material encountered cannot be based solely on routine engineering investigations and procedures and also reflects a lack of understanding of the soil behaviour. The present research was undertaken to determine the origin of the problems with a view to improving the data base for this class of material.

The material of interest is the lacustrine clay which will be referred to as **"Genesee Clay"** in this thesis and which serves as a foundation for the various components of the station. The clay has a thickness varying between 10 and 20 m and overlies a 2 to 20 m thick layer of ablation till which lies on bedrock. The Genesee Clay which was deposited during the last ice retreat from the region is of medium to high plasticity and soft to firm consistency; the upper weathered layer is stiff to very stiff. During the site investigation for the project, it was found that the clay is fissured and that there is a wide variation in undrained strength within short horizontal distances.

It is known that glacial deposits can exhibit variation in properties as a result of fluctuations in depositional environment, glacier ice overriding, erosion, slumping and sediment redistribution. In that respect, the Genesee Clay might have been affected by its depositional and post-depositional history and in a sense, the clay may be classified as a "geotechnically complex material" according to the definition of Morgenstern and Cruden (1979). In dealing with such materials, these authors suggested that "the analysis of geotechnical complexity requires the unravelling of the role of each of these processes (genetic, epigenetic and weathering) in order to establish sensible limits to detailed site investigations and material characterisation.". It was within this framework that the present investigation was undertaken since the preliminary information from the reports on the Genesee Power Project indicated that the processes mentioned above were instrumental in producing a complex deposit.

Although the Genesee Clay layer is thick and of lacustrine origin, it has an undulating surface topography which resembles that of a hummocky disintegration moraine suggesting the likelihood of deposition on ice-rich debris. This type of deposition is similar in nature to supraglacial deposition of till although there is some uncertainty as to the exact origin of the ice; the latter could have been buried glacial ice blocks or could have formed due to permafrost conditions prior to deposition of the clay. In fact, large areas of thick clay deposit with topographic features similar to those of Genesee Clay were identified in the Peace River region, Alberta by Odynsky (1971) and in other regions of Western Canada by Mollard (1983).

Since the present topography reflects the fact that the ice blocks within the till continued melting after complete deposition of the clay, differential vertical movements occurred at a time when at least part of the clay layer was already fully consolidated under the existing overburden and had developed resistance against deformation. At this stage, the clay could have been affected by the deformation resulting from the basal movements. Nevertheless, the engineering significance of these melt-out processes on the structure and stress history of the clay do not seem to have been recognised previously in the geotechnical literature; these effects could also be applicable to similar depositional sequences. Since preliminary data indicated that the present geotechnical characteristics of Genesee Clay may reflect this post-depositional history, it was decided to carry out an extensive investigation of the clay deposit. On the other hand, it is recognised that the properties of the clay were also affected by variations in depositional environment, weathering and stress history effects due to changes in effective stresses. Consequently, it was necessary to identify and assess these depositional variations and the individual effects of the post-depositional processes on the geotechnical properties of the clay. Therefore, reconstruction of the geological history is required. Although Genesee and its immediate surroundings had not been studied specifically in the past, the geology at Hugget which is about 15 km east of Genesee was studied by Shaw (1982) and the exposures at the borrow pits to the north of Genesee offered significant details on the local glacial history.

Six test sites were selected within the confines of the Genesee Power Project. Since the stresses induced due to the melt-out processes might be reflected in the topography, both topographic highs and lows were investigated. The field and laboratory investigations presented in this thesis were performed by the author during the period extending from 1983 to 1985. Both in-situ stress and undrained strength measurements were made at the sites in order to study the variability of these parameters within the deposit. The stress history of the clay has been studied by means of consolidation tests and yield envelopes. Laboratory tests were performed to study the present behaviour of the clay and the conclusions made were checked by backanalysis of the instrumented structures of the Genesee Power Project. Other pertinent data were drawn from the geotechnical reports of the consultants for the project which were EBA Engineering Consultants Ltd and Thurber Consultants Ltd of Edmonton and Golder Associates Ltd of Calgary.

In summary, the principal objectives of this thesis are:

1. to determine the depositional and post-depositional history of the Genesee Clay.
2. to assess the variability in the properties of the

deposit.

3. to determine the effects of the post-depositional bottom melt-out processes on the clay.
4. to determine appropriate design parameters for this class of material.

## 1.2 THE GENESEE POWER PROJECT

### 1.2.1 General description

The Genesee Power Project is located at Genesee which is about 60 km southwest of Edmonton, Alberta (Fig. 1.1). The development of the Project is aimed at the exploitation of the coal fields close to Genesee for the production of electrical power. A brief account of the proposed developments of the coal fields is given by Mulder (1981). As shown in Plate 1.1, the main components of construction are the cooling pond, power plant and the reconstruction of highway SR770. The cooling water pond which is surrounded by an earth dyke, which varies from 2 to 25 metres in height, covers an area of approximately 6.5 km². Water for the pond will be pumped from the North Saskatchewan River. The power plant consists of two 400-megawatt steam driven thermal generators with provision for the addition of 2 or more additional units. The coal handling facilities are located at the south end of the plant site and involve an excavation about 15 m below grade for the construction of a 170 m long coal storage slot and a 20 m deep hopper.

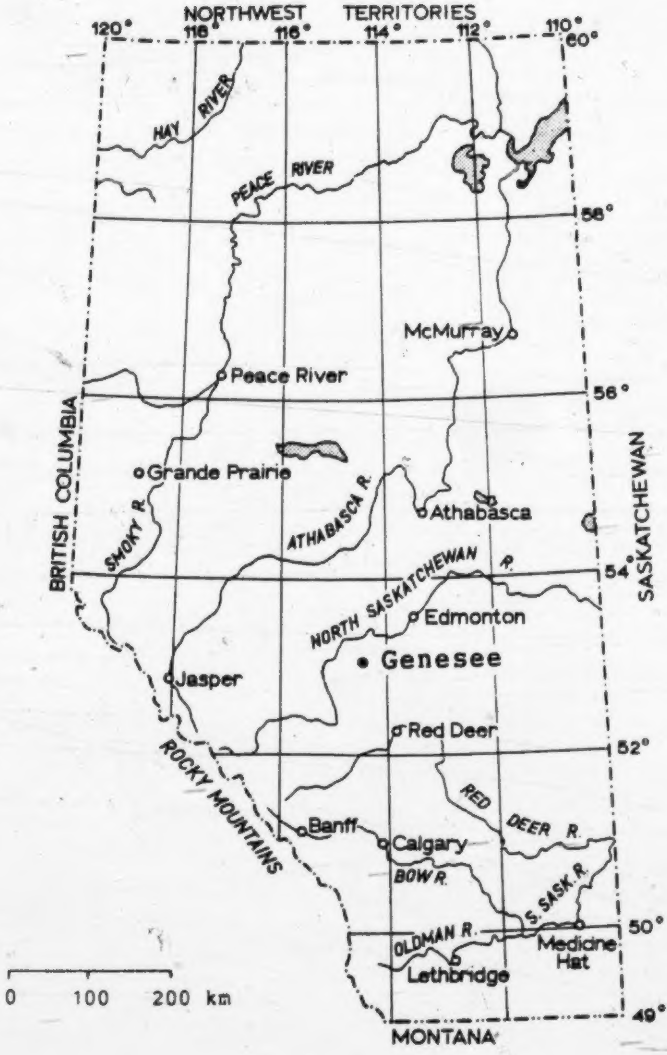
NORTHWEST TERRITORIES
120°
118°
116°
114°
112°
110°
60°
58°
56°
54°
52°
50°
49°
HAY RIVER
PEACE RIVER
McMurray
Peace River
Grande Prairie
SMOKY R.
ATHABASCA R.
Athabasca
NORTH SASKATCHEWAN R.
Edmonton
Genesee
Jasper
Red Deer
RED DEER R.
ROCKY MOUNTAINS
Banff
Calgary
BOW R.
S. SASK. R.
OLDMAN R.
Medicine Hat
Lethbridge
BRITISH COLUMBIA
SASKATCHEWAN
MONTANA
0
100
200 km

Figure 1.1 Location of study area, Genesee.

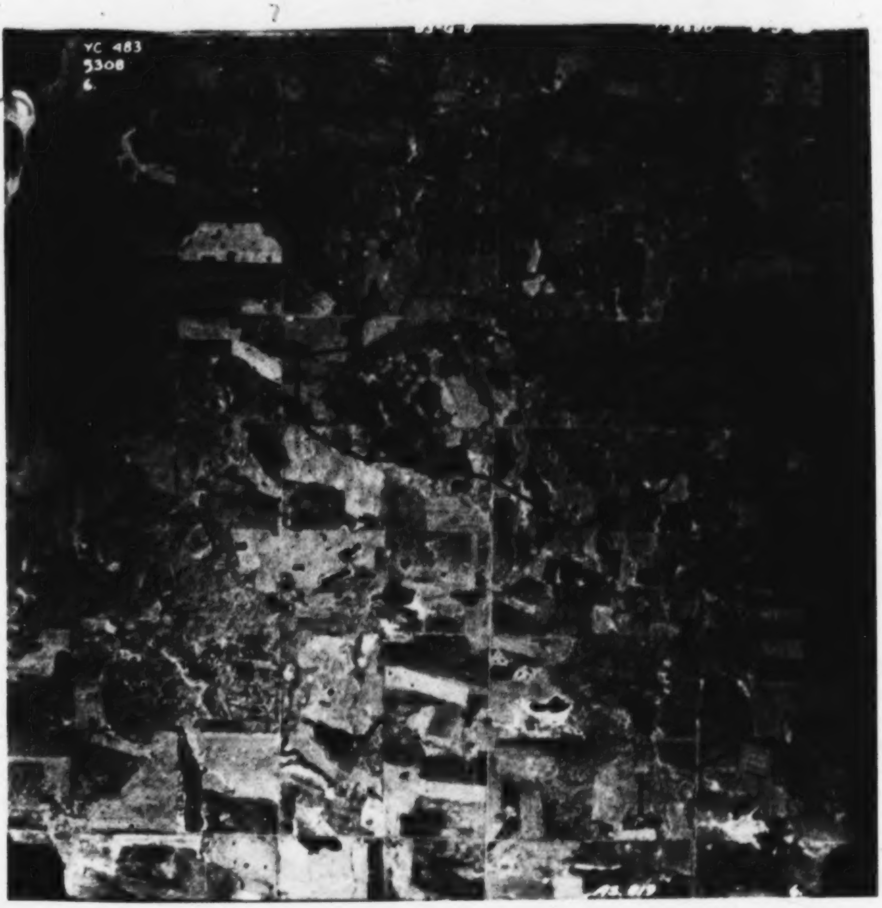

Airphoto no. YC 483-5308-6
Original scale 1:31680
Size reduction 0.67

Top of photograph is north.

Plate 1.1 Layout of Genesee Power Project.

The construction activities also include the relocation of the existing highway SR770 which traverses the cooling pond area. The new highway ,which incorporates an overpass structure to the southeast of the plant site, consists of 13 m high approach fills and a bridge over a mine haul road.

Construction of the project started in mid 1982.

### 1.2.2 Geotechnical problems

During the site investigation for the project, it was recognised that the lacustrine clay could present potential construction problems because it is slickensided, but the exact role of these discontinuities could not be evaluated since the intensity of their distribution was not known. On the other hand, EBA (1983) reported significant variation in the undrained strength over short distances of 30 m from cone penetration tests. Since there are insignificant differences in mineralogy and consolidation history over such short distances, the variation in undrained strength probably reflects variation in lateral stresses induced by the bottom melt-out processes.

During the construction of the project, the following major instabilities were encountered:

1. failure of the north approach fill side slopes at the overpass structure.
2. slope failure at the diversion ditch within the cooling pond.
3. large deformations in the lacustrine clay during

construction of the high dyke (greater than 18 m) at the cooling pond.

### 1.3 ORGANIZATION OF THESIS

In Chapter 2, the glacial geology of the study area is dicussed in relation to the the published data on the geology of Alberta, the findings of Shaw (1982) at Hugget and the field and laboratory investigations performed by the author. Description of the bedrock, till and lacustrine clay is also given in this chapter. Examples of macro and microstructures found in the Genesee Clay as well as a discussion of their origin are given in Chapter 3. The field and laboratory investigations are described in Chapters 4 and 5 respectively. The geotechnical properties of the Genesee Clay are discussed in Chapter 6 with particular emphasis on the effects of bottom melt-out processes. The instabilities encountered during the construction of the Genesee Power Project and the results of the backanalysis are discussed in Chapter 7. Chapter 8 contains the conclusions originating from this research.

---

# 2. GEOLOGY OF STUDY AREA

## 2.1 GLACIAL HISTORY

The close proximity of Genesee to Edmonton suggests that both regions have the same general geological history. According to Bayrock and Hughes (1962), the last ice sheet to cover the Edmonton district was of Wisconsin age, that is, over 31,000 years b.p. The glacier retreated from the area about 13,000 years b.p. in a north easterly direction. Since the land slopes downward from the Rocky Mountains towards Hudson Bay, large proglacial lakes formed in front of the retreating glacier. St. Onge (1972) identified seven phases of the proglacial lake formation in north-central Alberta and the lacustrine deposit at Genesee was deposited between phases 2 and 4 as shown in Fig. 2.1 which is reproduced from Quigley (1980). Drainage of the lake at Genesee took place in a southeasterly direction through a spillway southeast of Thorsby.

According to Gravenor and Bayrock (1965), the ice retreat from the Edmonton area was one of large scale downwasting which caused large ice blocks to separate from the main ice mass and to stagnate. An example of this stagnation is the pitted delta to the northeast of the Genesee lake deposit as shown on the surficial geology map (Fig. 2.2) which is reproduced from Andriashek et al (1979); the pitted delta acquired a hummocky topography as a result of the melting of buried ice blocks.

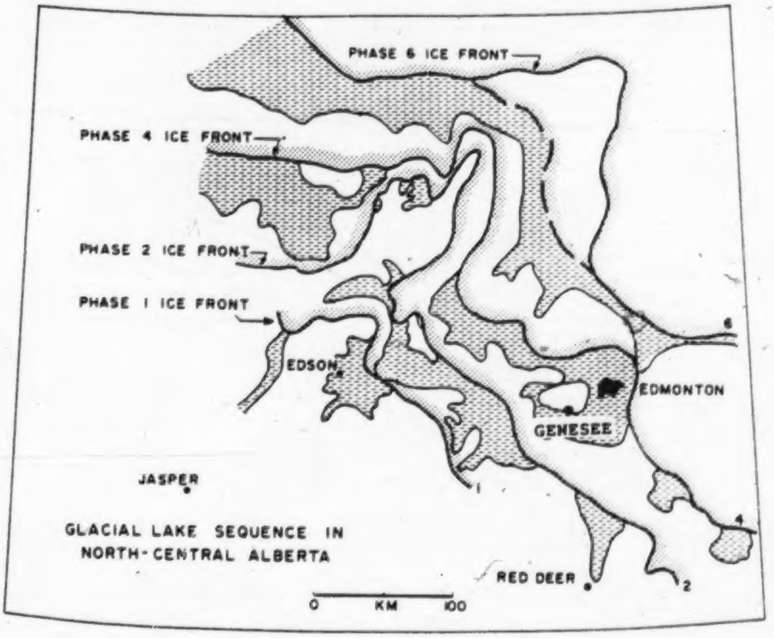
PHASE 6 ICE FRONT
PHASE 4 ICE FRONT
PHASE 2 ICE FRONT
PHASE 1 ICE FRONT
EDSON
EDMONTON
GENESEE
6
1
4
2
JASPER
GLACIAL LAKE SEQUENCE IN NORTH-CENTRAL ALBERTA
RED DEER
0 KM 100

Figure 2.1 Sequence of glacial lakes in north-central Alberta (modified after Quigley, 1980).

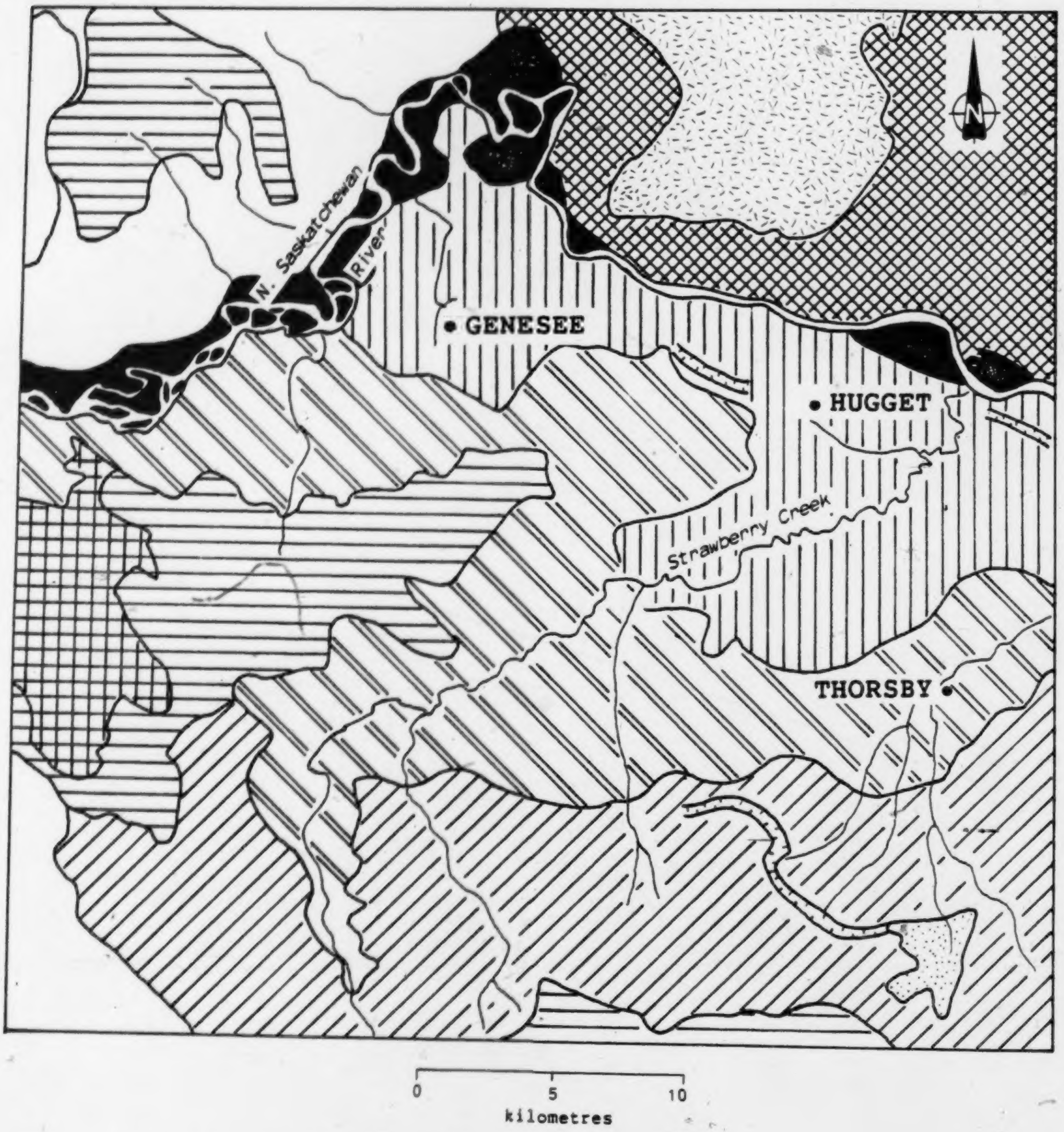
N. Saskatchewan River
GENESEE
HUGGET
Strawberry Creek
THORSBY
N
0
5
10
kilometres

Note - see next page for legend.

Figure 2.2 Simplified surficial geology map, Genesee and vicinity (modified after Andriashek et al, 1979).

## Legend for Figure 2.2

| | |
|---|---|
| ▥ | Glaciolacustrine clay and silt |
| ▧ | Mixed glaciolacustrine sediments; interbedded clay and silt with till layers and pockets |
| ▩ | Glaciolacustrine sand and silt |
| ░ | Pitted delta; sand, silt and sand, minor clay and gravel |
| □ | Undifferentiated glaciolacustrine clay or silty clay |
| ░ | Outwash sand and gravel |
| ▨ | Till |
| ▤ | Thin till cover over bedrock |
| ▦ | Bedrock |
| ■ | Depositional terraces |
| 〰 | Meltwater channel |

The glacier retreat was followed by local rejuvenation or readvance of small lobes from the main ice mass and Gravenor and Bayrock (1965) concluded that the stagnation - rejuvenation cycle occurred many times during the general retreat. A rejuvenation took place at Genesee as indicated by Plate 2.1 which shows the top 5 m. of the deposit to the north of the study area whose location is shown as C on the airphotograph (Plate 2.2). The photograph shows a layer of loose sand sandwiched between two layers of ice thrusted bedrock. The sand is medium coarse to fine grained, finely laminated to thinly bedded and does not show the cross-bedding normally associated with fluvial deposits. It is believed that this sand was associated with the beach of a former lake and that there was a readvance of the ice after the existence of the lake during an ablation period.

After the glacier retreat was complete, there were two major geological events, namely, the downcutting of the North Saskatchewan River Valley and the prevalence of a warm and dry climate which lasted from 7000 to 4000 years b.p (Bayrock and Hughes, 1962). There were only very minor modifications to the landscape after that period.

## 2.2 AIRPHOTO INTERPRETATION AND GEOLOGICAL MAP STUDY

The aerial photograph (Plate 2.2) shows the location of Genesee and indicates that the area consists of a depression where the ground surface elevation varies between 710 and 730 m whereas the ground elevation outside the depression

Plate 2.1 Ice-thrusted bedrock on sand.

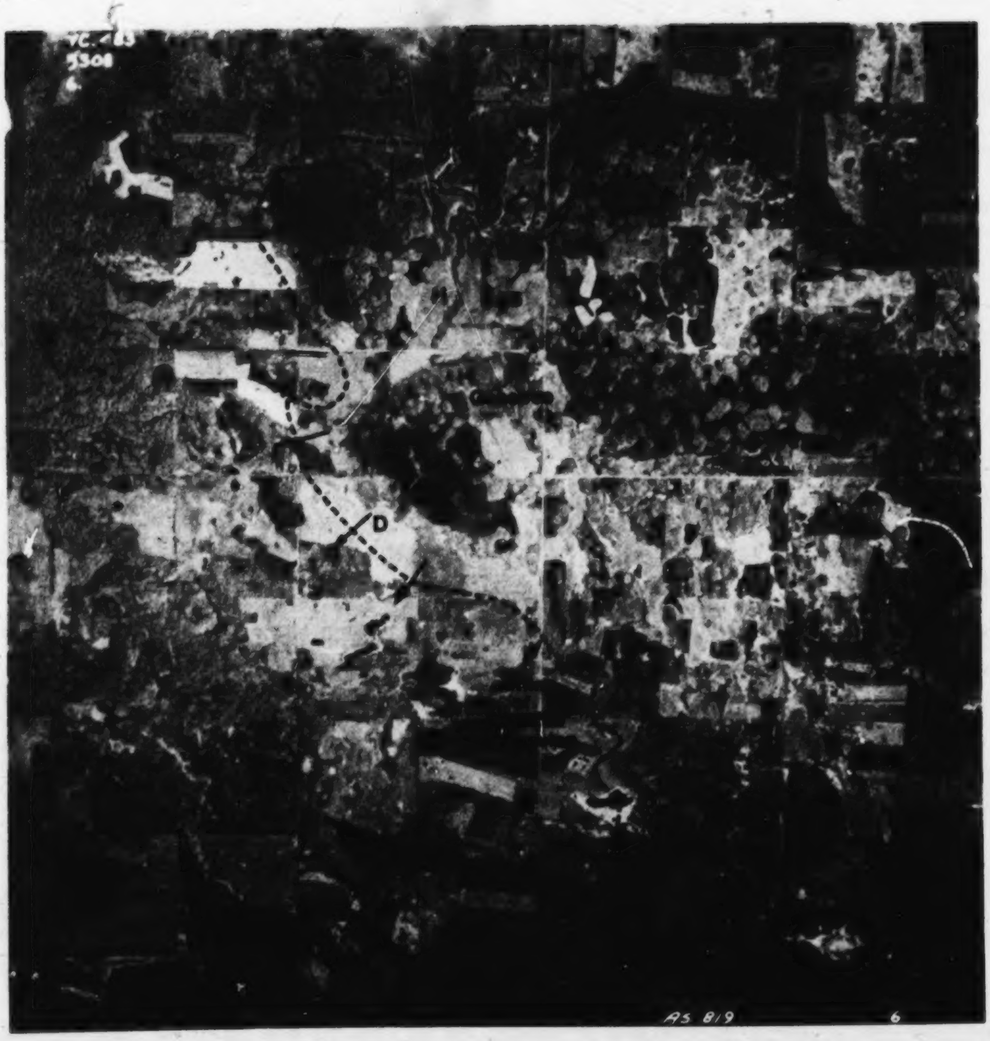
YC.483
5308
6
D
AS 819
6

Airphoto no. YC 483-5308-6
Original scale 1:31680
Size reduction 0.67

Top of photograph is north.

Plate 2.2 Airphotograph showing topographic features and test locations.

varies between 730 and 750 m. Borehole data (Thurber, 1982b) suggest that the general ground topography reflects that of the underlying bedrock with the boundary of the surface depression (Plate 2.2) corresponding to the ridge of a bedrock depression. This depression is 3 to 4 km wide. The bedrock topography map which is reproduced from Carlson (1970) is shown in Fig. 2.3 and the preglacial valleys in the vicinity of Genesee are shown in Fig. 2.4. Within the study area, the invert of the bedrock depression slopes downward towards the west at an angle of less than one degree. This has influenced the deposition of the overlying till and clay which become increasingly thicker in a westerly direction.

The surficial geology map (Fig. 2.2) gives an indication of the geological setting of deposition in the vicinity of Genesee. The lake covering that area was ponded against the higher bedrock surface to the south and the ice front to the north. The lake was fed by meltwater flowing from the northwest and by streams flowing on the surface of possibly stagnant ice to the northeast of Genesee; the latter streams deposited the deltas at the ice front which are at present classified as pitted deltas. Fine grained sediments were deposited in the deepest part of the lake, that is, the bedrock depression. The glaciolacustrine clay grades into sand and silt away from the depression. The lake level was most probably low since a thick (12 to 20 m) layer of clay was deposited only within the bedrock depression.

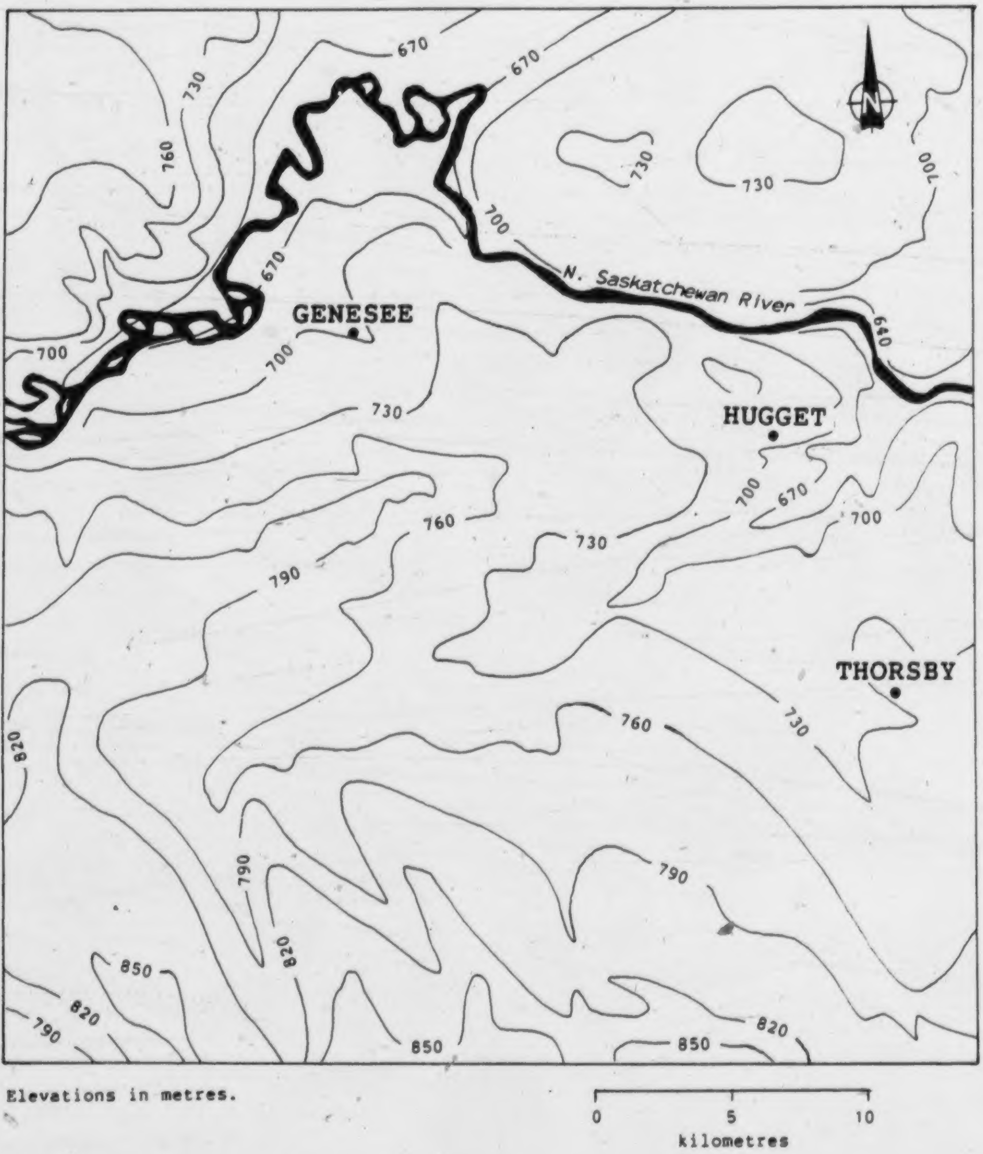
N
670
670
730
760
730
730
700
700
670
N. Saskatchewan River
690
GENESEE
700
700
730
HUGGET
700
670
700
760
730
790
THORSBY
820
760
730
790
790
820
850
820
790
850
850
820
Elevations in metres.
0
5
10
kilometres

Figure 2.3 Map of the bedrock topography (modified after Carlson, 1970).

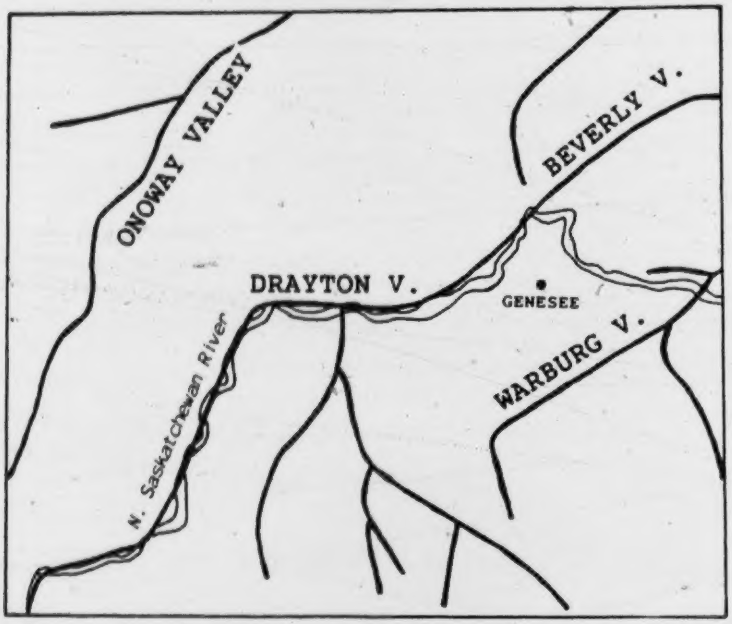
ONOWAY VALLEY
BEVERLY V.
DRAYTON V.
GENESEE
WARBURG V.
N. Saskatchewan River

Figure 2.4 Preglacial valleys in the Genesee area (modified after Andriashek et al, 1979).

There is an indication from the aerial photograph (Plate 2.2) that the level of the lake was at one time controlled by spillways (labelled D on Plate 2.2) just southwest of Genesee. Area E had been deeply cut by the flow of water from these spillways, indicating that, at one time, water was flowing in a southwest direction in that region. However, the regional flow of meltwater was in a general southeast direction. Therefore, the diversion of the water through these spillways represented local variation in the flow direction towards the southwest most probably caused by blockage of the main outlet at the southeast of the lake as explained in section 2.3.2. When the main outlet became functional again, the meltwater resumed its flow in the southeast direction cutting the channels in the deposit to the east of Genesee (Fig. 2.2). Presently, drainage is provided by Genesee Creek and its tributaries.

The surface topography of the clay deposit within the depression is undulating ( 1 to 4 degrees) to rolling ( 4 to 8 degrees) according to the glacial landform classification system of Clayton and Moran (1974). The topography, which resembles a field of mounds on the airphotograph, is similar to that of a dead ice disintegration moraine described by Gravenor and Kupsch (1959). The mounds have typically a basal width of 100 to 150 m and a height of 2 to 5 m (Plate 2.3); Fig. 2.5 shows a contour map of the area around the University of Alberta test locations within the cooling pond. There is no systematic distribution or orientation of

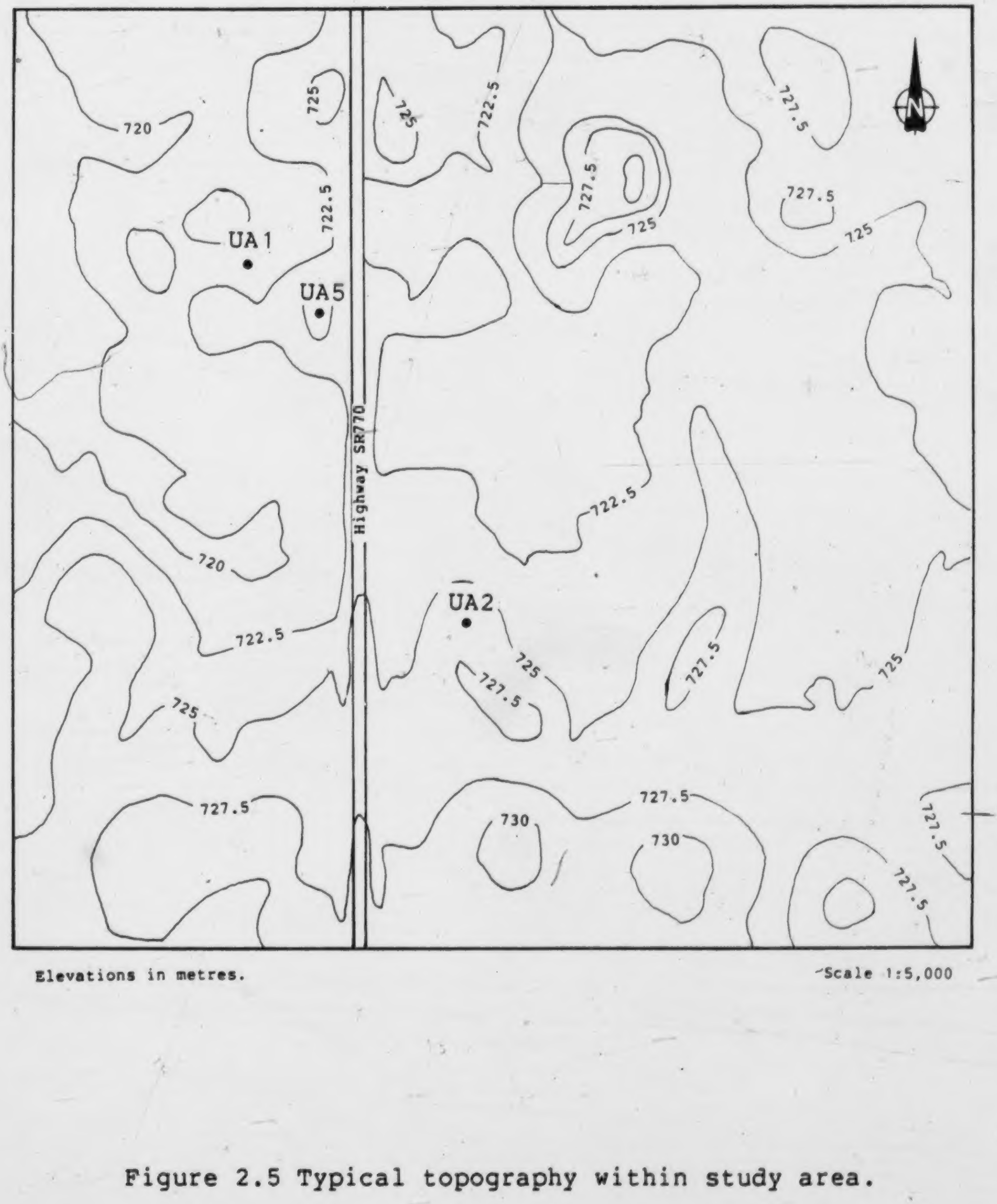
720
725
725
722.5
722.5
UA1
UA5
727.5
727.5
727.5
725
725
Highway SR770
722.5
720
UA2
722.5
725
727.5
727.5
725
725
727.5
727.5
730
730
727.5
727.5

Elevations in metres.

Scale 1:5,000

Figure 2.5 Typical topography within study area.

Plate 2.3 General view of hummocky terrain at Genesee.

the mounds and in some instances, the mounds lie within larger depressions such as F (Plate 2.2) which are now filled with peat. Three main types of mound formation can be identified, namely:

1. individual circular mounds with a central depression resembling the prairie mounds in till described by Gravenor (1955). These are labelled G and seem to be concentrated within the east part of the study area where the clay is thinner.
2. clusters or strings of 2 or more mounds such as H that coalesced during formation.
3. elongated mounds such as J which indicates that some flow took place during mound formation.

The formation of these mounds is discussed in section 2.6.

The following additional observations can be made from the airphotograph (Plate 2.2):

1. the presence of a perched lacustrine plain and ridge such as A and B respectively suggests that outside the depression, some deposition occurred within small ice-dammed lakes. These features confirm the presence of stagnant ice during ice retreat.
2. there is no evidence of ice thrusting or overriding on the clay deposit in the form of thrusted ridges or ice-scour markings.
3. the presence of small circular lakes, similar in appearance to sinkholes (K), which indicates substantial past subsidence.

4. because of the poor drainage of the region, ponding of water in the low lying areas has resulted in the development of peat over large portions of the study area.
5. outside the bedrock depression, the presence of numerous kettle holes indicates that ice blocks became buried during deposition of the till. The thinner overlying clay layer probably conforms to the till topography.

## 2.3 STRATIGRAPHY

The stratigraphy outside and inside the bedrock depression will be discussed separately. Shaw (1982) has studied the soil profile at Hugget which is situated at about 15 km east of Genesee (see Fig. 2.2).

### 2.3.1 Stratigraphy outside bedrock depression

The stratigraphy outside the bedrock depression at Genesee is important in that it gives some guidance as to the local geological history of the study area. This section will deal with the stratigraphy at the north of the bedrock depression because of the information obtained from exposures during excavation for borrow materials. Fig. 2.6 which is reproduced from Thurber (1982a) shows that the stratigraphy consists of a thin veneer (3 to 5 m) of lacustrine clay overlying about 5 m of till. Underlying these deposits is a complex succession of ice thrusted bedrock and glaciofluvial and glaciolacustrine deposits. As

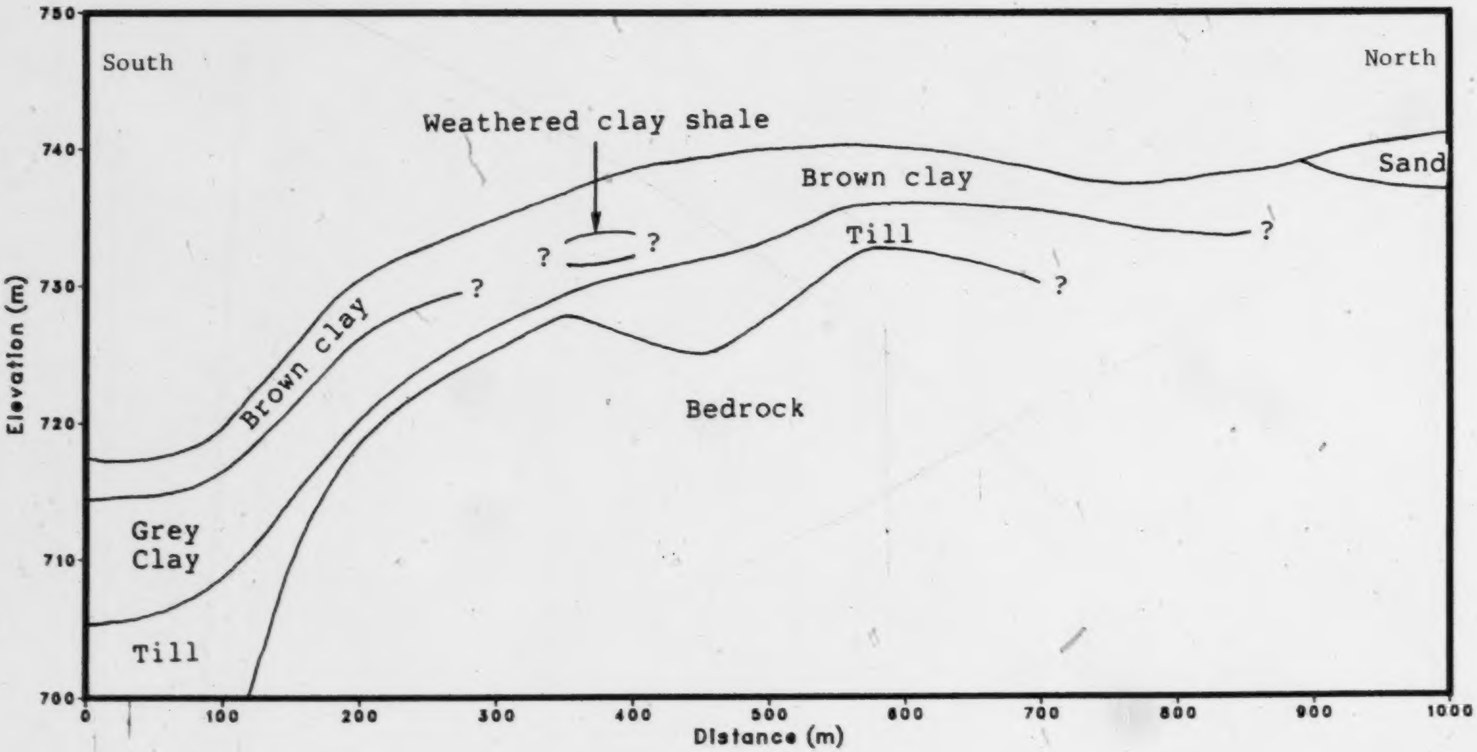
South
North
Weathered clay shale
Brown clay
Sand
?
?
?
Till
?
?
Brown clay
Grey
Clay
Till
Bedrock
750
740
730
720
710
700
Elevation (m)
0
100
200
300
400
500
600
700
800
900
1000
Distance (m)

Figure 2.6 Cross-section X-X (refer to Plate 2.2 for location).

mentioned in section 2.1, the stratigraphy at the north of the bedrock depression gives some evidence that the general ice retreat was characterised by ice stagnation - rejuvenation cycles of small lobes from the main ice mass. Observation of ice-thrust features such as those shown in Plate 2.4(a) indicates that this particular ice lobe advanced from the west. The presence of sand and till sandwiched between layers of thrusted bedrock as shown in Plates 2.1 and 2.4(b) suggests that the rejuvenation was preceded by glaciofluvial or glaciolacustrine conditions. The presence of distinct layering within the till of Plate 2.4(b) indicates that it was deposited under water during an ablation period. It is to be noted that the layer has been called "till" due to the presence of pebbles and coal chips but because of the limited exposure, it is not possible to say whether it is a waterlaid till as defined by Dreimanis (1976) or a flow till.

The presence of a 4 to 5 m thick layer of undisturbed clay, with distinct varves in certain areas, overlying the thrusted sequences indicates that significant sedimentation took place during the final phase of the ice retreat.

From the preceding information, it can be concluded that the lacustrine deposition took place in various sequences with possible cold periods existing between sequences. The cold periods existed during the rejuvenation of the glacier ice.

(a)

(b)

Plate 2.4 (a) South face of exposure (b) Till between ice thrusted bedrock.

### 2.3.2 Stratigraphy within bedrock depression

The soil profile at Genesee consists of lacustrine clay overlying a till layer which rests on the bedrock. The till has a thickness varying from 20 m at the cooling pond to 6 m at the plant site; but there are locations at the plant site where the till is only 1 to 2 m thick. The clay layer is 15 to 20 m thick at the cooling pond and 8 to 12 m thick at the plant site. As mentioned earlier, the thickness of these deposits was controlled by the sloping bedrock surface. The clay has an upper brown weathered layer which is between 6 and 10 m thick.

Shaw (1982) studied the soil profile at Hugget which lies on the side of the Strawberry Creek; the stratigraphy is reproduced in Fig. 2.7. While it is obvious that the bedrock depression in which Hugget lies is preglacial because of the presence of preglacial sands and gravels, such a conclusion cannot be made for the bedrock depression where Genesee is situated because of the absence of preglacial deposits. Therefore, it is possible that the bedrock depression at Genesee is similar to the stream-trenches described by Gravenor and Bayrock (1956) who believed that these trenches are contemporaneous with the retreat of the last ice and formed in openings in stagnant ice.

The difference in stratigraphy between Genesee and Hugget shows the influence of bedrock topography and ice position in controlling meltwater flow and hence deposition.

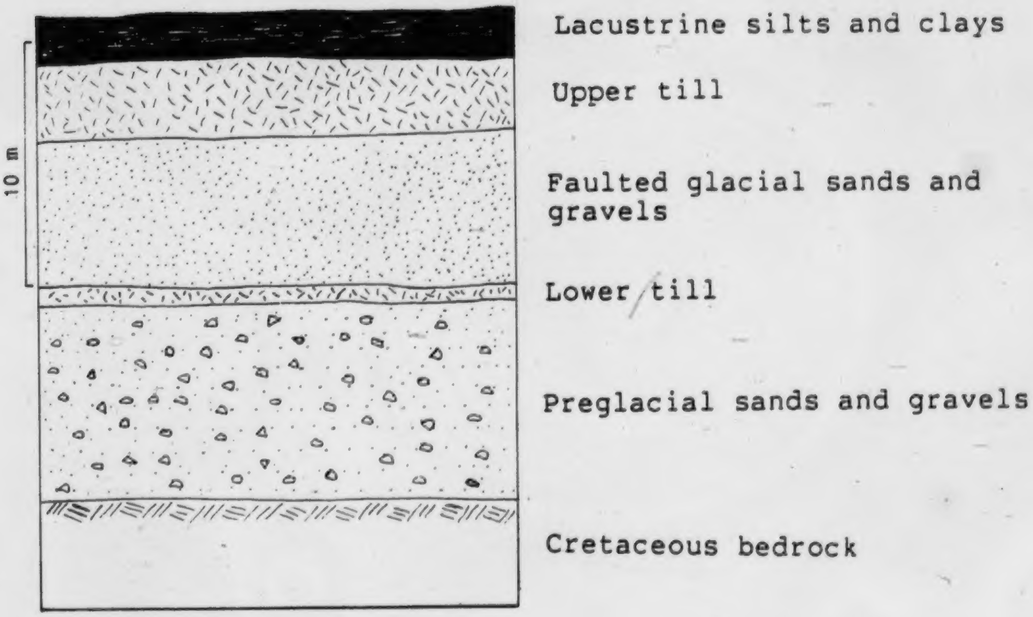
Lacustrine silts and clays
Upper till
10 m
Faulted glacial sands and gravels
Lower till
Preglacial sands and gravels
Cretaceous bedrock

Figure 2.7 Stratigraphy at Hugget.

The stratigraphy indicates deposition under lacustrine conditions at Genesee and glaciofluvial conditions at Hugget after deposition of the lower till. This was probably caused by the bedrock topography since Genesee and Hugget are separated by a bedrock plateau of higher elevation (Fig. 2.3) which enhanced the ponding of water at Genesee, whereas at Hugget there was free drainage. In section 2.1, the evidence was provided that there was at least one readvance of the glacier ice to the northwest of Genesee and in section 3.4, it is found that there were at least two sequences of deposition within the lake at Genesee with a low lake level between sequences. These observations are in agreement with the findings of Shaw (1982) based on the stratigraphy at Hugget. The presence of the two tills at Hugget (Fig. 2.7) has been interpreted by Shaw as an indication of two periods of ice occupation with glaciofluvial conditions prevailing between the two periods.

The general history of deposition at Genesee and at Hugget can be summarised as follows:

1. the till at Genesee and the lower till at Hugget were probably deposited during the first glacial advance.
2. during the ice retreat, lacustrine conditions existed at Genesee and glaciofluvial conditions at Hugget.
3. ice lobes rejuvenated over the region with obstruction of drainage in the east causing the lake level at Genesee to rise and overflow through the spillways to the southwest of Genesee (section 2.2). One ice lobe

deposited the upper till at Hugget and the one that moved from the northwest of Genesee did not override the already deposited clay.

4. the lake was then suddenly drained by the opening of outlets or by glacier retreat followed by exposure of the lake bottom.
5. during the final ice retreat, lacustrine conditions prevailed over the entire region with the deposition of the final few metres of sediment at Genesee and Hugget.

## 2.4 BEDROCK GEOLOGY

The bedrock is of the Paleocene Paskapoo Formation and consists of sequences of shales, sandstone and coal seams. Prior to glaciation, the bedrock was extensively eroded and a network of channels formed the drainage system. Fig. 2.4 shows the preglacial bedrock valleys which exist around Genesee and which are now buried by glacial deposits. On the other hand, Genesee itself is probably situated within a stream trench as explained earlier.

The upper 2 to 5 m of the bedrock is weathered and fractured with a moisture content of about 30 percent and compressive strentghs of 500 to 1300 kPa. The unweathered bedrock has a moisture content of abut 12 percent and compressive strengths of 1400 to 5000 kPa. With a Rock Quality Designation of over 75 percent, the unweathered bedrock can be considered to be of good quality.

The above properties of the bedrock have been drawn from EBA (1982).

## 2.5 TILL GEOLOGY

The till layer is light grey in colour and is homogeneous as shown in Plate A.1 (Appendix A). The grain size distribution curves in Fig. A.1 (Appendix A) show that the till is predominantly silt and sand with 10 to 20 percent clay sizes and traces of gravel and coal chips; it is of low to medium plasticity (Fig. A.2). X-ray diffraction tests on the clay size (less than 2 microns) gave the following mineral composition:

| | |
|---|---|
| Illite | 30% |
| Montmorillonite | 45% |
| Kaolinite | 25% |

These data agree with those given by Pawluk and Bayrock (1969) for Central Alberta and indicate that the till was derived locally from the weak and poorly consolidated sedimentary rocks of the Upper Cretaceous and Tertiary age (Scott, 1976).

In Western Canada, the till deposits are known to contain inclusions of sorted sediments such as sand lenses (May and Thomson, 1978) and lacustrine clay layers (Acton and Fehrenbacher, 1976) whose presence must be considered in the genetic classification of the till. The till at Genesee contains similar, but of smaller extent, sand lenses and clay layers as well as slabs of ice-transported bedrock

(EBA, 1982; and Thurber, 1982b) which are also found within the glacial till deposits of Edmonton (Kathol and McPherson, 1975). These large blocks of bedrock are believed to have been plucked out and transported by the ice during glaciation.

Because of the limited data, an independent genetic interpretation of the till at Genesee is not possible. However, due to the similarity between the characteristics of the till at Genesee and those found elsewhere in the Edmonton area, reference is made to the extensive study of the till within the Edmonton district. It is to be noted that an understanding of the genesis of the till at Genesee is important in classifying the post-depositional processes affecting the lacustrine clay.

In order to avoid confusion that may arise from the large number of terms found in the literature that describe the transport and deposition of debris, the terms used by Dreimanis (1976) have been adopted. In general, glacial debris can be transported in supraglacial, englacial or basal positions and depending on the mode of deposition can be classified as an ablation or basal till. An ablation till is deposited on or from the surface of a glacier due to the downmelting of the ice. In such a case, a till that did not undergo movement but remained in place is called a melt-out till whereas one that underwent movement is called a flow till. A basal till is one that was deposited beneath a glacier by either the melt-out or lodgement processes.

Shaw (1982) found evidence that the main body of till in the Edmonton area (Hugget is one of the two sites studied) was transported in a basal position and formed by the melt-out process. Shaw based this conclusion on the following facts:

1. the normal faulting in the fluvial sand overlying the lower till and the absence of faulting in the underlying preglacial deposit at Hugget indicate that the faulting was probably caused by the melting of preserved ice from the lower till.
2. the syndeposition of till and stratified sand lenses precludes deposition by lodgement or flow.
3. the preferred orientation of fabric in the till which is related to the regional ice flow direction is not compatible with deposition by lodgement or flow.
4. the preservation of angular clasts in the till is not expected from deposition by the lodgement process.

There is evidence that the deposition of the till at Genesee was not by lodgement. Standard penetration tests throughout the entire thickness of the till at both the cooling pond and the plant site yielded blow counts that were mostly between 10 and 20 (EBA, 1982; GA, 1982 and Thurber, 1982). These results show that the till at Genesee is even less stiff than the melt-out till in the Edmonton area as reported by May and Thomson (1978). Consolidation tests on the more clayey till layers at test location UA5 show that the till is normally consolidated (Fig. 6.3, Chapter 6). From these data, it can be said that the deposition of the till was not by lodgement; otherwise, it would be stiffer and be more overconsolidated. The clay layers within the till which indicate sorting and deposition within small lakes during ablation periods and the preservation of the bedrock slabs also preclude deposition by lodgement. On the other hand, the presence of high angle slickensides (described in Chapter 3) within the Genesee Clay favours the hypothesis that at least part of the till in the study area was deposited by the melt-out process and that ice persisted during deposition of the overlying clay. Therefore, based on the studies of Shaw and the above facts, it can be concluded that the main till body at Genesee can be classified as an ablation melt-out till.

On the other hand, tube samples indicate that the top 1 to 2 m of the till might have been deposited by flow. Plate 2.5 shows the contact between the lacustrine sediment and the till; the bottom 15 cm of the sample consists of lenses of sand, silt and till within a very silty clay matrix and has the appearance of having been "disturbed" during deposition indicating probable deposition by flow.

## 2.6 GEOLOGY OF GENESEE CLAY

This section reviews the origin of hummocky topography in lacustrine clays and discusses the case of the Genesee Clay. A brief description of the clay is given in the latter part of the section and the depositional and

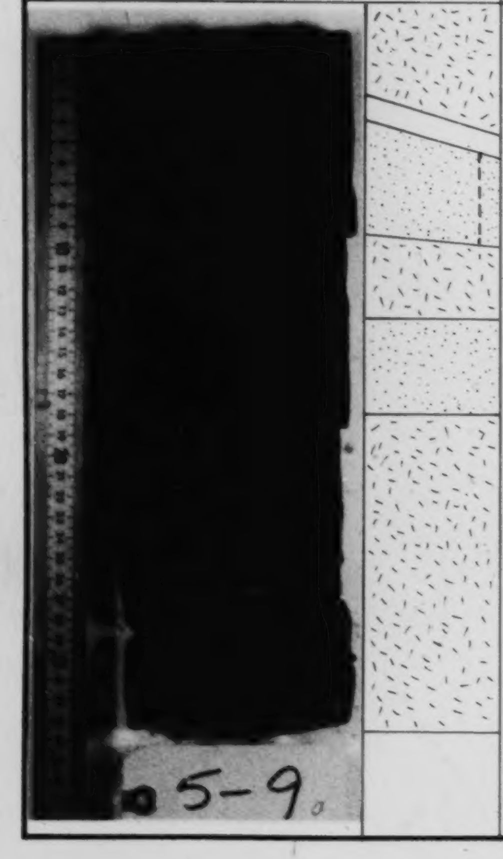

| Soil Description | Depositional Features | Structural Features | Water Content (%) w | Water Content (%) wp | Water Content (%) $w_L$ |
|---|---|---|---|---|---|
| Light grey clayey silt(till);medium plastic;occasional coal chips and pebbles | Homogeneous | | 23.6 | | |
| Dark grey clay,high plastic | Fine laminations (25° dip) | Intense minor slick along bedding,slight striations | 43.7 | | |
| Light grey silty clay,medium plastic | Fine laminations (15° dip),upward fining | Faint vertical crack, matt,planar,smooth, 100% sample area, easily separated | 40.1 | | |
| Light grey silty clay(till),low plastic | Homogeneous | | 30.8 | | |
| Light grey silty clay,medium to high plastic | 2-3mm laminations | | 41.2 | | |
| Grey clayey sand (till),low plastic, pockets of fine to medium coarse sand | Flow or slump | | 20.3 | | |

Plate 2.5 Depositional features of top 1 m of till.

post-depositional features are discussed in chapter 3.

### 2.6.1 Hummocky terrain in lacustrine clay - a literature review

Basically, a hummocky topography in lacustrine clay can be due to either a thin veneer of lake sediment reflecting the underlying hummocky disintegration moraine or post-depositional processes. In this study, only the second category will be considered as the Genesee Clay is thick enough to preclude the possibility that the surface topography is reflecting that of the underlying till. In fact, it is shown in Fig. 2.8 and 2.9 that the surface topography does not necessarily reflect that of the underlying till since a topographic high in the clay can lie above a trough in the till.

Hummocky topography in thick lake sediments has been given different names such as collapsed lake sediments (Clayton and Cherry, 1967), mounds or humpies (Odynski, 1971) and orbicular lakebed patterns (Mollard, 1983). Mollard (1983) summarised the possible post-depositional processes that could have produced such peculiar topography. In general, it is believed that the mounds have as their origin one of the following processes:

1. supraglacial deposition
2. subglacial deformation
3. periglacial processes
4. differential shrinkage or consolidation.

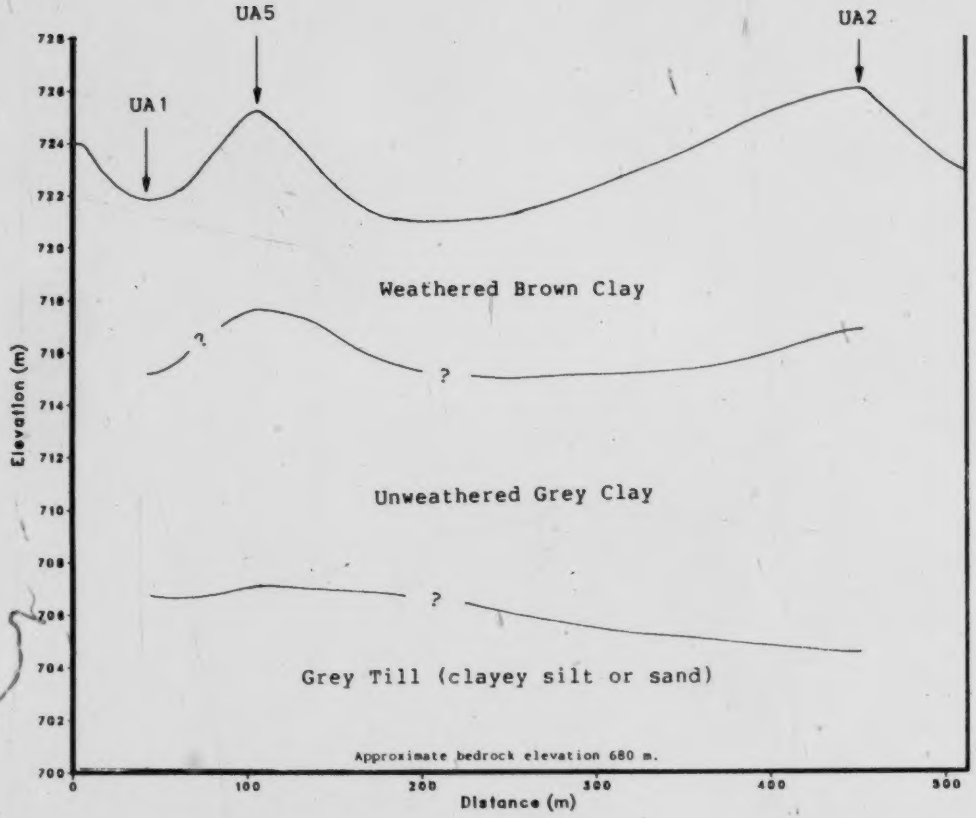
UA5
UA2
UA1
Weathered Brown Clay
?
?
Unweathered Grey Clay
?
Grey Till (clayey silt or sand)
Approximate bedrock elevation 680 m.
Elevation (m)
728
726
724
722
720
718
716
714
712
710
708
706
704
702
700
0
100
200
300
400
500
Distance (m)

Figure 2.8 Cross-section Y-Y (refer to Plate 2.2 for location).

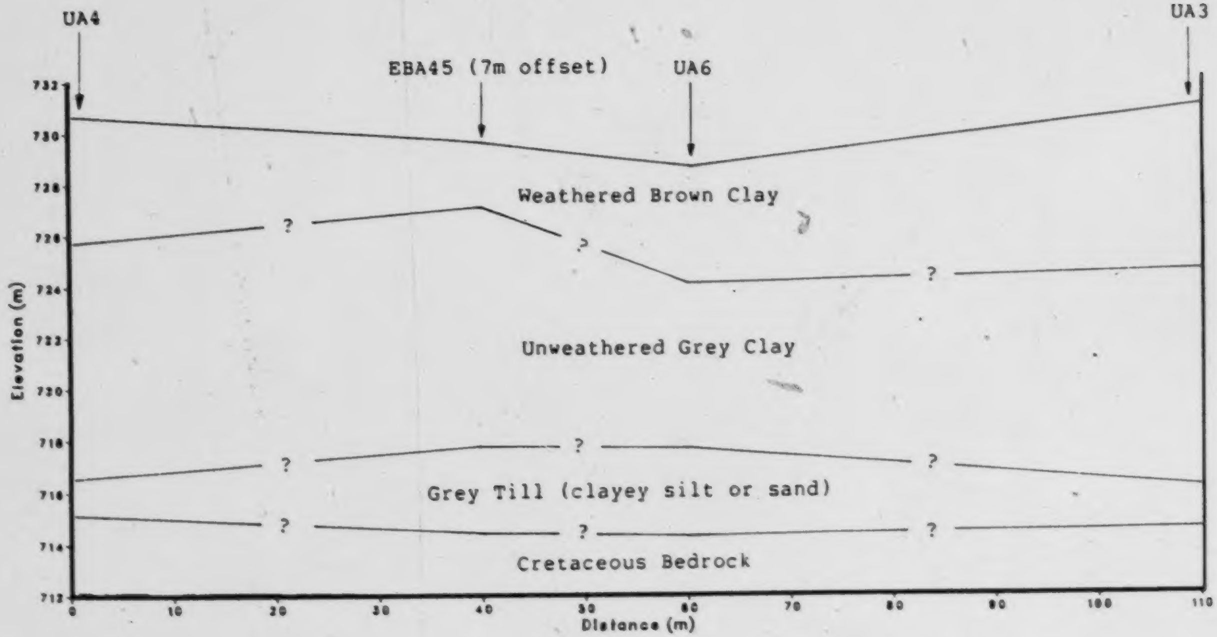
UA4
EBA45 (7m offset)
UA6
UA3
Weathered Brown Clay
Unweathered Grey Clay
Grey Till (clayey silt or sand)
Cretaceous Bedrock
?
Elevation (m)
732
730
728
726
724
722
720
718
716
714
712
Distance (m)
0
10
20
30
40
50
60
70
80
90
100
110

Figure 2.9 Cross-section Z-Z (refer to Plate 2.2 for location).

#### 2.6.1.1 Supraglacial origin

Supraglacial deposits are generally associated with till which was released at the surface of the glacier by the melt-out process; the till would normally flow as a result of reversal of topography (Boulton, 1968) and the rate of ice melting was controlled by the thickness of the drift. The various mechanisms which produced hummocky terrain in till were discussed by Gravenor and Kupsch (1959).

Clayton and Cherry (1967) were the first to report hummocky topography in thick lake sediments and attributed it to deposition within superglacial lakes formed on stagnant ice. According to Clayton and Cherry (1967), stagnant ice would stay at the bottom of the lake only if it contained enough debris to prevent it from floating and they found that a debris content of only 4.5 percent within or on the ice was required to satisfy this requirement. They also suggested that there must be an absence of active ice features for the supraglacial origin to apply.

Since the present day topography must have resulted from processes occurring after complete deposition of the clay, the buried ice blocks must have persisted for a long period. Clayton (1967) found from the geological history of North Dakota, that the stagnant ice could last for more than 3000 years. Mollard (1983) argued that the slow melting rate of the ice blocks was probably due to the temperature of the lake-bottom being close to freezing. During the melt-out of the buried ice, high pore pressures might be generated resulting in low effective stresses (McRoberts and Morgenstern, 1974) and hence, underconsolidation. Mollard (1983) believed that the formation of the mounds resulted from the loading of the soft lake clay into the underlying underconsolidated till.

#### 2.6.1.2 Subglacial origin

Hoppe (1952) suggested that till in a plastic state underneath stagnant ice could be squeezed into basal cavities or crevasses. In the case of the clay mounds, it was possible for floating ice to come to rest on the lake bottom due to the sudden lowering of the water level (Henderson, 1967). The clay, close to its liquid limit, would be squeezed sideways and upwards into basal cavities. Sangrey (1970) used this hypothesis to explain the highly distorted bedding and high preconsolidation pressures within a lake deposit near Kingston, Ontario. In such a case, it was highly probable that the floating ice would have produced scour markings and unless the ice was perfectly clear, inclusions of debris from the ice would be present in the lacustrine clay. On the other hand, Mollard (1983) found that in the Lake Agassiz clay, there were instances where the hummocky clay surface also showed ice-scoured markings but the latter seemed to post-date the processes producing the hummocky ground. Mollard also pointed out that this hypothesis does not explain the repetitive geometrical characteristics of the mounds.

#### 2.6.1.3 Periglacial origin

The ice-wedge origin was proposed by Henderson (1952). When the ground is frozen, it contracts and polygonally patterned tension cracks are formed. Ice wedges are formed in the cracks and growth of the ice wedges exerts high lateral pressures on the soil polygons which bulge into mounds. Melting of the ice wedges enhances the relief of the mounds. However, the size of the polygons would have to be unusually large to produce mounds of the sizes normally encountered. Burdick et al (1978) stated that the polygons in permafrost ground are usually less than 20 m across; this is not compatible with the size of clay mounds which are usually 100 m across.

A second postulate was proposed by Mathews (1963) who observed the mounds in lacustrine sediments at Fort St John, British Columbia and suggested a mechanism similar in nature to pingo formation. Mathews stated that the mounds were formed by movement of water saturated soil at depth instead of water alone, during the development of permafrost. This movement took place towards areas where the permafrost was thinnest. However, the existence and the mechanics of flow of a mobile soil-water mixture at the permafrost front have to be proved for this hypothesis to be valid.

#### 2.6.1.4 Differential shrinkage or consolidation

Mollard (1983) suggested this mechanism for a high plastic clay with clayey silt inclusions. With groundwater lowering and dessication, the volume of the soil was reduced by either shrinkage from a reduction of the water content to the shrinkage limit or consolidation from the high suction pressures set up. Since clay and clayey silt would change volume by a different amount under the same change in groundwater conditions, projections would result in an otherwise flat terrain. Such a mechanism cannot explain the repetitive geometrical characteristics and spatial arrangements normally encountered in hummocky terrain.

### 2.6.2 Hummocky terrain at Genesee

The preceding discussion has revealed the limitations of the various known hypotheses. However,considering the features associated with each hypothesis, it is believed that supraglacial deposition was the most likely mechanism that took place at Genesee. This is based on the fact that the airphotographs did not show ice-scour markings to suggest a subglacial origin and the Genesee Clay does not contain silt inclusions of the size that would produce relief of the order of 3 m as a result of differential shrinkage or consolidation. The periglacial origin has many difficulties in explaining the size and distribution of the mounds, Mollard (1983) also favours the supraglacial origin for the orbicular mounds which are geometrically similar to those at Genesee.

However, the main criterion to be satisfied in the supraglacial hypothesis is that the ice had to be preserved until after deposition of the clay was complete. Mollard (1983) suggested that the preservation of buried ice in sediments might have been enhanced by the cold water of the lakes. On the other hand, Clayton (1967) found that because of the insulating capacity of the sediment cover on the buried ice, the rate of melting could be reduced to less than 25 mm per year. Besides, at Hugget, Shaw (1982) concluded that ice persisted in the lower till until after deposition of a 6 to 8 m thick glaciofluvial sand and gravel layer and part of an upper till layer. Shaw inferred that cold permafrost conditions must have existed between the two glacial advances that were responsible for the two till depositions. Therefore, the conditions might have existed at Genesee whereby the ice in the underlying melt-out till was preserved until complete deposition of the clay.

Since the present surface topography of the Genesee Clay reflects the sequences in the final melting of the buried ice, Plate 2.2 shows that the formation of large depressions such as G which were due to the general melting of large ice sheets preceded that of the mounds which were due to the melting of remaining isolated ice blocks.

### 2.6.3 Characteristics of Genesee Clay

The clay deposit can be divided generally into an unweathered zone which is typically of a grey colour and an upper weathered zone which is brown or mottled brown and grey. In the low lying areas, there is a 1 to 2 m thick layer of grey clay with organic contents of less than 10 percent (EBA, 1982) overlying the weathered clay. However, this surficial clay, which is probably resedimented soil, is not of significance for the purpose of this study and has been omitted. In some instances, up to about 4 m of peat has developed on this surficial clay.

The micro and macrostructure of the weathered and unweathered clays are discussed in chapter 3.

#### 2.6.3.1 Weathered brown clay

Groundwater lowering and weathering have produced a thick stiff layer of 6 to 10 m. In some locations, there is a transition zone of 1 to 2 m of mottled brown and grey clay at the contact with the unweathered clay. The brown weathered clay is homogeneous and does not show well-defined bedding. Typically, it is made up of small angular to subangular nuggets or blocks of 2 to 5 mm, the size increasing with depth. Such features give the clay a crumbly texture. Within the brown crust, the moisture content is less than 25 percent whereas the mottled brown and grey clay has a moisture content of 35 to 40 percent. On the average, the brown clay has 50 to 70 percent clay size with the remainder being of silt

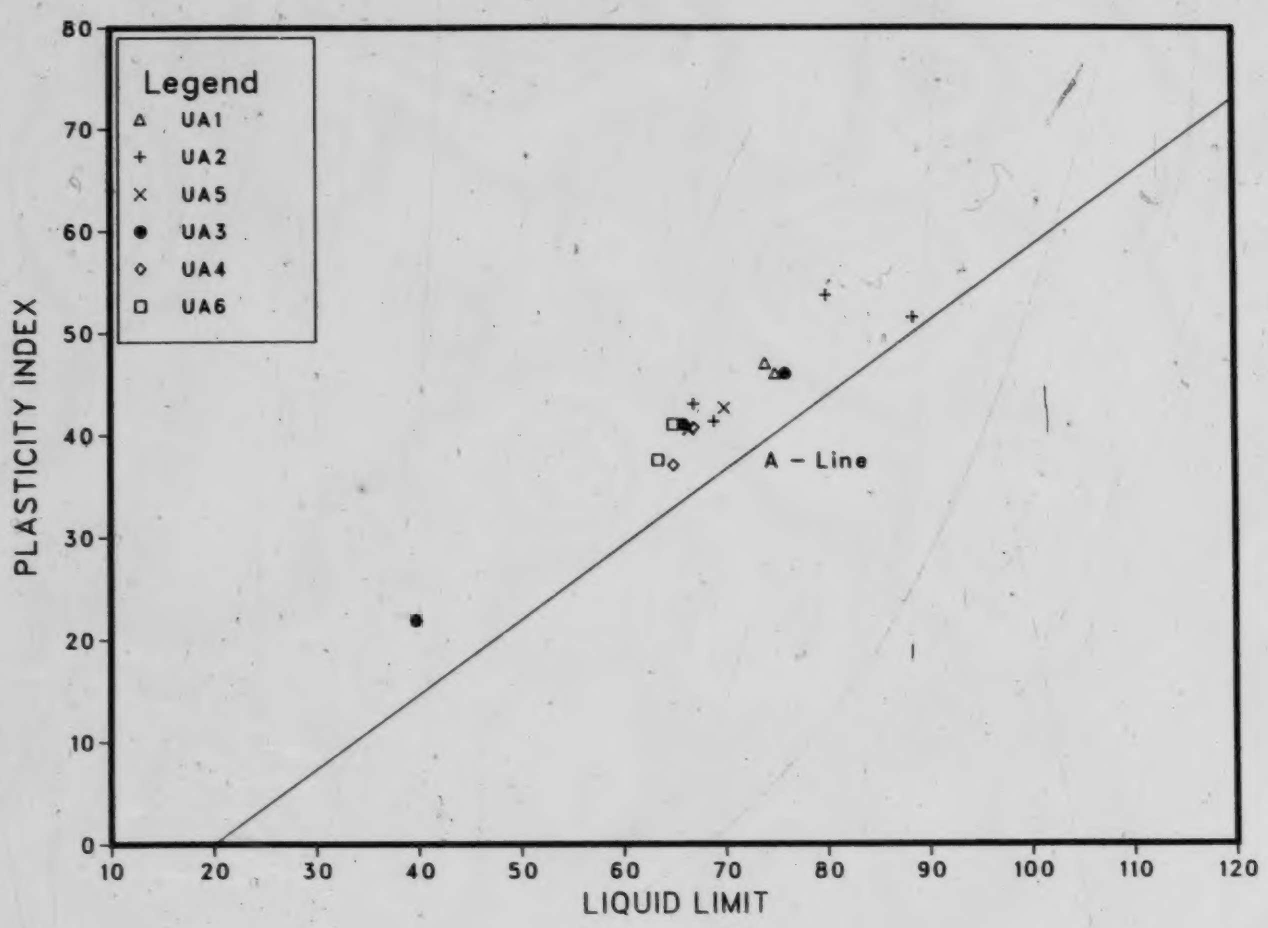

Figure 2.10 Plasticity characteristics of weathered brown clay.

size. The results of X-ray diffraction tests[1] on the clay size particles yielded the following:

| | |
|---|---|
| Illite | 50 % |
| Montmorillonite | 30 % |
| Kaolinite | 20 % |

Traces of chlorite, quartz and chlorite.

The brown clay is of medium plasticity with a Plasticity Index of 40 to 55 percent. Grain size distribution curves are given in Appendix B.

2.6.3.2 Unweathered grey clay

In general, the unweathered light grey clay in the cooling pond area is more or less homogeneous whereas at the plant site the entire thickness of the clay contains sequences of darker grey clay which are typically between 1 and 10 mm thick at a vertical spacing varying from 10 to 200 mm. The detailed sedimentology is given in Chapter 3.

Grain size analyses show that the light grey clay has between 55 and 65 percent clay size with the remainder being silt. The dark grey clay has between 65 and 80 percent clay size. The clays have Plasticity Indices of 30 to 50 percent and 60 to 80 percent respectively and are inactive with activity of 0.7 to

---

[1] All X-ray diffraction tests were performed and interpreted by the Alberta Research Council, Edmonton.

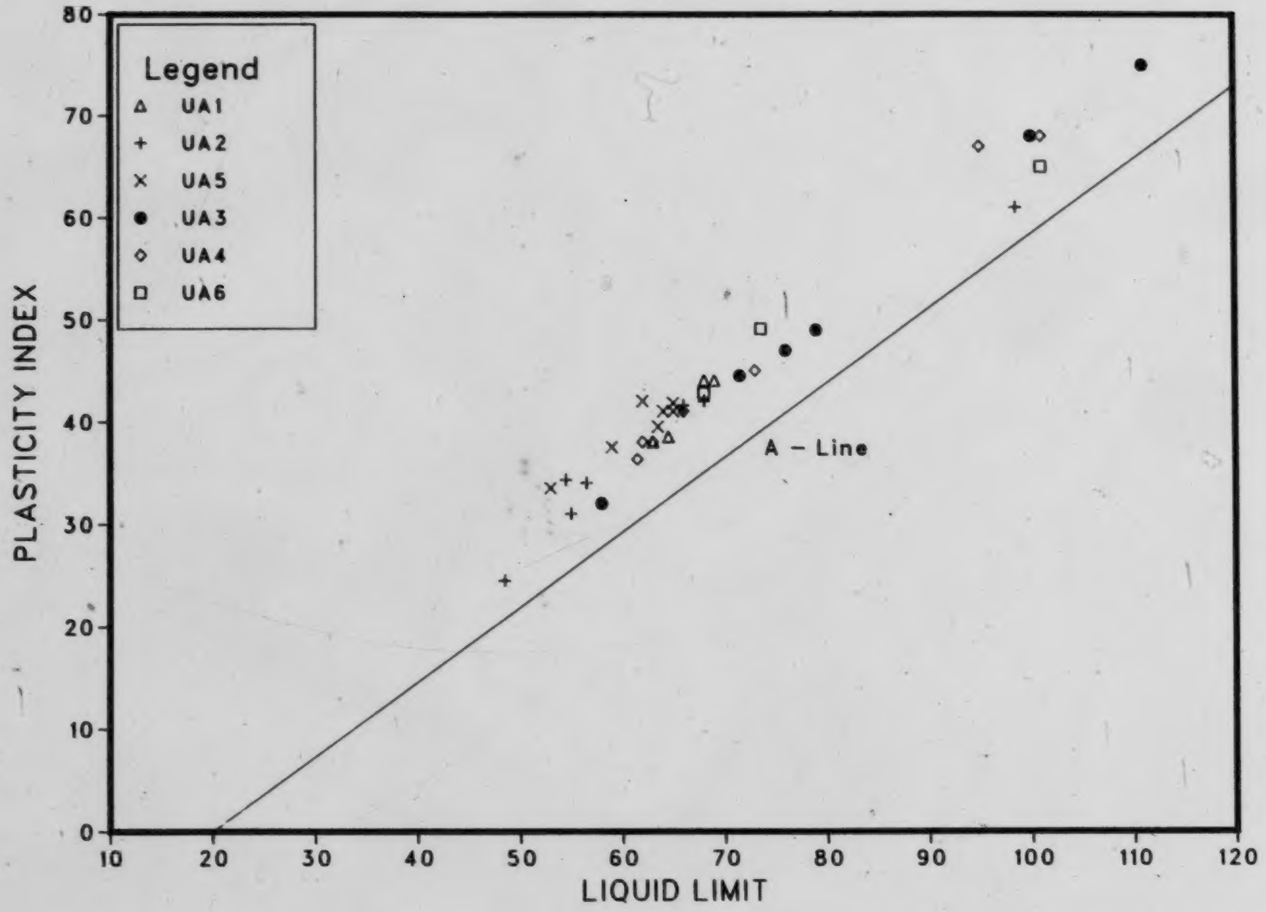

Figure 2.11 Plasticity characteristics of unweathered grey clay.

0.9.

Both clays have approximately the same mineral content namely:

| | |
|---|---|
| Illite | 40 % |
| Montmorillonite | 30 % |
| Chlorite | 10 % |
| Kaolinite | 20 % |

Traces of calcite, dolomite, feldspar and quartz.

Since the clay is highly fissured it is classified as a fissured medium to high plastic silty clay.

Grain size curves are given in Appendix B.

## 2.7 GROUNDWATER CONDITIONS

Based on piezometer readings as well as data from the consultants, the groundwater levels are at ground surface at the plant site and 2 to 5 m below the ground surface at the cooling pond. The lower water table at the latter site may be due to drainage by the Genesee Creek. There is no indication that artesian pressures exist. The groundwater flow in a hummocky disintegration moraine was studied by Meyboom (1966) but because of the low relief of the mounds at Genesee, the local groundwater flow pattern is not of engineering significance.

# 3. MACRO AND MICROSTRUCTURES OF GENESEE CLAY

## 3.1 INTRODUCTION

In this study, the generally accepted definitions found in the geotechnical literature (for example, Morgenstern (1967a)) for soil structure have been adopted. Macrostructures are discontinuities such as bedding planes, fissures, and shears or slickensides which can be observed by the naked eye whereas microstructures are features that can be recognised only through high magnification. Discontinuities are defined as the small features that divide an otherwise continuous mass of soil (Fookes and Denness, 1969). These discontinuities arise from both depositional and post-depositional processes and their identification and classification are necessary for understanding the geological history as well as the engineering behaviour of a deposit.

The studies of soil structure for the purpose of geotechnical engineering were carried out by researchers along the following lines:

1. Origin of discontinuities. Skempton and Northey (1953) explained the formation of fissures as a result of syneresis; Skempton (1966) discussed the formation of major and minor shear surfaces as a result of tectonic processes; the role of weathering in producing fissures was considered by Skempton et al (1969) and the minor shears in the London Clay were probably caused by high

lateral stresses as a result of erosion and weathering (Skempton, 1961). Fookes (1965) mentioned that unsheared discontinuities might be modified by later movements giving them polished or slickensided surfaces. The classification and characteristics of discontinuities according to their environment and mode of origin were summarised by Chandler (1973).

2. Description and classification of discontinuities. In general, the stages in classifying discontinuities consist of grouping similar features and relating the latter to each other within each independent group and of determining the relationship between the independent groups. The aim of this exercise is to classify discontinuities according to their mode of formation. Detailed classification schemes were suggested by Fookes and Denness (1969) and McGown et al (1980). The two approaches are basically similar although they might differ in specific details; in addition, McGown et al (1980) suggested methods for the quantitative evaluation of the engineering significance of the discontinuities.
3. Microstructural changes due to shearing. The studies of Morgenstern and Tchalenko (1967) have contributed largely to the understanding of the microscopic arrangements of clay platelets in sheared zones.
4. Effects of soil structures on engineering properties of a soil mass. Terzaghi (1936) drew attention to the weakening effects of discontinuities in stiff clays.

Skempton and Petley (1969) showed that the strength along discontinuities could be less than that of the intact soil. Skempton (1964) argued that, besides being planes of weakness, discontinuities could also act as stress concentrators. The influence of structural discontinuities on the other engineering properties such as compressibility and permeability of clays depends on their extent, distribution and most importantly on their porosity. On the other hand, layering, such as in varved clays, is the cause of anisotropy in the properties of these soils as discussed by Kenney (1976). The effects of test specimen size when dealing with fissured material were discussed by Bishop and Little (1967) and Rowe (1972) amongst others.

During the study of the Genesee Clay, numerous depositional and structural discontinuities were observed; this chapter will present a simplified descriptive scheme used for the logging of the clay samples as well as a discussion on the origin of the discontinuities. The effects of the latter on the engineering behaviour of the Genesee Clay are discussed in Chapter 6. For this study, the soil fabric was observed from 76 mm Shelby tube samples.

## 3.2 MACROSTRUCTURES

The macrostructures have been divided as sedimentary or depositional and structural following the terminology used by Skempton and Petley (1967); they are discussed separately in this section.

### 3.2.1 Method of investigation

The procedure adopted to study the macrostructures followed that recommended by Marsland et al (1982) and consisted of the following:

1. The soil sample was first observed by removing two thin slices (one perpendicular to the other for a three dimensional picture) of soil by means of a thin wire to expose unsmeared surfaces. Attention was paid to contrasting tones and textures which were normally indicative of bedding. In most instances,a major shear plane (one that had undergone large movement) could be detected at this stage.
2. The sample was then split into two halves. From the exposed surfaces, the nature of the contact between the layers was better defined; the internal structure of the layers and the discontinuities were easily recognised. In some cases, thin laminae were visible only after some drying had taken place. After the process of identification, description and measurements, samples were taken from the layers for moisture content determination and classification tests.

### 3.2.2 Depositional features

The transport and deposition of sediments into glacial lakes were discussed extensively by Kenney (1976). The significant characteristic of glacial deposits is their laminated nature and the term "varves" is used to describe the seasonally deposited laminae. Kenney (1976) also reviewed the role of lake currents such as turbulent gravity currents, interflows and overflows in the processes of varved clay deposition.

The Genesee Clay itself is not made up of the regularly spaced laminae as in classical varves and its deposition seems to have been influenced by frequent fluctuations in the depositional environment producing irregular layering. Therefore, in order to reconstruct the depositional history, it is necessary to log carefully the sedimentary units. A sedimentation unit, which normally reflects deposition under more or less constant physical conditions, is bounded by planes which represents stages of erosion, non-deposition or abrupt change in depositional conditions. These planes are recognisable because of some textural or compositional change from one sedimentation unit to the other. Therefore, a sedimentation unit yields information as to the environment operating during a certain period of time whereas the bounding plane represents a change in depositional environment. Consequently, the objective is to identify changes in depositional setting through the recognition of the sedimentary units.

#### 3.2.2.1 Descriptive scheme

The sedimentation unit is commonly known as a bed or lamina and the bounding planes are known as bedding planes. In the geological literature, there is disagreement over the differentiation of a bed from a lamina. Campbell (1967) discussed this problem extensively. However, in the present study, a bed will be considered to be a sedimentation unit which is thicker than 1 cm and a lamina as a unit which is less than 1 cm. This classification which is based on the bed thickness, was also adopted by Collinson and Thompson (1982) although Campbell (1967) argued that the differentiation between bed and lamina should be made on the basis of genesis. However, a bed can be made up of laminae which are produced as a result of some minor fluctuations in the environment during sedimentation of a bed. In the Genesee Clay, very thin (less than 1 mm thick) layers of sands or silts are occasionally found between beds and they are generally discontinuous. These are described as partings following the suggestion of Campbell (1967). It is to be noted that Marsland et al (1980) suggested descriptive terms to be used in the logging of layered soils and which are also based on the dimension of the sedimentation units. The dimensions used to classify the units are slightly different than those found in the geological literature; for example, a lamina is a unit between 0.5 and 5 mm thick. Since the terminology used is subjective, it was decided to retain as far as possible the definitions commonly found in the geological literature.

In describing the Genesee Clay, the following sedimentary features will be considered, namely, bedding planes, geometry and internal structure of the bed and soil composition of the bed.

The characteristics that were observed are as follows:

1. **Bedding plane**
   a. **Geometry.** The bedding plane can be "even, wavy and curved" following the definitions of Campbell (1967). In the Genesee Clay, the majority of the bedding planes are even so that their classification has been omitted from the soil logs; only wavy and curved bedding planes are classified when they occur.
   b. **Inclination.** This is given with reference to the horizontal.
   c. **Nature.** Where there are signs that the bed underwent erosion, the bedding plane is described as "erosional".
2. **Bed.**
   a. **Thickness.** In addition to the differentiation between bed and lamina discussed earlier, the laminae have been defined as "fine" when they are less than 1mm thick which is the most common case for the Genesee Clay.
   b. **Internal structure.** The terms used are:
      1) homogeneous - there are no visible

laminations.

2) laminated - laminae are parallel to bedding planes.

3) cross-laminated - laminae are inclined to bedding planes.

4) contorted - laminae are deformed relative to the original depositional plane. In most cases, the contortions are in the form of swirled laminae similar to those found in Winnipeg clays as described by Baracos (1977). It is to be noted that contorted beddings are penecontemporaneous rather than depositional features.

5) gradational - there is a change in the grain size from the lower to the upper bedding plane.

6) lenticular - lenses of limited lateral extent are visible.

3. **Soil description.**

Routine procedures such as those found in ASTM (1980) Designation D2488 were used for the visual description of the soil.

### 3.2.3 Examples of depositional features in Genesee Clay

In this section, typical features are described and illustrated; the logs of all the samples can be found in Appendix C.

#### 3.2.3.1 Sample 2-10 (Plate 3.1)

The sample shows the lenticular laminae of silt within a clay matrix; the laminae are also contorted. The lenticular bedding probably represents deposition of silt by turbidity currents alternating with deposition of clay under slack water conditions.

#### 3.2.3.2 Sample 4-9 (Plate 3.2)

This sample represents depositional sequences about 1 m above the till surface. The changing depositional environment is reflected in the layering of the clay; the dark grey clay is highly plastic (Plasticity Index greater than 65 percent) and has a clay content of about 80 percent whereas the light grey clay is of medium plasticity (Plasticity Index of about 40 percent) with about 50 percent clay sizes. The bedding is irregular with thick beds of the light grey clay and the transition between beds is sharp and abrupt. Slumping was prominent as indicated by the lenses of silt, sand or till within the clay beds and by the contorted beddings of the uppermost light grey clay. Shearing occurred along some of the bedding planes as indicated by the polished slickensides.

#### 3.2.3.3 Sample 6-6 (Plate 3.3)

This sample represents the depositional sequences of the main body of the unweathered clay layer at the plant site. Again, the alternate sequences of dark and

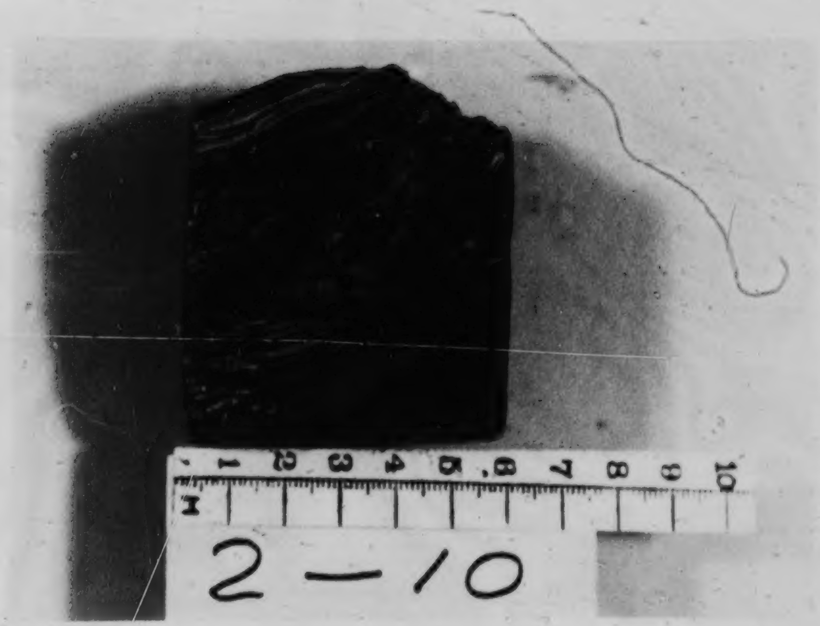
1 2 3 4 5 6 7 8 9 10
2—10

Plate 3.1 Lenticular laminae of silt within clay matrix-sample 2-10.

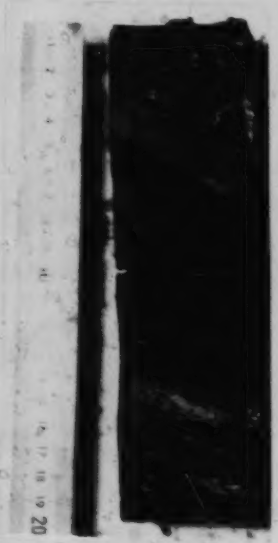

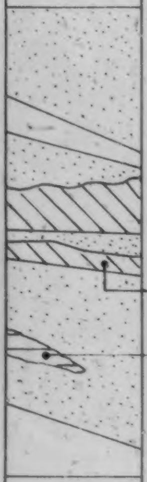

| Soil Description | Depositional Features | Structural Features | Water Content (%) w | $w_P$ | $w_L$ |
|---|---|---|---|---|---|
| Light grey clay, medium plastic, with swirlings of white silty clay | Contorted | | 38.6 | | |
| Dark grey clay, medium to high plastic | 40° dip bedding plane<br>Fine laminations | Bedding plane is polished no striations | 38.6<br>54.4 | | |
| Light grey clay, low plastic | Wavy bedding plane | | 23.3 | | |
| Medium dark grey clay, high plastic | Homogeneous | | 56.2 | | |
| Light grey clay, silty, low plastic | Erosional contact | | 29.0 | | |
| Medium dark grey clay, high plastic | Fine laminations | Intense minor slickensides along beddings | 59.8 | | |
| Sand lens, coal particles | | | | | |
| Light grey clay, medium plastic, silt partings | Lenticular laminae of silt | | 39.9 | | |
| Dark grey clay, high plastic | Fine laminations | Intense minor slickensides along beddings | 61.0 | | |

Plate 3.2 Depositional sequences in bottom 1 m of clay - sample 4-9.

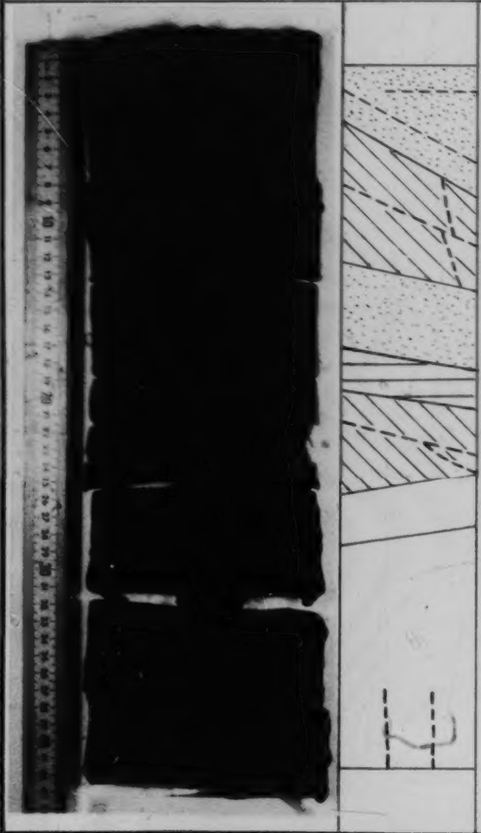

| Soil Description | Depositional Features | Structural Features | Water Content (%) | | |
|---|---|---|---|---|---|
| | | | w | $w_P$ | $w_L$ |
| Light grey clay, medium plastic | Homogeneous | Minor slickensides(30mm) no striations,horizontal<br>Major fissure,matt,partly smooth,otherwise flaky, easily separated,40° dip | 38.5 | 25 | 68 |
| | 50° dip bedding plane | | | | |
| Medium dark grey clay, medium to high plastic, with silt partings | Fine laminations, 40°-50° dip<br>30° dip bedding plane | Major slickenside,slight striations,along bedding 50° dip<br>Minor slickensides,matt, smooth,subvertical | 52.0 | | |
| Light grey clay, medium plastic | Homogeneous | | 44.2 | | |
| Fine sand | | | 18.9 | | |
| Medium dark grey clay, medium to high plastic | Fine laminations | Intense minor slickenside along beddings<br>Major slickenside,no striations,along bedding 30°-40° dip | 50.3 | | |
| Dark grey clay, high plastic | Laminated | Intense minor slickensides along beddings | 51.2 | | |
| Dark grey clay, high plastic, with silt partings along beddings | Fine laminations | Few minor slickensides along beddings<br>Minor fissures,matt, smooth,subvertical | 47.4 | 36 | 101 |

Plate 3.3 Depositional sequences in unweathered clay - sample 6-6.

light grey clay can be recognised. Although the darker grey clay tends to be slightly more plastic, there are at times only very slight differences in the plasticity of the dark and light grey clay; on the average, the Plasticity Index is 40 to 45 percent. Therefore, unless the samples are allowed to dry for a few hours as it is the case for this sample, the clay may have a homogeneous appearance. The thickness of the beds is variable and the bedding planes can have inclinations of up to 50 degrees. The internal laminated structure is dependent on the plasticity of the material forming the beds. The darker grey clay generally tends to be finely ( less than 1 mm thick) laminated whereas the less plastic light grey clay has no visible laminations and is homogeneous.

#### 3.2.3.4 Sample 5-3 (Plate 3.4)

Near the top of the unweathered zone, the clay tends to be mottled although there is no indication that the mottling is due to the effects of weathering. The clay has a disturbed internal structure which is similar to one induced by bioturbation. However, this type of structure may also be due to slumping.

### 3.2.4 Structural features

The post-depositional features of interest in this study are the fissures and shears which can cause weakening of the clay mass; they can originate from various

Plate 3.4 Mottled appearance of top of unweathered clay - sample 5-3.

environments and both their distribution and orientation reflect their mode of formation (Fookes and Denness, 1969). Shears were formed from relative movements between two surfaces whereas the characteristics of fissures are indicative of brittle fracture. In the case of Genesee, the discontinuities originated from penecontemporaneous slumping, differential movement within the till and weathering. These structural features are described according to a scheme presented below; typical examples are discussed in section 3.5. The logging of all samples is given in Appendix C.

#### 3.2.4.1 Descriptive scheme

Fookes and Denness (1969) identified six essential components in the description and classification of a sheared or fissured system. They are classification, size, surface geometry, surface markings, fabric and intensity. This guideline was also used by McGown et al (1980). For the present study, the scheme of Fookes and Denness has been modified for the logging of the tube samples. It should be noted that from the latter, information on the extent of discontinuities is very limited.

The following descriptive scheme is used:

1. **Type of discontinuity.** Two types have been encountered, namely, shears and fissures. Because of the polished appearance of the shears, the term "slickenside" is used.

2. **Size.** The discontinuities have been divided into two classes:
   a. Major - feature covers 100 percent of Shelby tube sample area (about 45 $cm^2$ in plan area).
   b. Minor - feature is less than the sample area.
3. **Surface geometry.** The majority of the discontinuities are planar with the exception of a few undulating ones. Therefore, only these two terms will be used.
4. **Surface markings.** The shears are normally polished and can be divided into three classes:
   a. Highly striated.
   b. Slightly striated.
   c. Unstriated.

   The fissures normally have matt surfaces and can vary from a plumose or flaky to smooth appearance. Examples of these fissures are illustrated in section 3.5.
5. **Orientation.** This is measured relative to the horizontal. The orientation is also given in terms of whether the fissure is along or across bedding.
6. **Intensity.** The intensity classification as proposed by Fookes and Denness (1969) is intended for determining the number or surface area of the discontinuities contained per unit volume of soil. In the case of tube samples, it is not possible to use such a classification system as the extent of

the features cannot be determined. Therefore, any statistical interpretation is of limited application. In the present case, a qualitative description is given. For example, the minor slickensides or fissures tend to be numerous and in this case, they are described as "intense" when there are more than 5 features per cm of the tube sample; otherwise, the number of features is given. The major slickensides or fissures are single discontinuities and their spacings are shown in the logs (Appendix C).

## 3.3 MICROSTRUCTURES

### 3.3.1 Method of investigation

The various methods of studying soil microstructures were reviewed by Tovey and Wong (1973). In this study, the scanning electron microscope (SEM) was used because of its high resolution for studying the grain arrangements.

The sample preparation consisted of trimming an undisturbed sample to about 1 cm square in cross-section and 3 to 4 cm in length. The sample was slightly notched at the planes where fractures were required. The sample was then frozen in liquid nitrogen and fractured along the notches producing a 1 cm cube specimen. The ice in the pores of the soil was removed by vacuum sublimation at -50 °C. The freeze-drying method has the advantage of minimising the drying shrinkage (Tovey and Wong, 1977); other methods of drying specimens are given by Gillott (1969). The specimen was then glued to a metal stub with silver paint and sputtered with gold to make the fractured surface electrically conductive. The Cambridge Stereoscan 250 of the Department of Entomology, University of Alberta, was used to view the specimens.

### 3.3.2 Examples of microstructures in Genesee Clay

The scanning electron micrographs which will be shown are for vertical fractures with the top of the micrographs representing the top of the specimen. Both the unweathered and weathered clays are described.

The SEM studies have given some insight into the particle arrangements within the Genesee Clay. Different types of particle arrangement were noted and are presented in this section. The main body of the clay which is light grey has an open flocculated structure (Plate 3.5(a)). The particle arrangement consists of individual particles forming face to face aggregations which in turn have face to face or edge to face contacts; the random particle orientation is an indication of the isotropic nature of the fabric. The flocculated structure of the Genesee Clay is consistent with the fabric of other glacial-lake clays (Kenney, 1976). However, the actual mechanism for the formation of a flocculated structure in glacial-lake clays is not fully understood. Kenney (1976) suggested that

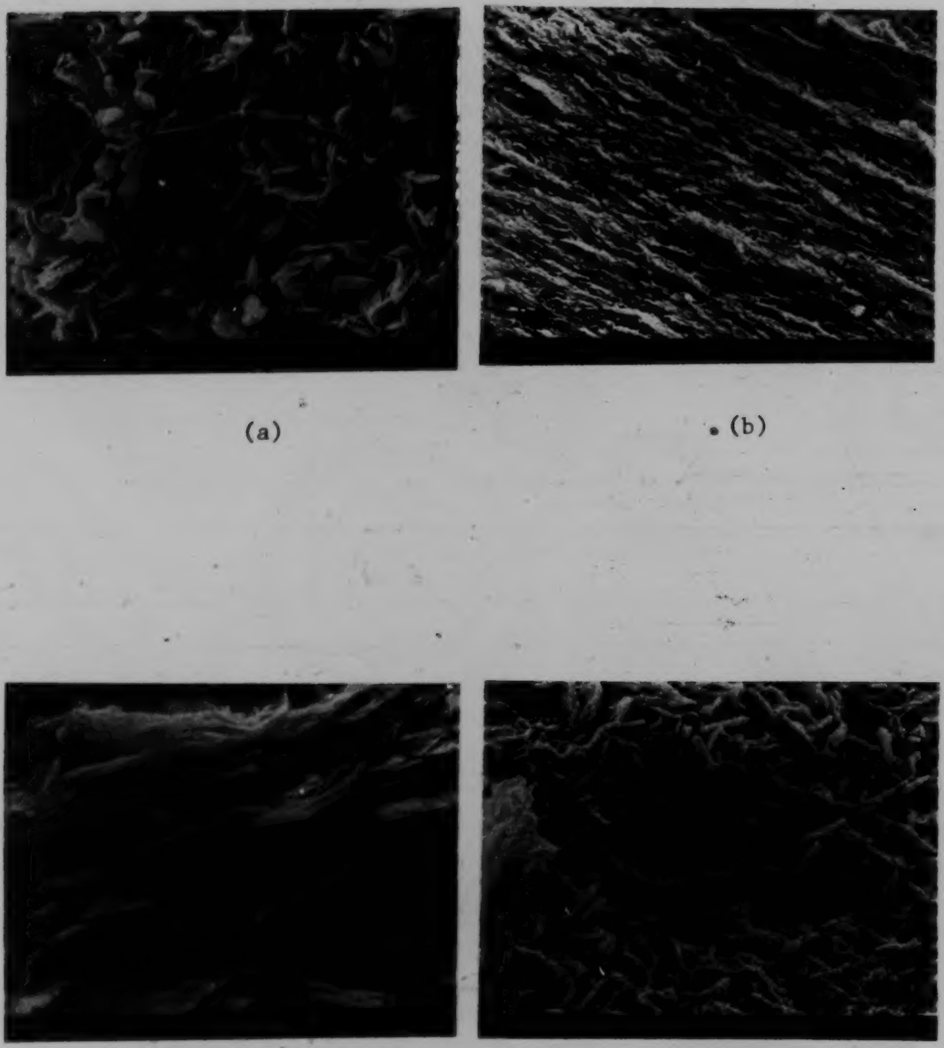

(a) (b)

(c) (d)

Plate 3.5 (a)Open flocculated structure-light grey clay
(b)Dispersed structure - dark grey clay
(c)Magnification of (b)
(d)Honeycomb structure.

because of the small sediment concentrations in glacial lakes, it is unlikely that significant flocculation occurred within the body of the lake water and proposed the hypothesis that flocculation occurred at the sediment surface.

On the other hand, the high plastic clay beds have a particle arrangement which shows a strong preferred orientation along the direction of the bedding (Plate 3.5(b) and (c)). Plate 3.5(b) shows two levels of grain arrangement. The individual clay platelets form compact laminae with relatively large voids between the laminae. This type of arrangement contributes to the high water content and compressibility of the dark grey clay as shown in Chapter 6. The strongly oriented arrangement is likely to be a depositional feature since the silt grain in the centre of Plate 3.5(c) had distorted the clay particles below it but not those above it; any post-depositional effects, such as shearing, causing the strong particle orientation would have resulted in the moulding of the clay platelets around the silt grain. The fissile appearance of the high plastic clay is consistent with the preferred orientation of the clay platelets. The difference in the soil fabric of the light grey clay and that of the dark grey clay cannot be explained readily since both clays have approximately the same mineralogy (see section 2.6.3). Quigley and Ogunbadjo (1972) argued that the high degree of in-situ parallelism may be due to the high rate of sedimentation resulting in a faster consolidation. Under these conditions, the initially flocculated structure could collapse before the development of Van der Waal's and cementation bonds. However, this mechanism does not satisfactorily explain the dispersed arrangement in the dark grey clay beds at Genesee. The dark grey clay which has a higher clay content than the light grey clay had a slower sedimentation rate. On the other hand, O'Brien (1968) observed similar particle parallelism in black shale and suggested that the existence of certain organic anions could have promoted the dispersion of clay suspensions by neutralising surface charges. Consequently, in the case of the Genesee Clay, there is the possibility that, during deposition, the dispersion of the clay particles within the dark grey layers was caused by the presence of organic material; the dark grey colour probably indicates a higher content of fine grained organic matter which was derived from the shale of the Cretaceous bedrock.

The honeycomb structure in Plate 3.5(d) shows the role of mineralogy in controlling grain arrangement; the difference in mineralogy is evident from the micrographs. However, the honeycomb structure can be considered a rare feature within the Genesee Clay as it was found in only one of the specimens observed. This structure is likely to collapse during consolidation of the sediments although some might be preserved by the arching of the surrounding particles. The other type of structure is the compact particle arrangement of a silty clay layer in Plate 3.6(a).

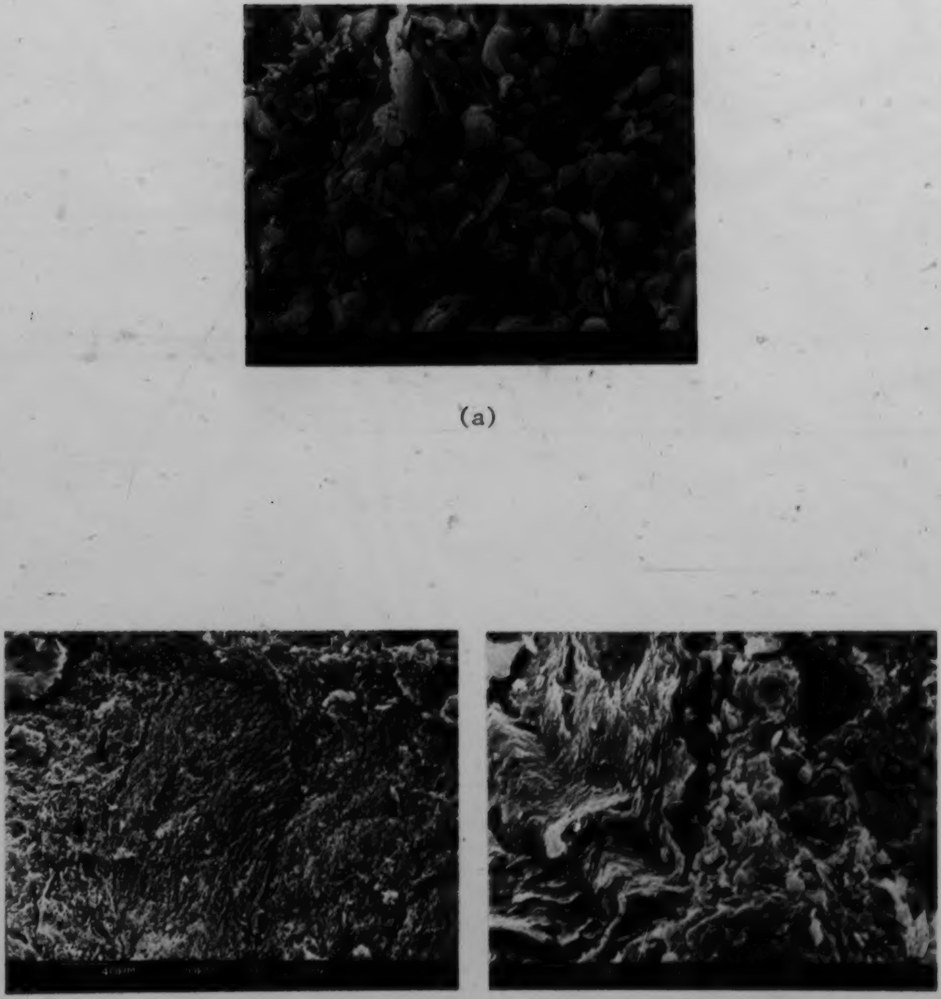

(a)

(b) (c)

Plate 3.6 (a) Compact arrangement of silty clay
(b) Micronodule in weathered clay
(c) Clay particles wrapping micronodules.

The structure within the weathered brown clay is shown in Plate 3.6(b) and (c). It has been found that the clay consists of intact lumps, as indicated by the preserved distinct particle orientation, surrounded by randomly oriented particles. In Plate 3.6(b) , the clay lump seems to have rotated through 90 degrees assuming that the initial orientation of the freshly deposited particles was horizontal. Plate 3.6(c) shows that the lumps are wrapped by an "onion skin" of clay particles (see the left of the micrograph); in this micrograph the intact clay had been plucked out during sample preparation. These micrographs show that the process of weathering took place by the disintegration of the clay into small blocks and that the clay matrix surrounding the blocks was remoulded and possibly resedimented from the drying and wetting action. There is also a difference between the particle arrangement within the remoulded clay and that within the intact material. There is a higher occurrence of stacked platelets in the remoulded matrix as shown in Plate 3.6(c).

The conclusion to be drawn from this study is that although the main body of the Genesee Clay is of high compressibility because of its open structure it does not display an unstable or collapsible structure.

## 3.4 DISCUSSION OF DEPOSITIONAL FEATURES

The predominance of fine grains in the Genesee lacustrine deposit indicates deposition beyond the limit of delta growth (section 2.2). During the initial deposition of the clay, the till surface which was hummocky as a result of its melt-out origin probably promoted the generation of turbidity currents within the depressions. As a result, lenticular laminae such as those shown in Plate 3.1 were produced. Initial deposition of the clay also occurred with the simultaneous release of soil from the till as a result of slumping. This is evident from the presence of till lenses such as that shown in Plate 3.2 within the bottom 1 to 2 m of the clay layer. Generally, the beds within this layer have a higher sand and silt content as shown in Fig 6.1 to 6.5 of Chapter 6. Deposition proceeded by the sedimentation of alternate beds of dark grey and light grey clays. Grain size analyses of the clay layers show that even the light grey clay, which represents periods of higher sediment concentration in the lake, contains more than 50 percent clay size indicating deposition by generally low-density currents. The colour changes reflect a grain size difference even though this may be slight. The thickness of the beds is very irregular as shown in Plate 3.3 varying from a few mm to about 200 mm. Generally, the dark grey clay tends to be the thinnest with thicknesses of 1 to 10 mm. Partings of sand or silt are commonly found along the bedding planes of the dark grey clay. The internal structure of the beds vary from very fine (less than 1 mm) laminated in the case of the dark grey clay of high plasticity to homogeneous and structureless for the less plastic light grey clay. The finely laminated and fissile appearance of the dark grey clay is reflected by the preferred orientation of the clay particles in the direction of the bedding.

The presence of rather thick beds and the lack of regularity in the sedimentation units suggest that deposition occurred under very frequent fluctuations in the lake conditions in terms of sediment supply. Moreover, higher sedimentation rates might have caused some minor slumping which formed the thick beds. The other characteristics that were associated with slumping are the high angle bedding planes of up to 50 degrees commonly observed in the Genesee Clay. Although penecontemporaneous slumping contributed to this feature, it is believed that later distortion of the soil as a result of deformation in the underlying till could have affected the inclination of the bedding planes.

On the other hand, while the layering is more visible at the plant site, the composition and texture of the beds at the cooling pond differ only slightly so that the clay is more or less massive with the exception of the bottom 1 to 2 m which is interbedded. This difference in the sedimentology between the two areas can be explained by referring to the sedimentation studies of Smith (1978) in Hector Lake, Alberta. Smith concluded that although layering could be found near the inlet delta, the layers decreased rapidly with distance becoming thin laminae or massive clays about 2 km from the inlet. According to Quigley (1980), this phenomenon is typical of postglacial lakes where the suspended sediment loads are low in the streams which enter the lakes as low density currents. The latter are inefficient for the sediment transport so that most of the coarser grains are not transported very far. Therefore, the area of the present plant site was probably closer to the sediment source than that of the cooling pond.

There are some indications that the clay was deposited in at least two sequences and that the lake bottom was most probably exposed between sequences resulting in the formation of stiff crusts with high overconsolidation ratios. These crusts are sandwiched between more or less normally consolidated clays. This is shown in Fig. 3.1 where a crust exists at about 13 m below ground level at UA2 in the cooling pond and at 14 m at the test locations in the plant site. Another observation is that just above this crust at the plant site, the clay contains layers or pockets of "till-like" deposit or very silty clays (refer to borehole log for UA6 in Appendix C); the presence of similar "till-like" layers at approximately the same depth was reported by EBA (1983) at another location in the plant site. These "till-like" layers indicate a major readvance of the ice with the subsequent release of ice-rafted sediments

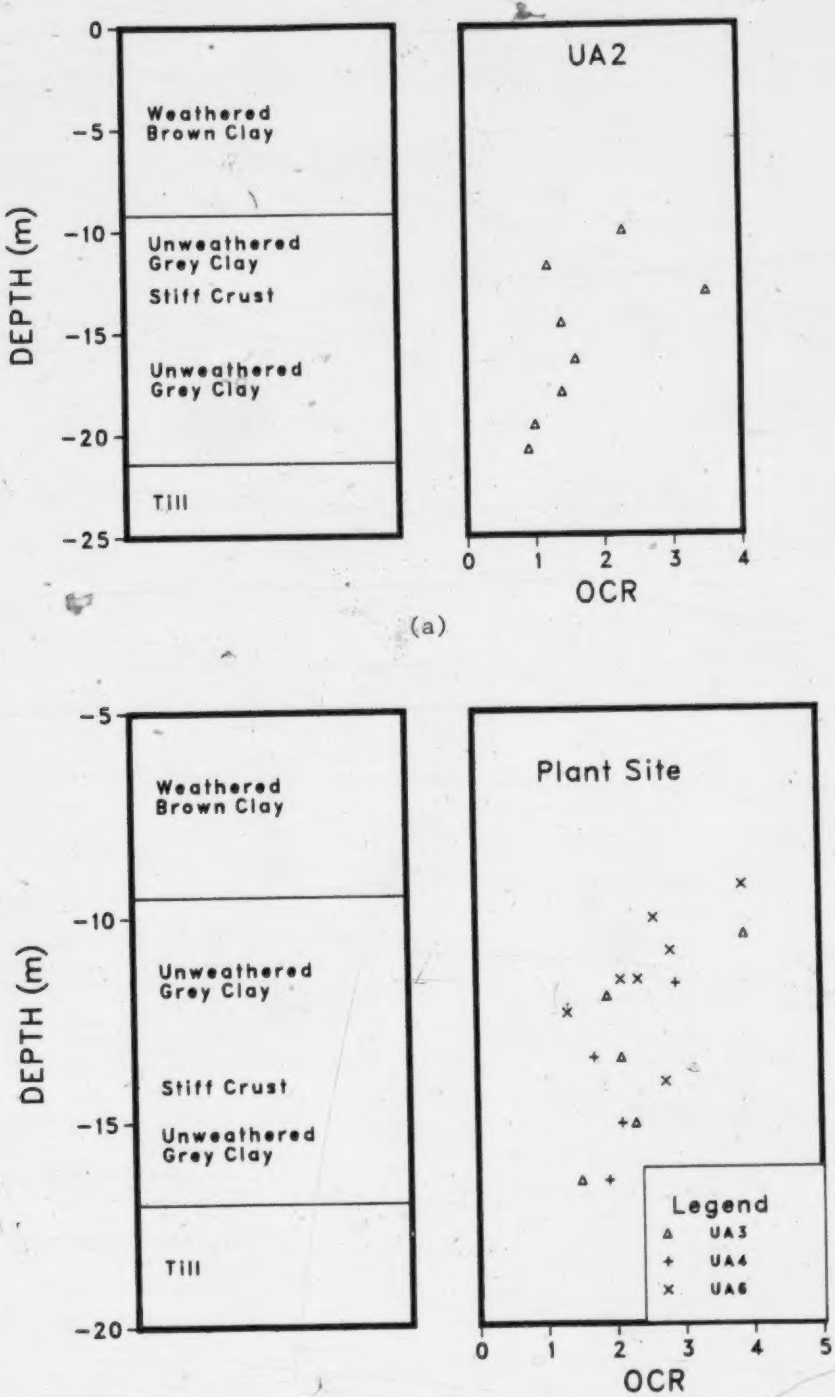

(a)

(b)

Figure 3.1 Variation of OCR with depth at (a) UA2 (b) plant site.

in the lake. Consequently, the level of the Genesee Lake was controlled by the cycles of the glacier ice retreat and advance which closed and opened the drainage outlet as discussed in the previous chapter. Similar observations had been reported for glacial Lake Agassiz by Quigley (1980). There are indications that large fluctuations in the level of Lake Agassiz were caused by the opening and closing of the Superior outlets by ice retreats and advances. These fluctuations resulted in the formation of intermediate stiff crusts within the main body of the Lake Agassiz clay as a result of the exposure of the lake bottom.

Therefore, it can be concluded that the Genesee Clay was deposited under fluctuating sedimentological conditions resulting in irregular layering which is in contrast to that of classical varved clays. Deposition was also interrupted by the opening of the drainage outlet of the Genesee lake resulting in the complete drainage of the lake; this caused drying of the lake bottom resulting in the formation of intermediate stiff crusts within the soft clay. The lake was flooded again when the outlet was closed by the ice readvance which was inferred from the presence of ice-rafted deposits. There was also no indication of large scale erosion during or after deposition of the clay.

## 3.5 DISCUSSION OF STRUCTURAL FEATURES

The post-depositional processes will be discussed on the basis of the macrostructures that have been encountered in the Genesee Clay. The macrostructures of interest are the features that were formed mainly during three stages that can be classified as follows:

1. Shortly after deposition. The discontinuities are mainly randomly oriented minor shears.
2. During physical weathering. The fissures are mainly subvertical and subhorizontal and can be very intense so that the clay has a nuggetty or blocky appearance. As discussed earlier, the physical weathering occurred during the intermittent exposure of the lake bottom as well as after complete deposition.
3. During the melt-out of ice within the underlying till. This process will be called basal melt-out. The discontinuities produced are high angle major shears.

The presence of randomly oriented fissures whose origin are unknown will also be discussed.

### 3.5.1 Minor shears formed shortly after deposition

It is a fact that shearing and slumping often occurs during deposition within a lake. Experiments by Einsele et al (1974) have shown that slumping or shearing along bedding planes occur as a result of sedimentation on tilted beds and high sedimentation rates. The internal deformation within a lacustrine deposit is likely to continue beyond these penecontemporaneous processes as a result of consolidation. Leckie and McCann (1980) have identified micro-faulting in lacustrine sediments from small movements within the underlying layers.

In the Genesee Clay, instabilities during deposition are indicated by the presence of swirled laminae bounded by intact beds. These contorted laminae do not in themselves contain structural discontinuities but the action of shearing and slumping might induce shear planes in the layers lying immediately below. Plate 3.7 shows a shear plane that is parallel to the bedding and the intense shearing had produced the tongue-like structure just above the shear plane. Experiments by Einsele et al (1974) have shown that such tongue-like intrastratal structures are formed by strong shear forces induced by the sliding of the surface layer during deposition on an inclined bed.

Minor penecontemporaneous slumping also took place with little mixing of sediments. Plate 3.8 shows the pull-apart and shearing features that could have been associated with a minor slump. This falls within Morgenstern's (1967b) definition of a coherent slump. Minor slickensides were present along the bedding planes and other sheared surfaces. Another set of minor slickensides was formed as a result of lateral compression as shown in Plate 3.9. Shearing took place across bedding as along planes A at angles of about 30 - 35 degrees to the horizontal which correspond to failure due to high lateral forces. The flow feature B indicates

Plate 3.7 Shearing along bedding with intrastratal flow structure.

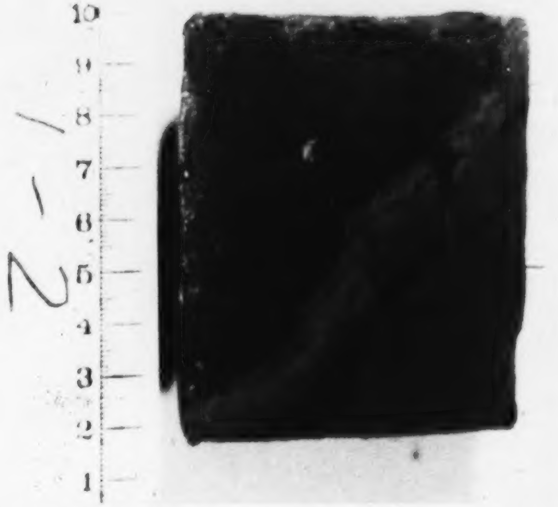
1-2
10
9
8
7
6
5
4
3
2
1

Plate 3.8 Minor coherent slump (sample 1-2).

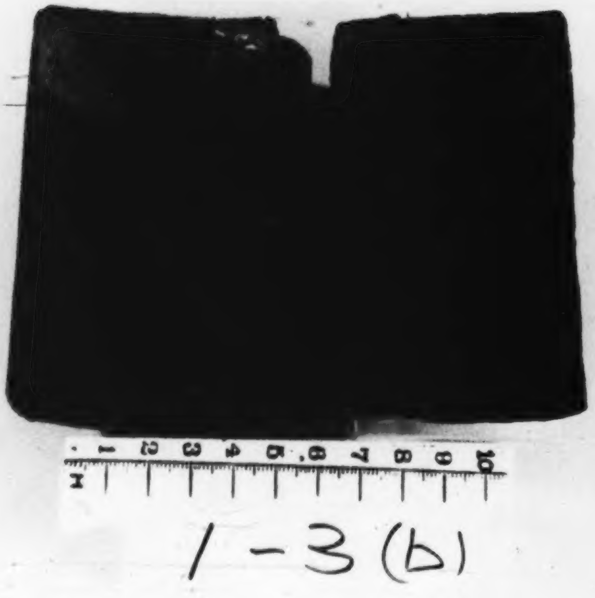
1 2 3 4 5 6 7 8 9 10
1 -3 (b)

Plate 3.9 Shearing due to lateral compression (sample 1-3).

that the shearing took place at high moisture content.

Minor slickensides (1 - 2 $cm^2$) were also present along beddings within the dark grey clay. The development of these slickensides was enhanced by the deposition of the strongly oriented particles discussed earlier so that small post-depositional movements due to consolidation and other types of stressing could cause the slickensides to form.

In these examples, the shear planes are characterised by polished surfaces with slight or no striations as shown in Plate 3.10. In addition, the slickensides have an area varying from a few $cm^2$ (Plate 3.10(a)) to the entire area of the sample depending on the magnitude of the shearing. It is to be noted that these sheared discontinuities might have originated as microfissures shortly after deposition as decribed by Einsele et al (1974) and later internal stressing caused renewed movement resulting in slickensided surfaces. The internal stressing might be due to either melting of ice within the till or differential consolidation in the underlying sediments.

### 3.5.2 Fissures due to weathering

Both the uppermost oxidised crust and the intermediate stiff layers whose presence was discussed earlier are considered in this section. The processes involved during the weathering action are mainly freezing and thawing and wetting and drying. These processes have produced a blocky or nuggetty structure within the upper clay. The individual

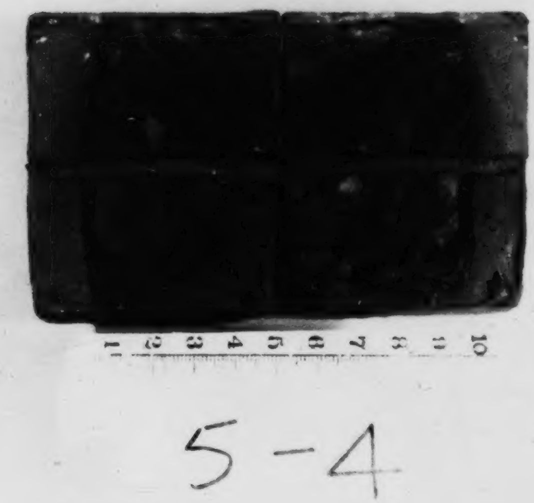
1 2 3 4 5 6 7 8 9 10
5-4

(a)

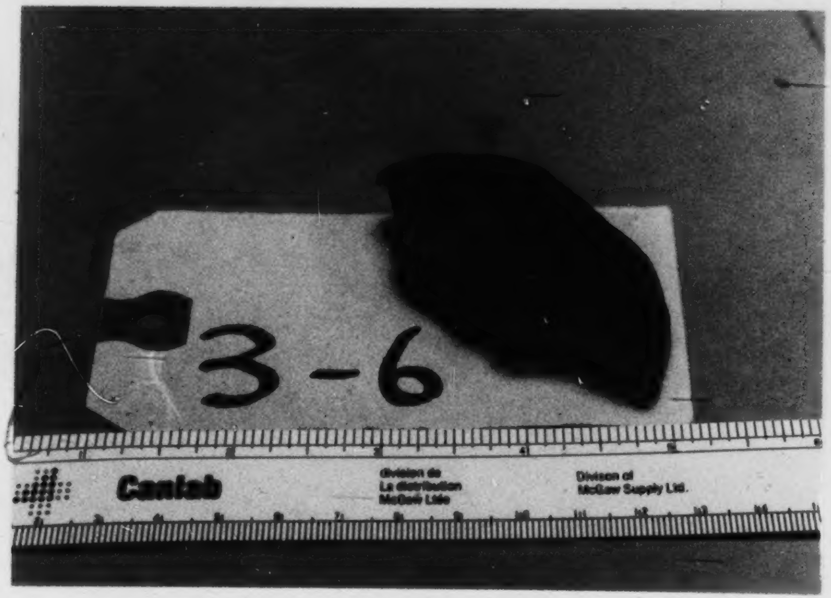
3-6
Canlab
division de La distribution McGaw Ltée
Division of McGaw Supply Ltd.

(b)

Plate 3.10 Slickenside with (a) no striation (b) slight striations

Plate 3.11 High angle major sheared fissure (sample 6-2).

Plate 3.12 Subhorizontal and subvertical major sheared fissures(sample 2-5).

blocks are angular to subangular and vary in size from 2 to 5 mm with the size of the blocks increasing with depth. At times, major high angle (greater than 60 degrees) shear planes are superimposed on the blocky structure as shown in Plate 3.11. Plate 3.12 shows a pair of subhorizontal and subvertical discontinuities in the intermediate stiff crusts within the unweathered clay; these stiff crusts did not show any sign of oxidation. The surfaces of the major discontinuities are polished with slight striations indicating shearing resulting most probably in association with the shrinkage and swelling action during weathering.

### 3.5.3 Major shears due to basal melt-out processes

Sanford (1959) made analytical and experimental studies of the response of a homogeneous rock layer subjected to basal vertical movements. High angle faults (dip of more than 45 degrees) were predicted as a result of the loss of support from underneath the layer. Similar faulting was observed in glaciofluvial sediments by McDonald and Shilts (1973) and Shaw (1982) and was attributed to the melting of buried ice in the stratum underneath the sediments concerned.

The melt-out of buried ice at Genesee was a process that lasted until the complete deposition of the clay based on the present hummocky terrain. Therefore, the ultimate melting of the ice was characterised by shearing as part of the clay gained enough strength to shear instead of undergoing plastic deformation. An example is shown in Plate 3.13 whereby a highly striated slickenside was produced. Such a sheared discontinuity was found in a sample from a depth of 15 m below ground level within the topographic low UA1 and the striae on the sheared surface indicate that movement changed from a direction indicated by arrow A to that shown by arrow B; the striae traced by a coal chip on the shear surface indicate that movement in the direction of B was at least 30 mm. The inclination of this shear surface is about 60 degrees to the horizontal. This high angle discontinuity is comparable to the normal faults in glaciofluvial deposits which were attributed to the melting of buried ice by McDonald and Shilts (1973) and Shaw (1982).

### 3.5.4 Unsheared fissures

Although the examples given above are sheared discontinuities showing varying degrees of movement, another set of discontinuities are the tension cracks or fissures that were found mostly in the more silty clay. Plate 3.14 shows such vertical fissures found in a block sample and the distinction between the appearance of the natural fissure and that of the fractures through the intact clay is clearly visible. The fissures have a matt, slightly undulated and more or less smooth surface whereas the fractures through the intact material have a "gummy" appearance. The layer within which the fissures occurred has a liquid limit of 55 %, plastic limit of 21 %, and natural moisture content of 38

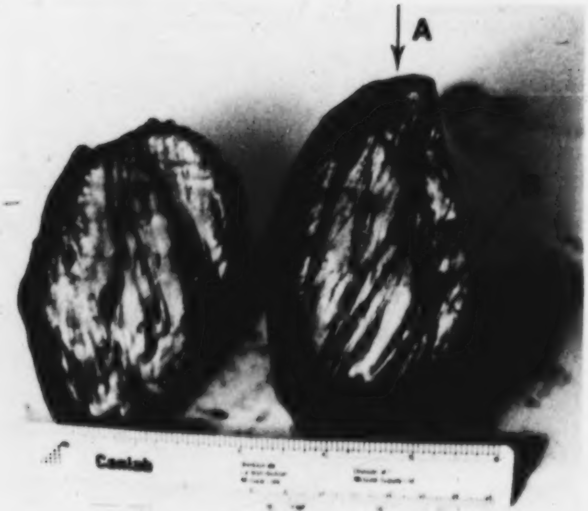

Plate 3.13 Highly striated high angle slickenside (sample 1-6).

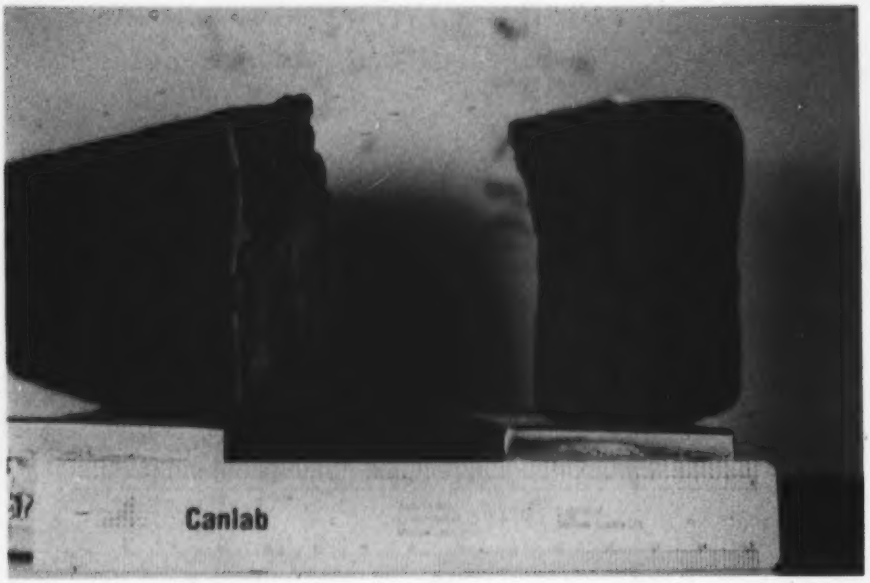

Plate 3.14 Smooth vertical fissures (block sample).

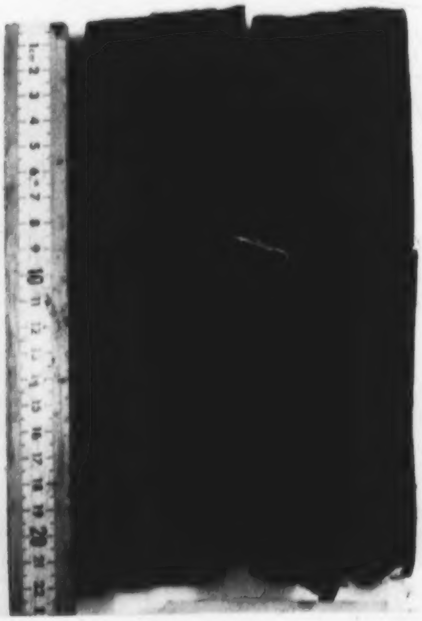

Plate 3.15 Randomly oriented fissures (sample 6-3).

% whereas the more plastic overlying layer has a liquid limit of 68 %, plastic limit of 24 % and natural moisture content of 48 %. On the other hand, Plate 3.15 shows a sample with intense randomly oriented faint fissures which divide the soil into small 1 cm cube blocks. These fissures most probably represent planes of weakness as manual distortion of the clay caused rupture along the fissures. Consolidated undrained triaxial test results on a specimen containing these fissures show that the clay exhibits strain-weakening behaviour as shown in Fig. 6.15 of Chapter 6.

The surface texture of these fissures can vary from a plumose or flaky appearance to the smooth appearance shown in Fig. 3.14. There are no indications that there was any shearing along these fissures. The latter tend to be of small size not exceeding 50 mm in length. Their exact origin is unknown but they could have formed during the internal stressing of the clay mass and might be bound by the major shear discontinuities. On the other hand, Eden and Mitchell (1970) described similar closely spaced hairline fractures in the Leda Clay of Eastern Canada and suggested that such fractures might originate from stress relief or the fatiguing effect of seasonal changes in temperature and/or groundwater pressures.

### 3.6 SUMMARY

The deposition of Genesee Clay was controlled by fluctuations in the depositional environment caused by cycles of ice retreat and readvance which resulted in very irregular layering of the deposit. Besides contorted bedding, the clay contains numerous structural discontinuities as a result of a combination of various post-depositional processes. Table 3.1 gives an indication of the intensity of the structural discontinuities within the unweathered clay and is not meant for statistical interpretation since the sampling was not continuous and some discontinuities might have been missed from the specimens used for laboratory tests.

In analysing Table 3.1, the following points should be noted:

1. UA1, UA2 and UA5 are boreholes within the cooling pond area and UA3, UA4 and UA6 are within the plant site.
2. The minor slickensides are found mostly in the dark grey clay and are oriented parallel to the bedding which may be inclined.
3. The minor fissures are found mostly in the light grey clay and are randomly oriented.
4. The single discontinuities include all the major shears irrespective of the mode of formation.
5. The weathered clay has not been included and is highly fissured and may contain major slickensides.
6. Discontinuities due to lithological contrast have not

Table 3.1 Structural discontinuities in unweathered clay.

| Borehole No | Total length of samples (cm) | Length containing intense minor slickensides (cm) | Length containing intense minor fissures (cm) | No. of single discontinuities |
|---|---|---|---|---|
| UA1 | 205 | 19 (9.3) | | 7 |
| UA2 | 305 | 60 (19.7) | 30 (9.8) | 14 |
| UA5 | 200 | 7 (3.5) | | 7 |
| UA3 | 192 | 21 (10.9) | 30 (15.6) | 5 |
| UA4 | 220 | 35 (15.9) | 123(55.9) | 4 |
| UA6 | 156 | 46 (29.5) | 31 (19.9) | 5 |

Numbers in bracket indicate the percentage of the total length of sample.

been included although it is shown in Chapter 6 that they can be planes of weakness.

Table 3.1 shows that there is quite a variation in the intensity of the minor slickensides and fissures with a higher intensity at the plant site. The fact that the length of the samples at UA4 containing the minor discontinuities form a combined percentage of about 72% of the total length of samples should be of significance since these discontinuities are potential weakening agents as shown in Chapter 6. On the other hand, there seems to be a higher occurrence of the single discontinuities at the cooling pond.

# 4. FIELD INVESTIGATION

## 4.1 INTRODUCTION

The purpose of the field investigations was to assess the variability in the engineering properties of the Genesee Clay and to determine the causes of this variability. As the clay is not highly variable in terms of mineralogical composition, the variability is thought to be due to the stress history and structure. Therefore, it was decided to determine variability in the in-situ stresses as well as in the undrained strength. Sampling was done to establish the soil profiles, study the soil fabric and perform laboratory tests. The in-situ porewater pressures were measured by the piezometer used for the hydraulic fracture tests. The investigations were carried out in November and December, 1983 with the exception of lateral stress measurements at test locations UA5 and UA6 which were carried out in March, 1985.

## 4.2 LOCATION OF TEST SITES

The test locations were selected so as to be away from any influence of the structures being built. Three locations were selected at the plant site and at the cooling pond so that both the topographic highs and lows were investigated. The test locations are shown in Plate 2.2 and the profiles tested are shown in Fig. 2.8 and Fig. 2.9 of Chapter 2. The test sites are labelled UA1 to UA6. It is to be noted that

Table 4.1 List of in-situ tests performed.

| Test Site | Depth of test (m) | | | | | |
|---|---|---|---|---|---|---|
| | pwp | HF | TSC N-S | TSC E-W | DMT N-S | FV |
| UA1 | 8.4<br>11.4 | 8.4<br>11.4<br>14.4<br>16.0 | 8.4<br>11.4<br>13.4 | 11.4<br>13.4<br>14.4 | From 6.0 to 20.0 | From 5.4 to 15.8 |
| UA2 | 10.8<br>13.8 | 10.8<br>13.8 | 10.8<br>13.8<br>16.8<br>20.5 | 13.8<br>16.8<br>18.1 | From 8.0 to 20.0 | From 8.3 to 20.3 |
| UA5 | | | 10.4<br>13.4 | 10.2<br>13.2 | | From 6.8 to 14.0 |
| UA3 | 8.3<br>10.6<br>12.3 | 8.3<br>10.3 | 8.3<br>10.3<br>12.3<br>15.3 | | From 7.0 to 17.5 | From 7.0 to 14.5 |
| UA4 | 7.7<br>9.7<br>11.7 | 9.7<br>11.7 | 9.7<br>11.7<br>14.7 | | From 9.5 to 13.0 | From 8.5 to 13.0 |
| UA6 | | | 11.6 | | | From 9.7 to 13.7 |

pwp - porewater pressure measured by piezometer.

HF - hydraulic fracture.

TSC N-S - total stress cell in north-south orientation.

TSC E-W - total stress cell in east-west orientation.

DMT - Marchetti flat plate dilatometer.

FV - field vane shear test.

the plant site had been graded at the time of the present investigation and approximately 2.5 m of peat was excavated and replaced by 4 m of clay and shale fill one and a half year earlier.

At each location, the test holes were drilled so that they were about 5 m or more from each other. Table 4.1 gives a summary of the tests performed at each location.

### 4.3 IN-SITU MEASUREMENT OF LATERAL STRESSES

In this section, the most common methods of measurement will be reviewed, followed by a discussion of the selection of the methods used at Genesee and a comparison of the results obtained.

The in-situ lateral stresses are expressed in terms of $K_0$ which is defined as the ratio of lateral effective stress to the vertical effective stress (Bishop, 1958) assuming that the stresses are principal stresses.

#### 4.3.1 General review

The importance of knowing the in-situ state of stress for the design of geotechnical structures has been emphasized by Morgenstern and Eisenstein (1970). On the other hand, a knowledge of the present state of the ground stresses can be used to reconstruct the stress history of the soil in the manner reported by Skempton (1961) for the London Clay. The measurement of lateral stresses at Genesee was performed primarily to investigate the effect of basal melt-out processes on the stress history of the clay.

The measurement of lateral stresses in clays has been discussed in detail by Wroth (1975). On the other hand, the measurement of the actual undisturbed lateral stresses is impossible because of the disturbance caused by the insertion of the measuring probe. Therefore, the development of measuring devices has evolved around the minimisation of the disturbances.

The first attempt to make a direct measurement of lateral stresses in a soft clay was made by Kenney (1967) who inserted a hollow steel pile instrumented with load cells. Massarsch (1975) reported the successful use of a thin Glotzl cell hydraulically jacked into the ground. Hydraulic fracture tests similar to those used in rock have been reported by Bjerrum et al (1972). The most successful device in terms of minimising disturbance appears to be the self-boring pressuremeter developed independently by Wroth and Hughes (1973) and Baguelin et al (1972).

The method normally used to account for disturbance due to insertion of the probe is to allow for the dissipation and stabilisation of the excess pore pressures with the assumption that the measured lateral stresses will reach a value close to that which existed before the cell was inserted. More recently, Marchetti (1979) and Handy et al (1982) have developed methods which do not depend on stress relaxation. Marchetti used empirical relationships to take account of the disturbance whereas Handy et al established relationships between known levels of disturbance and measured stress and then extrapolate to zero disturbance.

Besides the error caused by the instrument, the lateral stress if expressed in terms of the coefficient $K_0$ is also subjected to errors in the evaluation of the vertical stresses and porewater pressures. Massarsch et al (1975) and Tavenas et al (1975) discussed these problems extensively; Tavenas et al (1975) estimated the probable error in the measured $K_0$ to be in the range of ± 0.3.

### 4.3.2 Evaluation of test methods

This section will evaluate the known methods of measuring in-situ lateral stresses in clays such as:

- self-boring pressuremeter
- push-in stress cell
- Iowa stepped blade
- Marchetti flat plate dilatometer
- hydraulic fracture

and is based on published data.

#### 4.3.2.1 Self-boring pressuremeter

The measurement of lateral stresses by the self-boring pressuremeter can be performed in two ways:

- expansion of a flexible membrane by applying gas pressure and the pressure corresponding to a zero lateral strain condition of the borehole wall is considered to be the in-situ lateral stress (this is known as the expansion pressuremeter)

- direct measurement by load cells mounted on the outside of the probe (this is known as the Camkometer)

Ideally, the self-boring pressuremeter should be the best method for measuring in-situ lateral stresses. However, at present, there is still some uncertainty as to the accuracy with which this pressuremeter can measure the actual lateral stresses. The main problems associated with the method are:

- disturbance caused by installation procedures
- errors in the interpretation of test data when the expansion pressuremeter curves are used.

The success of the self-boring pressuremeter in minimising disturbance depends on the rate of advance to avoid clogging and the subsequent use of excessive flushing pressures which can cause hydraulic fracture (Windle and Wroth, 1977). Even with the appropriate advance rate, the generation of porewater pressures during insertion indicates the presence of disturbance; Clough and Denby (1980) found that pore pressures in the high plastic San Francisco Bay Mud required up to 6 hours for dissipation and stabilisation. However, the problems remain in that there is at present no standardised procedures for performing the tests in terms of penetration rate, flushing pressure and cutter setting. Denby and Clough (1980) found that the techniques to be used for the best results would vary depending on the soil type, depth and in-situ stress. Therefore, there is a need to carry out trial tests at each new site before appropriate testing procedures can be established so that the cost can be prohibitive.

The problems associated with installation techniques are also shown by the fact that the self-boring technique has not produced consistent results. Tedd and Charles (1983) reported much lower values of lateral stresses with the Camkometer than with the expansion pressuremeter. Massarsch and Broms (1976) found that the Camkometer gave very erratic results and some of the measured lateral stresses were lower than the Rankine active earth pressure.

In the case of the expansion pressuremeter, Lacasse and Lunne (1982) discussed eight methods of estimating lateral stresses of which only five provided what were believed to be satisfactory estimates. Even then, errors of up to ±10 % could be expected.

Therefore, unless the problems are solved, the self-boring pressuremeter may not necessarily give better results than the other methods.

#### 4.3.2.2 Push-in stress cell

Stress cells have been used in various forms to measure the in-situ lateral stresses. Massarsch (1975), Massarsch et al (1975) and Tavenas et al (1975) have obtained satisfactory results in soft clays with undrained strengths of 10 to 30 kPa both in terms of limited soil disturbance around the cell and good reproducibility of the results. Tavenas et al (1975) reported that measurements made at the same depth by three different cells were within ± 1 kPa of each other. Massarsch and Broms (1976) have found good agreement between the 3 mm thick Glotzl earth pressure cells and the self-boring pressuremeter. Massarsch (1979) performed tests whereby the lateral pressure in a soft soil mass could be varied by means of inflatable rubber cushions and the stress cell was inserted after the pressure had been set to a particular value. Massarsch found that the lateral pressure measured by the pressure cell was 3 % lower than the increase in the applied pressure.

More recently, Tedd and Charles (1981,1983) have experimented with the installation of stress cells in the stiff London Clay and came to the conclusion that the cells could overread by an amount found empirically to be one half the undrained strength. Therefore, the stress cells are best suited for soft to firm soil whereas for stiff soil some correction factor has to be applied. The other problem with the push-in method of insertion is the non-verticality of the probes during insertion; this is especially important at great depths. However, Campanella and Robertson (1983) found that in a soft deposit, good verticality could be maintained for penetration depths in excess of 15 m.

Another disadvantage of the stress cells is that it takes up to about a week for the excess pore pressures to dissipate; the dissipation is accompanied by loss of water from the disturbed zone around the cell in the case of normally or lightly overconsolidated soils so that at equilibrium the soil surrounding the probe is overconsolidated with respect to its original conditions. Therefore, even though the pore pressure is allowed to dissipate, the initial ground stress is not recovered.

### 4.3.2.3 Iowa stepped blade

~~The Iowa stepped~~ blade is another version of the push-in stress cell and consists of three thicknesses of blades to measure soil pressures which are then extrapolated for the zero blade thickness (Handy et al, 1982). The readings are taken without waiting for the dissipation of the excess porewater pressures. Handy et al found good agreement between the stepped blade and self-boring pressuremeter tests. The problem with methods that do not allow for stress relaxation is the fact that the time at which the reading is taken is critical. For all methods involving jacking of the probe, immediately after the vertical pressure is released at the end of the insertion, there is a rapid drop in the monitored pressure so that the time interval between the end of push and the reading of the horizontal pressure should be kept constant. It would be interesting to estimate the lateral stresses based on the data after the complete dissipation of porewater pressures and then determine the stress for zero blade thickness which represents a state closer to the in-situ stresses.

#### 4.3.2.4 Marchetti flat plate dilatometer

The flat plate dilatometer (DMT) was developed by Marchetti (1980). In terms of measuring lateral stresses, the DMT functions in a similar fashion to the Iowa stepped blade. However, the DMT has the additional capacity of estimating undrained strengths and deformation moduli. In this method, all measurements are made under undrained conditions just after the instrument has been jacked into position. Similar to the stepped blade, the time at which the reading is taken has to be consistent. Since the measurements are corrected by empirical relationships, the testing procedures cannot deviate from those established to derive these relationships. There is also the need to expand the data base to improve the empirical correlations. At present, the experience with the DMT is rather limited, but Lacasse and Lunne (1983) and Campanella and Robertson (1983) reported satisfactory results for clays.

#### 4.3.2.5 Hydraulic fracture test

This simple method for measuring lateral stresses in soil was first proposed by Bjerrum and Andersen (1972). It consists of noting the pressure required to generate a crack in the soil when water is injected from the tip of a piezometer. Theoretically, the crack forms in a direction perpendicular to the minor principal stress. Because of the disturbance due to driving and the influence of the tensile strength of a clay on the fracture pressure, Bjerrum et al (1972) proposed the use of the pressure at which the crack closes as the estimated minor principal stress. Experimental evidence by Bjerrum and Andersen (1972) showed that this assumption was acceptable. Bozozuk (1974) and Wilkes (1974) found that it was difficult to define the closure pressure on the basis of the plot of pressure against rate of flow suggested by Bjerrum and Andersen (1972). While Bozozuk proposed a different graphical technique, Wilkes suggested a modified testing procedure. According to Tavenas et al (1975), the Bjerrum and Andersen method gives the minimum possible closure pressure whereas the Bozozuk method gives a higher closure pressure; Wilkes method has the disadvantage of requiring a larger number of tests.

The problems associated with the hydraulic fracture test are not restricted to the interpretation of the test results only. Tavenas et al (1975) found that in cemented clays, the disturbance due to insertion of the piezometer could take up to 100 days to stabilise so that tests performed after a shorter period could overestimate the lateral stress. On the other hand, Massarsch et al (1975) pointed out that the direction of cracking may not be uniquely controlled by the minor principal stress but also by the presence of varves, fissures and non-homogeneities. Penman (1975) found that the horizontal features within a clay fill due to compaction could cause the closure pressure to be higher than the minor principal stress. Massarsch (1978) argued that only vertical fractures are likely to form within the plastic zone originating from the installation of the piezometer even within overconsolidated clays and therefore, $K_0$ values greater than unity can be expected. By sampling the soil after a fracture test, Lefebvre et al (1981) found that both vertical and horizontal cracks were generated. However, in such a case, the final closure pressure may be equal to the minor principal stress. Cracks will close progressively, and those that are perpendicular to the minor principal stress are the last to close.

There have been conflicting views on the reliability of the hydraulic fracture tests. Andersen et al (1972) and Wroth and Hughes (1973) reported hydraulic fracture results which compared favourably with those of stress cells and self-boring pressuremeter respectively whereas publications by Tavenas et al (1975) and Massarsch et al (1975) showed large differences in hydraulic fracture and stress cell results.

### 4.3.3 Methods used at Genesee

From the above discussion, it can be seen that the self-boring pressuremeter and the push-in stress cell are the most reliable instruments because of the limited disturbance and of the fact that excess pore pressures are allowed to dissipate. Undoubtedly, the pressuremeter would have been the best tool if the right installation procedures and interpretation method were used. However, at present, the literature shows that for soft clays the push-in stress cell gives data comparable to the self-boring pressuremeter at a much lower cost. Since the Genesee Clay is a soft to firm clay with in-situ vane strength of 30 to 60 kPa, the amount of overreading in stress cells is not likely to be very serious when compared to the range of scatter in some of the published results of the self-boring pressuremeter. Consequently, based on the good performance of the stress cell in soft clays, it was decided to use this method as the main tool for estimating lateral stresses at Genesee. Because of its low cost and simple operation, the flat plate dilatometer was used to assess its performance and to build up a data base for the use of this instrument in Alberta. Finally, the piezometers used for measuring the local porewater pressures were designed for hydraulic fracture tests.

### 4.3.4 Test procedures

4.3.4.1 Total stress cell (TSC)

The cell used was the Irad Gage vibrating wire earth pressure cell model EPC (Irad Gage, 1982). Essentially, it consists of an oil-filled cell (230 mm in diameter and 6 mm thick) which is connected by a short length of thick wall steel tubing to a vibrating wire diaphragm pressure gage. The cell has an aspect ratio (ratio of cell thickness to active diameter) of 0.03 and a stiffness (ratio of diameter of the active diaphragm to the deflection of the diaphragm) of 20,000. For the present study, the cell was protected by means of a flat steel frame which has the shape of a spade for easy insertion. Plate 4.1 shows the protected cell in the upper part of the photograph, an unprotected cell in the lower part, and the readout unit for the vibrating wire gage. The total area of the frame and cell is about 2.6 times that of the cell alone; according to Audibert and Tavenas (1975), this ratio is satisfactory in eliminating errors due to edge stress concentration and arching of the surrounding soil.

For insertion of the cell at Genesee, a 425 mm diameter pilot hole was first drilled down to a depth of approximately 7 m in order to penetrate the full thickness of the weathered brown clay. This also

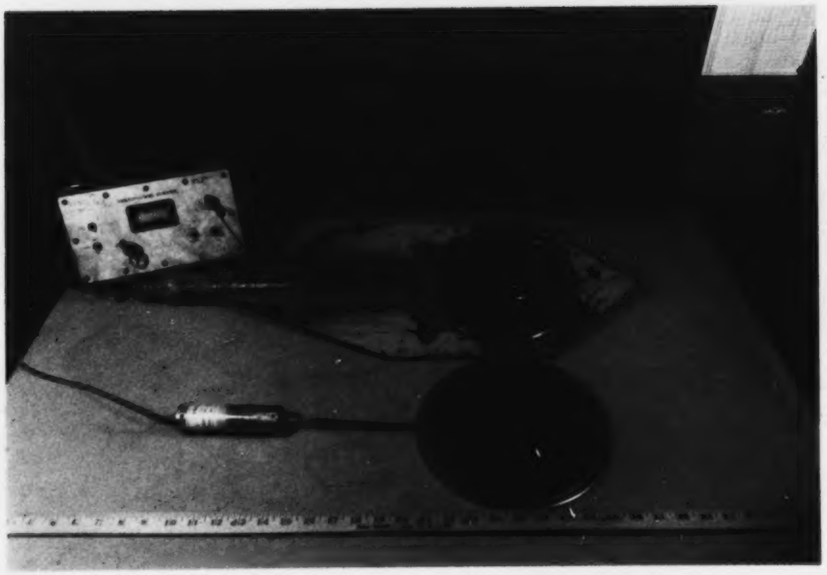

Plate 4.1 Total stress cell and protective casing.

represents the approximate depth that can be left unsupported. The cell was first connected to a 3 m length of 46 mm AW rod and 76 mm CHD rods were used for additional lengths. CHD rods were used to reduce buckling of the drill rods when the cell was pushed into the soil. A steel guide was placed at the top of the pilot hole to keep the rod as vertical as possible.

The cell was pushed at a rate of about 1.5 cm per second and the first measurement was made at 3 m beyond the bottom of the pilot hole in order to be outside the range of disturbance caused by the drilling. Readings of pressure were taken at intervals of time until the cell pressure came to equilibrium when it is believed that the pore pressure generated by insertion of the cell had dissipated. For the Genesee Clay, it took from 5 to 10 days for the excess pore pressures to dissipate because of the low permeability of the soil whereas, for a trial test within the Lake Edmonton Clay, it took only 2 days for the measured pressure to come to equilibrium. An example of the relaxation of pressure with time is given in Fig. 4.1; plots for other tests are given in Appendix D.

For this study, four different cells were used and they were calibrated in the laboratory within a sealed chamber (Plate D.1, Appendix D) by means of pressurised water. The cells were pushed down to a depth of 13 m beyond the bottom of the borehole without difficulties.

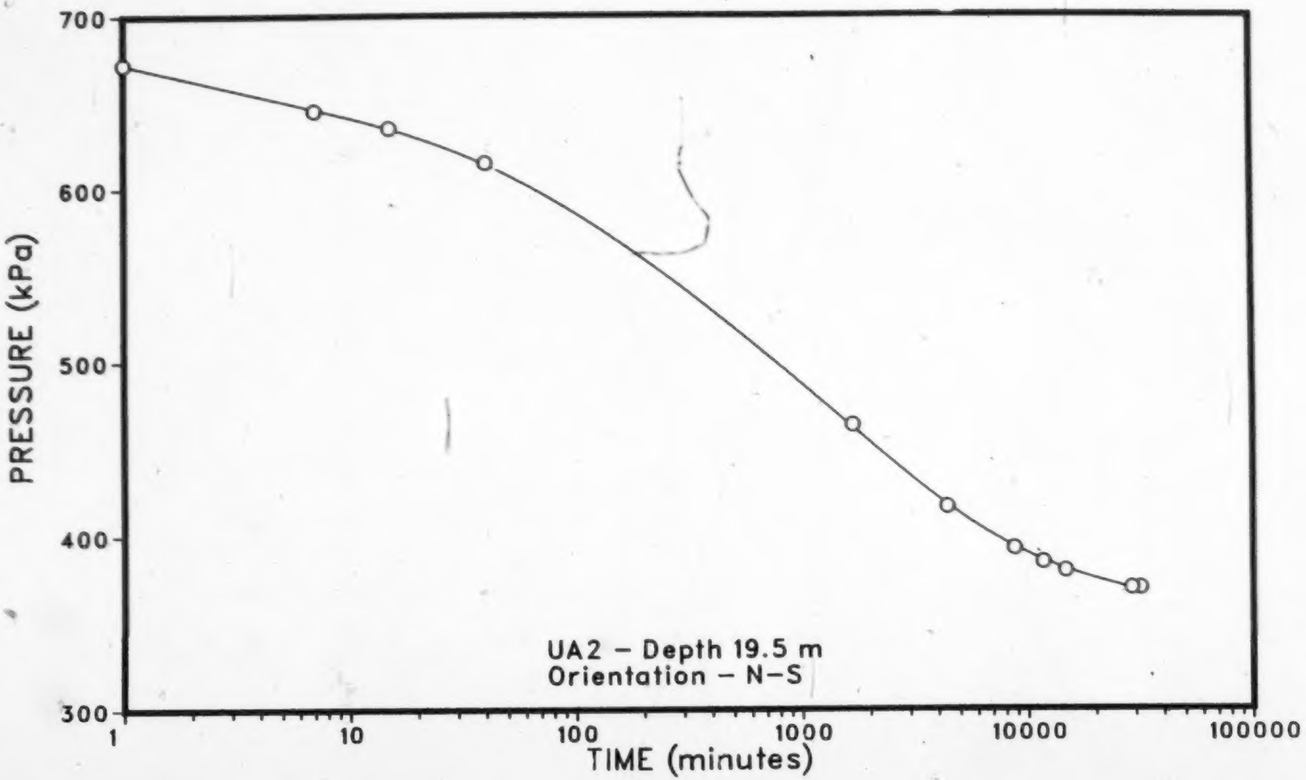

Figure 4.1 Example of dissipation of TSC pressure with time.

The four cells were used for measurements at 25 positions. Only one of the cells was damaged when the cell encountered a gravel or compact sand lens near the till surface.

### 4.3.4.2 Marchetti flat plate dilatometer (DMT)

The dilatometer used is the one described by Marchetti and Crapps (1981). It consists of a stainless steel blade 14 mm thick, 95 mm wide and 220 mm long (Plate 4.2). A thin flat circular expandable steel membrane,A, 60 mm in diameter is located on one side of the blade and rests on a sensing disc connected to a buzzer in the control unit. When the membrane starts to lift off, the buzzer is turned off. The buzzer is turned on again after the membrane centre has moved 1 mm into the soil. Before and after each test, the corrections ΔA and ΔB were measured. They were respectively the suction required to keep the membrane in contact with the seating and the pressure to lift the membrane centre by 1 mm from its seating in free air.

The blade was pushed into the ground from the bottom of a 150 mm diameter pilot hole at the rate of 2 mm per second and the membrane was inflated by means of pressurised gas immediately after reaching the required depth; for this project, the tests were done at intervals of 0.5 m. During inflation of the membrane, the pressures required to just lift the membrane off the sensing disc and to cause 1 mm movement of the membrane

Plate 4.2 Marchetti flat plate dilatometer.

centre were recorded. These were pressures A and B respectively.

Using $\Delta A$ and $\Delta B$, $p_0$ and $p_1$ were calculated from the following equations:

$p_0 = 1.05(A+\Delta A) - 0.05(B-\Delta B)$ ...............(4.1)

$p_1 = B-\Delta B$ ..............................(4.2)

The following parameters were then calculated:

$I_D = (p_1 - p_0)/(p_0 - u_0)$ ...............(4.3)

$K_D = (p_0 - u_0)/\sigma_v'$ .....................(4.4)

$E_D = 34.6(p_1 - p_0)$ .....................(4.5)

where $I_D$ = material index,

$K_D$ = horizontal stress index,

$E_D$ = dilatometer modulus,

$u_0$ = in-situ porewater pressure,

$\sigma_v'$ = vertical effective stress.

$I_D$, $K_D$ and $E_D$ were used in empirical relationships to evaluate $K_0$, OCR, undrained shear strength ($c_u$), constrained modulus (M)[2] and friction angle (in the case of sandy silt and sand). For the Genesee Clay, the following relevant equations were used:

---

[2] M is equal to $1/m_v$ at $\sigma_v'$.

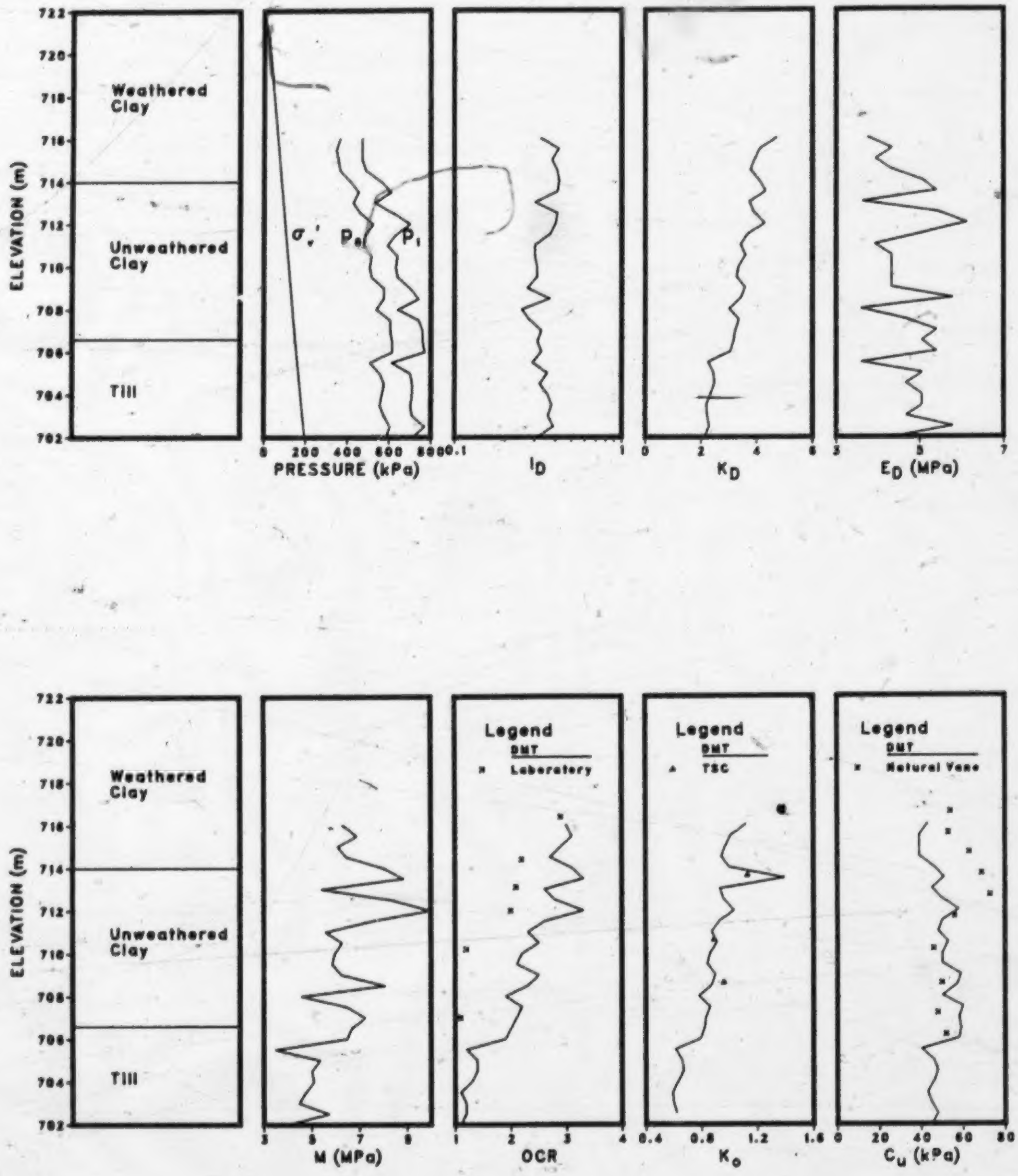

Figure 4.2 Example of DMT results (test location UA1).

$$OCR = (0.5K_D)^{1.56} \quad \ldots\ldots\ldots\ldots\ldots\ldots\ldots\ldots\ldots (4.6)$$

$$K_0 = (K_D/1.5)^{0.46} - 0.6 \quad \ldots\ldots\ldots\ldots\ldots\ldots\ldots (4.7)$$

$$c_u = 0.22\sigma'_v (0.5K_D)^{1.25} \quad \ldots\ldots\ldots\ldots\ldots\ldots\ldots (4.8)$$

$$M = (0.14 + 2.36(\log K_D)E_D \quad \ldots\ldots\ldots\ldots\ldots\ldots (4.9)$$

Equations 4.1 to 4.9 were obtained from Marchetti and Crapps(1981). For this project, the computations were programmed on an HP 41CV.

An example of the data obtained from the DMT is given in Fig. 4.2; data for the other sites are presented in Appendix D. It is to be noted that at all sites the DMT tests were performed with the blade oriented in the north-south direction.

### 4.3.4.3 Hydraulic fracture test

The piezometer used is shown in Plate 4.3(a). It consists of a 100 mm long and 25 mm outside diameter high air entry filter stone,A, and was provided with an electrical pressure transducer,B, which was connected to a readout unit at ground level. The piezometer was deaired through nylon leads connected to the inlet,C, and outlet,D, to the piezometer. The pressure system consisted of an air-water pressure cylinder,E, and a volume change device,F, (Plate 4.3(b)). The pressure was supplied from a nitrogen gas bottle,G, through a pressure regulator,H.

The nylon and electrical leads were enclosed in a plastic tube which was sealed at the top of the

6
7
10
11
12
13
14
27
28
29
30

(a)

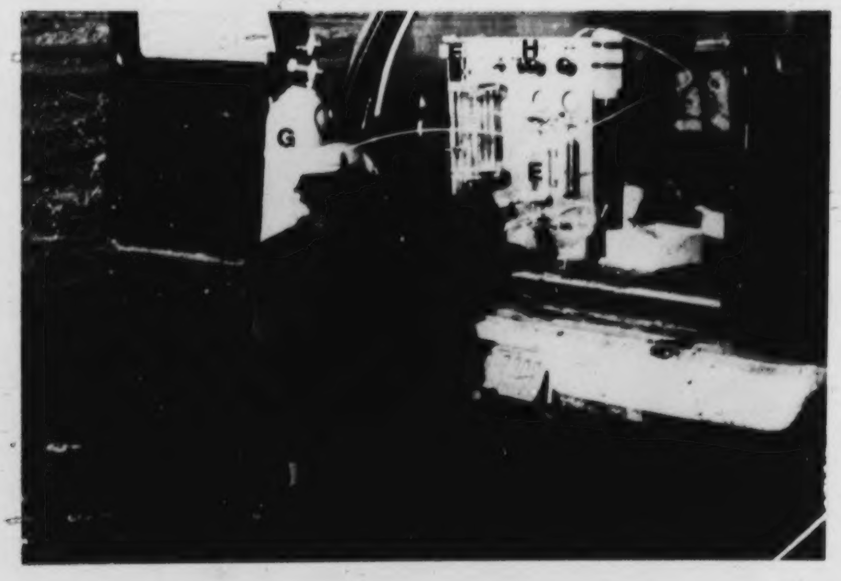

(b)

Plate 4.3 (a) Piezometer (b) Pressure system and volume change device.

piezometer to provide a water tight chamber for the pressure transducer. The plastic tube was threaded first through a 46 mm AW rod and then through 76 mm CHD rods. All the leads and the piezometer were completely saturated and the leads were plugged before installation. The piezometer was pushed at a rate of 2 cm per second for a distance of 3 m below the bottom of a 150 mm pilot hole and the excess pore pressure generated was allowed to dissipate with the leads vented to the atmosphere. Normally, it took about 1 week for the pressure indicated by the electrical transducer to become stable, but all tests were performed 10 to 14 days after installing the piezometer. Before performing the test, water was circulated through the piezometer under a small pressure to remove trapped air. Immediately after, one of the nylon leads was plugged and the water pressure was increased at a rate of about 10 kPa per sec by means of the air pressure regulator. Fracture occurred between 0.5 and 1 minute when a sudden increase in the flow rate was noticed on the volume change device. Normally, 10 to 15 $cm^3$ of water were pumped by the time the fracture occurred. After fracture, a falling head permeability test was performed by shutting off the pressure supply. The pressure drop and the associated rate of flow were measured at intervals; an example of the results is given in Fig. 4.3 and other test data are given in Appendix D. The

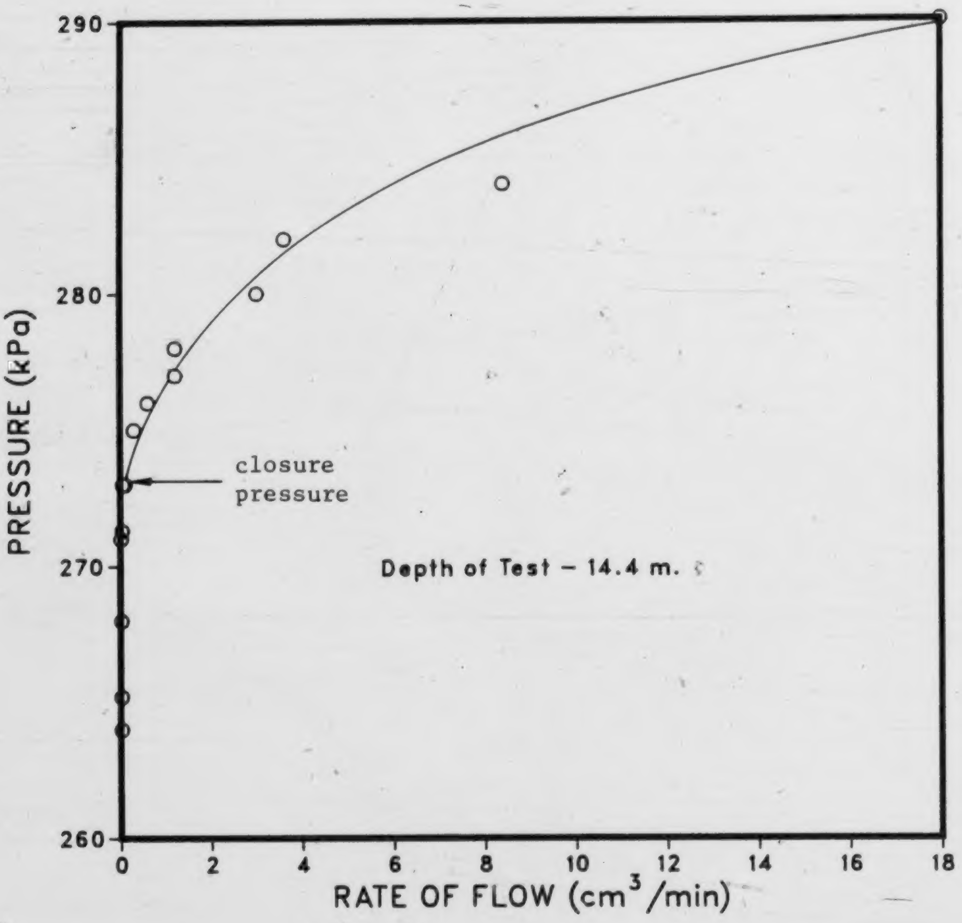

Figure 4.3 Determination of closure pressure from hydraulic fracture.

closure pressure is the point corresponding to a sudden decrease in rate of flow. By subtracting the in-situ porewater pressure prior to the test from the closure pressure and then dividing by the effective overburden pressure, $K_0$ is obtained.

Two major problems were encountered, namely:

1. after a few weeks, some of the electrical transducers within the piezometers were damaged by humidity and it was not possible to monitor the in-situ porewater pressures but it was possible to carry out the hydraulic fracture test by monitoring with a pressure transducer connected to the pressure system at ground level.
2. as the tests were done in the month of December, when the temperature dropped to -30 °C the water in the leads froze and it was not possible to conduct further tests.

### 4.3.5 Discussion of test results

#### 4.3.5.1 Total stress cell

Immediately after insertion of the cell, the pressure recorded is nearly twice that reached at equilibrium. Fig. 4.4 which shows a plot of the cell pressure one minute after insertion against the equilibrium pressure indicates that there is a relationship between the two pressures. The relationship is most likely nonlinear and passes through the origin.

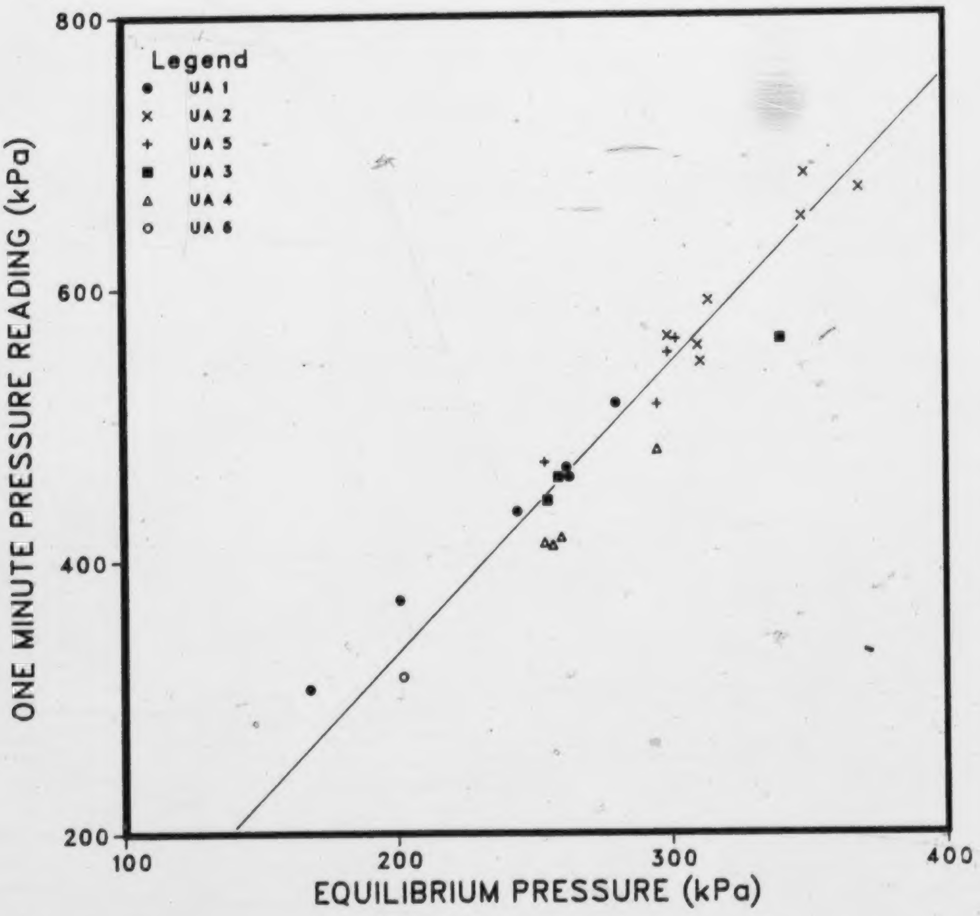

Figure 4.4 TSC one-minute pressure against equilibrium pressure.

Therefore, the cell pressure just after insertion is a function of the initial horizontal stress. By using such a relationship, it is possible to obtain rough estimates of the lateral stress without having to wait for equilibrium; however, such a relationship is probably unique for each deposit. This explains why, for the DMT, the empirical relationship to calculate the in-situ lateral stress from the pressure reading after insertion of the dilatometer gives satisfactory results.

As shown in Fig. 4.5 to 4.7, the stress cell has given very consistent results in the sense that there was not much scatter in the data. In these figures, the lateral pressures plotted are total and not effective. The good performance of the total stress cells is reflected in the repeatability of the results when the stresses were measured in two perpendicular directions (North-South and East-West) at the test locations UA1, UA2 and UA5 with a different cell for each direction. As discussed in Chapter 6, there is a certain anisotropy in the lateral stresses at certain depths at these three locations, such as elevation 709 m at UA2, but below and above these depths the different stress cells gave the same lateral stresses at each location. Therefore, this method gives consistent results.

#### 4.3.5.2 Marchetti flat plate dilatometer

Although this section deals mainly with lateral stresses, the prediction of overconsolidated ratio (OCR)

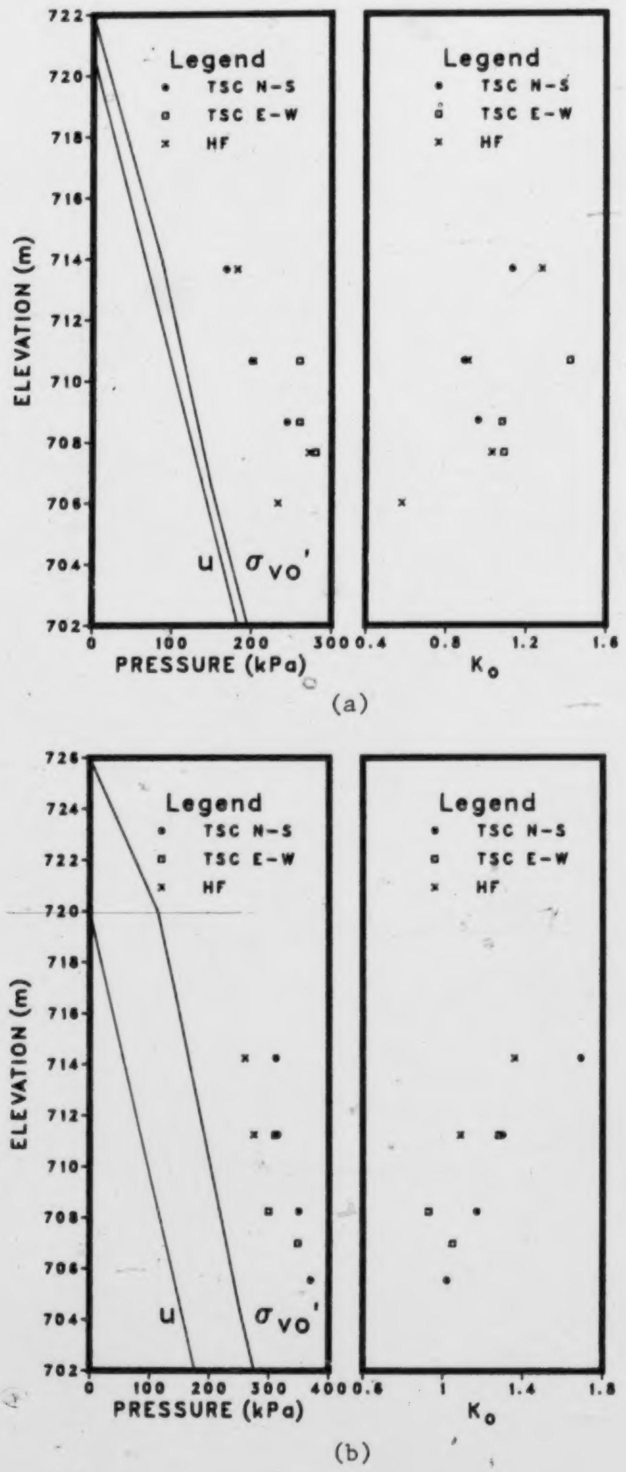

(a)

(b)

Figure 4.5 Measurement of $K_0$ at (a) UA1 (b) UA2.

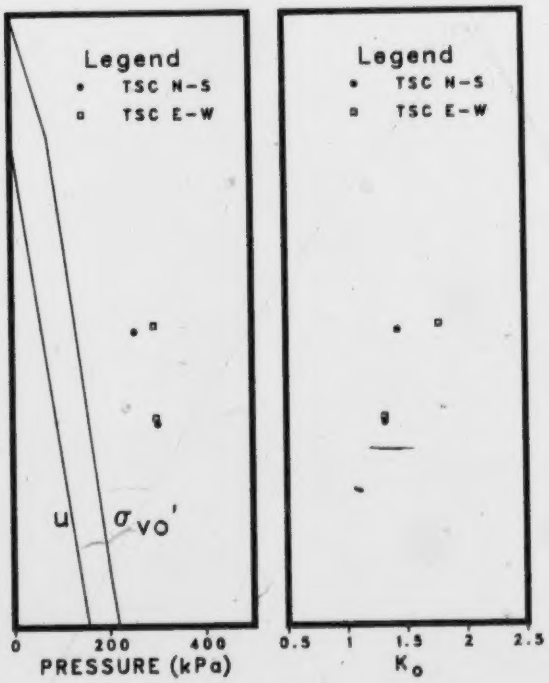

Figure 4.6 Measurement of $K_o$ at UA5.

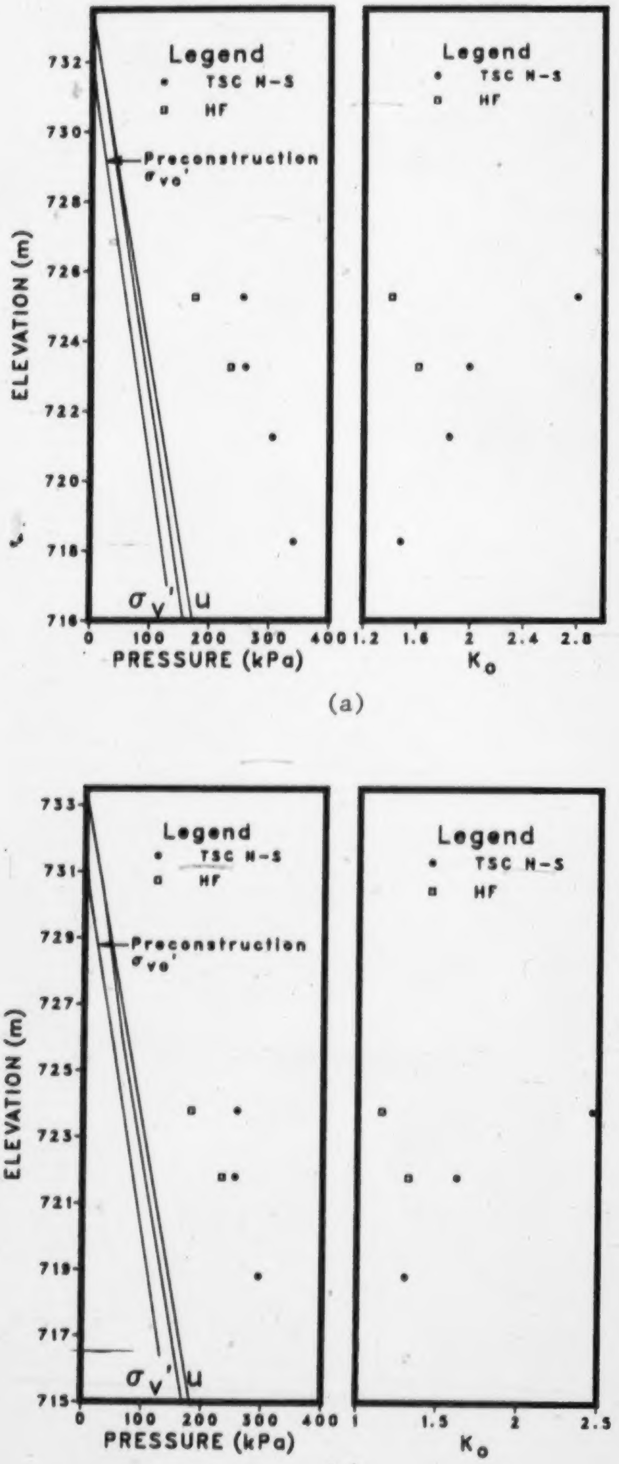

Figure 4.7 Measurement of $K_o$ at (a) UA3 (b) UA4.

and undrained strength ($c_u$) by the DMT will also be discussed. To enable a comparison of the DMT results with other test methods, OCR, $c_u$ and $K_0$ obtained from laboratory tests, field vane and total stress cells respectively are also plotted on the DMT data sheets. It was noted earlier that the plant site was graded with about 4 m of fill when the present testing program was started. However, the DMT measurements have not been corrected to obtain estimated values for the preconstruction conditions at the plant site. Therefore, for this section only, all the values of $K_0$, OCR and $c_u/\sigma_{vo}'$ for the plant site were calculated on the basis of the effective stresses at the time of investigation. This will not cause any error in the interpretation as this section compares the DMT results against other methods of measurement.

The variability in the DMT measurements can be detected by comparing the results with other methods of measurement at the various test sites; for that purpose Fig. 4.8 is given for comparison with Fig. 4.2. For the case of UA1 in Fig. 4.2, it can be found that the DMT OCR is higher than that determined in the laboratory whereas the DMT $K_0$ is comparable to the TSC $K_0$. On the other hand, for UA2 in Fig. 4.8, the DMT OCR falls within the range of the laboratory OCR but the DMT $K_0$ is much lower than the TSC $K_0$. Therefore, taken individually, the DMT correlations may give what appears

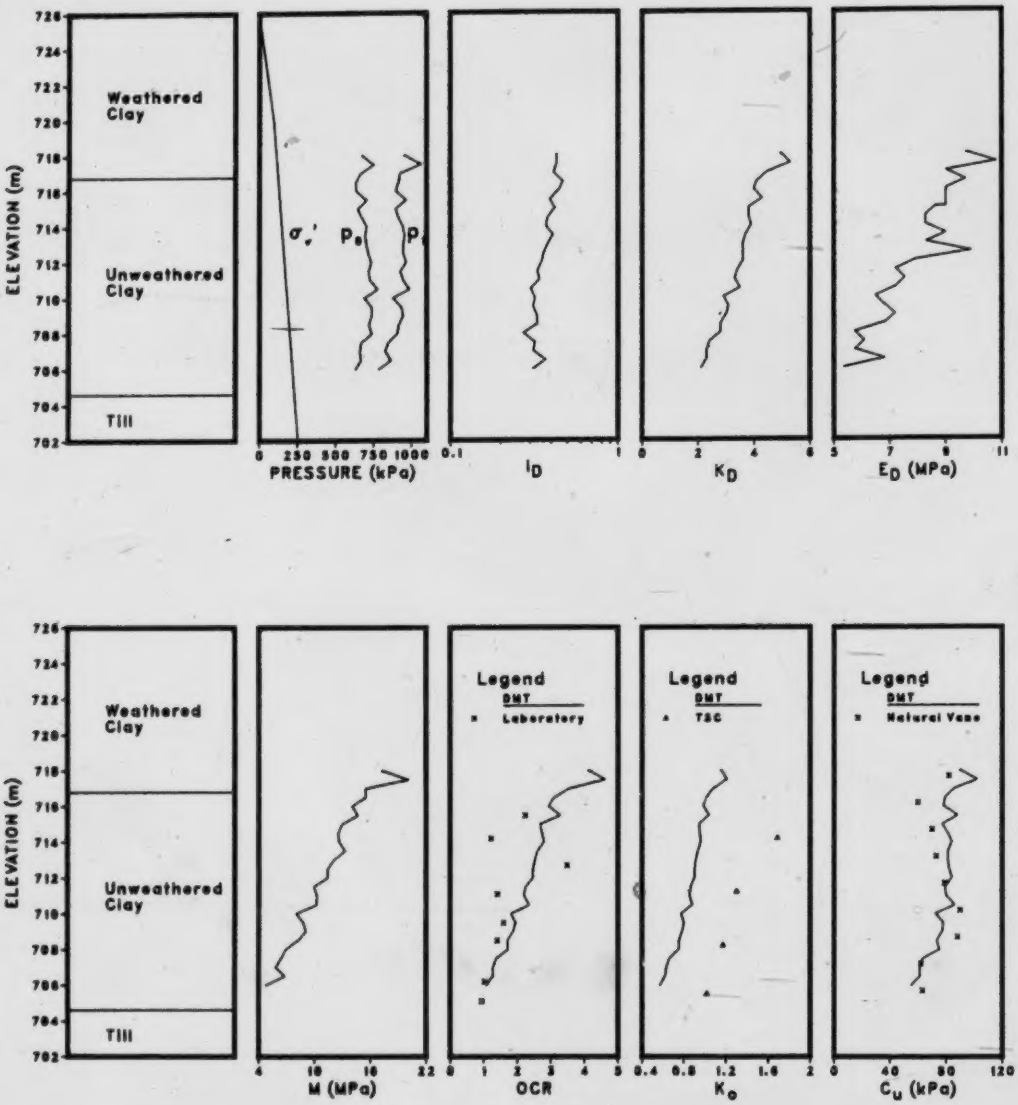

Figure 4.8 DMT test results at UA2.

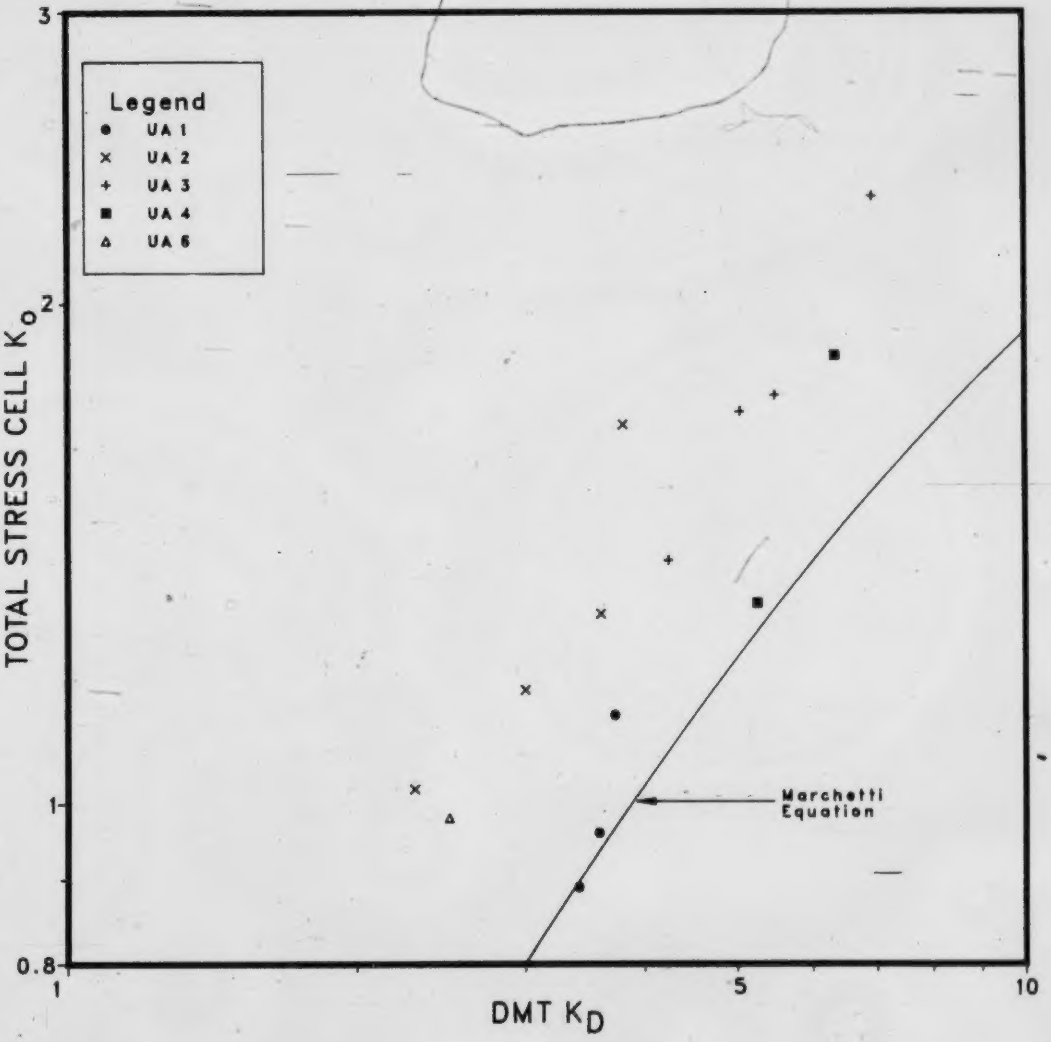

Figure 4.9 TSC $K_o$ against DMT $K_D$.

to be good results. So it was decided to determine the reliability of the DMT correlations by considering the data from all the sites as a whole. It is to be noted that the DMT tests were not performed at UA6 as part of this project but data from DMT tests by EBA (1983) for test hole EBA BH77 (about 20 m away from UA6) were used as being equivalent to conditions at UA6.

Since the DMT $K_0$ is obtained from the DMT horizontal stress index $K_D$ through empirical correlations, the TSC $K_0$ is plotted against $K_D$ in Fig. 4.9 which shows that although there is an apparent correlation between TSC $K_0$ and $K_D$, Marchetti's equation underpredicts the TSC $K_0$ at Genesee by as much as 50 %.

The laboratory OCR against $K_D$ is plotted in Fig. 4.10. There is a general overestimate of OCR (except for UA6) if the Marchetti relationship is used. Therefore, the Genesee Clay falls within the category of "abnormal" clay according to Marchetti (1979); the latter defines deposits as "abnormal" for the purpose of DMT interpretation when the horizontal stresses are in excess (positive or negative) of those for cases of simple unloading. Since the Genesee Clay has a complex stress history as discussed in Chapter 6, Marchetti (1979) suggested that the measured $K_D$ would be higher than those predicted by the available empirical correlations. Nevertheless, the correlation of Marchetti between $c_u/\sigma_v'$ and $K_D$ seems to predict the average field

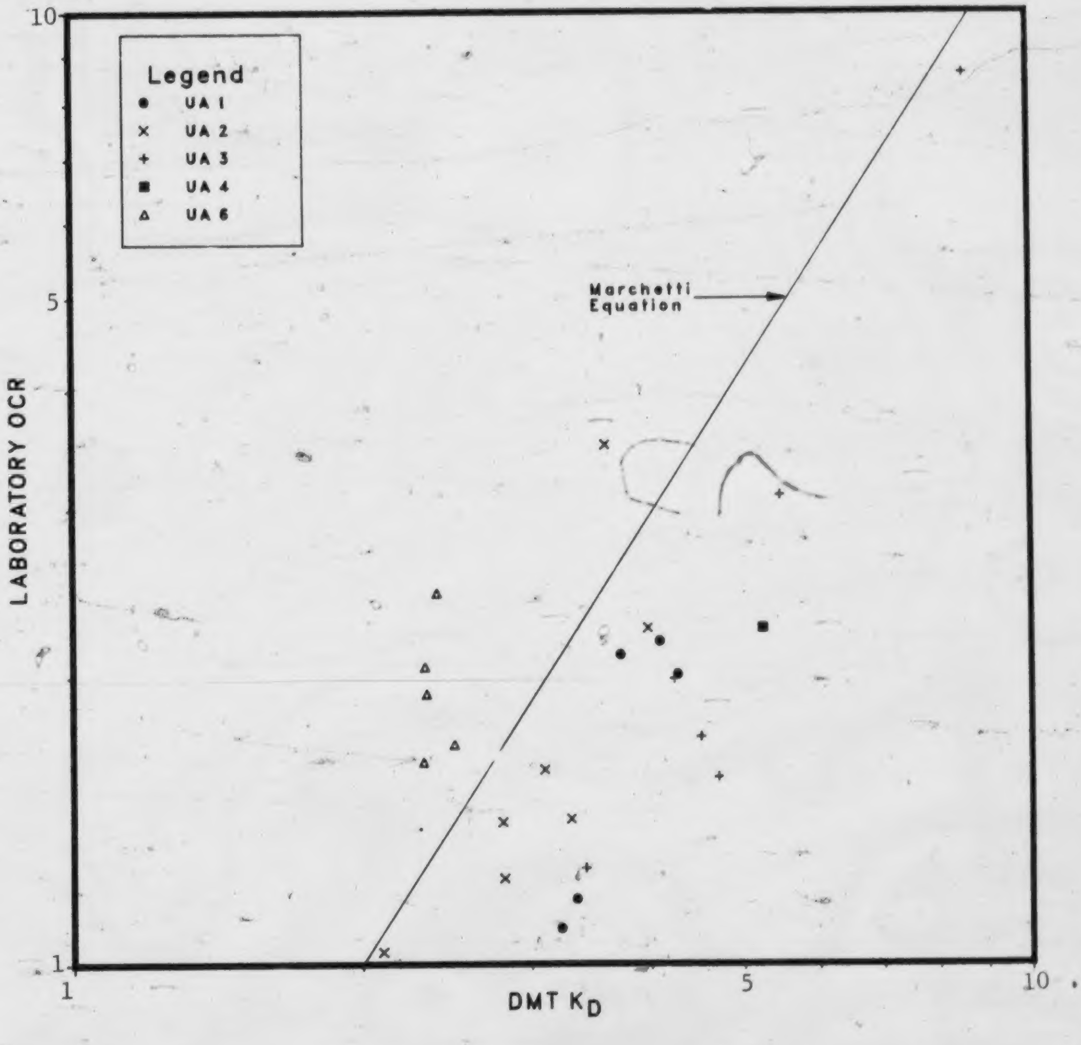

Figure 4.10 Laboratory OCR against DMT $K_D$.

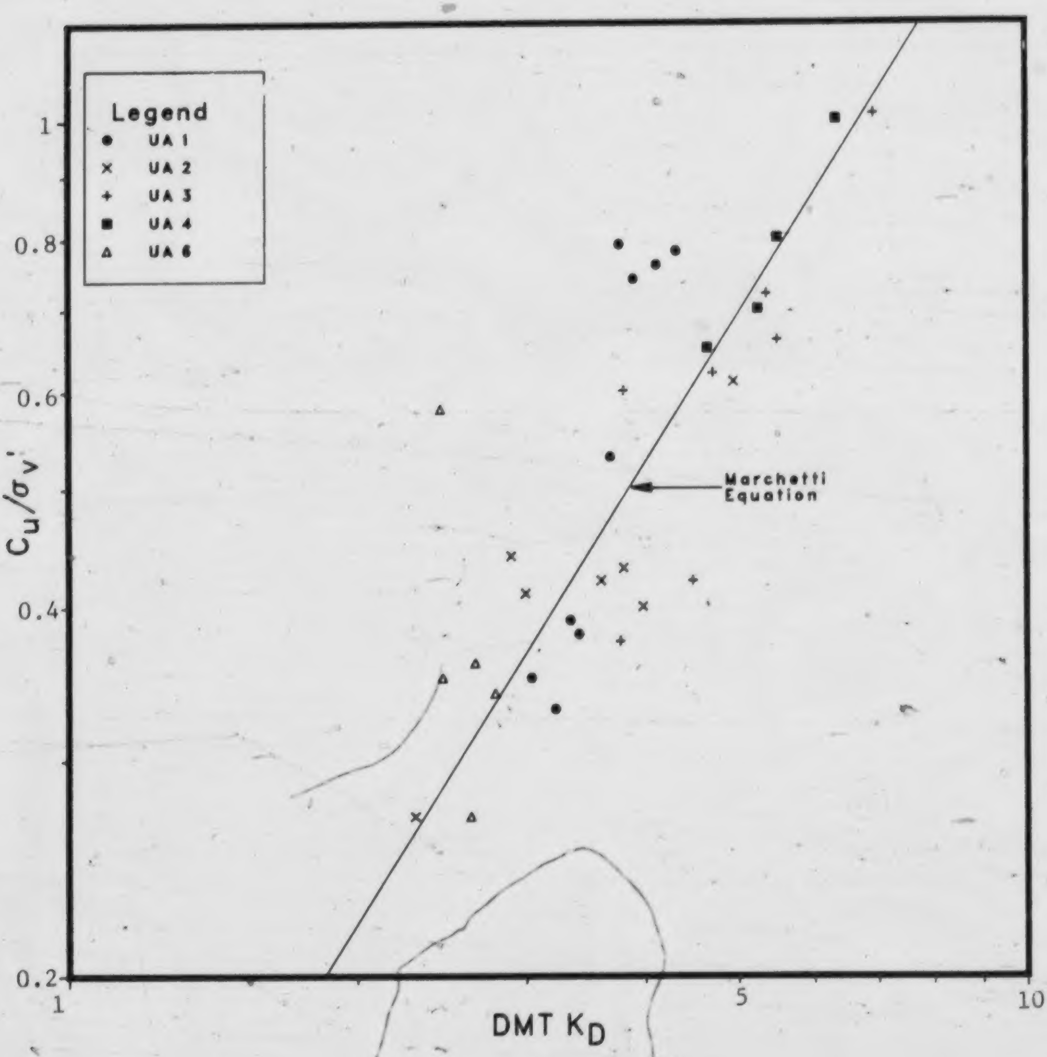

Figure 4.11 Normalised field vane strength against DMT $K_D$.

vane strength as shown in Fig. 4.11. Consequently, the DMT might not give reliable estimate of $K_0$ in the case of the Genesee Clay which has a complex geological history. The above show that the other DMT results should be used with care and there is a need to explore further its limitations.

### 4.3.5.3 Hydraulic fracture test

At Genesee, the values of $K_0$ by the hydraulic fracture method are consistent with those of the spade cell for $K_0$ equal to or less than unity. This is seen in Fig. 4.5 and it is also shown that, at a particular depth, the hydraulic fracture test generally measured the lower of the $K_0$ predicted by the stress cells which is consistent with the fact that the fracture test measures the minor principal stress. However, the situation became confusing for $K_0$ greater than one, when the hydraulic fracture gave an estimated lateral stress smaller than the spade cell but higher than the overburden pressure. Although the hydraulic fracture test should not be used for $K_0$ greater than unity, the question is whether that test really measures the minor principal stress. The exact reason for the fracture pressure to be greater than the overburden pressure is not known but since the soil fabric studies show that the soil is fissured, it is possible that the crack due to hydraulic fracture was influenced by the fissures. Since the water pressure,

$u_f$, to generate a fracture is given by Vaughan (1971) as

$u_f=m\sigma_3+\sigma_t$ ..............................(4.10)

where $\sigma_3$=minor total principal stress

$\sigma_t$=tensile strength of the soil

it is found that the fracture pressure can be about 2 times higher than the minor principal stress since m varies between 1 and 2. Where a crack exists m is equal to 1 and $\sigma_t$ is equal to zero. Therefore, where natural fissures exist in the soil and these fissures are not perpendicular to the minor principal stress, the fracture pressure may be that which just opens the fissures and is not high enough to generate cracks perpendicular to the minor principal stress. Therefore, in such a case, the closure pressure need not indicate the minor principal stress in fissured clays; other reasons were discussed in section 4.3.2.5.

Consequently, even though the hydraulic fracture test gave what appears to be good result for the case of $K_0$ less than one, the fact that the minor principal stress was not measured for the case of $K_0$ greater than one suggest that the theoretical basis for fracturing in soil is more complex than assumed by Bjerrum et al (1972). Therefore, the results should be interpreted with care.

#### 4.3.5.4 Summary

It was found that among the tools used for measuring lateral stresses, the total stress cell has given the most consistent results.

### 4.4 IN-SITU VANE TEST

A Nilcon vane was used for determining the in-situ undrained strength. A detailed description of the equipment is given in the instruction manual by Roctest (1982). Schmertmann (1975) reported that this vane "has among the smallest relative vane volume displacement, the thinnest blade edges, an accurate vane torque measuring system". This method makes use of unsleeved torque rods and is provided with a slip coupling situated just above the vane to enable the determination of the torque required to turn the rods only.

The 130 x 65 mm vane was used at UA1 and 110 x 50 mm vane was used at the other test sites. The vane was rotated at about 10 degrees per minute so that failure took place within 3 minutes. After the peak strength, the vane was rotated 20 times to achieve complete remoulding and the remoulded strength was determined.

The results were recorded on charts such as the one shown in Plate 4.4. T represents the torque required to turn the rods only and P is the maximum torque to turn both the rods and the vane. The difference (P-T) is used to determine the peak shear strength and (R-T) is used to determine the

Plate 4.4 Example of field vane shear test chart.

remoulded shear strength.

The results of the field vane tests are given in Fig 6.1 to 6.6 of Chapter 6.

## 4.5 IN-SITU POREWATER PRESSURE MEASUREMENT

The measurement of the in-situ porewater pressure was done by the piezometer used for the hydraulic fracture test. The porewater pressure measured at different depths was very consistent after the dissipation of excess pore pressure due to the insertion of the piezometer. The range of fluctuation over a few days was less than 10 kPa and was probably due to slight fluctuations in the zero readings of the electrical pressure transducer.

# 5. LABORATORY INVESTIGATIONS

## 5.1 INTRODUCTION

The samples for the laboratory investigations were obtained by means of 76 mm Shelby tubes at intervals of 1.5 m down to the top of the till. In addition, three 250 mm cube block samples were obtained at a depth of 6 m from the side of the diversion ditch (labelled L on Plate 2.2) within the cooling pond. The soil samples were extruded and waxed as soon as they were brought into the laboratory and were stored within a humidity and temperature controlled room. During extrusion, samples were taken for moisture content determination and laboratory vane tests were performed.

The specimens were labelled as follows:

1. those trimmed from the block samples were labelled as, for example, B3-1 where B specifies the specimen is from a block sample, 3 is the block sample number and 1 is the specimen number.
2. the tube samples were labelled as,for example, 1-5 where 1 represents the test location and 5 is the sample number. The description of the samples are given in the borehole logs in Appendix C.

## 5.2 CLASSIFICATION TESTS

The Atterberg limits were performed on specimen remoulded at their natural moisture content instead of ovendried specimens. Specific gravity determinations and hydrometer analyses were performed according to standard procedures described in Head (1981). An average specific gravity of 2.78 was found for the clay.

## 5.3 ONE-DIMENSIONAL CONSOLIDATION TEST

One-dimensional consolidation tests were performed in floating ring and fixed ring cells. The specimens were 63.5 mm in diameter and 25 mm thick for the floating ring and 19.3 mm thick for the fixed ring.

For all test specimens, the initial swelling pressure was measured. As the soil was rather soft, the conventional load increment ratio of 1 was not used. The recommendation of Brumund et al (1975) to use reduced load increment ratios in the vicinity of the preconsolidation pressure ($\sigma_p'$) was adopted to prevent squeezing of soil out of the consolidation ring. The load increment duration of 24 hours was used and the log-time method was adopted for analysing the settlement-time variation and for computing the coefficient of consolidation, $c_v$. The most probable preconsolidation pressure was determined from void ratio (e) against log $\sigma_v'$ curves using Casagrande's method.

A summary of the consolidation test results is given in Tables E.1 and E.2 in Appendix E.

## 5.4 DIRECT SHEAR TEST

The standard direct shear test on 60x60x20 mm specimen was used to determine the residual strength parameters. The test was performed under drained conditions with the rate of shearing calculated from the time to failure equation for drained tests given by Bishop and Henkel (1962) and the $c_v$ obtained during the consolidation stages of the test. The rate of shearing was between 0.0117 and 0.02 cm per hour. It was found that between 5 to 7 shears were required to reach the residual strength. The results, in tabular and graphical form, of the test are given in Appendix E for both the weathered brown and unweathered grey clay.

## 5.5 CONSOLIDATED UNDRAINED TRIAXIAL TESTS

Isotropically consolidated undrained (CIU) tests were performed in conventional triaxial equipment; anisotropically consolidated (CAU) tests were performed in the hydraulic stress path equipment designed by Bishop and Wesley (1975). The Bishop and Wesley cell and the electronic controller for operating the cell are briefly described in the Appendix F. In both cases, the specimens were 38mm x 76mm.

The types of test performed and the samples are listed below.

1. CIU tests on 7 specimens trimmed vertically and 6 specimens trimmed horizontally from the block samples. The range of consolidation pressures were from 0 to 450

kPa. The purpose was to obtain strength parameters within the overconsolidated and normally consolidated range of stresses and to investigate anisotropic behaviour.

2. CIU tests on unweathered clay tube samples consolidated isotropically to the estimated effective overburden stress. The following samples were tested:
    a. UA1 - samples 1-2, 1-3, 1-4, 1-6a.
    b. UA2 - samples 2-4, 2-6, 2-8b, 2-10.
    c. UA5 - samples 5-4a, 5-6a, 5-6b, 5-8, 5-9.
    d. UA3 - samples 3-7, 3-8, 3-9.
    e. UA4 - samples 4-4, 4-6, 4-7a, 4-8a, 4-9.
3. CAU tests on unweathered clay tube samples consolidated anisotropically to in-situ stresses where the lateral stresses were the measured ones. The following samples were tested:
    a. UA5 - sample 5-4b.
    b. UA4 - samples 4-7b, 4-8b.

    It is to be noted that the measured $K_0$ was in many cases close to unity and although the samples were consolidated to the in-situ stresses with a $K_0$ of one they are classified as CIU tests.
4. CAU tests on unweathered clay tube samples consolidated to the effective overburden stress under conditions of zero lateral strain. The following samples were tested: UA2 - samples 2-8a and 2-9.
5. CIU tests on weathered brown clay tube samples

consolidated isotropically to

a. the estimated overburden stress. The samples were 1-1A, 2-1, 5-2 and 3-4.

b. stresses past the preconsolidation pressures. The samples were 5-1a, 5-1b.

The test results on these samples are given in Appendix E.

All samples tested were 38 mm in diameter and 76 mm high and the procedures adopted are those described by Bishop and Henkel (1962). A backpressure of 200 kPa was used in all tests and was found to be adequate for sample saturation, generally giving B values larger than 0.97. Side drains for more efficient porewater equalization and 0.3 mm rubber membranes were used. The rate of strain in all tests was 0.5 percent per hour.

In the present study, tests were carried to large strain of about 15% so that corrections had to be made to account for the restraint imposed by the rubber membrane and side drain. Bishop and Henkel (1962) estimated that the correction is of the order of 12 kPa at 15 percent strain. Theoretical expressions for membrane corrections were derived by Henkel and Gilbert (1952) for samples failing in a plastic configuration and by LaRochelle (1967) for samples failing along a single plane. Since all the samples of the Genesee Clay failed along a single plane, an attempt was made to use LaRochelle's approach. However, the latter yielded unreasonably high corrections for the combined membrane and side drain effects. Therefore, it is believed that because of the complexity of the corrections, empirical correlations are likely to be more reliable. Empirical corrections for membrane are given by Chandler (1966) and for membrane and side drain by Balkir and Marsh (1974).

For the tests on the Genesee Clay, the soil samples normally bulged until the peak strength was reached and then shearing occurred along a single plane. It is to be noted that for samples containing slickensides, movement normally started along different planes before finally failing along one of these planes. However, for the correction, the displacement was assumed to have occurred along the plane with the most movement. Therefore, for the area correction, the specimen was assumed to increase in area until the peak strength and thereafter, the area decreased with strain when shearing starts on a single plane. For samples failing along a single plane, the area of contact, A, is easily shown to be equal to:

$$A = \left[2r^2\sin^{-1}(x/r) + 2x\sqrt{(r^2-x^2)}\right]_{x=\frac{\Delta h\cot\alpha}{2}}^{x=r} \quad \ldots\ldots\ldots(5.1)$$

where r=radius of sample

$\Delta h$=axial displacement

$\alpha$=angle of inclination of the failure plane to the horizontal.

For membrane and side drain correction, it was found that the correction due to bulging was minimal (of the order of 3 to 4 kPa) up to the peak strength and was, therefore, neglected. The Balkir and Marsh (1974) empirical correlations were used to correct the triaxial test results; it should be noted that these corrections were obtained from simulated failures along a surface inclined at 52° to the horizontal and since most of the shear failures occurred at about 55° in the present case, these corrections are believed to be appropriate.

For comparison, the curve produced after applying Chandler's correction for membrane restraint only is also drawn on Fig. 5.1 which is an example of the stress-strain curve for a very brittle failure. If the side drain correction is added to that of the membrane in this example, both corrections by Chandler (1966) and Balkir and Marsh (1974) are in agreement.

## 5.6 LABORATORY DETERMINATION OF THE COEFFICIENTS OF EARTH PRESSURES

### 5.6.1 Introduction

The coefficients of earth pressure referred to in this section are:

1. the $K_0$ of the clay in its normally consolidated state which is also referred as $K_0(nc)$,
2. the existing in-situ $K_0$,
3. the maximum horizontal stress or the horizontal preconsolidation pressure that the clay experienced in

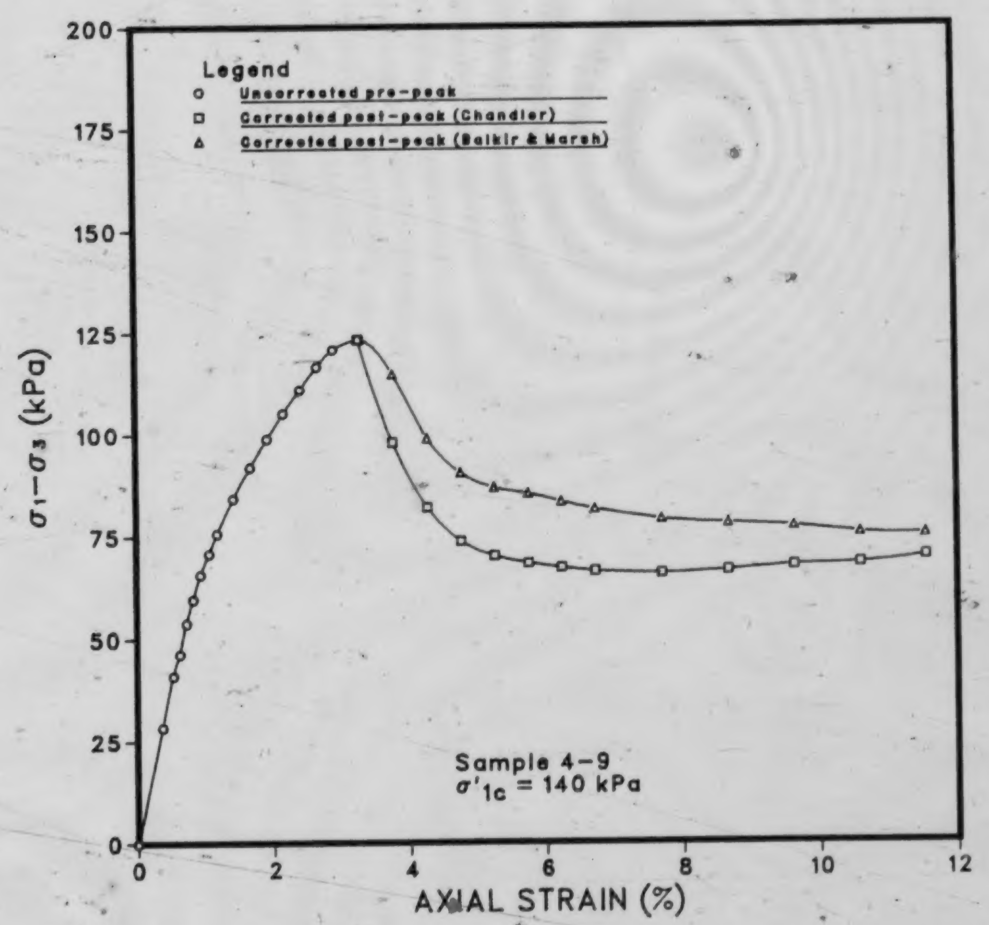

Figure 5.1 Corrected stress-strain curve for brittle failure.

the past.

These parameters will be used as a basis of comparison against the lateral stresses measured from in-situ tests.

### 5.6.2 Determination of the normally consolidated $K_0$

The normally consolidated $K_0$ can be determined by the method proposed by Bishop (1958) whereby a soil sample is consolidated under a combination of vertical and lateral stresses so that the condition of zero lateral strain is satisfied. However, the soil has to be stressed beyond the preconsolidation pressure when the curve of horizontal stress against vertical stress merged with the virgin compression line (Chandler, 1967). In the case of clay, Bishop (1958) recommended a steady but very slow rate of loading to avoid built-up of significant porewater pressure gradients in order to satisfy the zero lateral strain condition. Various methods of checking the lateral strain on the specimen are described by Bishop and Henkel (1962) and Al-Hussaini (1981). In this study, the burette method was used and consisted of adjusting the axial and cell pressures so that the volumetric and axial strains were equal.

The test was performed on a 38x76 mm specimen in the hydraulic stress path cell designed by Bishop and Wesley (1974). As the test duration was long, 2 membranes with a thin film of silicone grease between them were used to reduce the infiltration of water from the cell into the soil specimen. Crooks and Graham (1976) reported that such an arrangement reduced the leakage to about 0.1 $cm^3$ per day. Fig. 5.2 shows the results of the test on a specimen from a block sample. The estimated in-situ vertical stress for the sample is 60 kPa and the preconsolidation pressure is 120 kPa. The $K_0$ for the normally consolidated range is 0.6 which gives a $\phi'$ of 23° if Jaky's formula that

$$K_0 = 1 - \sin\phi' \quad \ldots\ldots\ldots\ldots\ldots\ldots\ldots\ldots\ldots\ldots (5.2)$$

is assumed. This value of $\phi'$ is in agreement with the value of 20° determined in consolidated undrained triaxial tests.

Using the rebound curve, a laboratory relationship of the overconsolidation ratio (OCR) against $K_0$ is plotted in Fig. 5.3; this relationship will be used in Chapter 6.

### 5.6.3 Estimation of the existing in-situ $K_0$

An indirect method of measuring the existing in-situ $K_0$ was proposed by Skempton (1961) and consisted of determining the capillary pressure in undisturbed samples. Skempton suggested four methods of determining the capillary pressure of which the measurement of porewater suction is the most direct method. Wroth (1975) discussed the assumptions on which the method is based; the most important assumption is that there is no loss of capillary suction due to sampling disturbance and to the delay between sampling and testing. The laboratory experiments of Kirkpatrick and Rennie (1975) showed that samples of kaolin lost 80% of the suction after

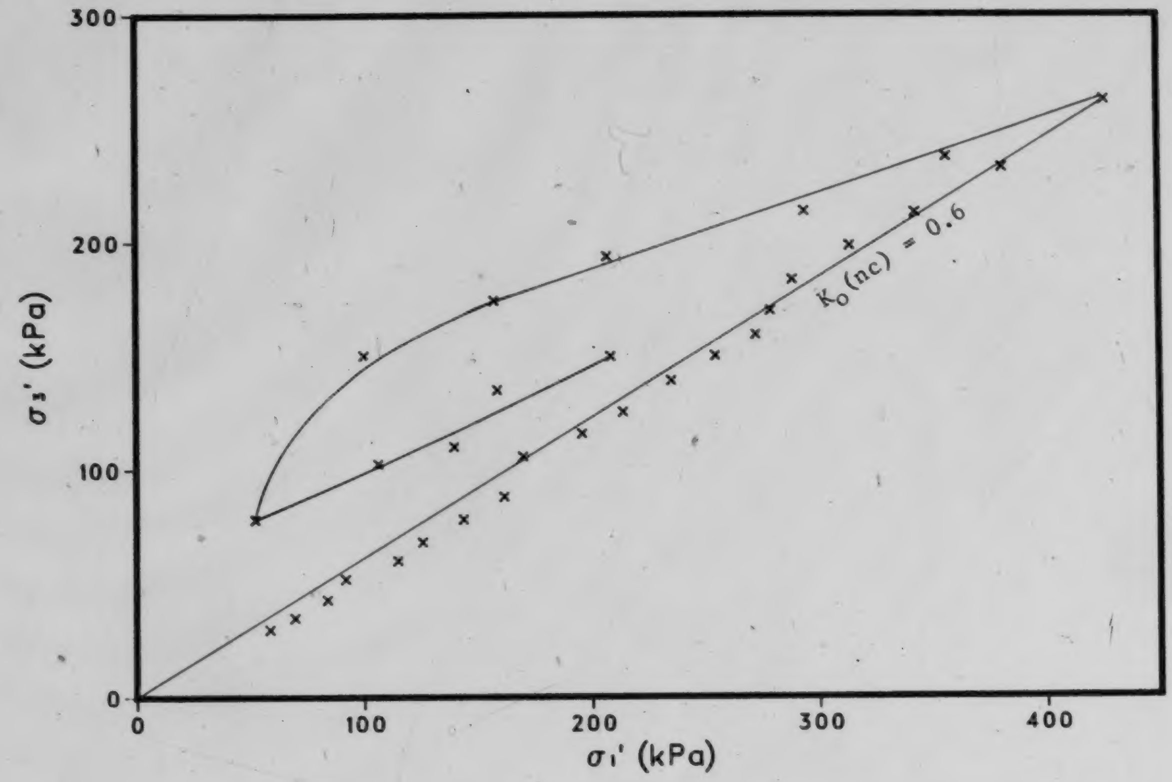

Figure 5.2 Determination of normally consolidated $K_o$.

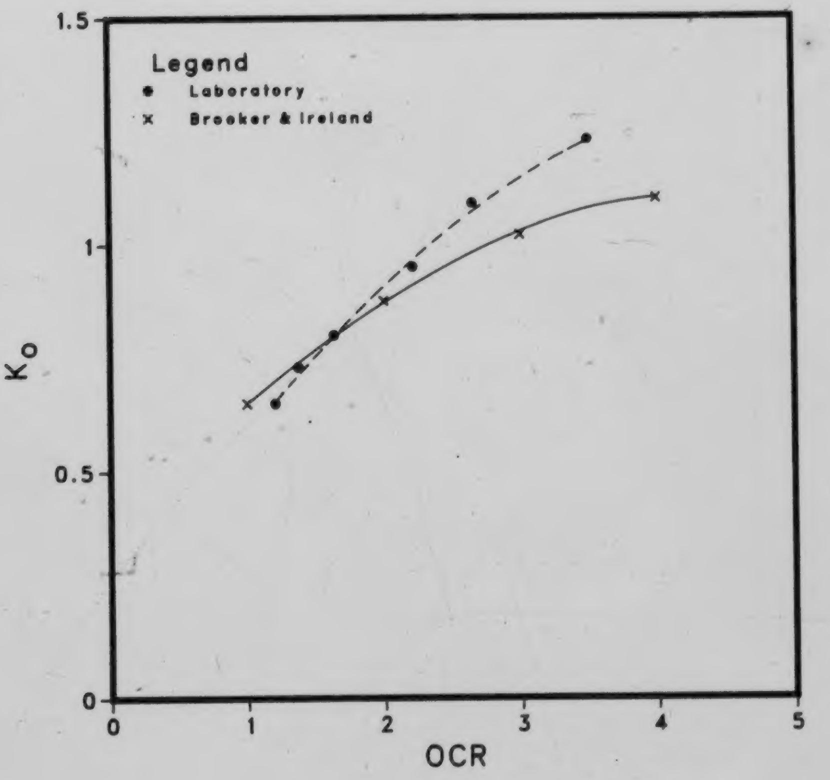

Figure 5.3 Variation of $K_0$ with OCR.

50 days storage whereas Hight et al (1985) reported that loss of suction in low plastic clay samples was insignificant during a two-year period. Moreover, Burland and Maswoswe (1982) found that the porewater suction method on specimens trimmed from 105 mm diameter thin-walled tube samples gave reasonably good estimates of $K_0$ when compared to the self-boring pressuremeter tests although the storage time was not mentioned.

In this study, the porewater suction was measured by following the procedures described by Burland and Maswoswe (1982). The test was performed on a 38x76 mm specimen and care was taken to eliminate loss of suction pressure before measurement was made. This included mounting the specimen on a ring of thin wire to prevent contact with the saturated porous disc. Side drains were not used and silicone grease was applied on the perimeter of the top cap and sample pedestal of the triaxial cell to eliminate seepage of water underneath the membrane. The other precaution taken was to calibrate the pressure transducer just before the test and the transducer for measuring the porewater pressure was also used to set the cell pressure to be applied. This was done to eliminate the errors induced by using different transducers to measure the porewater and cell pressure.

The test was performed on a specimen from a block sample after about 2 months of storage and a cell pressure of 500 kPa was applied over a period of about 2 days. On application of this high pressure, contact of the sample with the porous disc was made as the thin wire became embedded into the clay and the porewater pressure was monitored from the base of the cell. The difference between the cell and porewater pressure generated was the suction pressure existing in the sample. The value of $K_0$ was derived from the following expression:

$$K_0 = (p_k'/\sigma_{vo}' - A_s)/(1 - A_s) \quad ...............(5.3)$$

where $p_k'$ = initial suction pressure,

$\sigma_{vo}'$ = estimated in-situ vertical stress,

$A_s$ = pore pressure coefficient.

For the block sample, the measured $p_k'$ was 67 kPa and $\sigma_{vo}'$ was 60 kPa. After the suction measurement,the specimen had a B value of 0.97 which was comparable to those of 0.97 and 0.99 achieved in the tests by Burland and Maswoswe (1982). Using the above equation and typical values of $A_s$ of 1/2 and 1/3, the following values of $K_0$ were obtained:

$A_s$ = 1/2, $K_0$ = 1.24

$A_s$ = 1/3, $K_0$ = 1.18

Therefore, $K_0$ for the block sample is approximately 1.2. This value of $K_0$ is consistent with the values of lateral stresses measured in the region as shown in Chapter 6.

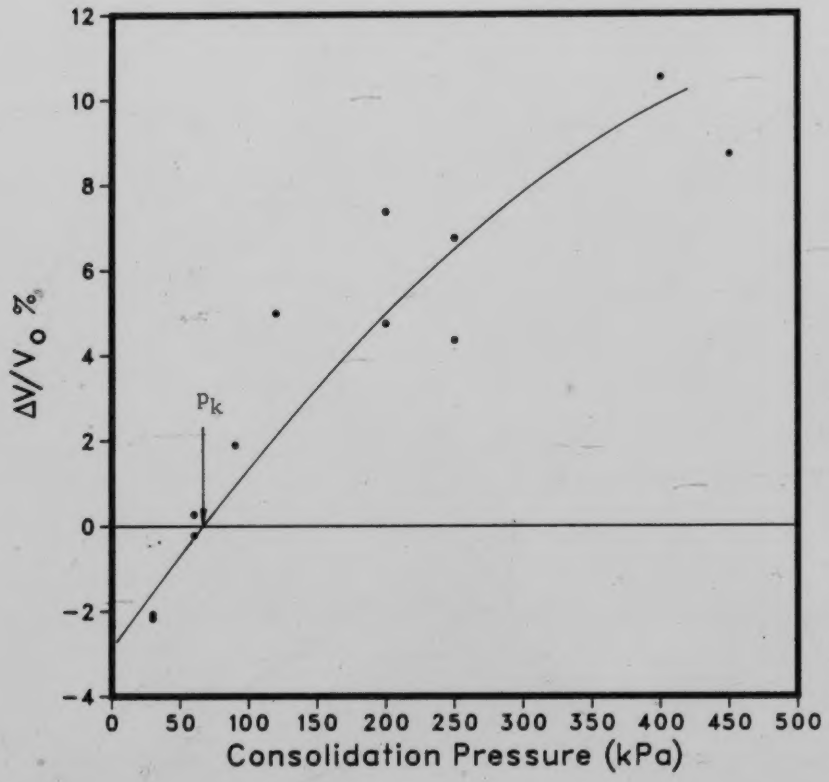

Figure 5.4 Volume change against isotropic consolidation pressure.

The value of the suction pressure is confirmed by the plot of $\Delta V/V_0$ (where $\Delta V$ is the volume change and $V_0$ is the initial volume of the specimen) against isotropic consolidation pressure presented in Fig. 5.4; the latter was obtained from the consolidation stage of isotropically consolidated undrained triaxial tests on specimens from the block samples. The estimated suction when $\Delta V$ is zero is between 60 and 65 kPa.

Suction tests were performed on some of the tube samples, but the suction pressures measured gave values of $K_0$ which were lower than the $K_0$(nc) of 0.6 and were not comparable to the field measurement. These data indicate that the tube samples have lost some of their suction pressures as a result of the sampling disturbance.

Another method for estimating the in-situ horizontal stresses was described by Poulos and Davis (1972). This test was performed in the Bishop and Wesley cell on 1 specimen from the block sample to investigate its application for lightly overconsolidated clays. The specimen was first consolidated with a ratio of lateral effective stress to vertical effective stress of 0.5 where the vertical effective stress is equal to the effective overburden stress. The sample swelled under that pressure as was expected and was allowed to do so before the next increment of pressure was applied; this stage was considered the datum for the measurement of volume change during consolidation. Consolidation of the specimens was continued with increasing lateral stress while the vertical stress was kept constant. The volume change as well as the axial deformation were monitored. A graph of volume change against lateral stress was plotted in Fig. 5.5 where a change in slope indicates the onset of yielding which Poulos and Davis (1972) considered as representing the estimated in-situ horizontal stress. But the question is whether the suggestion of Poulos and Davis that this method gives an estimate of the in-situ state of stress is valid. This is explained by considering Fig. 5.6 which shows the stress path followed during the test and the yield envelope for the block sample determined as explained in section 5.8. It is known that the position of the yield envelope is controlled by the past maximum state of stress and unless the soil had a stress history other than one of normal consolidation, the yield point obtained by the Poulos and Davis method is just another point on the yield envelope and does not represent the present state of stress. Therefore, the method is not valid for determining the state of stress for a lightly overconsolidated soil.

## 5.7 DETERMINATION OF HORIZONTAL PRECONSOLIDATION PRESSURE

This test consists of performing a one-dimensional consolidation test on a specimen that has been trimmed in a horizontal direction. The horizontal preconsolidation pressure was first suggested by Zeevaert (1953) as a means of estimating the in-situ lateral stresses. This method was

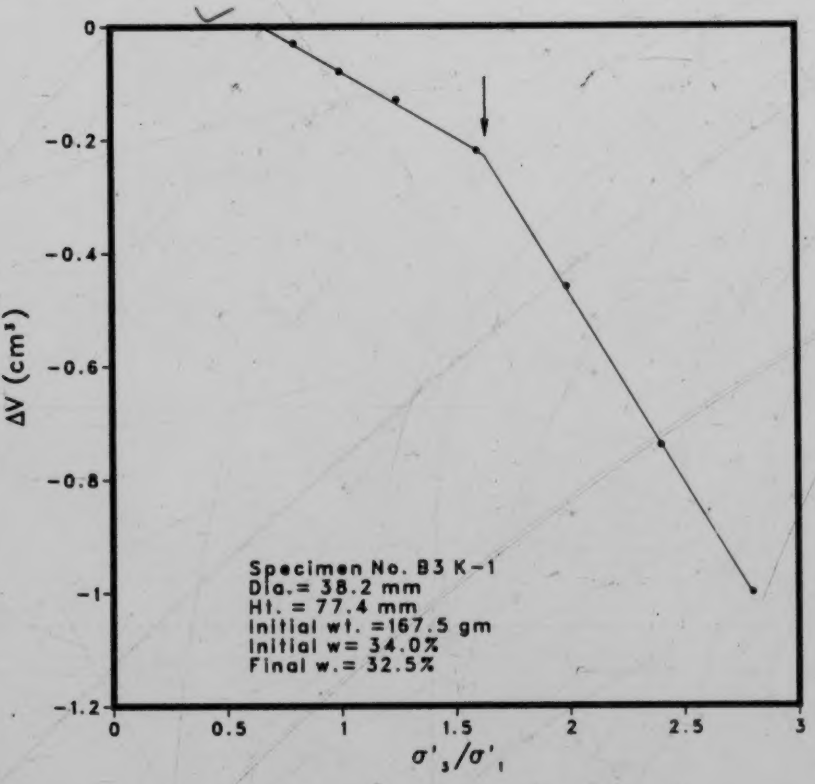

Figure 5.5 Determination of lateral yield point by Poulos and Davis method.

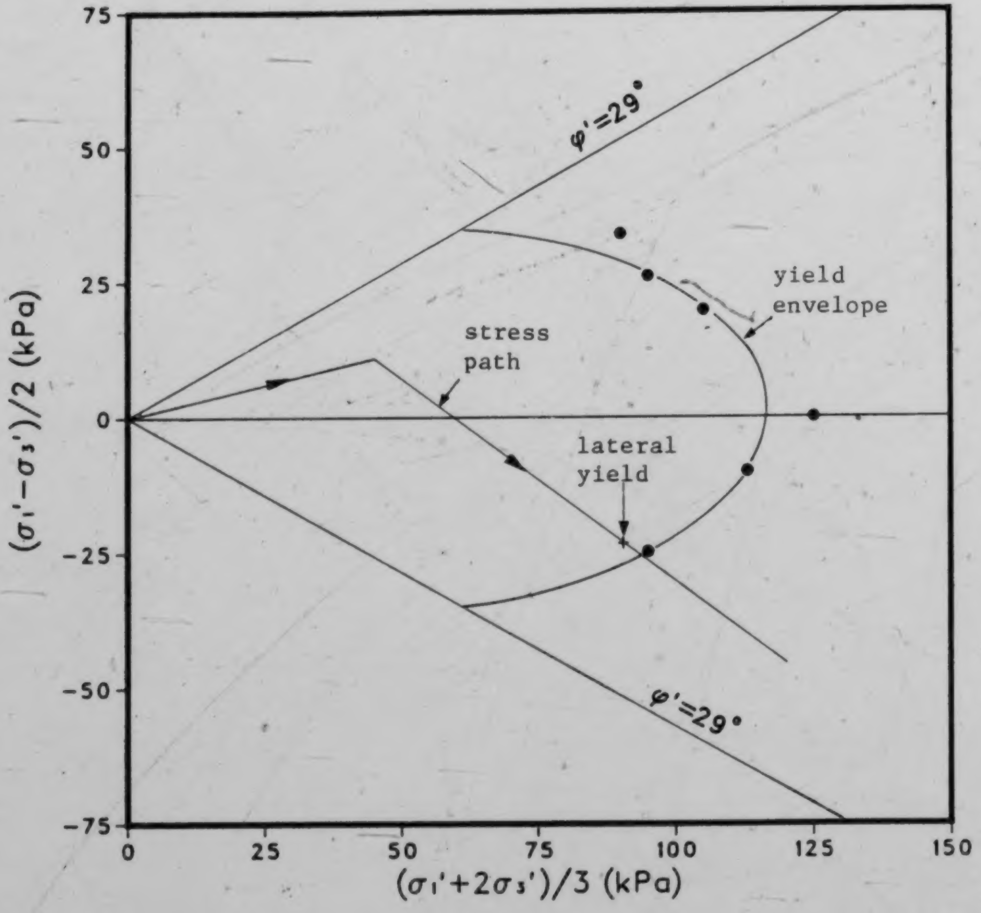

Figure 5.6 Stress path followed in Davis and Poulos method.

used by Esu and Calabresi (1969) to determine the high lateral stresses in a clay deposit. Kenney and Folkes (1979) stated that "a measure of the maximum past induced radial stress could be determined from oedometer consolidation tests performed on specimens rotated 90°". The use of the horizontal preconsolidation pressure was further amplified by Tavenas et al (1975) who suggested that the ratio of the horizontal preconsolidation pressure to the vertical one is equivalent to the in-situ $K_0$.

Consequently, the horizontal preconsolidation pressure was determined for tube samples from different elevations so that samples subjected to a wide range of in-situ $K_0$ were tested. The results are summarised in Table 5.1. In this table, the horizontal preconsolidation pressure is denoted as $\sigma_{ph}'$ whereas the vertical one is represented as $\sigma_p'$ and the $K_0$ values were obtained from the total stress cell measurements. The ratios $\sigma_{ph}'/\sigma_p'$ should approximate $K_0(nc)$ if it is assumed that the $\sigma_{ph}'$ was induced when the vertical effective stress of the soil reached the maximum value of $\sigma_p'$ during the consolidation history. However, the ratios $\sigma_{ph}'/\sigma_p'$ presented in Table 5.1 do not approach the value of 0.6 for $K_0(nc)$. There are two possible explanations for this deviation: either the high value of $\sigma_{ph}'/\sigma_p'$ indicates that lateral stresses other than those due to vertical effective stress changes were induced or the stress path followed in the consolidation test is such that an apparent horizontal preconsolidation pressure is obtained. However, unless the

Table 5.1 Consolidation test results on vertical and horizontal samples.

| Sample No | Orientation | $K_o$ | $\sigma'_{vo}$ (kPa) | $\sigma'_{p}$ (kPa) | $\sigma'_{ph}$ (kPa) | OCR | $\frac{\sigma'_{ph}}{\sigma'_{vo}}$ | $\frac{\sigma'_{ph}}{\sigma'_{p}}$ |
|---|---|---|---|---|---|---|---|---|
| 1-4 | vert | 0.89 to 1.42 | 120 | 140 | | 1.17 | | |
| | horz | | | | 140 | | 1.17 | 1.00 |
| 2-8 | vert | 1.05 | 220 | 310 | | 1.41 | | |
| | horz | | | | 260 | | 1.18 | 0.84 |
| 5-5 | vert | 1.43 to 1.78 | 140 | 310 | | 2.21 | | |
| | horz | | | | 230 | | 1.64 | 0.74 |
| 5-7 | vert | | 165 | 255 | | 1.55 | | |
| | horz | | | | 215 | | 1.30 | 0.84 |
| 3-6 | vert | 1.99 | 77.6 | 300 | | 3.90 | | |
| | horz | | | | 270 | | 3.50 | 0.90 |
| 3-7 | vert | 1.84 | 90.7 | 175 | | 1.93 | | |
| | horz | | | | 205 | | 2.30 | 1.17 |
| 3-8 | vert | | 103.8 | 215 | | 2.07 | | |
| | horz | | | | 260 | | 2.50 | 1.21 |
| 6-4 | vert | 0.98 | 76.7 | 180 | | 2.35 | | |
| | horz | | | | 160 | | 2.09 | 0.89 |
| B1 | vert | 1.20 | 60.0 | 115 | | 1.92 | | |
| | horz | | | | 120 | | 2.00 | 1.04 |

stress path followed in the test is known, it is not possible to give any meaningful interpretation to $\sigma_{ph}'$. Consequently, the suggestion of Tavenas et al (1975) to use the ratio $\sigma_{ph}'/\sigma_{vo}'$ (where $\sigma_{vo}'$ is the effective overburden pressure) as a means of evaluating the in-situ $K_0$ does not appear to be valid.

## 5.8 DETERMINATION OF YIELD ENVELOPE

When a soil mass is loaded, yielding is said to occur at the point of transition from elastic to plastic behaviour. In fact, the vertical and horizontal preconsolidation pressures and the lateral stress determined by the Poulos and Davis method represent points on the yield envelope. Yield envelopes for postglacial clays had been investigated by Mitchell (1970), Crooks and Graham (1976), Tavenas and Leroueil (1977) and Baracos et al (1980). The various features associated with yield envelopes for undisturbed clays were discussed by Crooks and Graham (1976) and Tavenas and Leroueil (1977). The position of the yield envelope within a stress space is necessarily governed by its past stress history and Tavenas and Leroueil (1979) found that this position is fixed by the preconsolidation pressure.

In the present study, the purpose of determining the yield envelope is to evaluate the effects of the past stress history on the characteristics of the clay and to predict the response of the clay to stress history due to construction work as shown in Chapter 7.

### 5.8.1 Laboratory procedures

Both undrained and drained tests can be used to determine the yield envelope (Parry and Wroth, 1981). The undrained tests consist of applying stresses on the soil sample and measuring the pore pressures developed; yielding is indicated by a sharp increase in pore pressure. This test procedure has the advantage that it is faster than the drained test but there is no control on the effective stress path. However, the drained and undrained tests do not identify the same yield envelope (Graham, 1985).

For this study, drained tests were used because the exact stress path can be imposed on the soil sample. Mitchell's (1970) approach of consolidating the sample from an initial state of zero stresses was adopted although other researchers such as Crooks and Graham (1976) recommended initial consolidation to the estimated in-situ stresses prior to loading along different paths. It is believed that the yield envelope is independent of the stress path followed within the elastic range so that both approaches will give the same envelope.

The dimensions of the samples were 38x76 mm and the tests were performed in the Bishop and Wesley stress path cell. A backpressure of 200 kPa was applied and side drains were used to facilitate drainage. The samples were surrounded by two membranes coated with silicone grease in order to reduce the infiltration of water from the cell into the sample. The specimens were consolidated at various constant stress ratios. The stress increments were applied for a duration of 24 hours and a mean effective stress, $(\sigma_1'+2\sigma_3')/3$, increment of 15 to 20 kPa was applied at each stage. Volume change and axial deformation were measured at intervals and it was found that consolidation was completed within 24 hours. The lateral strain was calculated from the volumetric and axial strain assuming that :

volumetric strain = axial strain + 2 x lateral strain.

Difficulties were encountered in the interpretation of the results (Crooks et al, 1976 and Tavenas et al,1979) since yielding was sometimes not well defined along certain stress paths when components of strain were plotted against stresses. Crooks et al (1976) proposed the use of strain energy absorbed during consolidation as an indicator for locating yielding. The strain energy was computed after each stage of loading increment from the following:

$$W = \Sigma\{\sigma_1\delta\epsilon_1 + 2\sigma_3\delta\epsilon_3\} \quad \ldots\ldots\ldots\ldots\ldots\ldots\ldots\ldots(5.4)$$

where W = strain energy per unit volume

$\sigma_1$ and $\sigma_3$ = average effective stresses

$\delta\epsilon_1$ and $\delta\epsilon_3$ = strain increment.

The test results can then be plotted in the form of strain energy,W against the mean effective stress,$(\sigma_1 + 2\sigma_3)/3$. However, this method cannot be applied to tests at constant mean effective stress (Graham, 1985). Test results for a block sample are given in Fig. 5.7 and the stress paths investigated together with the resulting yield envelope are given in Fig. 5.8. The block sample has the following characteristics:

$\sigma'_{vo}$ = 60 kPa

$\sigma'_{p}$=120 kPa

Natural moisture content = 37%

Liquid Limit = 58%

Plastic Limit = 21%

% clay = 55

$\phi'$ = 29° within overconsolidated range (Fig. 6.21).

A discussion on the geotechnical application of the yield envelope for the Genesee Clay is found in Chapter 6 and 7.

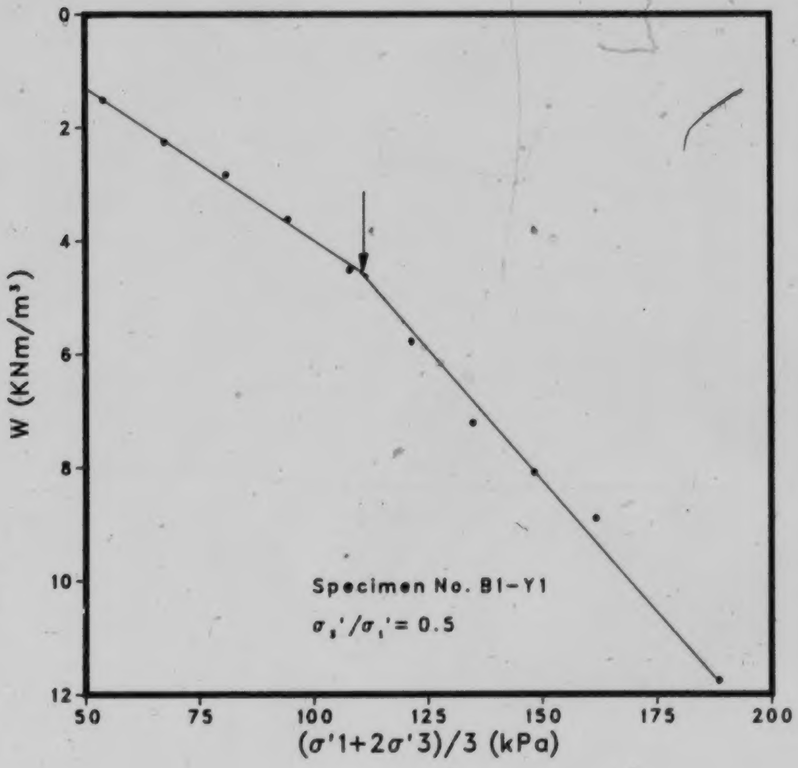

Figure 5.7 Example of determination of yield point.

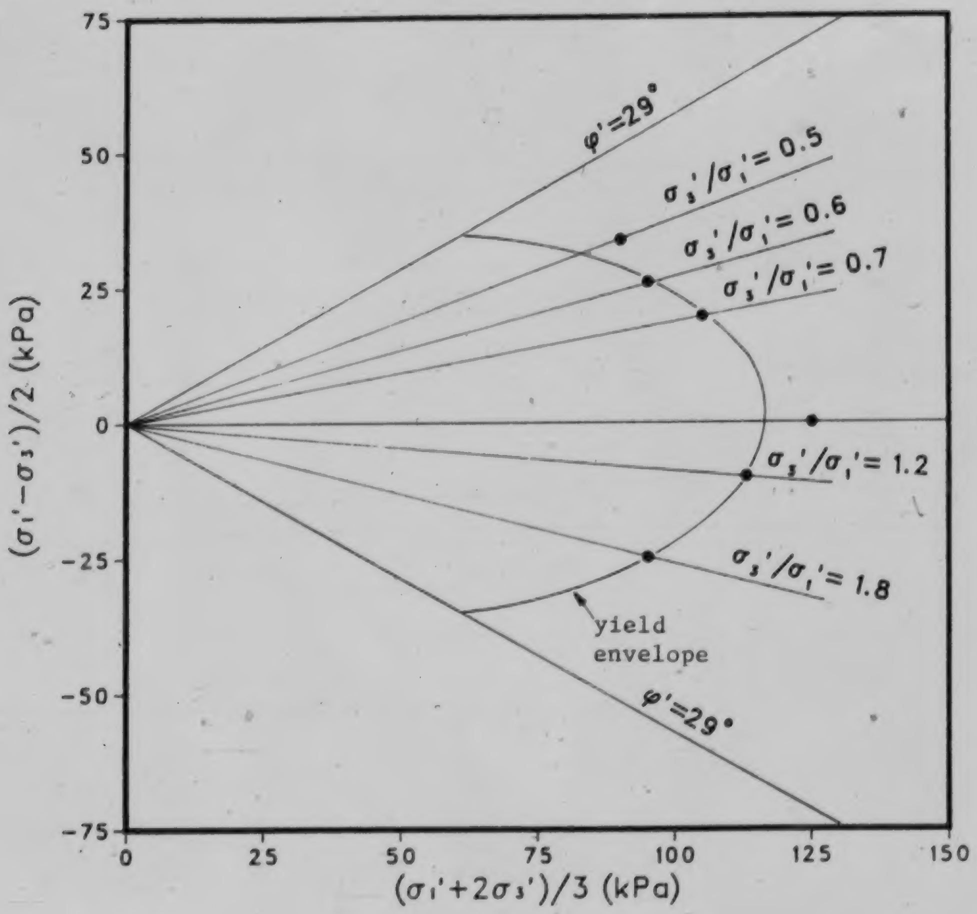

Figure 5.8 Yield envelope for Genesee Clay.

# 6. GEOTECHNICAL CHARACTERISTICS OF GENESEE CLAY

The engineering properties of the clay are discussed with reference to the geological characteristics described in Chapter 2 and 3. The main test results are summarised in Fig. 6.1 to 6.6 and the detailed laboratory test data are given in Appendix E.

## 6.1 CLASSIFICATION

Classification of clays was discussed by Terzaghi (1936), Skempton and Hutchinson (1969) and Bjerrum (1973). Terzaghi (1936) distinguished between soft and stiff clays on the basis of Liquidity Index so that soft clays have Liquidity Indices equal to or greater than 0.5 whereas stiff clays have Liquidity Indices closer to zero. Skempton and Hutchinson (1969) subdivided clays according to their plasticity characteristics and the two subdivision of interest for this project are the medium plasticity with liquid limit of 50 to 90 percent and high plasticity with liquid limit greater than 90 percent.

Based on the above guidelines and the plasticity characteristics given in Fig. 2.10 and 2.11 (Chapter 2), the Genesee Clay can be classified broadly as stiff fissured and medium plastic for the upper weathered brown layer and soft fissured and medium to high plastic for the unweathered clay layer. Besides, the weathered clay is heavily overconsolidated with overconsolidation ratio (OCR) greater than 5 and Liquidity Index of 0.1 to 0.2 whereas the

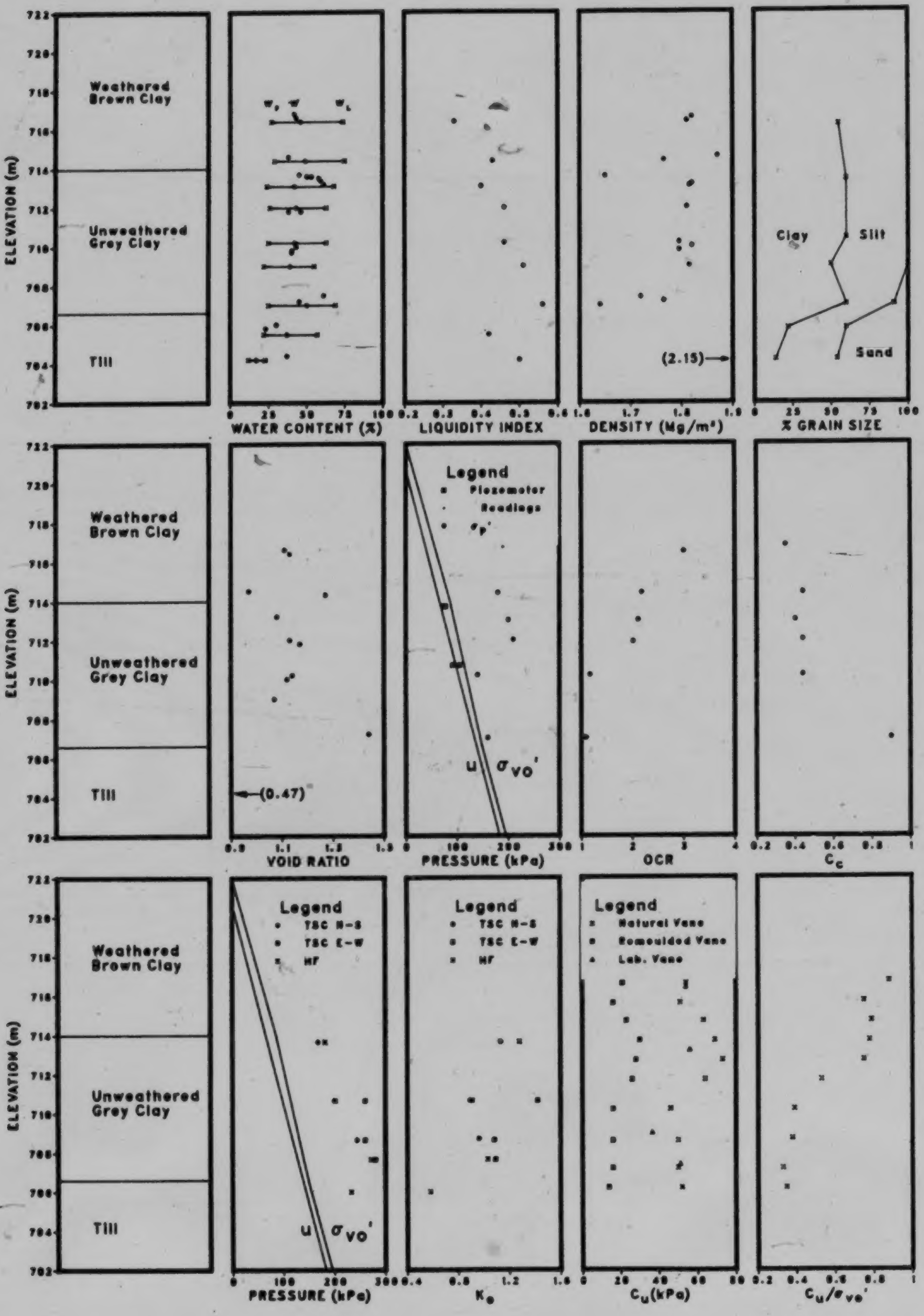

Figure 6.1 Summary of test results for UA1.

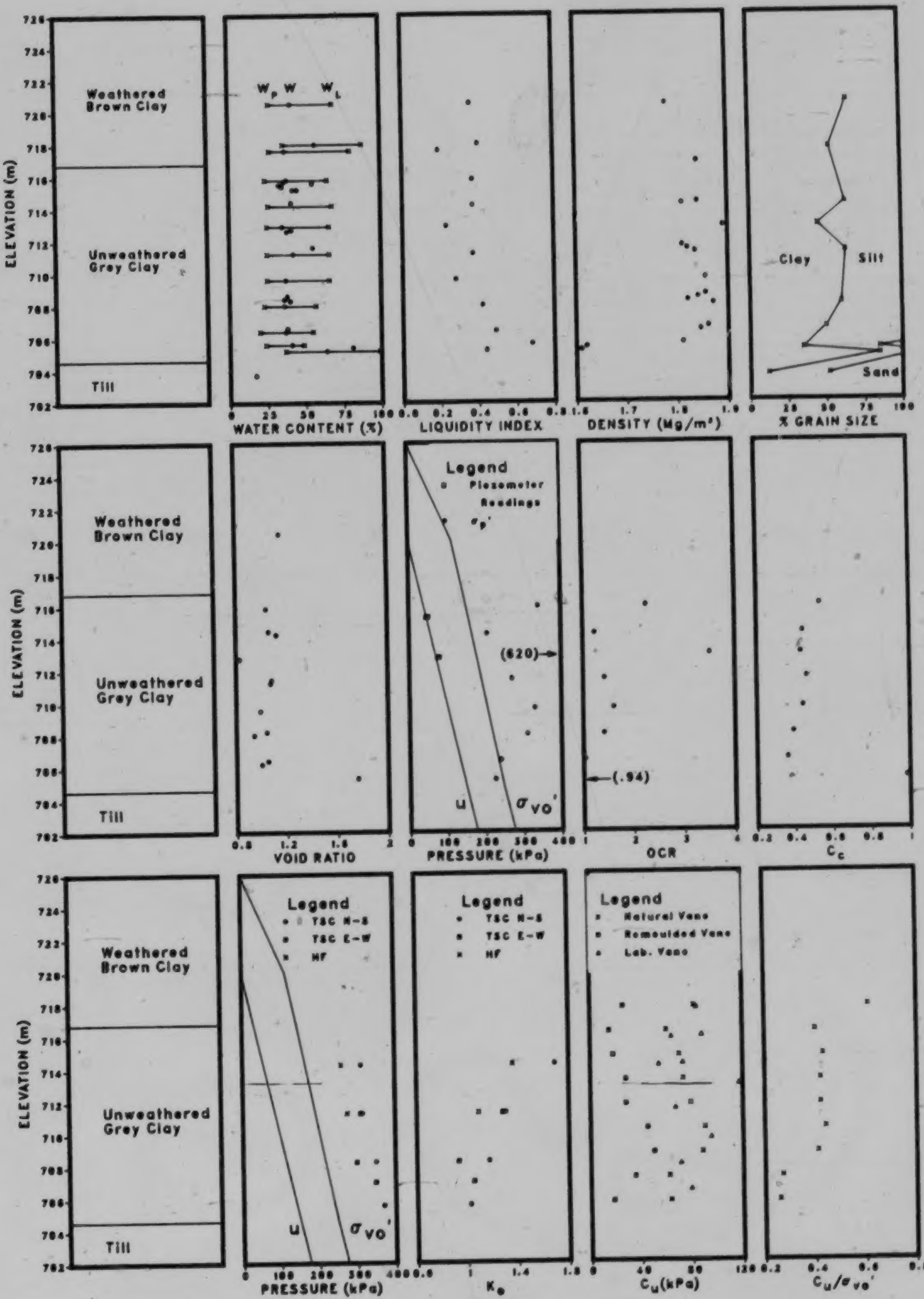

Figure 6.2 Summary of test results for UA2.

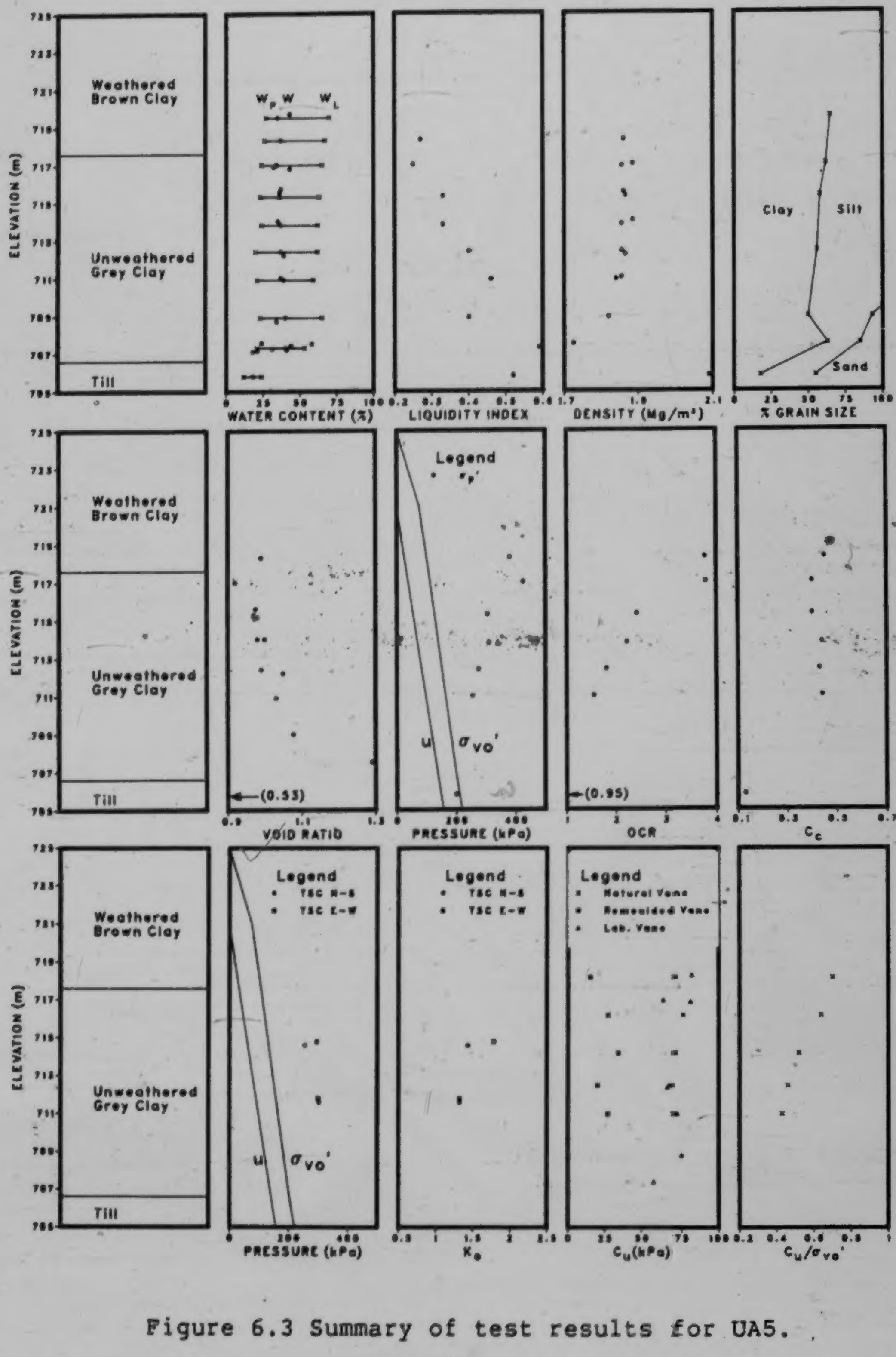

Figure 6.3 Summary of test results for UA5.

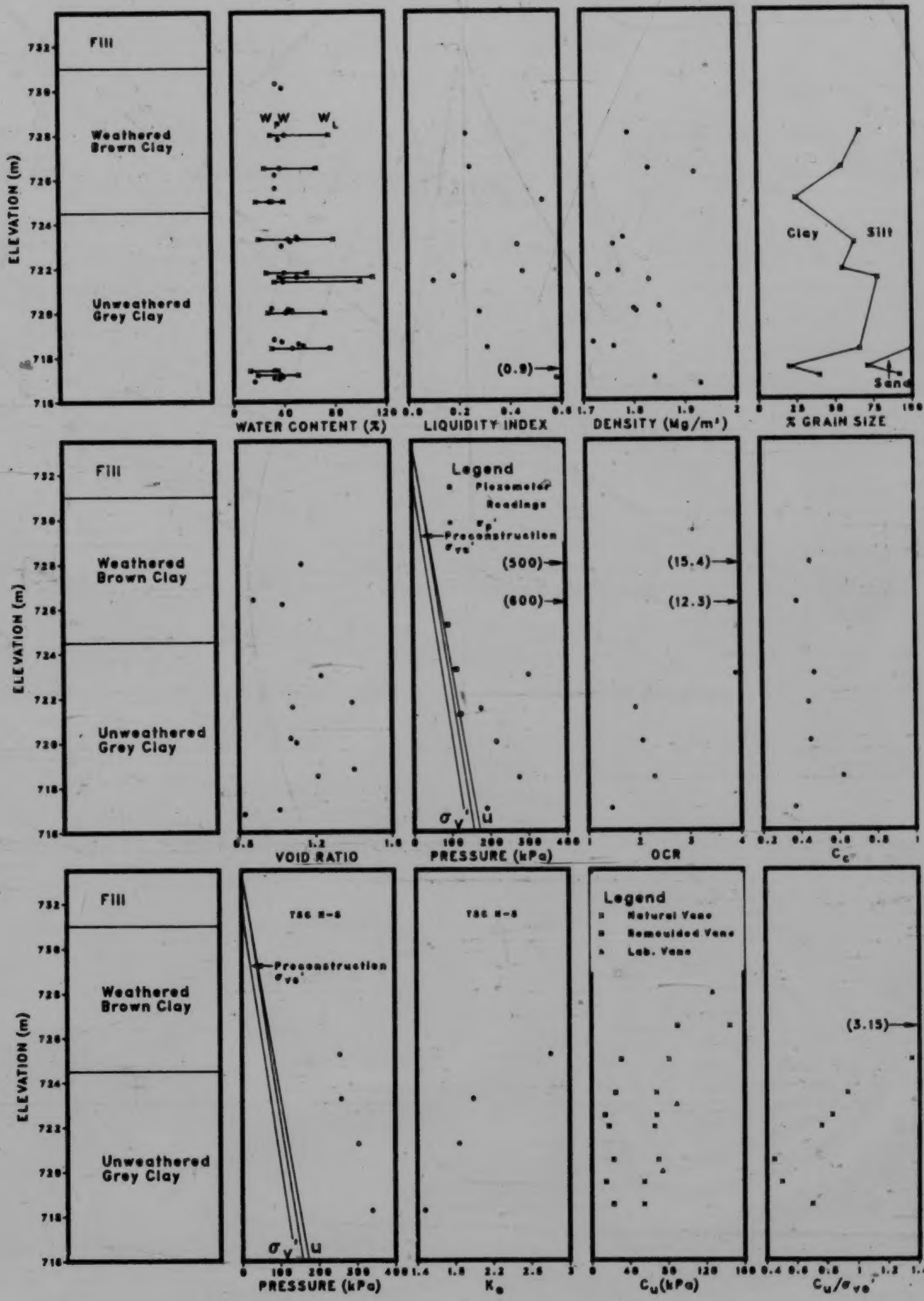

Figure 6.4 Summary of test results for UA3.

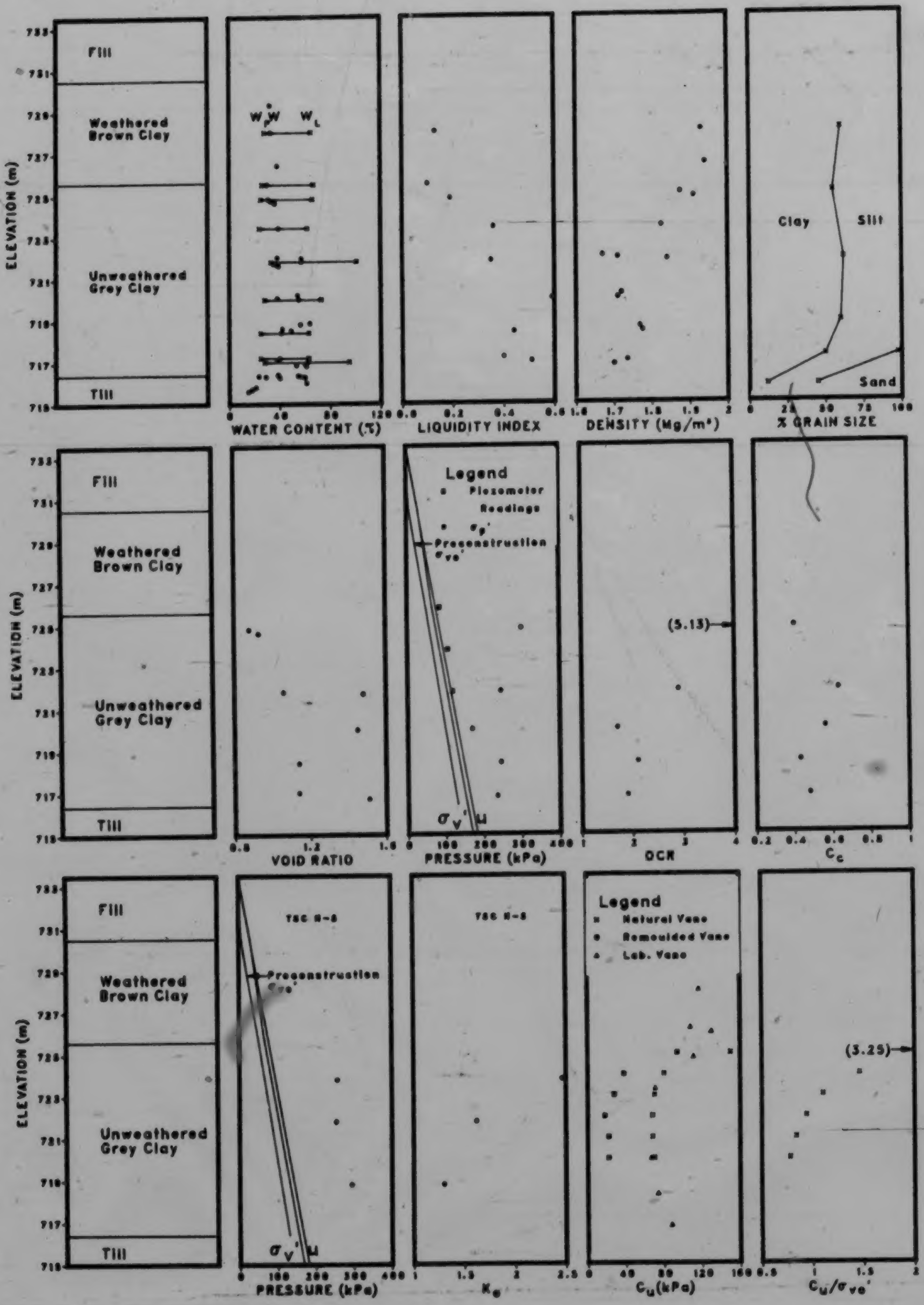

Figure 6.5 Summary of test results for UA4.

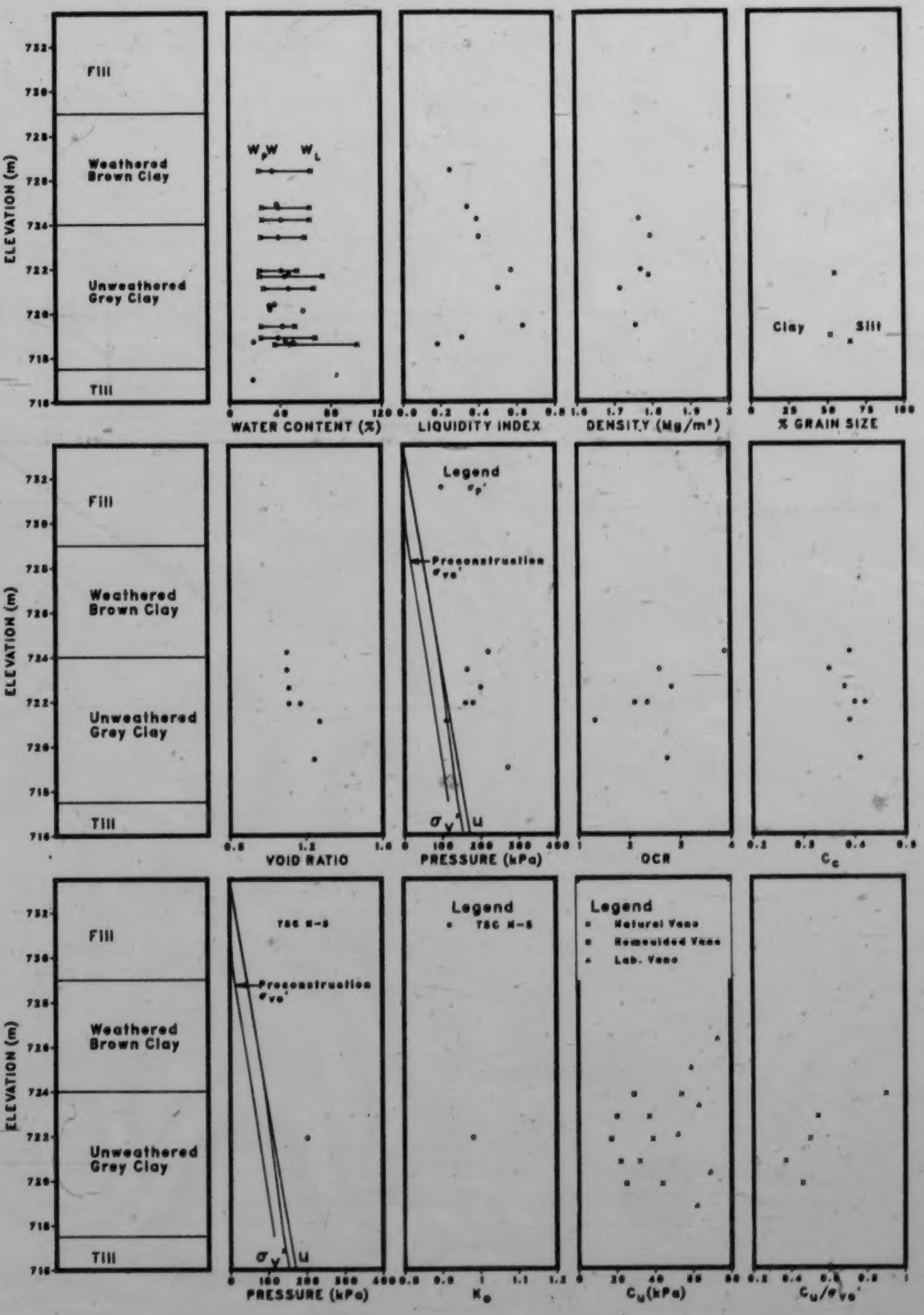

Figure 6.6 Summary of test results for UA6.

unweathered clay is lightly overconsolidated with OCR between 1 and 3. Based on the in-situ vane tests, the sensitivity of the clay is between 2 and 3.

## 6.2 CONSOLIDATION CHARACTERISTICS

The consolidation history was dominated by lowering of the groundwater table after deposition; this has produced an upper weathered zone with overconsolidation ratio higher than 5 due to dessication. The intermediate exposure of the lake bottom affected the deposit only by producing a thin layer (about 1 metre thick) of stiff fissured crust but did not affect the clay immediately below the crust which is only lightly overconsolidated. The variation in overconsolidation is also reflected in the Liquidity Index as shown in Fig. 6.1 to 6.6. On the other hand, based on the OCR - Depth profiles, there is no indication of significant delayed consolidation or erosion.

The swelling pressures measured in the oedometer are mostly in the range of 20 to 35 kPa with the high plastic dark grey layers having a higher swelling potential. The swelling pressures for all the test samples are given in Table E.2 (Appendix E).

The compression index,Cc, of the unweathered medium plastic light grey clay varies from 0.4 to 0.5 which agrees with relationships such as

$$Cc = 0.009(w_L - 10) \quad \ldots\ldots\ldots\ldots\ldots\ldots\ldots\ldots (6.1)$$

given by Terzaghi and Peck (1967) for normally consolidated clays. On the other hand, the compression index of the high plastic dark grey clay varies from 0.6 to 1.0 and is due to the presence of large voids between the microlaminae as explained in section 2.3.2. However, the dark grey clay itself is not likely to cause serious consolidation problems because of its limited thickness within the clay mass.

An example of the variation of the coefficient of consolidation, $c_v$, with pressure is shown in Fig. 6.7 for the samples from UA1. As expected, there is a drop in $c_v$ after the preconsolidation pressure is exceeded. This drop in $c_v$ is accompanied by a drop in $m_v$ as shown in the examples given in Fig. 6.8, an indication of the structural breakdown after the preconsolidation pressure.

Consolidation tests were also performed on samples trimmed horizontally; a comparison of the void ratio against log pressure curves for vertical and horizontal samples are given in Fig. 6.9. Parry and Wroth (1981) have shown that in consolidation tests on lightly overconsolidated clays for stress increments in the pre-yield range just in excess of the field stresses, the volume compressibility, $m_v$, in the horizontal direction is almost double that in the vertical direction as a result of structural anisotropy which is lost at consolidation pressures equal to 2.5 to 3 times the preconsolidation pressure. However, the tests on the Genesee Clay samples show that there is little difference in $m_v$ in the two directions as indicated in Fig. 6.10. This indicates

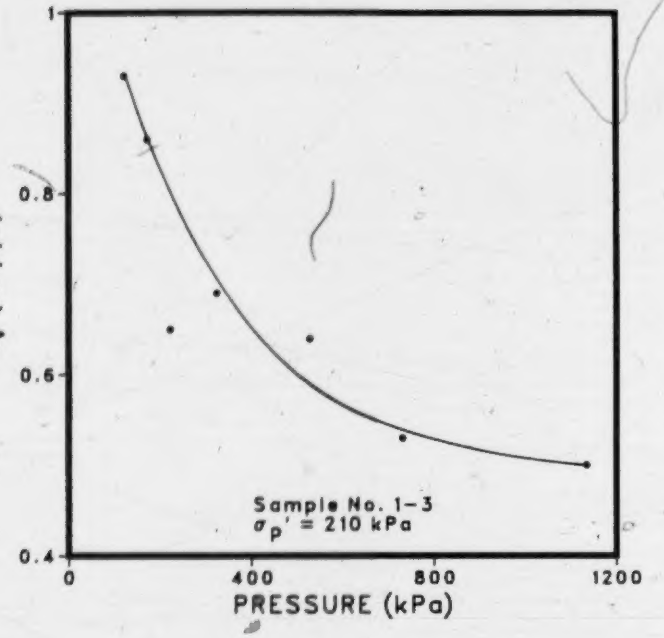

Figure 6.7 Variation of $c_v$ with pressure.

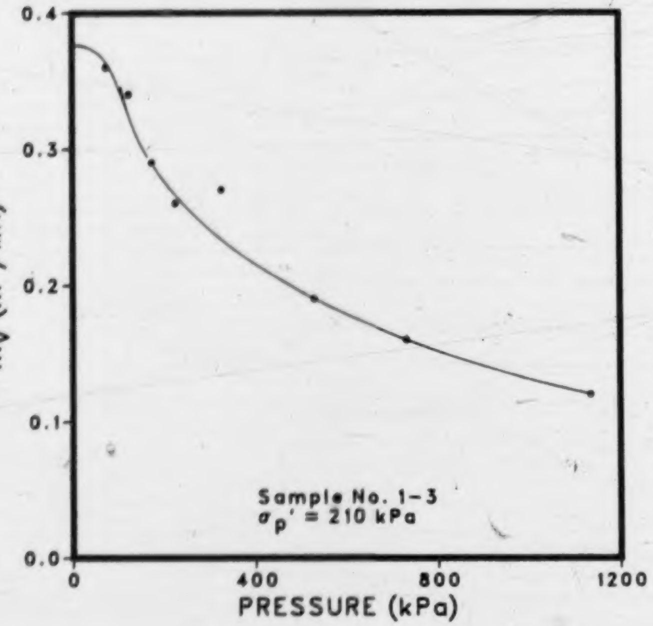

Figure 6.8 Variation of $m_v$ with pressure.

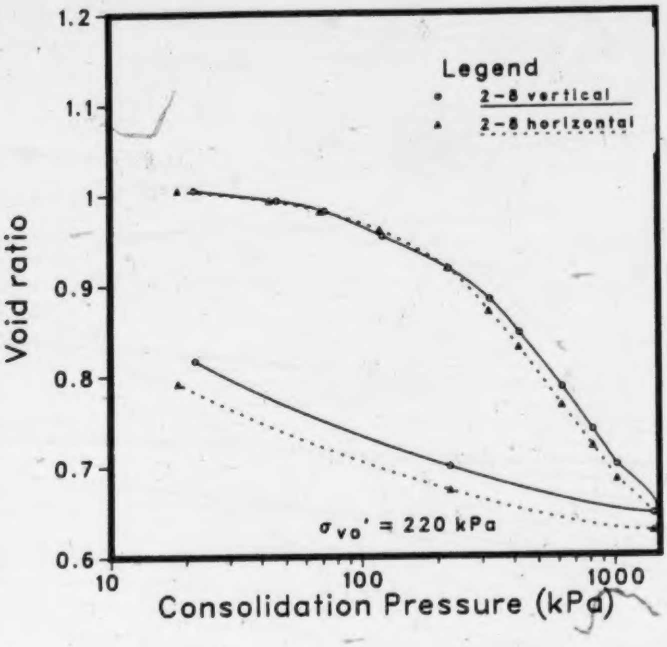

Figure 6.9 e-log $\sigma_v$ for vertical and horizontal specimens.

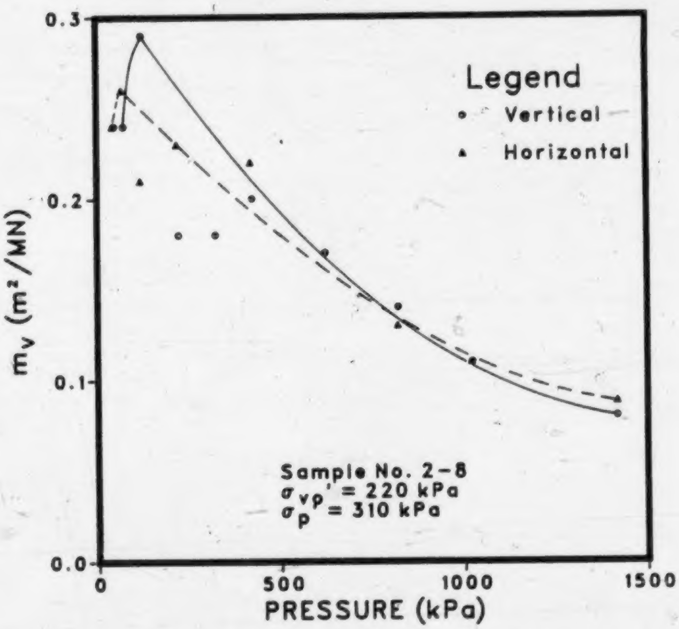

Figure 6.10 Comparison of $m_v$ for vertical and horizontal specimens.

the lack of structural anisotropy in the light grey clay as evidenced by the absence of particle orientation in Plate 3.5(a).

## 6.3 VARIATION IN LATERAL STRESSES

In the case of the simple geological process of sedimentation and subsequent erosion, the in-situ lateral stresses can be estimated from $K_0$-OCR relationships which have been proposed by many, for example, Brooker and Ireland (1965), Schmidt (1966), Wroth (1975) and Mayne and Kulhawy (1982). However, the warning of Burland (1979) against these oversimplifications is justified since the effects of various cycles of unloading and reloading on $K_0$ are still unknown and the lateral stresses can be affected by lateral unloading such as river downcutting (Morgenstern and Eisenstein, 1970), by tectonic forces (Henkel, 1970), by the bending of a stratum due to consolidation of an underlying stratum (Esu and Calabresi, 1969) and by manmade activities. Other unsolved problems related to $K_0$ are the effects of soil grain arrangement (Abdelhamid and Krizek, 1976) and of secondary compression (Mayne and Kulhawy, 1983 and Schmertmann, 1983). The field measurements at Genesee showed that the lateral stresses deviate from the $K_0$ - OCR relationships given by the references mentioned above and the important question to ask is whether the bottom meltout processes had any effect on the present in-situ stresses.

The discussion that follows is based on the results of the total stress cell measurements which were proved to be reliable as discussed in Chapter 4. Measurements were made in the north-south (N-S) and east-west (E-W) directions and in the north-south direction at the plant site. The results are presented in Fig. 6.1 to 6.6 and are given in terms of the orientation of the stress cells. Within the weathered clay, the lateral stresses are high with a $K_0$ approaching passive failure; this is shown in Fig. 6.4 for UA3 where a $K_0$ of 2.8 was measured and is approximately equal to the passive coefficient, Kp, calculated from

$$Kp = (1 + \sin\phi')/(1 - \sin\phi') \quad \ldots\ldots\ldots\ldots\ldots(6.2)$$

for $\phi'=27.8°$ from data presented in Fig. 6.20; however, $K_0$ decreases rapidly with depth within the unweathered clay.

The other observation that can be made is that there is an areal variation in the lateral stresses within the unweathered clay; this variation seems to be related to the topography since UA1 which is a topographic low has a lower $K_0$ than the topographic highs UA2 and UA5 at the cooling pond; similarly, at the plant site, a lower $K_0$ was measured at UA6 than at UA3 and UA4. This is made clear in Fig. 6.11 and 6.12 which are the combined data for the unweathered clay from Fig. 6.1 to 6.6. It is to be noted that in Fig. 6.11 and 6.12, the directions of the measured stresses and not those of the cells are given. It has been found

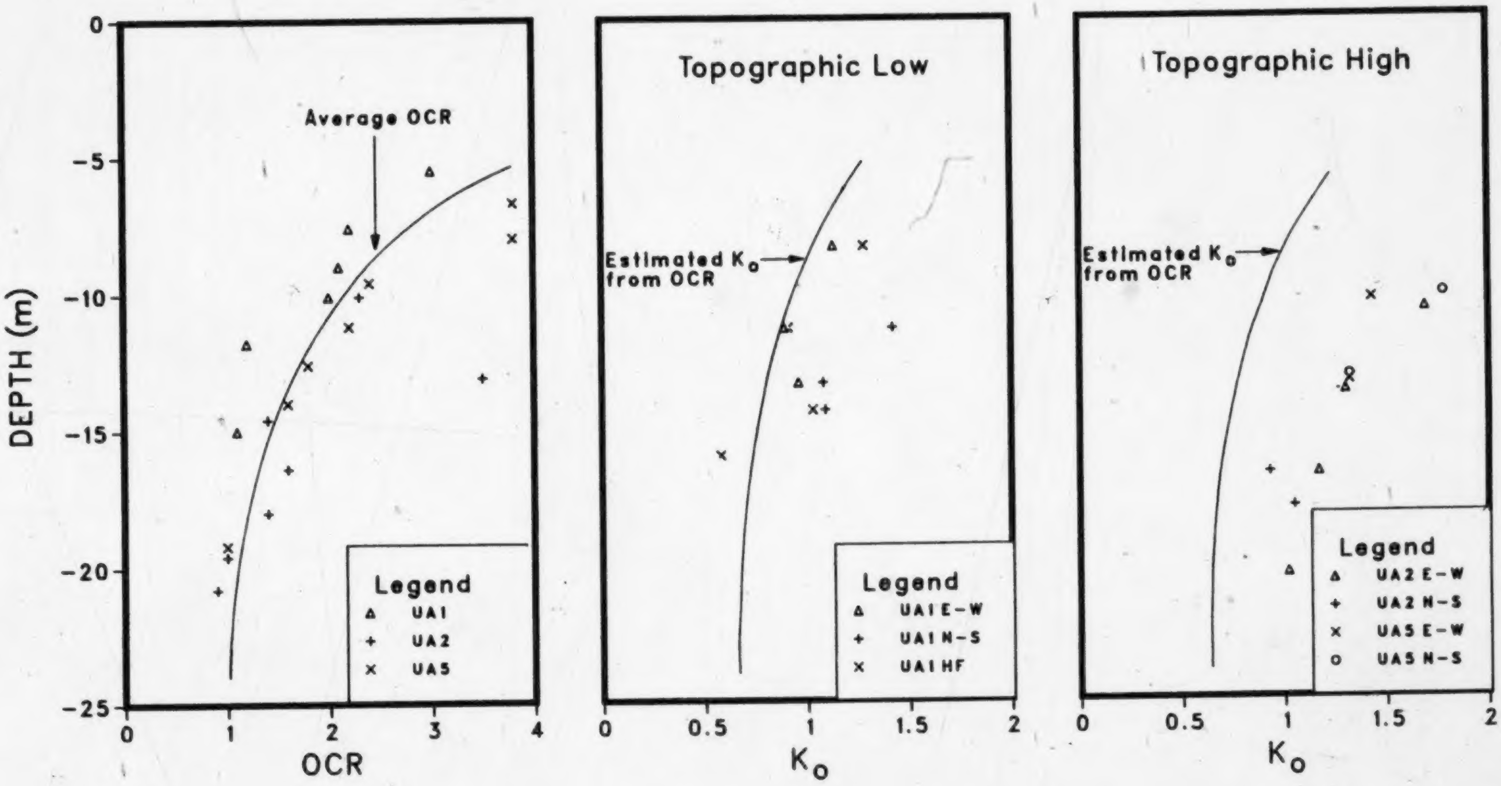

Figure 6.11 Variation of OCR and $K_o$ with depth at cooling pond.

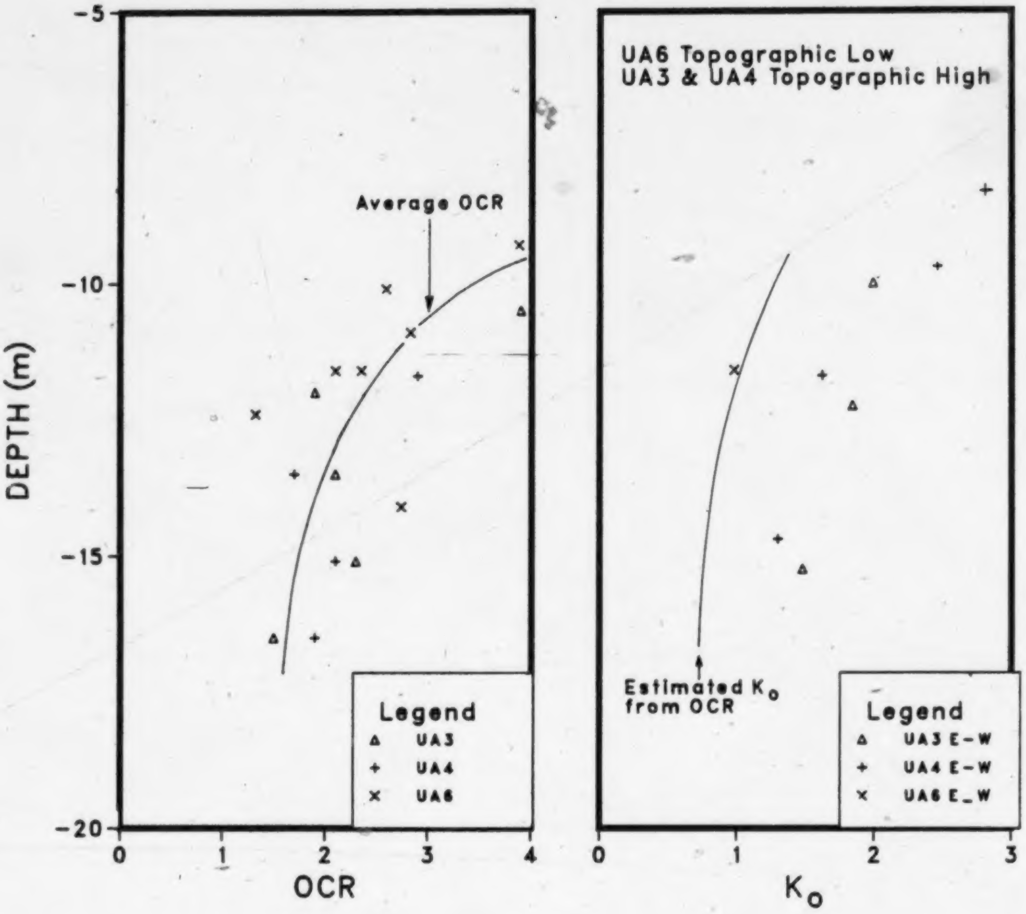

Figure 6.12 Variation of OCR and $K_0$ with depth at plant site.

necessary to separate data for the cooling pond area from those for the plant site because of the slight difference in consolidation history. Generally, it can be found that there is little deviation from the average OCR line at each location. Consequently, the apparent trend in the variation of $K_0$ with topography together with the information on the geological history of the deposit indicate that the bottom melt-out processes had influenced the in-situ state of stress.

The estimated $K_0$ for the average OCR line has also been drawn from the laboratory determined OCR - $K_0$ relationship of Fig. 5.3. Besides the difference between the values of $K_0$ at the topographic lows and those at the topographic highs, there is a remarkable agreement in the $K_0$ at the topographic highs at each location; furthermore, the estimated $K_0$ - Depth profile serves as a lower bound on which the lowest values of $K_0$ at the topographic lows lie.

Fig. 6.11 shows that there is some directional anisotropy in $K_0$ but this anisotropy is confined to certain layers only such as between 10 and 13 m and possibly between 15 and 17 m at both the topographic lows and highs. These anisotropic zones probably reflect the rotation of principal stresses and the arching effects as a result of the basal movements. Here it is worth repeating that, in section 3.5.3, it was shown that movement was not unidirectional as a result of the underlying ice melting. Consequently, the straining accompanying these multidirectional movements could have caused the anisotropy in $K_0$. Because of the erratic nature of the movements, there is no preferred orientation of the anisotropy, that is, the lateral stresses are not necessarily higher in a particular direction.

The variation of $K_0$ with OCR was investigated from Fig. 6.13, where the points are plotted with values of the field $K_0$ but the OCR were estimated from the average OCR line drawn in Fig. 6.11 and 6.12. This was done to reduce the scatter in the OCR. It is seen that the overconsolidation controls the lowest values of $K_0$ whereas the other values of $K_0$ are controlled by the internal stressing due to the bottom meltout processes; there is no doubt that there has been a complex superposition of the two effects. However, there are no indications of $K_0$ within the unweathered clay being close to either the active coefficient, $K_A$, of 0.36 or the passive coefficient, $K_P$, of 2.8 although some of the patterns of shearing discussed in Chapter 3 indicate the possibility of active and passive failure having occurred. This may be due to the stress relaxation or redistribution that took place since the bottom melt-out processes ceased.

Therefore, it can be concluded that stress history effects due to bottom melt-out processes still dominate those associated with vertical effective stress changes alone.

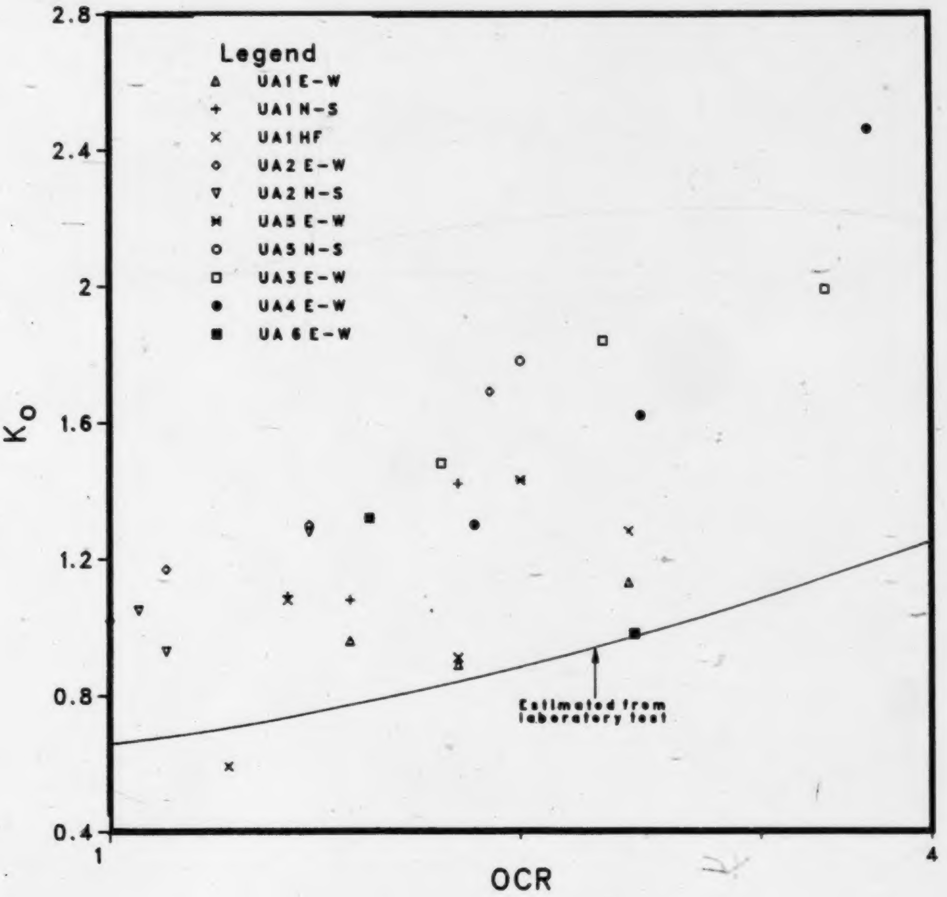

Figure 6.13 K$_o$ against OCR for Genesee Clay.

## 6.4 STRESS - STRAIN BEHAVIOUR

### 6.4.1 Unweathered grey clay

The summary of the triaxial test data is presented in Tables E.4 to E.8 and the stress - strain curves and stress paths are plotted in Fig. E.9 to E.18 in Appendix E.

Because of the presence of discontinuities, the peak strength measured varied widely from failure along intact material to failure along single discontinuities. The intact soil itself does not exhibit significant strain weakening behaviour within the range of strain obtainable in the laboratory as shown by the example in Fig. 6.14. On the other hand, examples of stress - strain curves and stress paths of the various modes of failure due to discontinuities are given in Fig. 6.15 and 6.16 respectively. Fig. 6.16 also contains the stress path for the intact sample of Fig. 6.14. The discontinuities encountered are as follows:

- sample 2-10 - shearing along 55° major slickenside;
- sample 5-6a - shearing along 55° bedding plane;
- sample 3-9 - multiple shearing along minor slickensides;
- sample 4-4 - multiple shearing along unsheared fissures.

The inclinations are given with respect to the horizontal and the samples were tested in their normal vertical position. All these samples were first consolidated isotropically under a cell pressure equal to the estimated

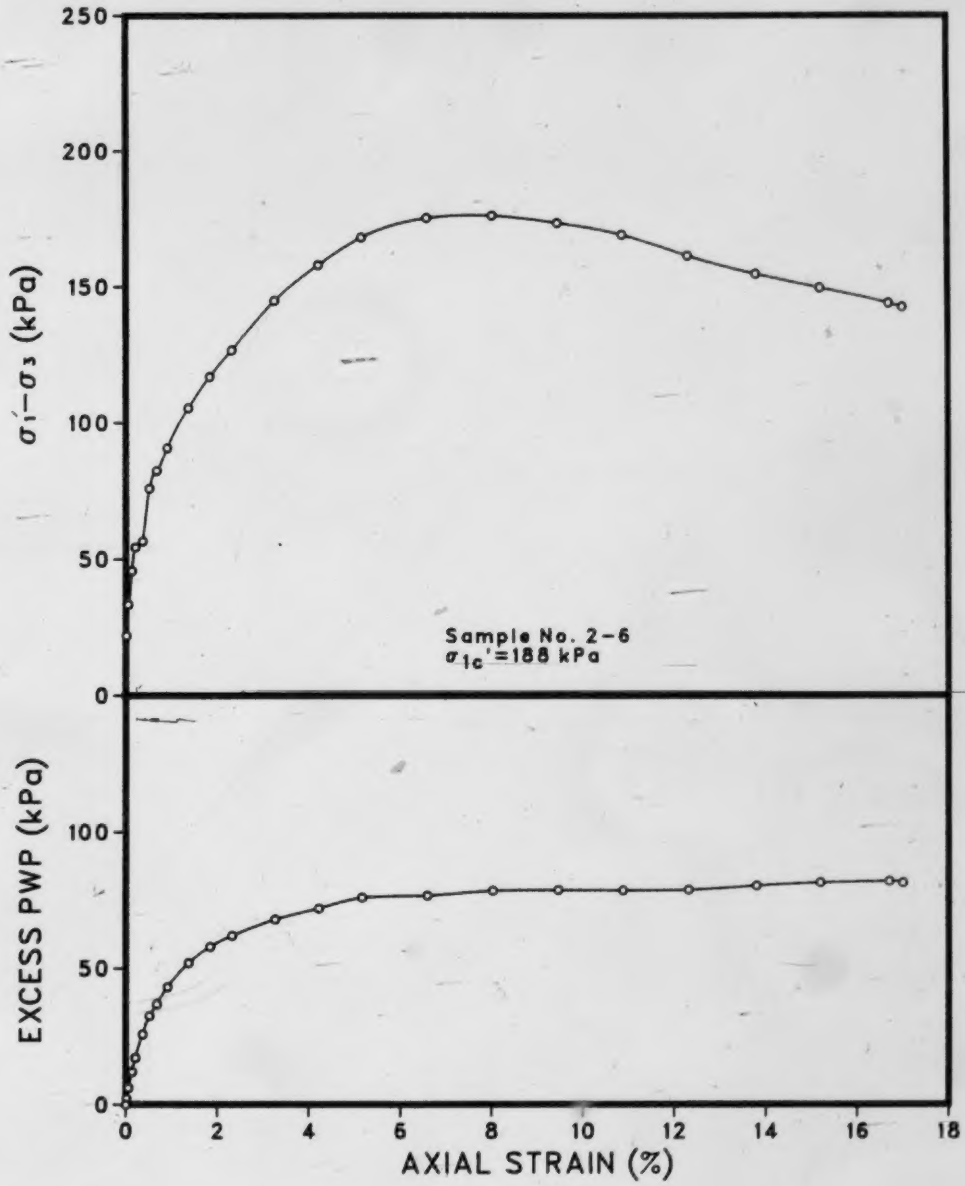

Figure 6.14 Example of CIU test results for intact unweathered clay.

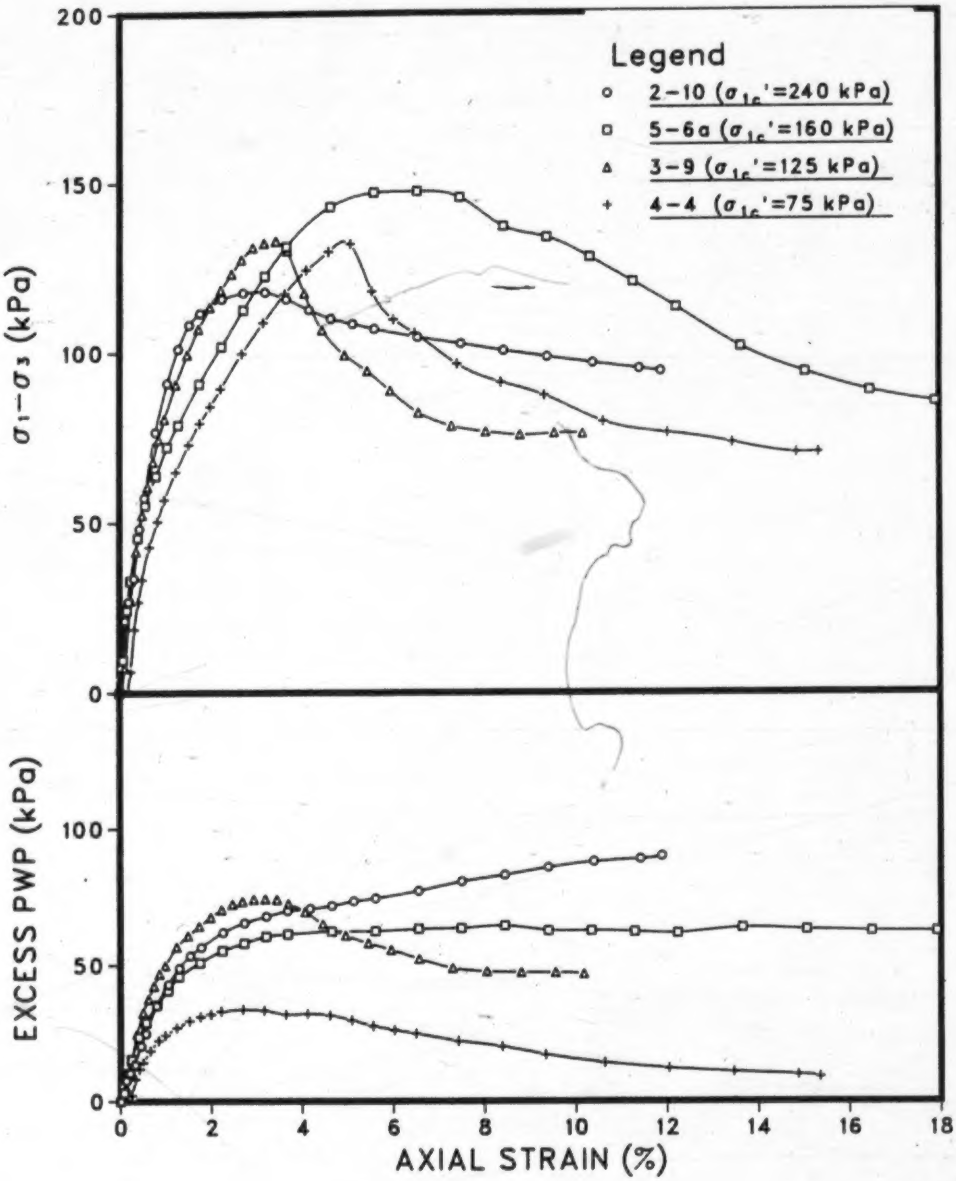

Figure 6.15 CIU test results on unweathered clay with discontinuities.

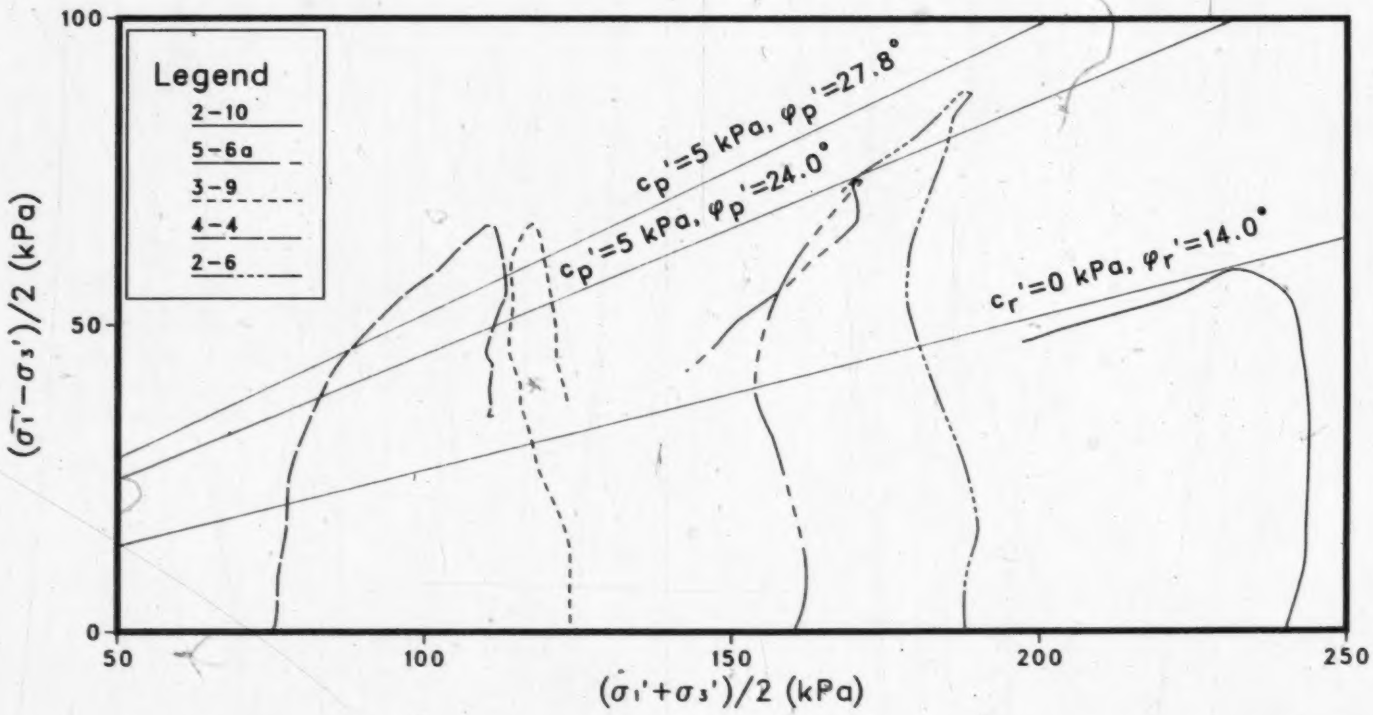

Figure 6.16 Stress paths for CIU tests in Fig. 6.14 and 6.15.

effective overburden pressure. For the multiple shearing, failure within the sample started initially along multiple planes with final shearing along planes inclined at 55° to 60° to the horizontal. The stress paths followed by the samples during the undrained shear indicate that prior to reaching peak strength, the soil behaves in the usual lightly overconsolidated to normally consolidated manner. Sample 2-10 shows that the strength along the major slickenside has a peak which is well below the actual peak of the intact material (Fig. 6.16); the strength of this sample after the peak lies close to the residual strength. This type of behaviour along a sheared discontinuity is similar to that discussed by Skempton and Petley (1967) and is believed to be due to the orientation of the particles along the sheared plane. It is noted that, because of its higher plasticity, sample 2-10 has a smaller residual angle of friction than that presented in Fig. 6.16 which was obtained from the direct shear tests on the samples of medium plasticity.

Sample 5-6a which failed along the bedding plane exhibits a strain - weakening behaviour; the peak strength was close to the peak envelope for the intact material and the reduction in strength was very gradual with strain. This is consistent with failure along a discontinuity along which little or no previous movement occurred. Of particular interest are the behaviour of samples 3-9 and 4-4 which contained the randomly oriented small area slickensides and fissures respectively. These samples displayed brittle failure. That is, there was a sudden drop in strength after the peak was reached. The strain at which peak occurred depended on the intensity of the fissuring but was normally around 3 to 4 %. The porewater pressure response shows that sample 5-6a which failed along the bedding plane was non-dilatant whereas samples 3-9 and 4-4 containing the small discontinuities were strongly dilatant. Similar dilatant behaviour caused by microfissures in the Leda clay was described by Mitchell (1970). The weakening behaviour is in agreement with the view expressed by Morgenstern (1977) that the weakening at low stresses might be in response to the changing dilatant characteristics of the fissured system.

### 6.4.2 Weathered brown clay

As shown in Chapter 3, the weathered clay is highly fissured and usually contains a large area of polished surface. As a result, the brown clay exhibits a strain - weakening behaviour as shown in Fig. 6.17 which gives CIU test results on the following:

- samples 1-1a, 2-1, 5-2 and 3-4 which were consolidated to the estimated effective overburden pressures;
- sample 5-1b which was consolidated to the normally consolidated state;
- sample 5-1a which was consolidated to an intermediate range.

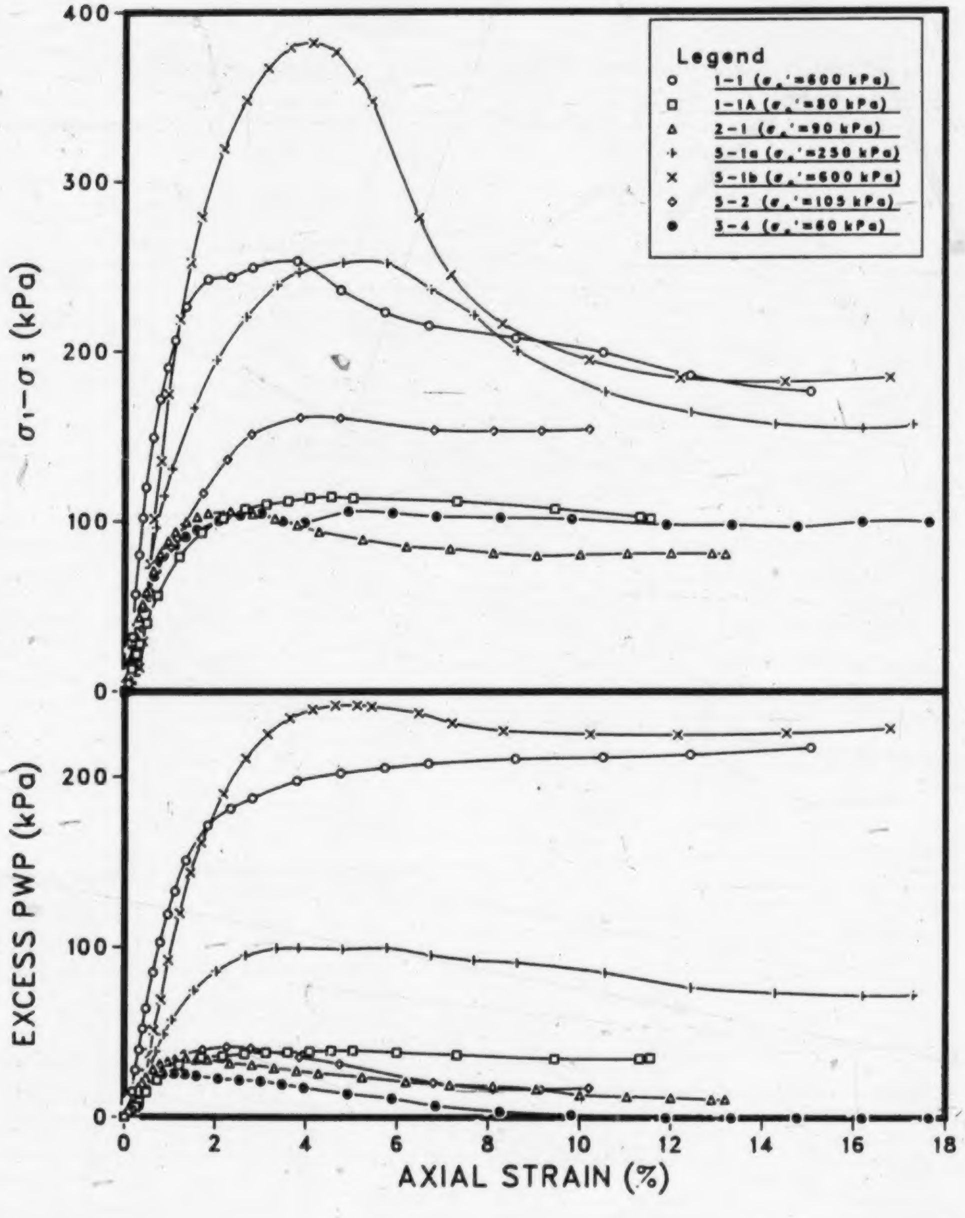

Figure 6.17 CIU test results on weathered brown clay.

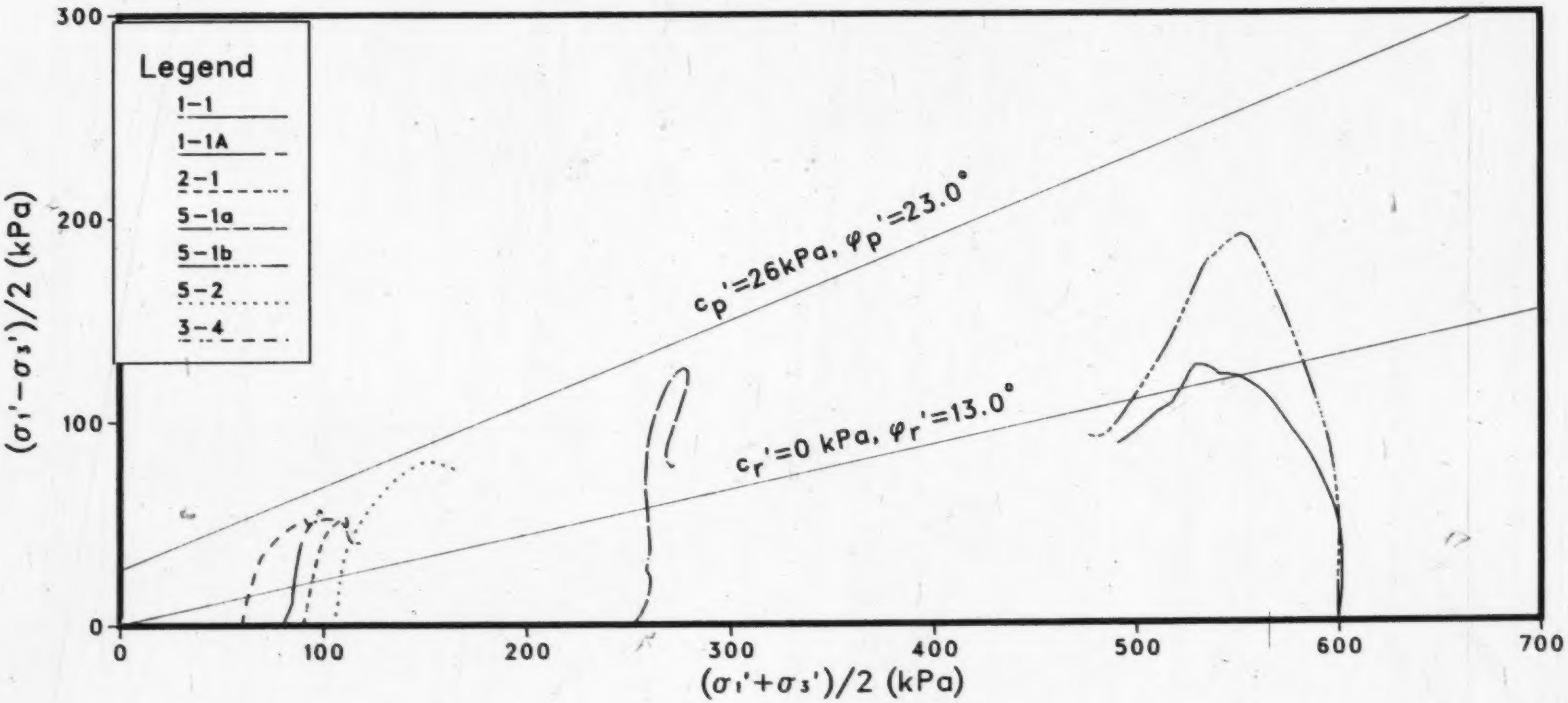

Figure 6.18 Stress paths of tests shown in Fig. 6.17.

Fig. 6.18 which gives the stress paths for these tests indicates that the peak strength does not reach the peak envelope obtained from the direct shear tests which force failure to occur through the intact material. At large strains of about 10%, the strength of some of the samples drop close to the direct shear test residual envelope as shown in Fig. 6.18; this large strain strength probably shows the control of the larger slickensides rather than the small fissures on the stress - strain behaviour of the brown clay.

## 6.5 STRENGTH PARAMETERS

### 6.5.1 Unweathered grey clay

The variability in the clay content of the layers and in the consolidation history as well as the presence of structural discontinuities affects the determination of strength parameters for the Genesee Clay. The effect of anisotropic consolidation on strength parameters will be discussed in the next section. To determine the peak strength parameters, it was decided to reject data from samples failing along a single existing slickenside since it was shown earlier that the strength is closer to residual than to peak. To take into consideration the difference in OCR, the data for the cooling pond and plant site were plotted separately in Fig. 6.19 and 6.20 respectively. The clay at the cooling pond shows slightly more scatter with an

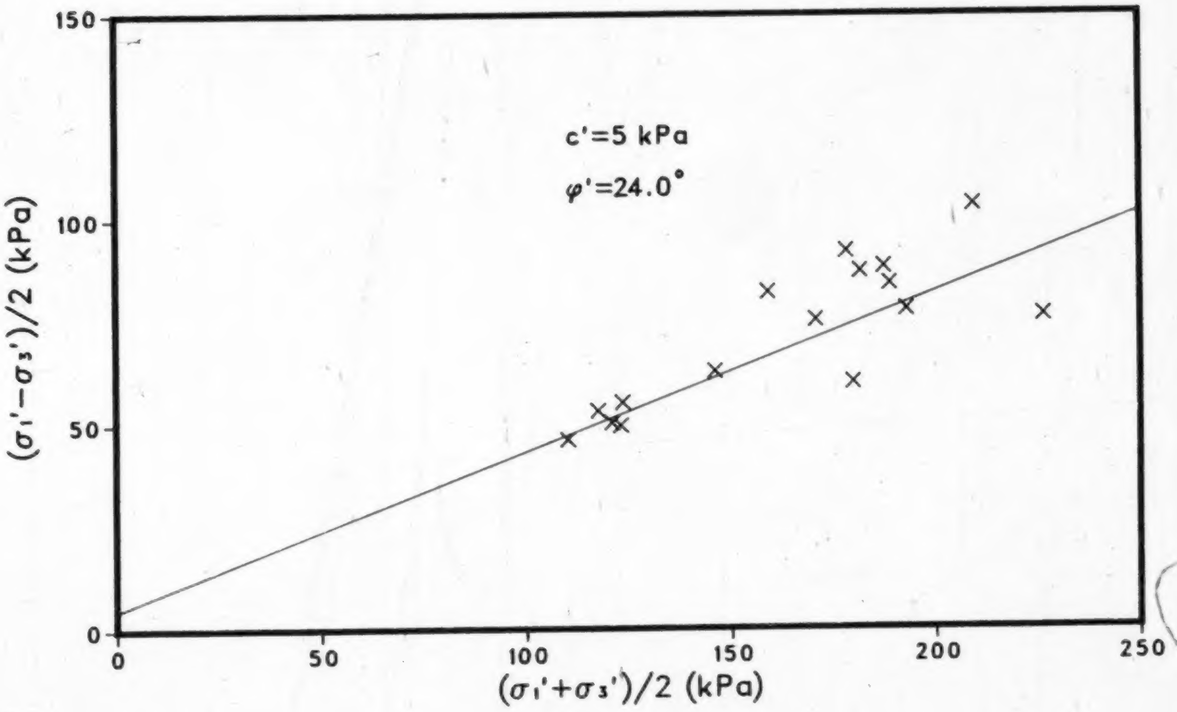

Figure 6.19 Peak strength envelope of grey clay at cooling pond.

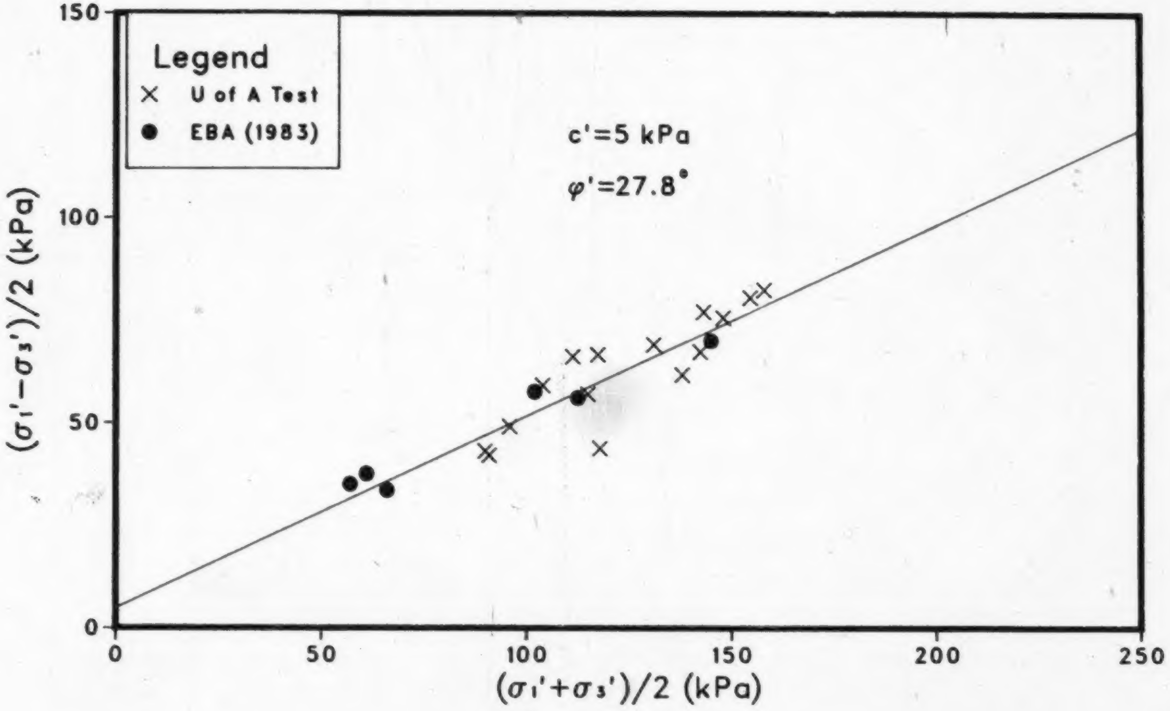

Figure 6.20 Peak strength envelope of grey clay at plant site.

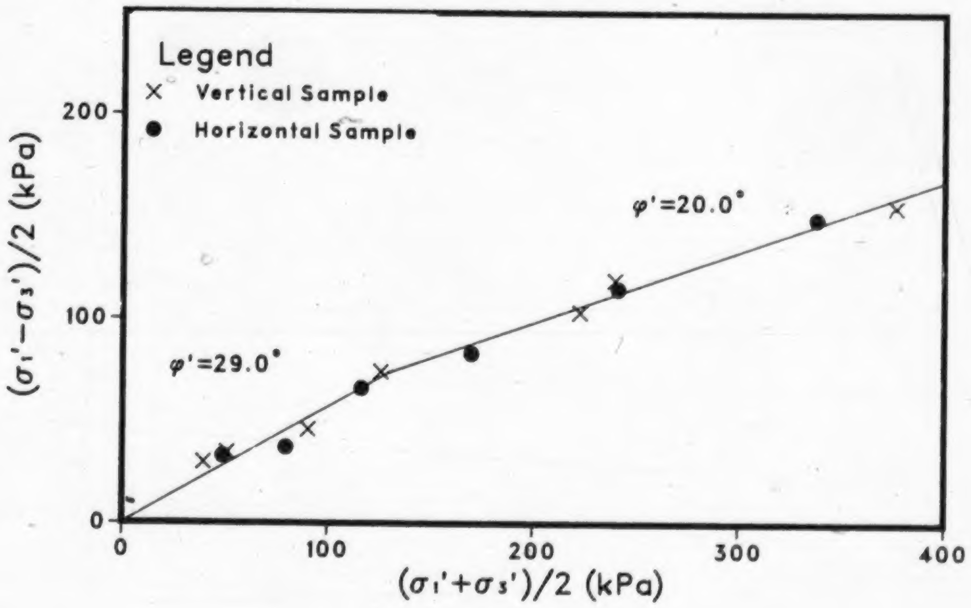

Figure 6.21 Bilinear peak strength envelope of grey clay.

average peak c'= 5 kPa and $\phi$'= 24° whereas for the plant site, c'=5 kPa and $\phi$'= 27.8°.

It is of interest to note that CIU tests on specimens not including visible fissures show that the peak strength envelope is bilinear with the change in slope occurring at approximately the preconsolidation pressure. Fig. 6.21 shows that within the overconsolidated range, $\phi$'= 29° and within the normally consolidated range, $\phi$'= 20°; there is the possibility that the envelope is curved instead of bilinear. The actual cause of this phenomenon is not known; however, it is believed that there are two possibilities:

1. according to Larsson (1981), clay particles form aggregates which can be assumed to act as units below the preconsolidation stresses. When the latter are exceeded, the aggregates breakdown and the friction angle depends on the shape of the particles instead of the aggregates.
2. the same phenomenon as (1) may occur at the macroscopic scale; the soil is divided into macroscopic blocks by non-visible microfissures so that it behaves as a frictional material at low stresses.

Fig. 6.21 which also includes test results on horizontal samples shows that the strength parameters are not anisotropic to sample orientation. It is to be noted that the block samples are made up primarily of the light grey clay whose particle arrangements did not reveal distinct orientation. On the other hand, Bishop et al (1965) found no significant anisotropy in c' and $\phi$'in the London Clay although its fabric has a distinct orientation whereas Baracos (1977) found anisotropy in c' and $\phi$' in the Winnipeg clay whose particles have a preferred horizontal orientation. Consequently, it can be observed that the anisotropy in c' and $\phi$' is not totally dependent on particle orientation.

Direct shear tests on specimens from one of the block samples gave an average peak c'= 0 and $\phi$'= 25° and residual parameters $c'_r = 0$ and $\phi'_r = 14°$ (Fig. 6.22).

Backanalysis (Chapter 7) shows that the operational strength of the Genesee Clay is not peak due to the presence of discontinuities; on the other hand, the random distribution of the latter and the unlikelihood of the failures occurring on a preexisting shear surface suggest that the operational strength is not residual although the strength along some of the discontinuities can be residual. Therefore, the question that is asked is which strength parameters can be obtained from the laboratory tests. Tentatively, the large strain strength envelope from the undrained triaxial tests has been drawn for the strain - weakening samples at the stabilised strength after the peak. The associated large strain is normally between 10 and 15 %. The data are plotted in Fig. 6.23 and the large strain strength parameters are approximately c'= 0 and $\phi$'= 20°. These parameters are supported by the study of Pilot et al (1982) who found that the strength parameters measured by

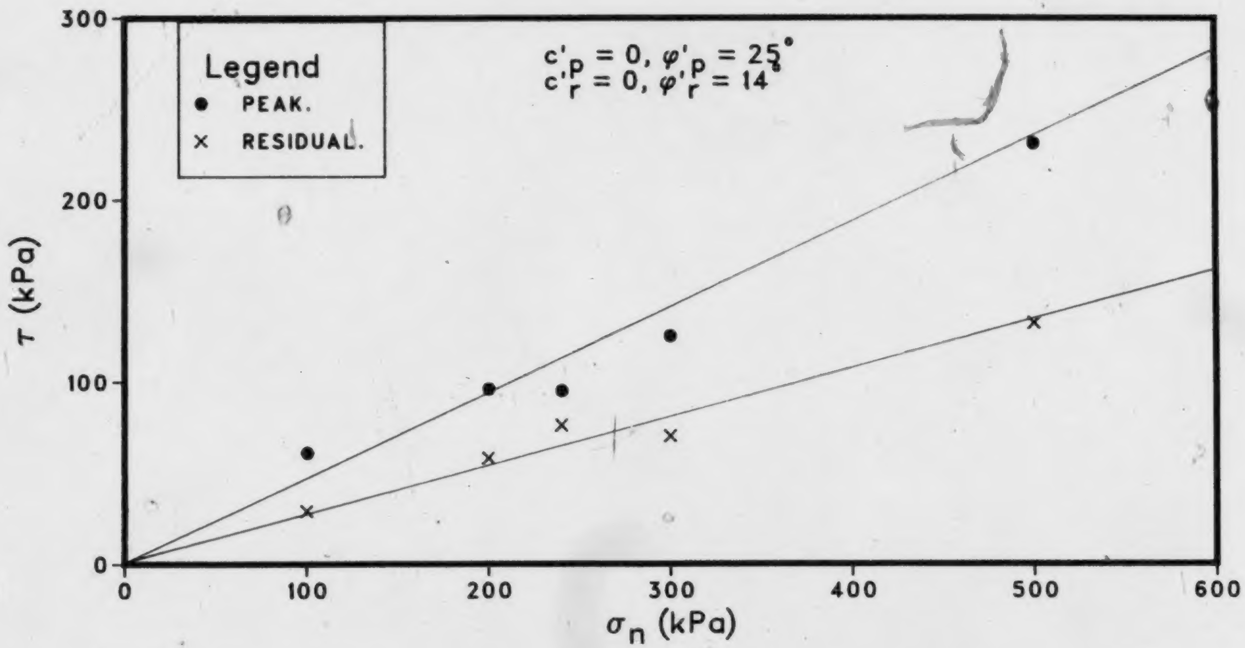

Figure 6.22 Strength parameters from direct shear test on grey clay.

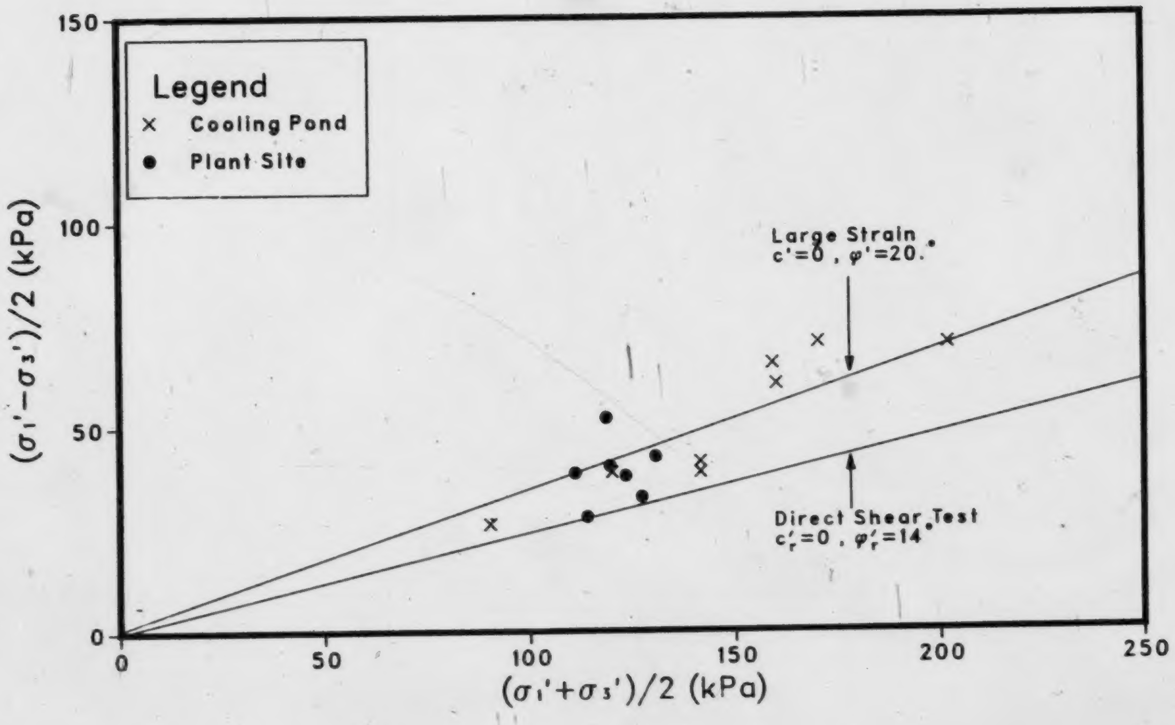

Figure 6.23 Large strain strength envelope of grey clay.

triaxial tests carried out to large strains (15 %) and at confining pressures corresponding to the overconsolidated state gave satisfactory results for the effective stress analysis of four test embankments.

### 6.5.2 Weathered brown clay

The strength parameters derived from the direct shear test results are shown in Fig. 6.24. As shown in section 6.4.2, the strength of the weathered clay samples was affected by the type of discontinuities within them. Therefore, only the peak stress points from the CIU tests are plotted in Fig. 6.24. However, the large strain strength envelope for the samples believed not to contain major slickensides is also shown in Fig. 6.24. The large strain strength parameters of $c'=0$ and $\phi'=18.5°$ have been found to be satisfactory parameters for the backanalysis discussed in Chapter 7.

## 6.6 VARIATION OF $A_f$ WITH OCR AND $K_0$

The variation of Skempton's (1954) parameter $A_f$ with OCR is well known; examples of this variation are given by Bishop and Henkel (1962) and Ladd et al (1977) among others. The relationship between $A_f$ and OCR for Genesee Clay is given in Fig. 6.25. For OCR higher than 1.5, $A_f$ for the Genesee Clay is higher than the results for remoulded Weald Clay given in Bishop and Henkel (1962).The high values of $A_f$ have been attributed to the collapsible nature of the soil

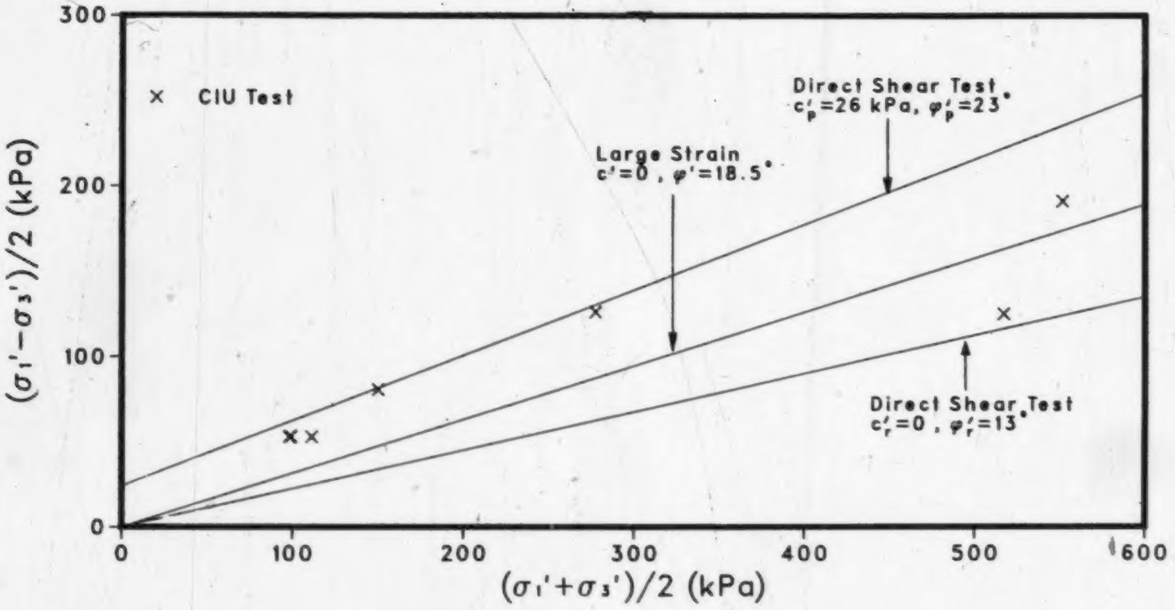

Figure 6.24 Strength parameters from direct shear tests on brown clay.

structure by Graham and Au (1985) based on their study of Winnipeg Clay. However, there is no indication that the Genesee Clay is behaving in a similar manner.

Fig. 6.26 shows the variation of $A_f$ with $K_0$ values calculated from measurements made by the total stress cells. For samples from the cooling pond area, the average values of $K_0$ obtained from measurements in the two different orientations were used. Samples suspected of being affected by discontinuities were not included. It is found that there is not too much scatter in the data and it possible to define a relationship between $A_f$ and $K_0$. It is interesting to note that samples consolidated anisotropically to the measured in-situ stresses agree closely with that relationship. This suggests that isotropic consolidation to the in-situ vertical effective stresses did not disturb the soil fabric within the sample.

The point of interest is that there is a relationship between $A_f$ and OCR on the one hand and $A_f$ and $K_0$ on the other; however, it has been shown in Fig. 6.13 that there is no relationship between OCR and $K_0$. Since $A_f$ is dependent on the soil structure, it is possible that within the range of OCR and $K_0$ prevailing in the Genesee Clay, there is not much change in the soil structure with changes in either OCR or $K_0$. In fact, at an OCR greater than 1.5 or a $K_0$ greater than 1.0 the drop in $A_f$ with increasing OCR or $K_0$ is very small. It can be concluded that both OCR and $K_0$ had an effect on the structure of the clay and after a threshold value of $K_0$

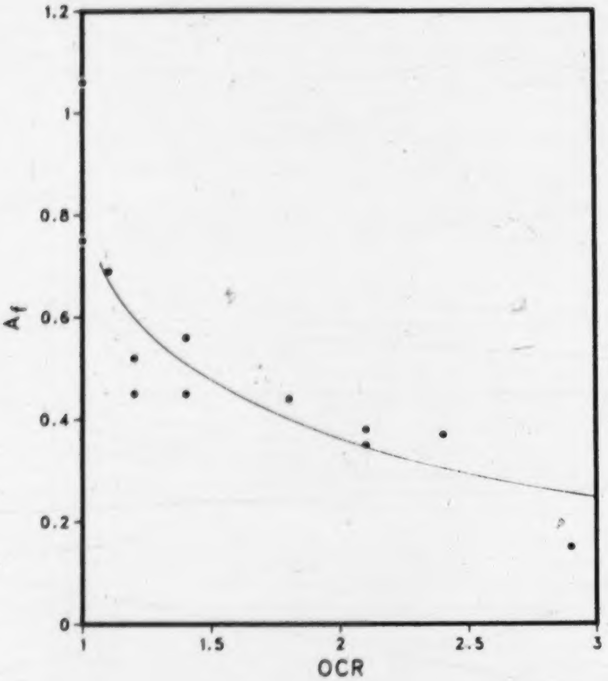

Figure 6.25 Variation of $A_f$ with OCR.

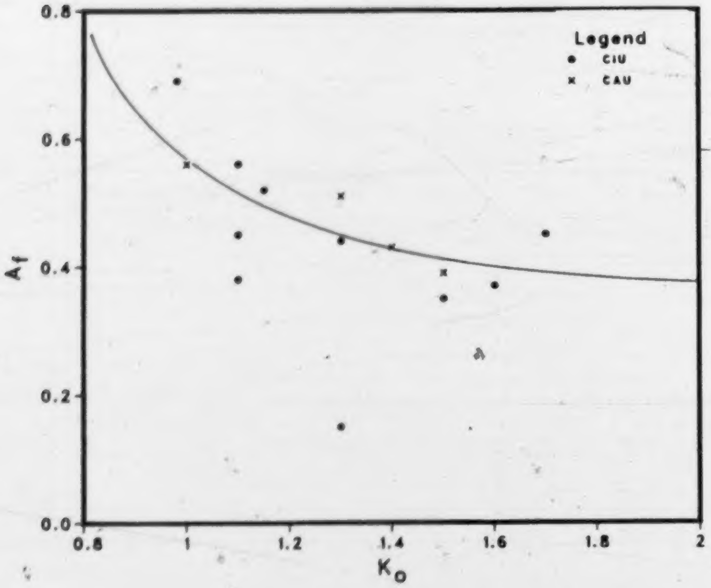

Figure 6.26 Variation of $A_f$ with $K_o$.

or OCR there is only very small modification of the soil fabric with increasing OCR or $K_0$ or a combination of both.

## 6.7 ANISOTROPY IN GENESEE CLAY

As this research is also concerned with the stability of the Genesee Clay as a foundation material, the effect of anisotropy with respect to the shear strength of the soil was investigated. The importance of strength anisotropy in stability problems has been emphasized by Lo (1965), Duncan and Seed (1966b) and many others. Essentially, there are two types of anisotropy.

The first is an inherent anisotropy caused by particle orientation or macrostructures such as discontinuities and layering as in varved glacial lake clays. The effect of preferred orientation of particles was studied by Duncan and Seed (1966a) who found that although sample orientation had no effect on the c' and $\phi'$ from tests on samples of overconsolidated kaolinite, the undrained strength of the vertical samples is about 10 % higher than that of horizontal samples as a result of a lower pore pressure parameter $A_f$. This shows the effect of grain structure anisotropy on pore pressure response. Strength anisotropy due to the preferred orientation of discontinuities has been studied by Lo and Vallee (1970) who derived theoretical expressions for strength variation of a soil containing parallel planes of weakness. Anisotropic shear strength properties in varved clays for both drained and undrained conditions have been studied by Kenney (1976) who found that directional anisotropy in $\phi'$ in drained tests due to the presence of alternate layers of clay and silt is very small. In the case of undrained failure, Kenney (1976) reported that the degree of anisotropic shear strength is greatly influenced by the rate of strain and equalisation of porewater pressures in the different layers.

The second type of anisotropy is induced by the stress system acting on the soil. Hansen and Gibson (1949) drew attention to this stress induced anisotropy and derived an expression for the undrained strength, $c_u$ in terms of $K_0$, $c'$, $\phi'$ and $A_f$ and inclination of the failure plane. In deriving this expression, it was assumed that there is no anisotropy in terms of $c'$, $\phi'$ and $A_f$. On the other hand, experiments by Ladd (1965) and Donaghe and Townsend (1978) showed that $\phi'$ and $A_f$ are affected by anisotropic consolidation.

Based on the above discussion, the question to be asked is whether the Genesee Clay exhibits anisotropic behaviour in the sense that lower strength is obtained in certain orientations. First, the unfissured light grey clay does not show anisotropy in $c'$ and $\phi'$ as discussed in section 6.5.1 and this is assumed to be due to the isotropic fabric in these layers. The isotropic behaviour is also confirmed by the consolidation tests on horizontal samples as discussed in section 6.2. CIU tests on horizontal and vertical specimens from the same block sample and consolidated at pressures within the overconsolidated and normally consolidated range showed that the stress paths for each pair of vertical and horizontal specimens are identical and the undrained strength of the horizontal specimens is about 0.95 times that of the vertical ones. These are shown in Fig. 6.27 for the stress - strain relationships and Fig. 6.28 for the stress paths. It can be noted in Fig. 6.27 that the pore pressure response does not show any influence of inherent anisotropy. On the other hand, the dark grey clay layers are likely to exhibit anisotropic strength as a result of both the preferred orientation in particle arrangements and the presence of small area slickensides as discussed in Chapter 3. Drained direct shear test results (Fig. 6.29) on a layer of dark grey clay, consolidated to the in-situ stresses and sheared parallel to the bedding, showed that the strength drops to the residual value on the second shearing. It was not possible to do the tests perpendicular to the beddings because of the limited thickness of these dark grey clay layers; but it is obvious that shearing along the bedding represents the lowest strength.

The major shears will cause anisotropy due to orientation in the manner discussed by Lo and Vallee (1970) but the orientation of these shears seem to be governed by the differential melting processes of the underlying ice and therefore, is likely to vary with location.

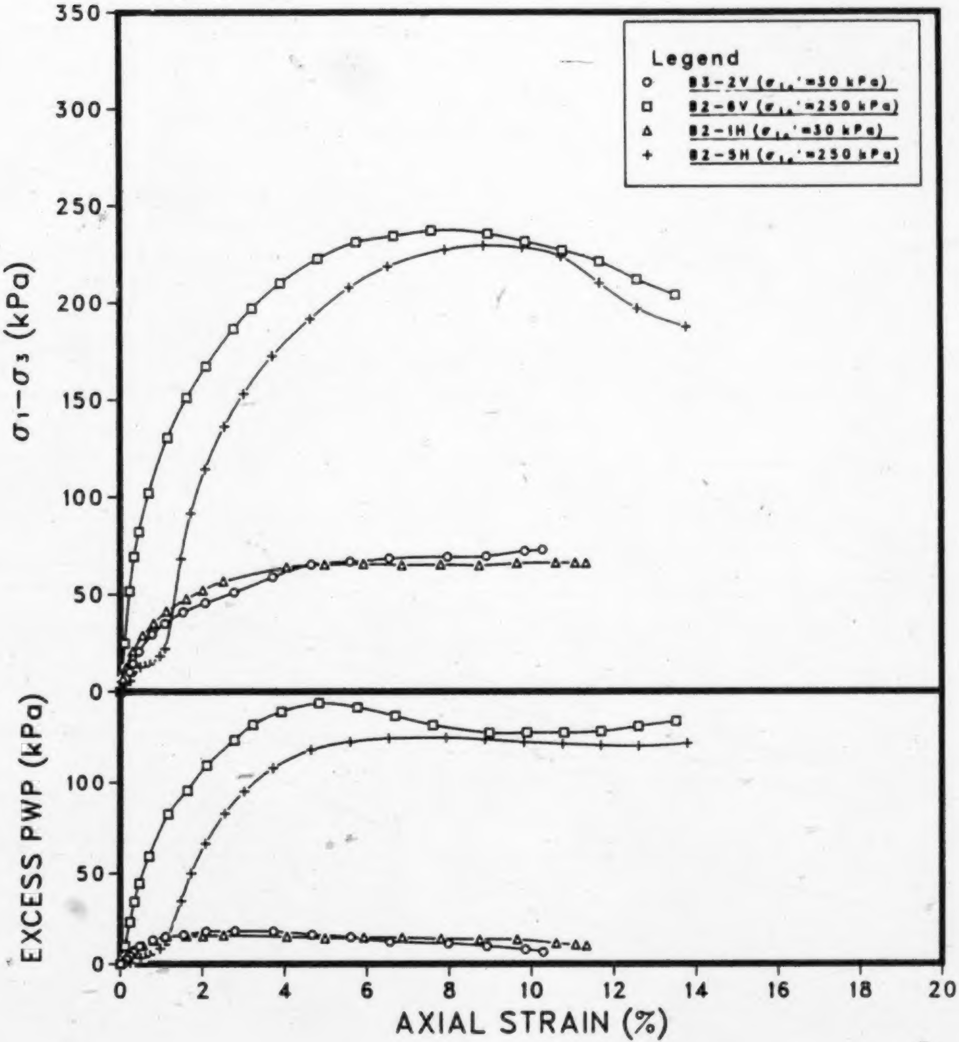

Figure 6.27 CIU test results on vertical and horizontal samples.

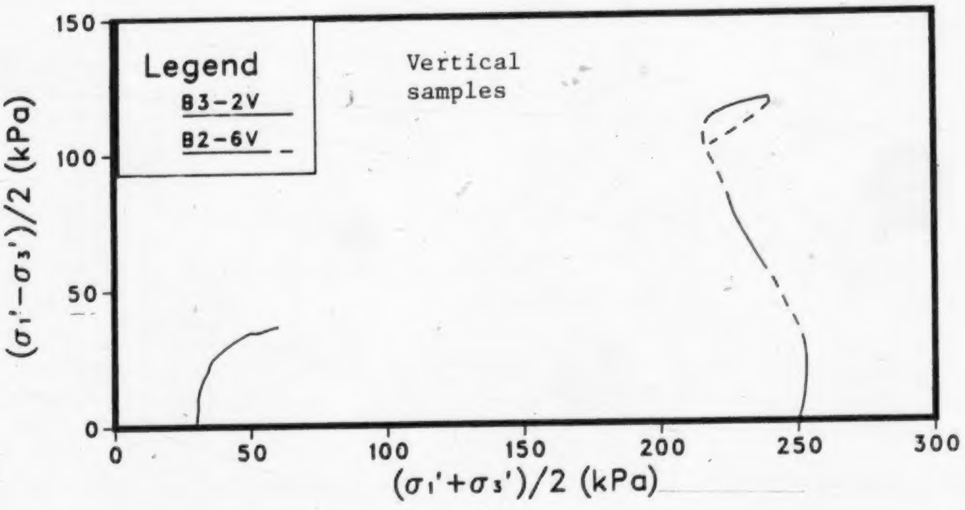

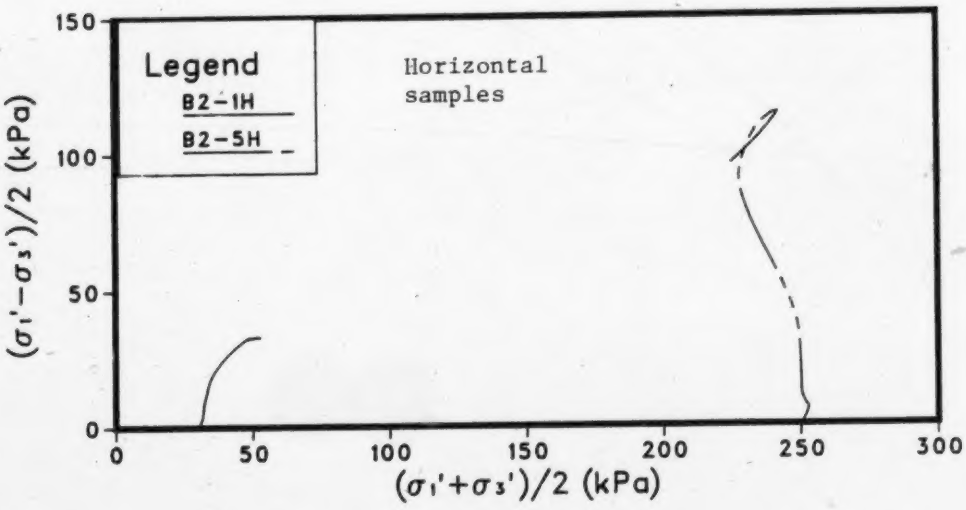

Figure 6.28 Stress paths of tests shown in Fig. 6.27.

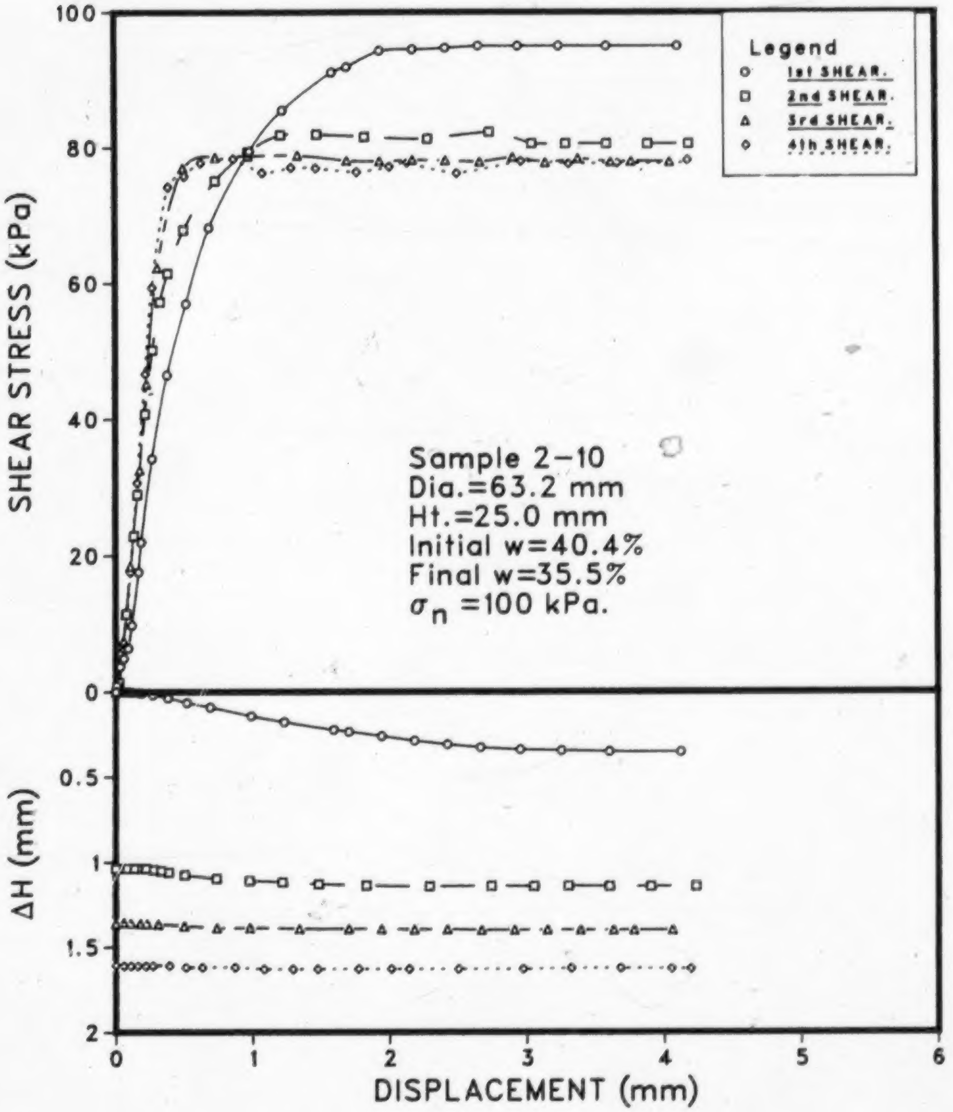

Figure 6.29 Drained shear test results on dark grey clay.

Finally, an attempt was made to investigate the effects of anisotropic consolidation on the clay. Undrained triaxial tests were performed on isotropically (CIU) and consolidated anisotropically (CAU) samples. In both cases, the vertical consolidation pressure is equal to the estimated effective overburden pressure and for the CAU tests, the horizontal pressure applied is the one measured in the field. Samples were chosen from zones of highest $K_0$ in the unweathered clays and for these tests, $K_0$ were in the range of 1.3 to 1.5. The samples tested were 5-4a and 5-4b, 4-7a and 4-7b and 4-8a and 4-8b; 5-4a, 4-7a and 4-8a were consolidated isotropically while the others were consolidated anisotropically. On the other hand, samples 2-8a and 2-9 were consolidated under conditions of zero lateral strain up to the estimated effective overburden pressure; the ratio $\sigma_3'$ to $\sigma_1'$ obtained were 0.64 and 0.6 respectively. The test results are summarised in Appendix E. Nevertheless, these tests were unsuccessful in determining the effects of anisotropic consolidation conditions as one or both of each pair of samples were affected by the discontinuities.

Therefore, to summarise, it can be said that the light grey clay of which the main body of Genesee Clay is composed does not show anisotropic behaviour with sample orientation and this is due to the isotropic soil fabric as well as the near isotropic in-situ state of stress of the samples tested. Anisotropic consolidation does not seem to have a large effect on $A_f$ and $\phi'$ for $K_0$ larger than unity; it is possible that the effect is more pronounced in the lower $K_0$ range and the variation of $A_f$ against $K_0$ in Fig. 6.26 seems to show this trend. On the other hand, individual soil specimens may exhibit anisotropy as a result of lithological contrasts and structural discontinuities. But, when Genesee Clay deposit is considered as a whole, the random arrangements of these features are not likely to cause global directional effects. On the other hand, it is believed that the operational strength of the Genesee Clay is controlled to a greater extent by the randomly oriented minor discontinuities.

## 6.8 VARIATION IN UNDRAINED STRENGTH

In this section, undrained strength is considered with reference to the intact material. The effects of stress history on the undrained strength of clays are well known; they are reflected in the excess pore pressures generated at failure. As shown earlier, pore pressures are known to depend on the OCR of the clay and consequently, attempts were made to find empirical corelations between the undrained strength, $c_u$ and OCR. For example, the relationship by Ladd et al (1977) is expressed as:

$$\frac{(c_u/\sigma_v')(oc)}{(c_u/\sigma_v')(nc)} = OCR^m \quad \ldots\ldots\ldots\ldots\ldots\ldots\ldots\ldots\ldots\ldots\ldots (6.3)$$

where m is a parameter which varies between 0.85 and 0.75 with increasing OCR. Using critical state soil mechanics principles, Wroth (1984) confirmed the theoretical validity of the above empirical expression.

On the other hand, Skempton and Bishop (1954) proposed a theoretical expression relating undrained strength to the coefficient of earth pressure, $K_0$ as follows:

$$\frac{c_u}{\sigma'_{vo}} = \frac{c'\cos\varphi'/\sigma'_{vo} + [K_o + A_f(1-K_o)]\sin\varphi'}{[1 + (2A_f-1)\sin\varphi']} \quad \text{...........(6.4)}$$

where $\sigma'_{vo}$ = vertical effective stress;

$A_f$ = pore pressure parameter at failure;

c' and $\phi'$=effective shear strength parameters.

This equation is based on the following assumptions:

1. there is no rotation of principal stresses;
2. $A_f$, c' and $\phi'$ are not anisotropic.

The field investigations at Genesee showed that there is a marked variation in the vane undrained strength both in profile and in plan as indicated by the data presented in Fig. 6.1 to 6.6. The vane strength is not likely to be affected by the planar discontinuities unless the latter coincide with the failure surface generated by the vane. The variation of strength in profile is due to the presence of slightly stiffer layers formed as a result of the intermittent submergence and exposure of the lake bottom during deposition as discussed in Chapter 3. On the other hand, there is a slight variation in the strength profile as shown by the laboratory vane tests because of the slight variation in the clay content of the layers. However, the discussion will be based solely on the field vane tests. It is found that there is a marked variation in the undrained strength over short horizontal distances although there is not much difference in the degree of overconsolidation. The present investigation shows that the undrained strength at UA1 is of the order of 40 to 50 kPa whereas at UA2 and UA5 it is in the range of 75 to 80 kPa; at UA6, the undrained strength is between 35 and 40 kPa whereas at UA3 and UA4, it is closer to the 75 to 80 kPa range. Similar observations were reported by EBA (1983) and Crooks et al (1985). Since it was shown in Fig. 6.11 and 6.12 that there is only a very slight difference in OCR between UA1,UA2 and UA5 and between UA3, UA4 and UA6, it was decided to explore the variation of the ratio $c_u/\sigma_{vo}'$ against $K_0$. The data for the cooling pond and the plant site are plotted separately in Fig. 6.30 and 6.31 respectively.

Equation no. 6.4 was used to provide bounds for $c' = 0$ and $\phi'$ of 24° and 27.8° for the clay at the cooling pond area and plant site respectively. The range of $A_f$ values were those obtained from the triaxial tests (see Fig. 6.25). Fig. 6.30 and 6.31 show that the measured $K_0$ and $c_u/\sigma_{vo}'$ fall reasonably well within the bounds predicted by equation no. 6.4. Consequently, it can be concluded that the undrained strength is a function of $K_0$ and the field vane

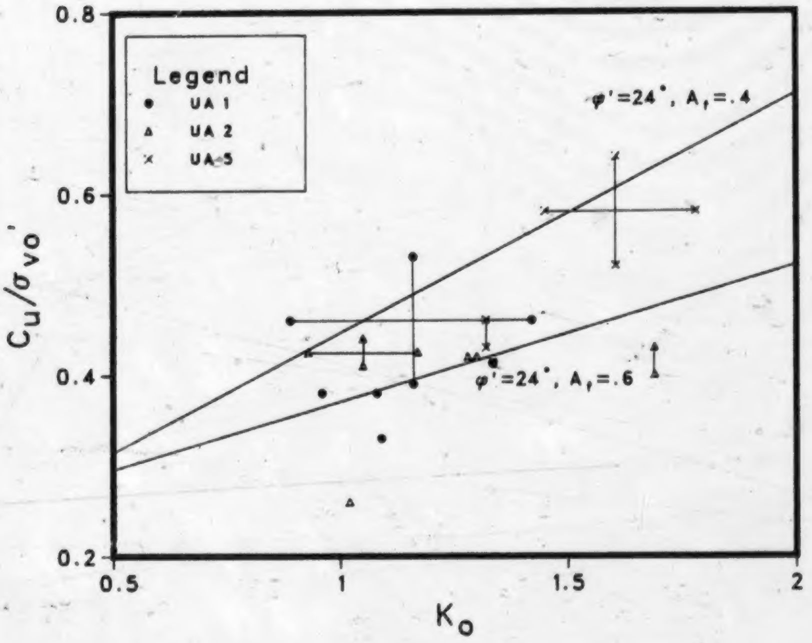

Figure 6.30 $c_u/\sigma_{vo}'$ against $K_0$ for cooling pond area.

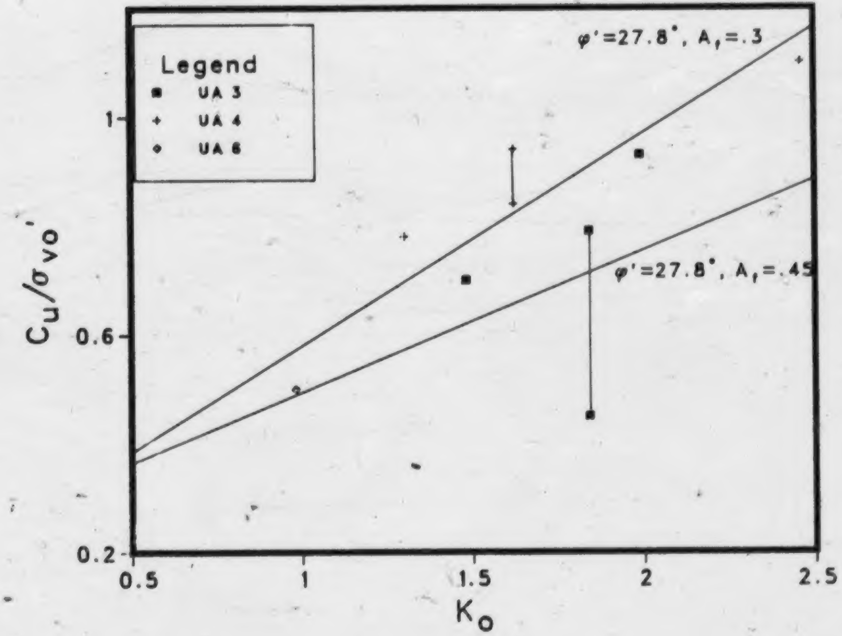

Figure 6.30 $c_u/\sigma_{vo}'$ against $K_0$ for plant site area.

strength is showing a variation in $K_0$ which is believed to have been caused by the bottom melt-out processes as discussed earlier. However, this variation in $K_0$ was also influenced by the complex consolidation history.

### 6.9 YIELDING IN GENESEE CLAY

The yield envelope has been determined for specimens trimmed from a block sample of the light grey clay and is plotted in Fig. 5.8 (Chapter 5). The major feature that can be noticed is that the envelope for the Genesee light grey clay appears to be symmetrical about the isotropic stress axis whereas data published by Mitchell (1970), Tavenas and Leroueil (1979) and Crooks and Graham (1976) show that the yield envelopes are more or less symmetrical about the $K_0$ consolidation line. As shown earlier, the Genesee light grey clay exhibits isotropic behaviour in terms of strength and compressibility properties and these characteristics confirm the shape of the yield envelope. The data seem to indicate that the envelope is not symmetrical about the $K_0$=1.2 axis which represents the present state of stress. Therefore, the shape of the yield envelope is a complex response to both stress history and particle arrangement.

# 7. STABILITY ANALYSIS OF SLOPES AND EMBANKMENTS ON GENESEE CLAY

## 7.1 INTRODUCTION

During the construction of the Genesee Power Project, various instabilities occurred with the planes of movement being located mainly within the unweathered clay. Two cases of failure are backanalysed and another case where large deformations were detected is briefly described. These cases are important in understanding the behaviour of this class of material. The methods of analysis used are the Bishop (1955) method of slices for circular failure surfaces and the Morgenstern and Price (1965) method for non circular surfaces; the Bishop analysis was performed by using the ICES computer program LEASE. Both total and effective stress analyses were conducted on the failure surfaces.

## 7.2 SLOPE FAILURE AT DIVERSION DITCH

The failure at the diversion ditch is described based mainly on verbal information from Thurber Consultants and additional site visits by the author after the failure.

The diversion ditch was excavated to drain water from the Genesee Creek to enable construction of the high dyke. Excavation of the ditch with sideslopes of 2 horizontal to 1 vertical was started in early October, 1982 and completed in about 1.5 months; the depth of the ditch was between 5 and 10 m. Instabilities along the sides of the excavation as

Plate 7.1 Slope failure at diversion ditch.

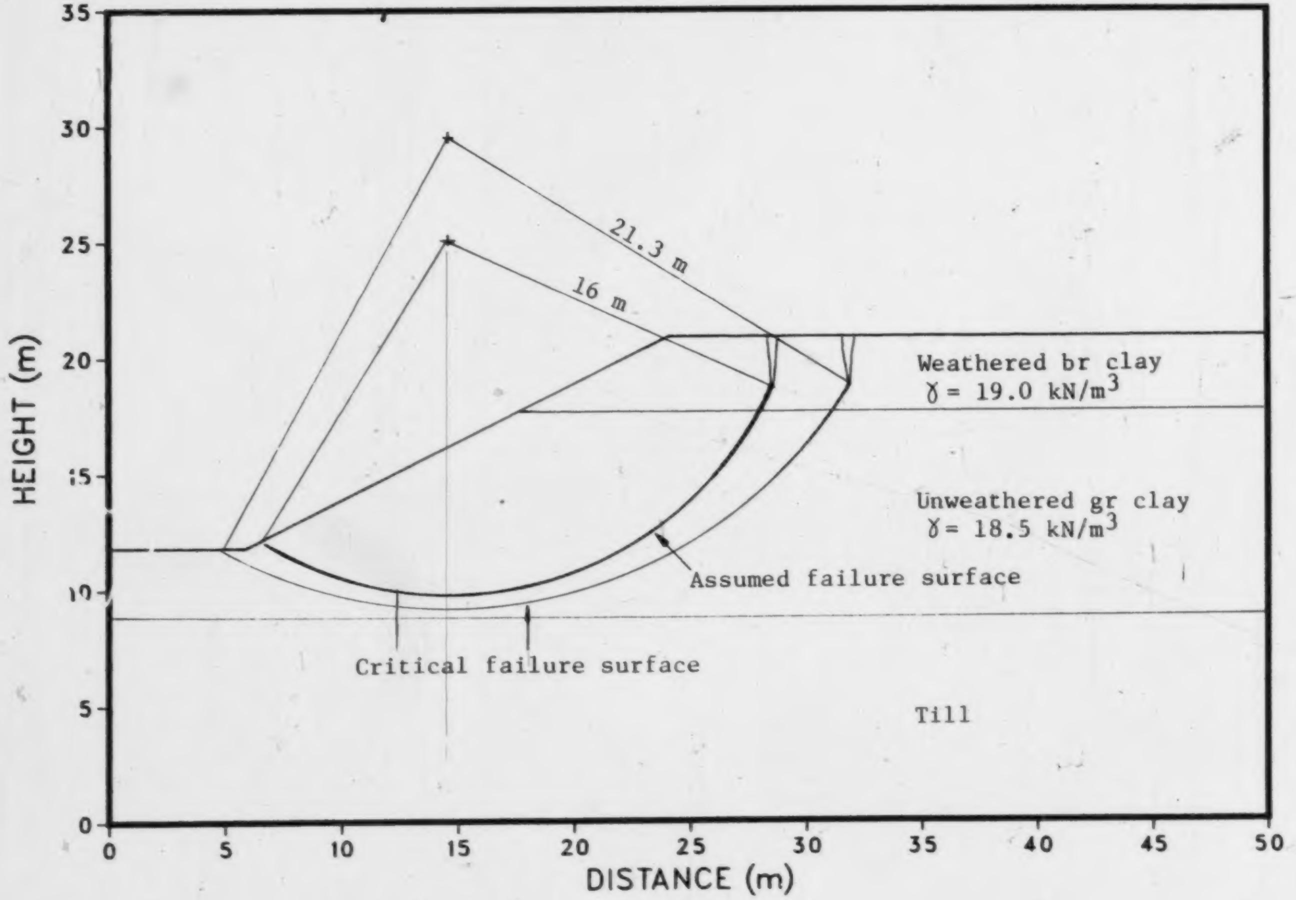
HEIGHT (m)
35
30
25
20
15
10
5
0
DISTANCE (m)
0
5
10
15
20
25
30
35
40
45
50
21.3 m
16 m
Weathered br clay
$\gamma = 19.0$ kN/m$^3$
Unweathered gr clay
$\gamma = 18.5$ kN/m$^3$
Assumed failure surface
Critical failure surface
Till

Figure 7.1 Assumed failure surface at diversion ditch.

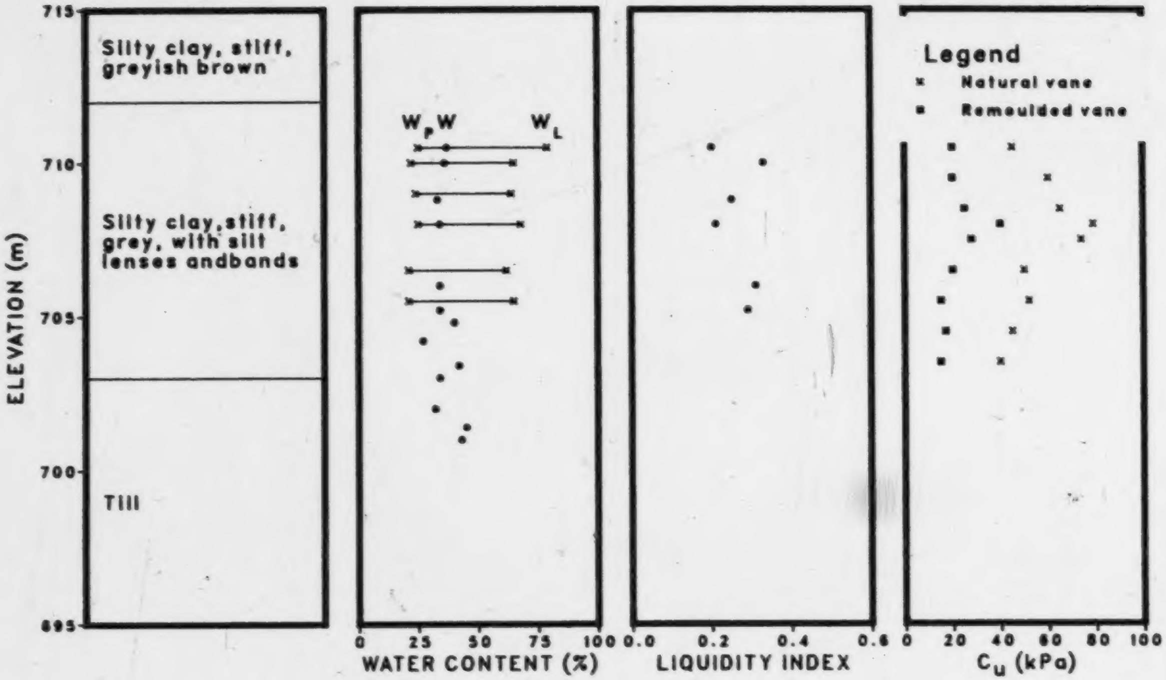

Figure 7.2 Soil properties at location close to diversion ditch.

well as tension cracks were observed as from February, 1983. One of the instabilities developed into the failure shown in Plate 7.1 and prior to failure, a tension crack estimated to be 2.3 m deep had formed. Fig. 7.1 gives the assumed failure surface based on the geometry of failure whereas the soil profile and field vane shear strength are given in Fig. 7.2 which is drawn from data obtained from Thurber (1982b). Based on previous investigations, the groundwater table prior to excavation is located approximately at the ground surface; however, there was no information on the porewater pressures at the time of failure.

A total stress analysis was carried by using Bishop's method and the 2.3 m deep tension crack was assumed to exist at the time of failure. Certain assumptions had to be made concerning the strength of the brown clay although the rather shallow depth of the brown clay is not likely to affect the results significantly. The vane shear tests within the cooling pond showed that the undrained strength of the brown clay could vary from 60 to 80 kPa. However, in Fig. 6.17 of Chapter 6, the CIU tests on the brown clay samples consolidated to the overburden stress show that because of its fissured nature, the brown clay had a peak strength of about 50 kPa with a tendency to strain weaken after that. The lowest measured undrained strength at large strains is about 40 kPa. Consequently, the analysis was run with an undrained strength of 40 to 60 kPa for the brown clay layer. The results are presented in Fig. 7.3. It can be

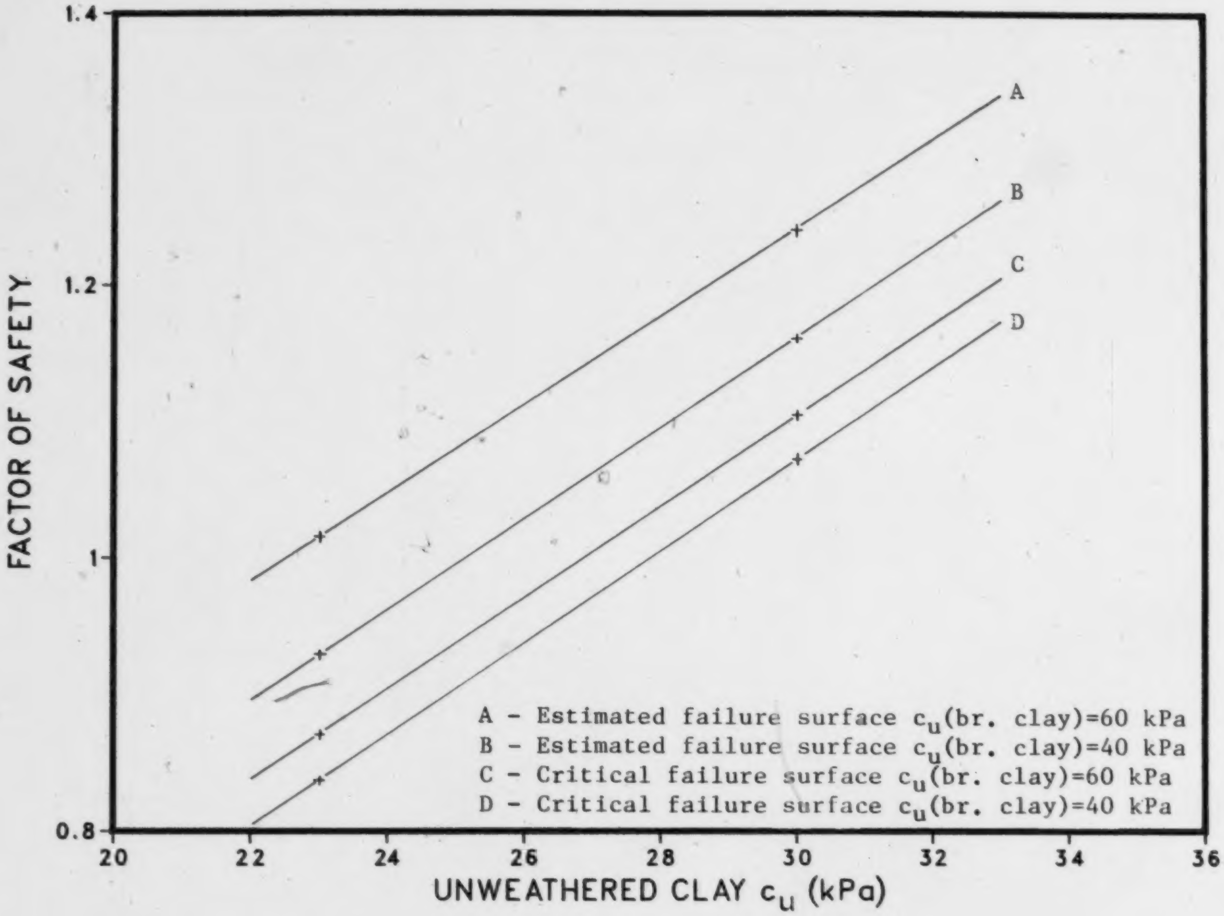

Figure 7.3 Total stress analysis of slope at diversion ditch.

found that at the time of failure, the mobilised undrained strength within the unweathered grey clay is estimated to be between 23 and 28 kPa.

The field vane tests indicated that the intact unweathered clay has an undrained strength between 40 and 60 kPa and therefore, the inadequacy of the vane test to accurately predict the strength of the clay is clearly shown. Bjerrum (1972) considered extensively the problems of the vane shear test and proposed correction factors to take into account rate effects and anisotropy. For a plasticity index of 40 to 50 %, Bjerrum's correction factor, $\mu$, of about 0.8 should be applied to the Genesee Clay; therefore, assuming the minimum field vane peak strength of 40 kPa, the predicted mobilised strength is 32 kPa which does not fall within the range of values obtained from the backanalysis. Another method of estimating undrained strength for the total stress analysis was proposed by Mesri (1975) who suggested that

$$c_u = 0.22\sigma_p' \quad \ldots\ldots\ldots\ldots\ldots\ldots\ldots\ldots\ldots\ldots(7.1)$$

where $\sigma_p'$ is the preconsolidation pressure. Based on the result of consolidation tests on samples from the cooling pond, a constant preconsolidation pressure of 150 kPa can be assumed yielding a predicted mobilised strength of 33 kPa according to Mesri's method. Again, this method could not predict the field strength of the unweathered clay.

However, it is to be noted that the slope failed 4 months after excavation and that delayed failure might have been the result of pore pressure dissipation as dicussed by Vaughan and Walbancke (1973). Due to swelling, there could have been an increase in water content and therefore, a decrease in undrained strength. However, based on the fact that the coefficient of consolidation is small (of the order of 0.35 $m^2$/yr for tests on a block sample from the side of the ditch), the charts given by Eigenbrod (1975) show that only a small amount of pore pressure dissipation could have taken place. Therefore, the moisture content could not have changed by a large amount to cause a substantial reduction in undrained strength. Consequently, the lower operational strength was probably caused by the presence of structural discontinuities; this is supported by the undrained analysis of the SR770 embankment failure where the estimated operational strength of the unweathered clay is between 22 and 29 kPa which falls within the range of strength estimated for this case.

## 7.3 BACKANALYSIS OF SR770 EMBANKMENT FAILURE

A detailed description of the embankment failure is given by Crooks et al (1985). The overpass structure was one of the components in the relocation of the highway SR770 and its site was shown in Plate 1.1. The approach fills to the overpass were designed to a maximum height of approximately 13 m. The construction of the north approach fill started in

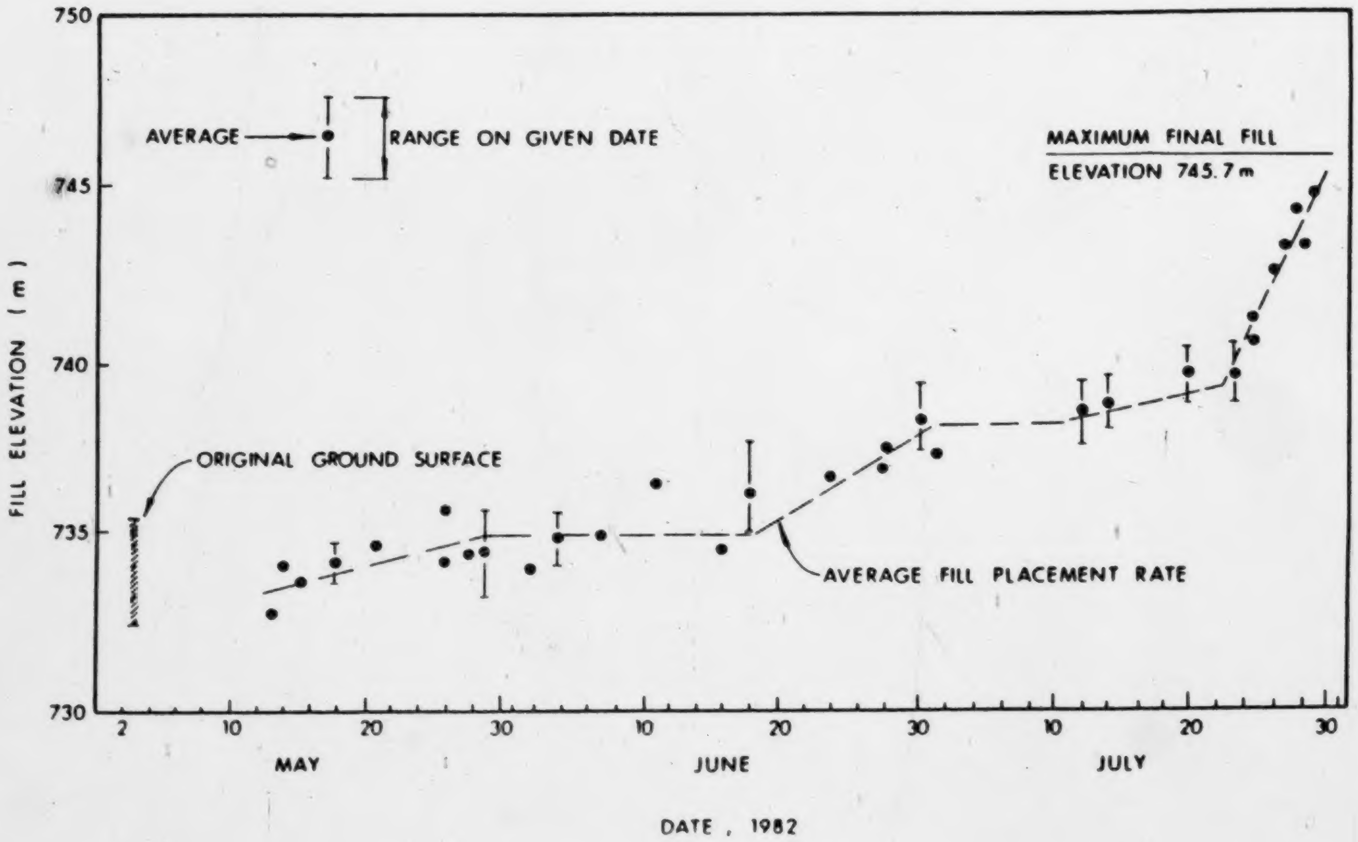

Figure 7.4 Construction history of SR770 embankment fill.

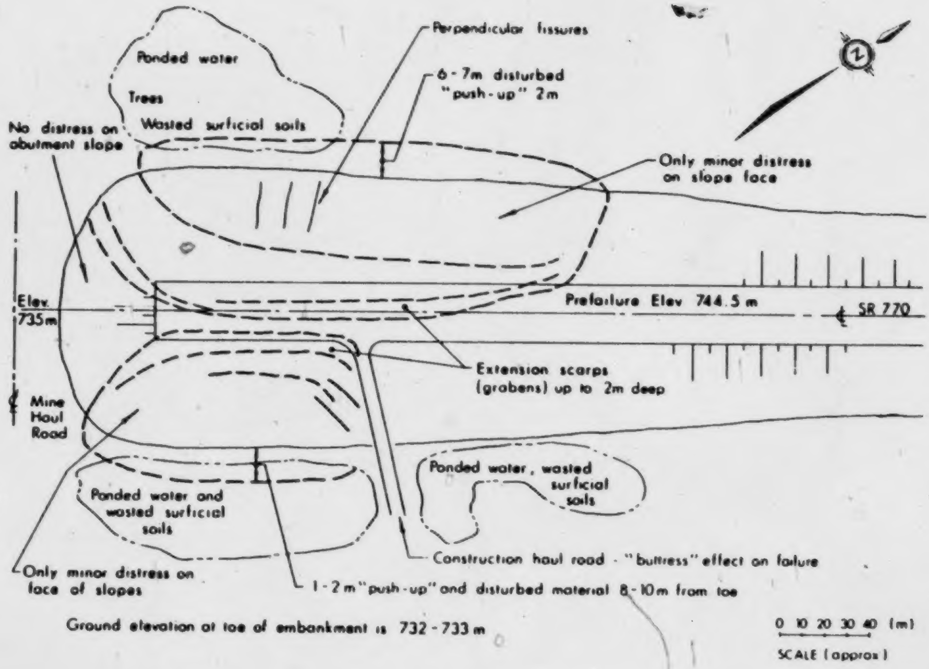
Ponded water
Trees
Wasted surficial soils
No distress on abutment slope
Perpendicular fissures
6 - 7m disturbed "push - up" 2m
N
Only minor distress on slope face
Elev. 735m
Prefailure Elev 744.5 m
℄ SR 770
Extension scarps (grabens) up to 2m deep
℄ Mine Haul Road
Ponded water, wasted surficial soils
Ponded water and wasted surficial soils
Construction haul road - "buttress" effect on failure
Only minor distress on face of slopes
1 - 2 m "push - up" and disturbed material 8 - 10m from toe
Ground elevation at toe of embankment is 732 - 733 m
0 10 20 30 40 (m)
SCALE (approx)

Figure 7.5 Plan view of SR770 embankment failure.

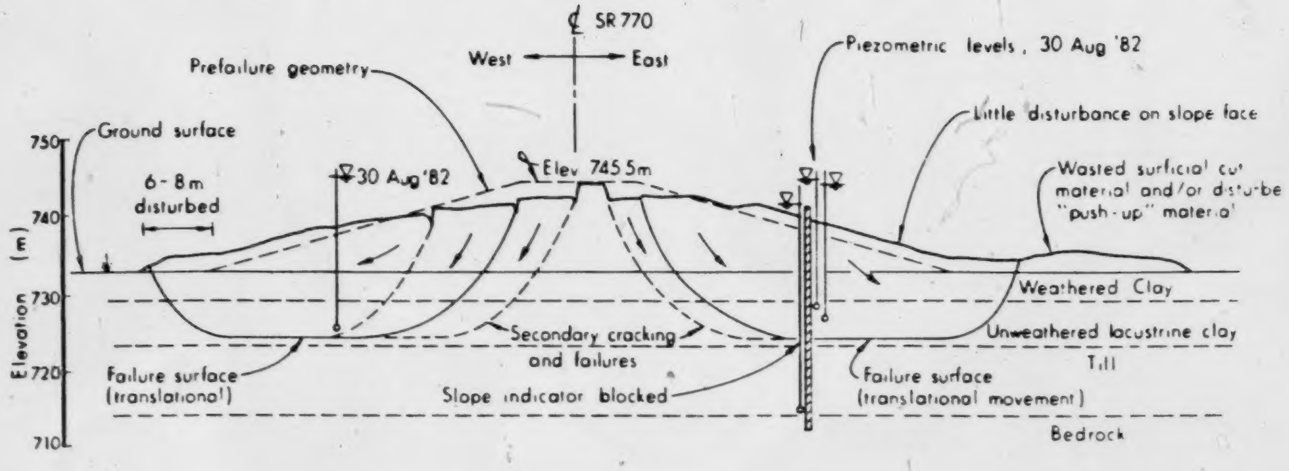
℄ SR 770
West
East
Prefailure geometry
Piezometric levels, 30 Aug '82
Little disturbance on slope face
Wasted surficial cut material and/or disturbe "push-up" material
Ground surface
750
740
730
720
710
Elevation (m)
6 - 8m disturbed
30 Aug '82
Elev 745.5m
Weathered Clay
Unweathered lacustrine clay
Till
Bedrock
Secondary cracking and failures
Failure surface (translational)
Slope indicator blocked
Failure surface (translational movement)

Figure 7.6 Cross section of SR770 embankment.

the spring of 1982 and consisted mainly of compacted silty clay. The sides were built to a slope of 3.5 horizontal to 1 vertical. When a height of approximately 12 m was reached, failures occurred on both sides of the embankment. The construction history of the embankment is given in Fig. 7.4 and a plan view and cross section of the main features of the failure are given in Fig. 7.5 and 7.6 respectively. These three figures are reproduced from Crooks et al (1985).

Instrumentation to measure lateral displacements and porewater pressures were installed two weeks after the failure and the position of these mesurements are shown in Fig. 7.6. However, from the deflection of the slope indicator, it was possible to infer that failure occurred within the unweathered clay although the complete geometry of the failure surface could not be obtained. The fact that the piezometers were installed 2 weeks after the failure implies that some pore pressure could have dissipated but considering the low $c_v$ of the material, the amount of dissipation was assumed to be insignificant. In addition, the porewater pressure measured in the unweathered clay yielded a B of 0.8 which is consistent with values obtained for the dyke of the cooling pond; B is defined as the ratio of the increase in porewater pressure to the increase in vertical stress due to the placement of fill.

### 7.3.1 Total stress analysis

In performing the backanalysis, appropriate assumptions had to be made about the undrained strength of the fill and brown clay. The brown clay was assumed to have an undrained strength of 40 kPa which represents the large strain strength of this material. The mobilisation of shear strength in the embankment fill for backanalysis was discussed by Bjerrum (1972); when no crack is observed prior to failure, the full strength could be assumed to have been mobilised whereas in the case where cracks are observed, the assumption is made that the crack remains open during failure and the extreme case would be to assume that the crack occurs throughout the depth of the fill in the case of a brittle material. In the SR770 embankment failure, cracks were observed on the crest prior to failure but because of the uncertainty concerning the depth of these cracks it was decided to perform the stability analysis using reduced undrained strength in the fill. Vane shear tests by Thurber Consultants on the fill of the cooling pond dyke gave undrained strengths of 75 to over 100 kPa and trial values of 40 and 60 kPa were adopted. The stability analyses were run using both the Bishop method for circular failure and the Morgenstern and Price method for non-circular failure. The results of the analysis for the most critical failure surfaces shown in Fig. 7.7 are presented in Fig. 7.8. The analysis shows that the critical failure surfaces from both Bishop and Morgenstern and Price methods of analysis are

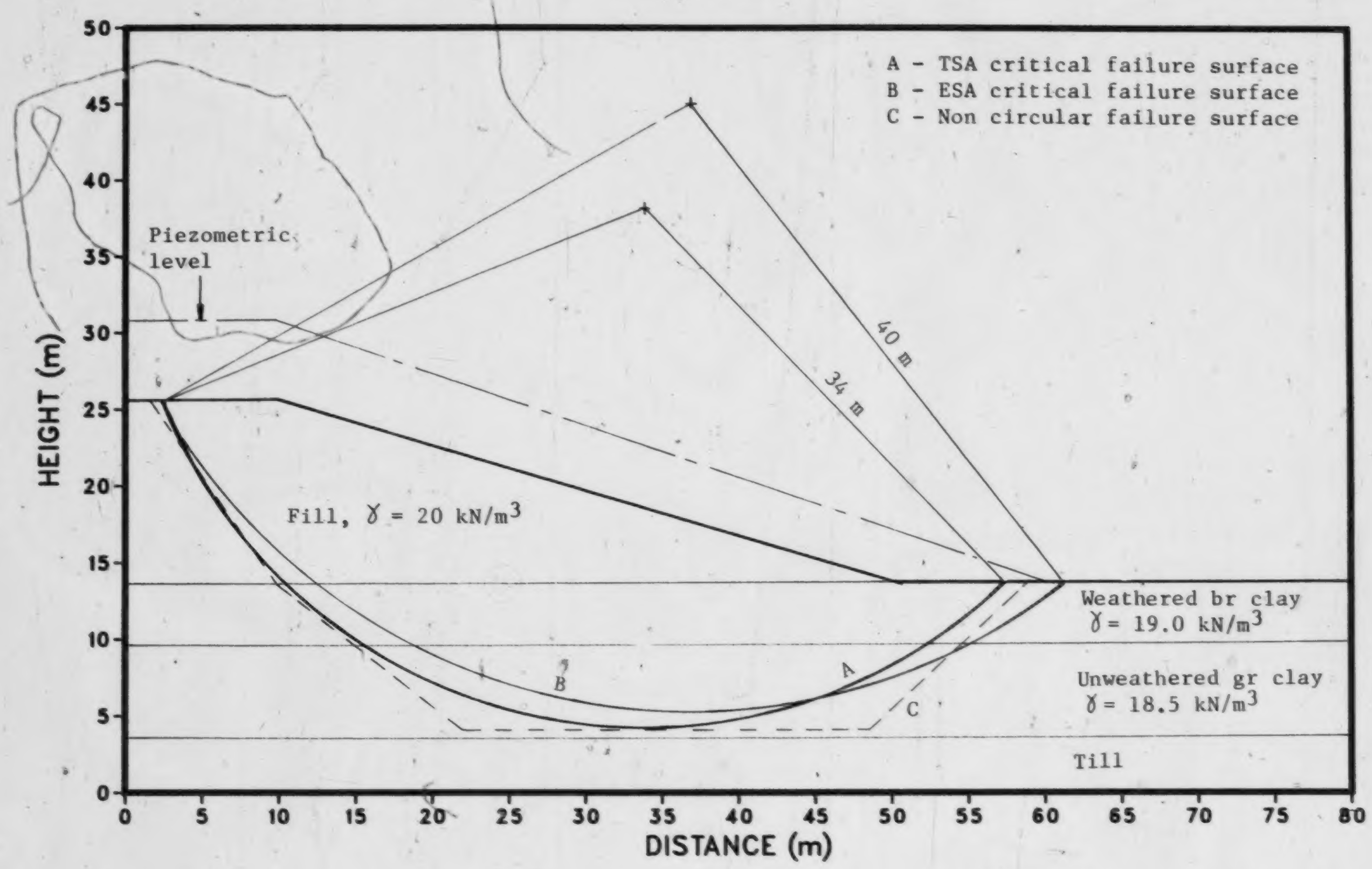
A - TSA critical failure surface
B - ESA critical failure surface
C - Non circular failure surface
Piezometric level
40 m
34 m
Fill, $\gamma = 20$ kN/m$^3$
Weathered br clay
$\gamma = 19.0$ kN/m$^3$
Unweathered gr clay
$\gamma = 18.5$ kN/m$^3$
Till
A
B
C
HEIGHT (m)
DISTANCE (m)
0
5
10
15
20
25
30
35
40
45
50
55
60
65
70
75
80

Figure 7.7 Critical failure surfaces for SR770 embankment.

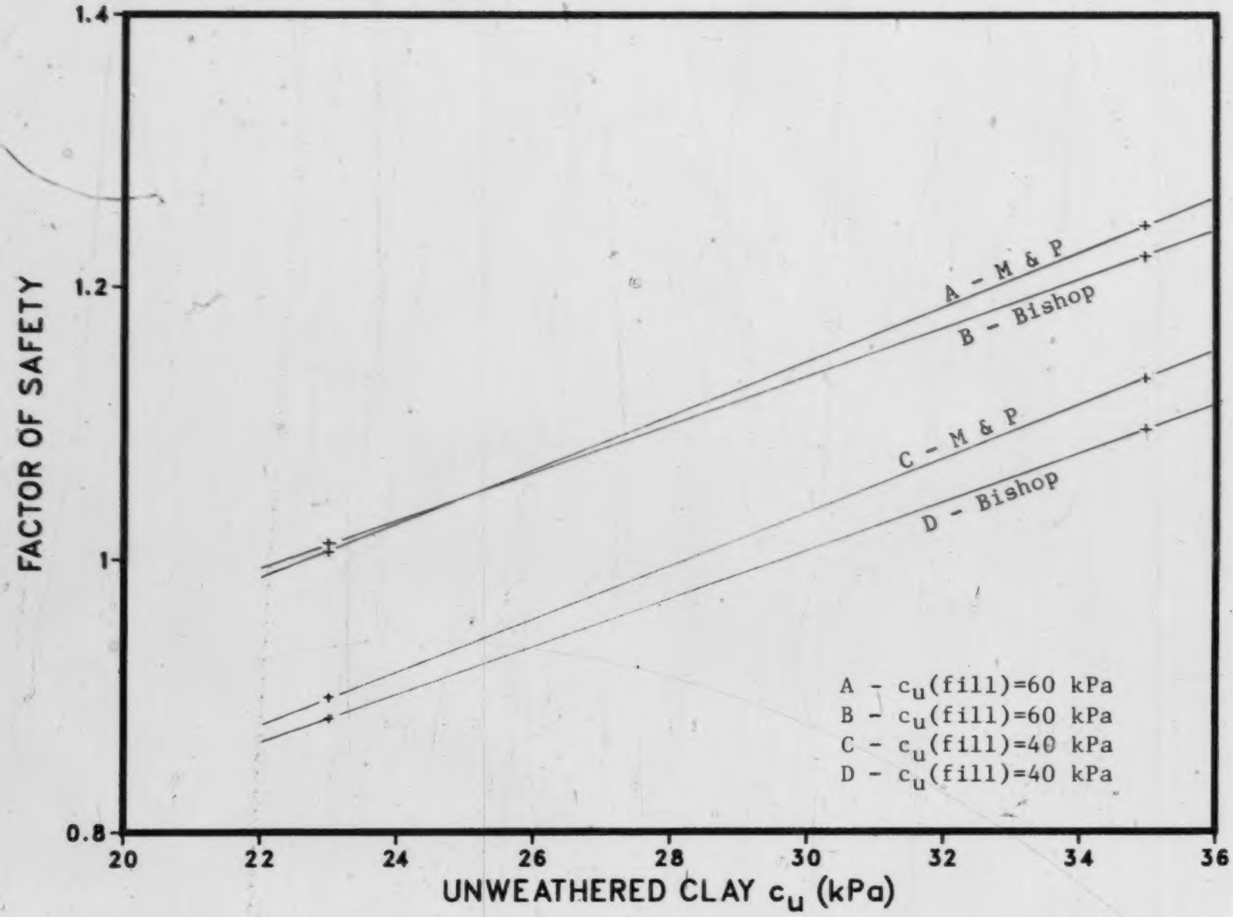

Figure 7.8 Total stress analysis results of SR770 embankment.

consistent with the observed geometry at the time of failure. The analysis also shows that the assumption of the fill strength of 40 to 60 kPa gave undrained strength within the unweathered clay of the order of 22 to 29 kPa which agrees with values obtained from the backanalysis of the slope failure at the diversion ditch. Therefore, this confirms that the operational strength of the Genesee Clay could not be predicted by the field vane strength after application of the correction factors.

### 7.3.2 Effective stress analysis

The analyses were performed based on the following assumptions:

1. Because pore pressures were not measured in the fill and the weathered clay, it was decided to assume undrained strengths in these two materials as part of the parametric study. The author recognised that it is not normal practice to adopt such an approach. The analysis was conducted in order to explore the possible range of assumptions that could be made.

   The fill strength was assumed to vary between 40 and 60 kPa based on the results of the total stress analysis. The brown clay was assigned a strength equivalent to the large strain strength of 40 kPa. For the unweathered clay, c' was assigned a value of 0 and $\phi'$ was varied. The piezometric line assumed is shown in Fig. 7.7 and is based on the piezometer readings in Fig.

7.6 and on the fact that B is generally about 0.8 for the unweathered clay. The Morgenstern and Price method was used. Bishop analysis was only performed for the case of the fill strength of 40 kPa.

2. The charts by Rivard and Goodwin (1978) were used to determine drained parameters for the fill. For a liquid limit of the fill of 55%, c' = 20 kPa and $\phi'$ = 23° were obtained. The large strain strength parameters of c' = 0 and $\phi'$ = 18.5° for the brown clay were assumed. Since no pore pressure measurements were made in the fill or brown clay, $r_u$ values of 0.4 were assumed in these materials based on measurements at the high dyke given in Thurber (1985); the piezometric line in the unweathered clay is the one shown in Fig. 7.7. The effect of using the peak strength parameters of c' = 26 kPa and $\phi'$ = 23° for the brown clay was also investigated. Only the Morgenstern and Price analysis was performed and the results are given in Fig. 7.9.

It is to be noted that the Bishop method gave a slightly different critical failure surface for the total and effective stress analysis; however, the same critical surface was obtained for both undrained and drained analyses for the Morgenstern and Price method.

Fig. 7.9 shows that the mobilised $\phi'$ in the unweathered clay at failure is between 17° and 20° for the assumptions made. It is of interest to note that the average large strain strength envelope of Fig. 6.23 gave a $\phi'$ of 20° and

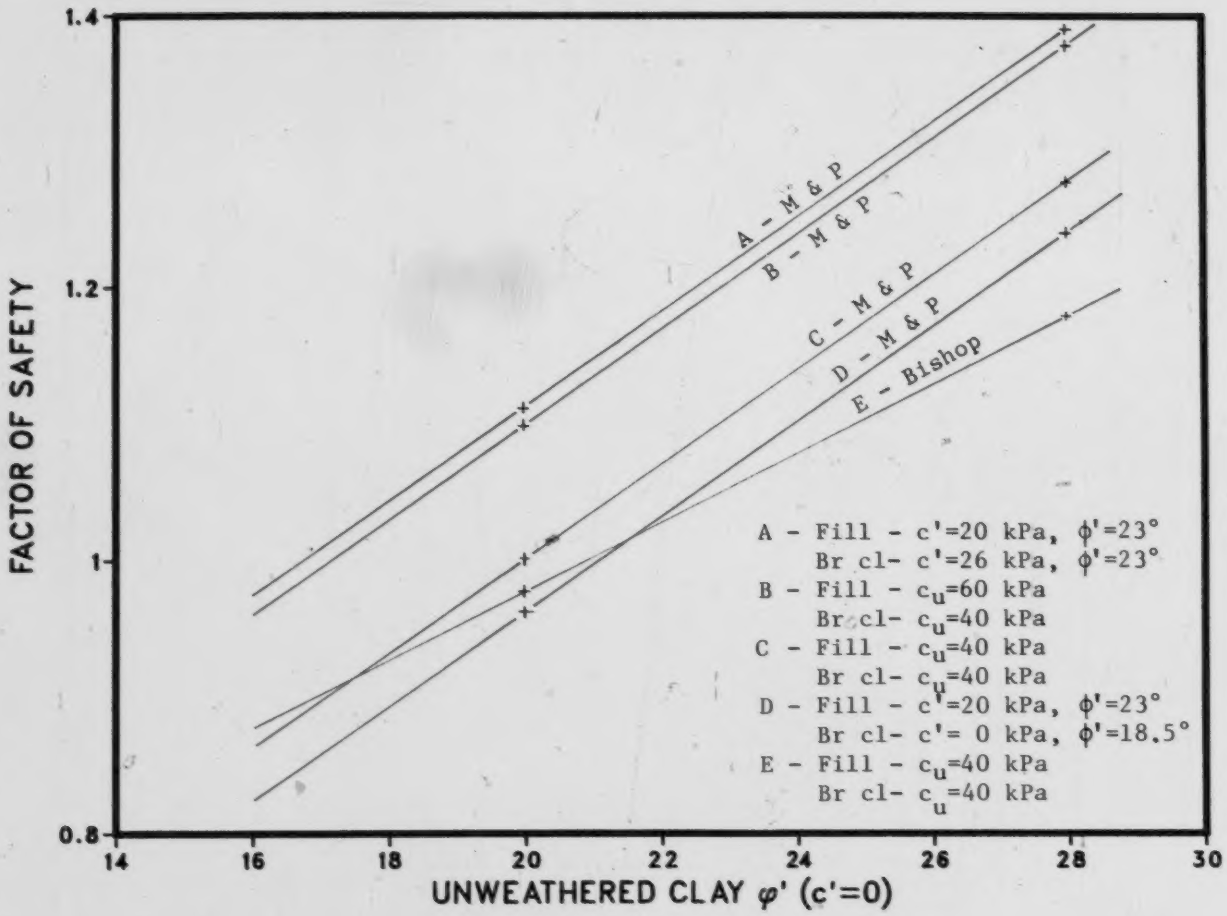

Figure 7.9 Effective stress analysis of SR770 embankment.

the backanalysis shows that this value of $\phi'$ is mobilised when the large strain parameters for the brown clay were used. It is also worth noting that the effective stress parameters for the fill obtained from Rivard and Goodwin (1978) gave reasonable results. Consequently, the mobilised $\phi'$ is between the peak and residual values and since there is no evidence that failure occurred along a presheared surface, there is the likelihood that progressive failure mechanisms were operational. Since the Genesee Clay is strain-weakening because of the presence of randomly oriented discontinuities, the process of taking the soil past the peak strength was probably due to the discontinuities acting as stress concentrators (Skempton, 1970).

## 7.4 LARGE DEFORMATION AT HIGH DYKE

The basic soil properties at the high dyke is shown in Fig. 7.2. Fig. 7.10 gives a cross section of the dyke which was built in 4 stages with the remaining fifth lift still left to be placed. The schedule of the construction was as follows:

Stage 1 - September - November, 1982.
Stage 2 - July - September, 1983.
Stage 3 - September - October, 1983.
Stage 4 - November, 1983.

The pore pressure response within the unweathered grey clay against construction activities along the centreline of the

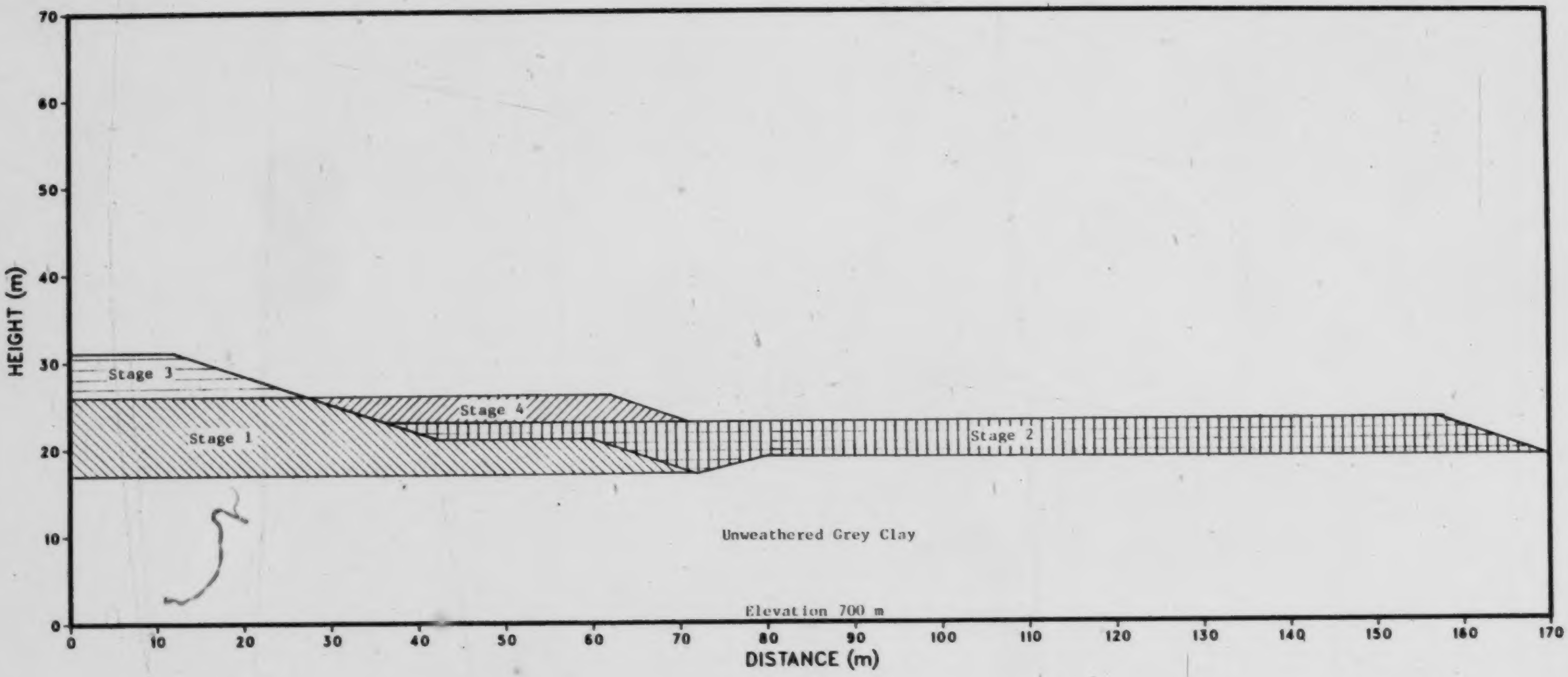
HEIGHT (m)
70
60
50
40
30
20
10
0
Stage 3
Stage 4
Stage 1
Stage 2
Unweathered Grey Clay
Elevation 700 m
0
10
20
30
40
50
60
70
80
90
100
110
120
130
140
150
160
170
DISTANCE (m)

Figure 7.10 Stages in construction of high dyke.

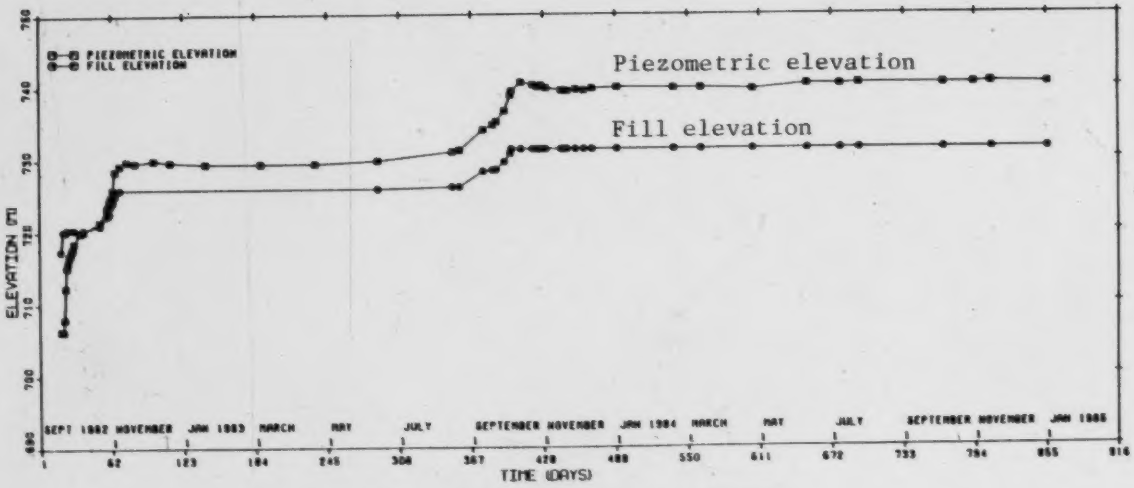

GENESEE COOLING POND DYKE PIEZOMETER HDP23

TIP INSTALLED IN CH-GREY CLAY - ELEV.=706.00

SEPT 1,1982:DAY 1.INITIAL READING SEPT 20,1982

Figure 7.11 Pore pressure response with construction activities under centreline of dyke.

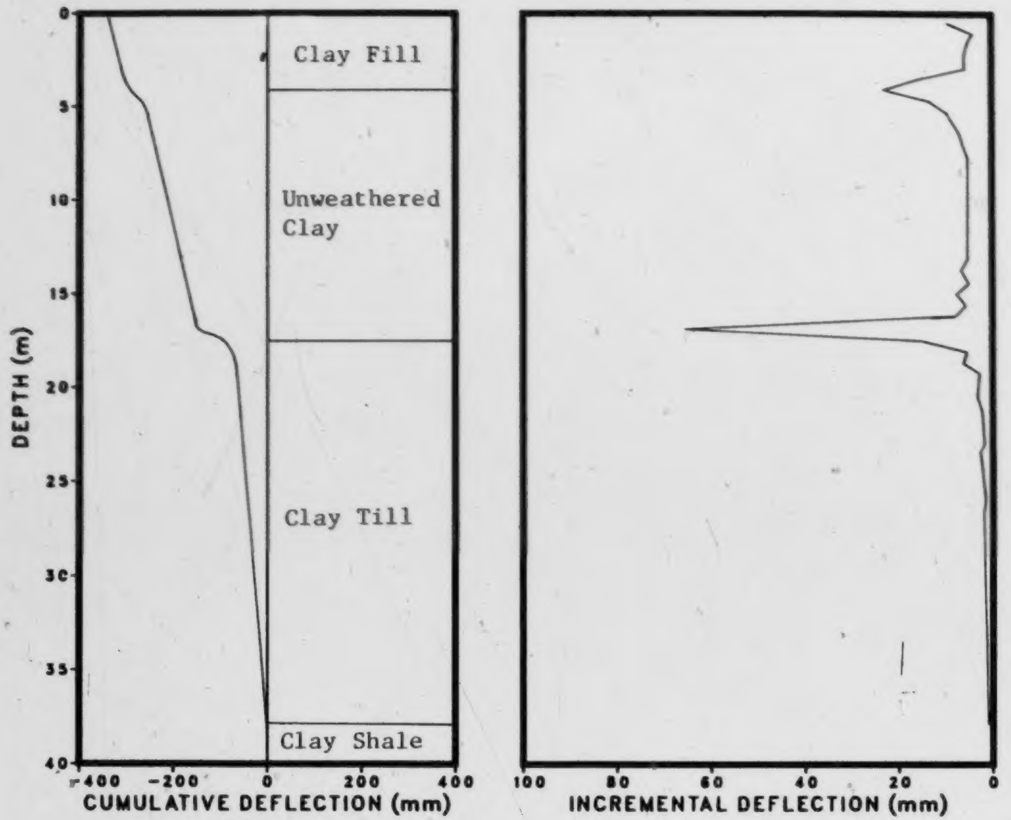

Note: Slope indicator was installed on Oct. 28,1982 prior to start of construction. Deflection shown was measured on July 27, 1984 and represented movement perpendicular to centreline of dyke.

Figure 7.12 Movement registered by Thurber SI5 slope indicator.

dyke is shown in Fig. 7.11. It can be seen that there was insignificant pore pressure dissipation between construction stages. A slope indicator (Thurber SI5) installed prior to the start of construction at the position shown in Fig. 7.14 indicates that large movements started just after stage 3 was completed as shown in Fig. 7.12. Yielding was occurring just above the interface (depth of 17.6 m) of the unweathered grey clay with the underlying clay till although movements also occurred at the fill and clay interface. Cracking at the crest of the dyke was also observed. Fig. 7.13 shows that about 30 mm of shear displacement had occurred at the clay and till interface before the stabilising berm 4 was placed; it is to be noted that less than 10 mm of deflection was recorded in the slope indicator prior to construction of stage 3.

The stability of the high dyke after stage 3 was studied by assuming a non-circular failure surface and the critical one is shown in Fig. 7.14. For the fill, undrained strength of 40 kPa was assumed for total stress analysis and $c' = 20$ kPa and $\phi' = 23°$ for effective stress analysis; the zone of weathered clay was not encountered in this area. An $r_u$ of 0.4 was assumed in the fill and the piezometric line for the unweathered clay is shown in Fig. 7.14; this line was drawn based on the readings of piezometers Thurber HDP 23 and 29. The readings of these piezometers are given in Fig. 7.11 and 7.15 respectively.

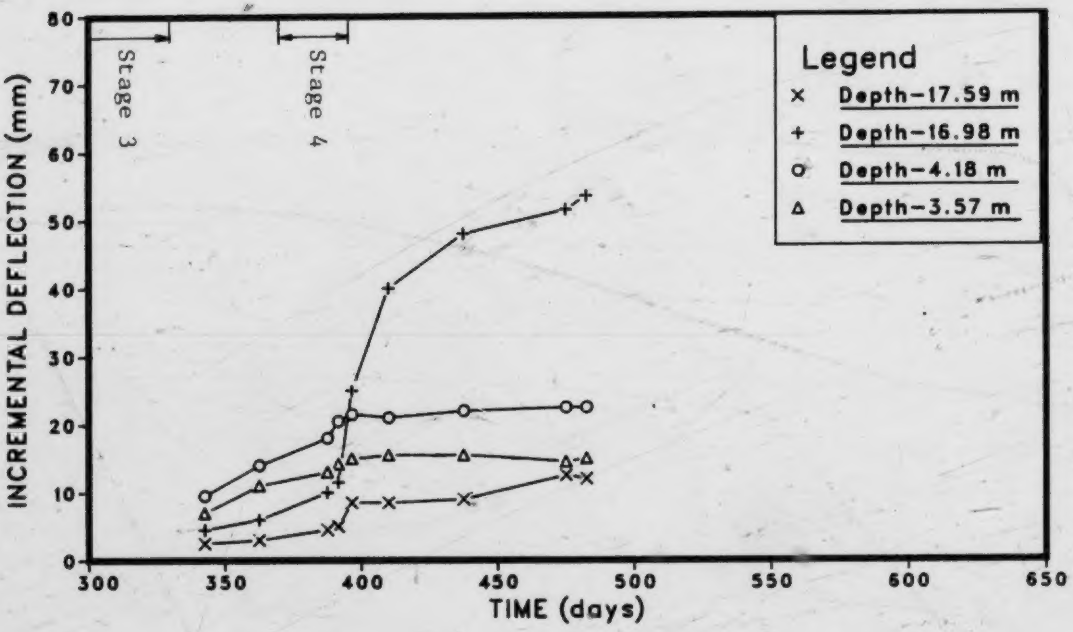

Figure 7.13 Variation of movement of slope indicator SI5 with time.

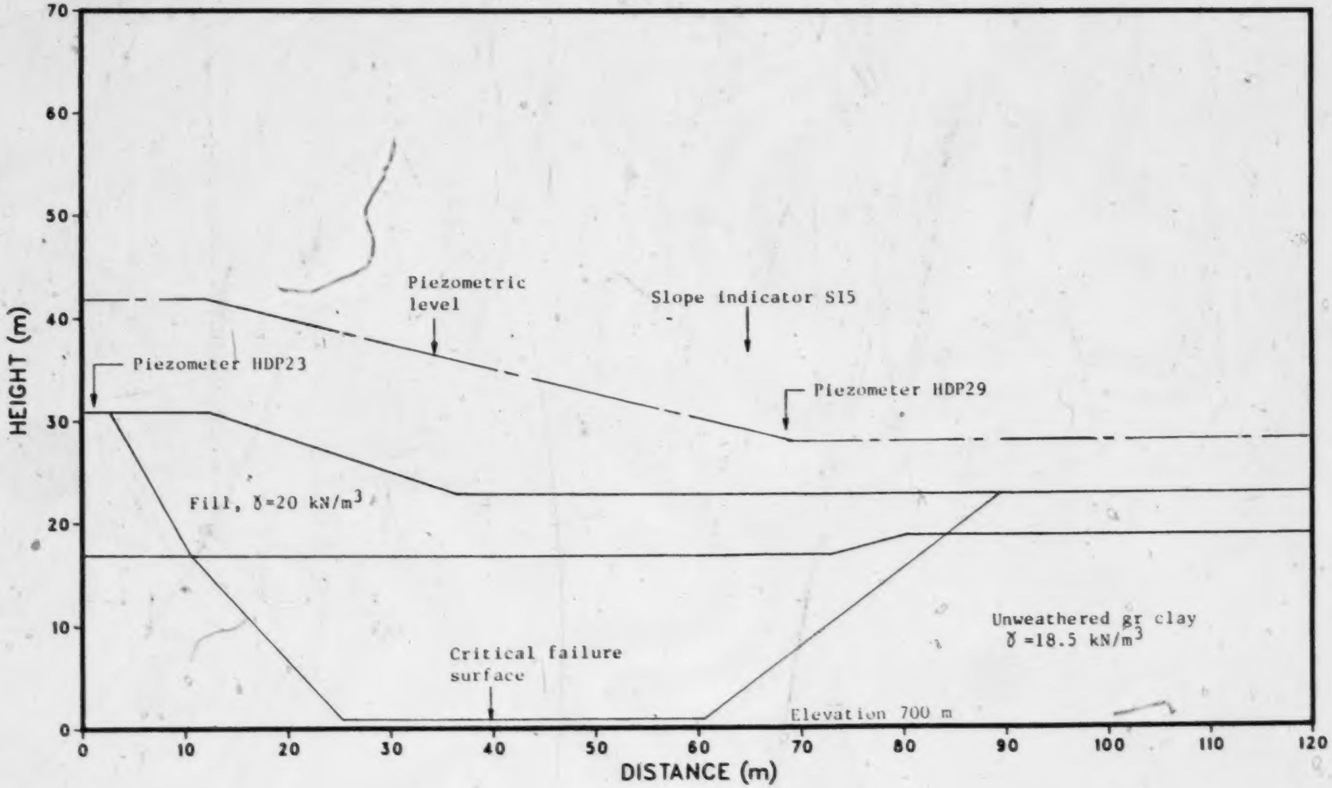
HEIGHT (m)
70
60
50
40
30
20
10
0
Piezometric level
Slope indicator S15
Piezometer HDP23
Piezometer HDP29
Fill, $\gamma$=20 kN/m$^3$
Unweathered gr clay
$\gamma$ =18.5 kN/m$^3$
Critical failure surface
Elevation 700 m
0
10
20
30
40
50
60
70
80
90
100
110
120
DISTANCE (m)

Figure 7.14 Cross section of high dyke for stability analysis.

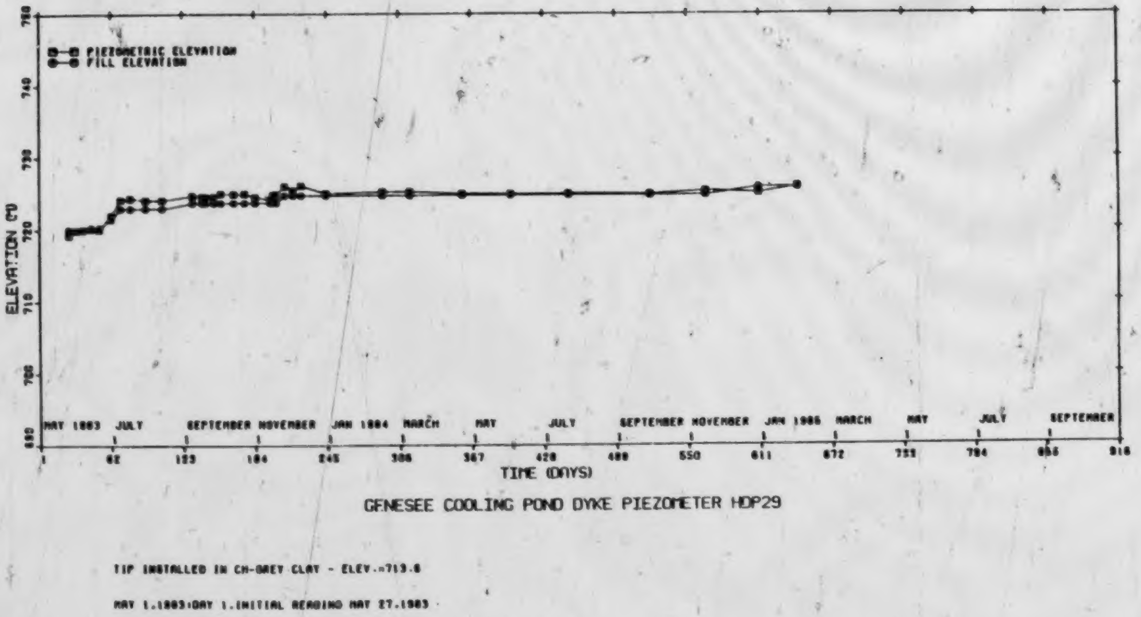

Figure 7.15 Pore pressure response of piezometer Thurber HDP29.

These analyses show that assuming the operational strength obtained from the previous backanalyses the factor of safety is higher than 1.3 (Fig. 7.16 and 7.17). However, the large deformations within the unweathered clay and the cracking of the fill suggest that there was an onset of yielding. This is shown in Fig. 7.18 where the pore pressure observed by the piezometer HDP 23 indicates that yielding started when the fill reached the elevation of approximately 726 m. The stress path at HDP 23 is shown in Fig. 7.19. At that particular point, the in-situ $K_0$ is assumed to be 1 based on measurements at the other test locations in the cooling pond. The total stress path was constructed using the elastic stress distributions given in Poulos and Davis (1974) for a vertical embankment loading on a semi-infinite mass. The effective stress path was then drawn by subtracting the observed porewater pressure from the total stresses. The yield envelope for the block sample (Fig. 5.8) is also shown in Fig. 7.19 in order to compare it with the in-situ yielding characteristics. The following comments can be made concerning the behaviour of the Genesee Clay under loading:

1. the initial part of the calculated effective stress path suggests that $\Delta u/\Delta\sigma_{oct}$ is 0.56 which is in agreement with observations made by Pender et al (1975). However, this ratio predicted from isotropic elasticity is 1.0 (Parry and Wroth, 1981). This deviation could have been due to an anisotropic response although it was shown in

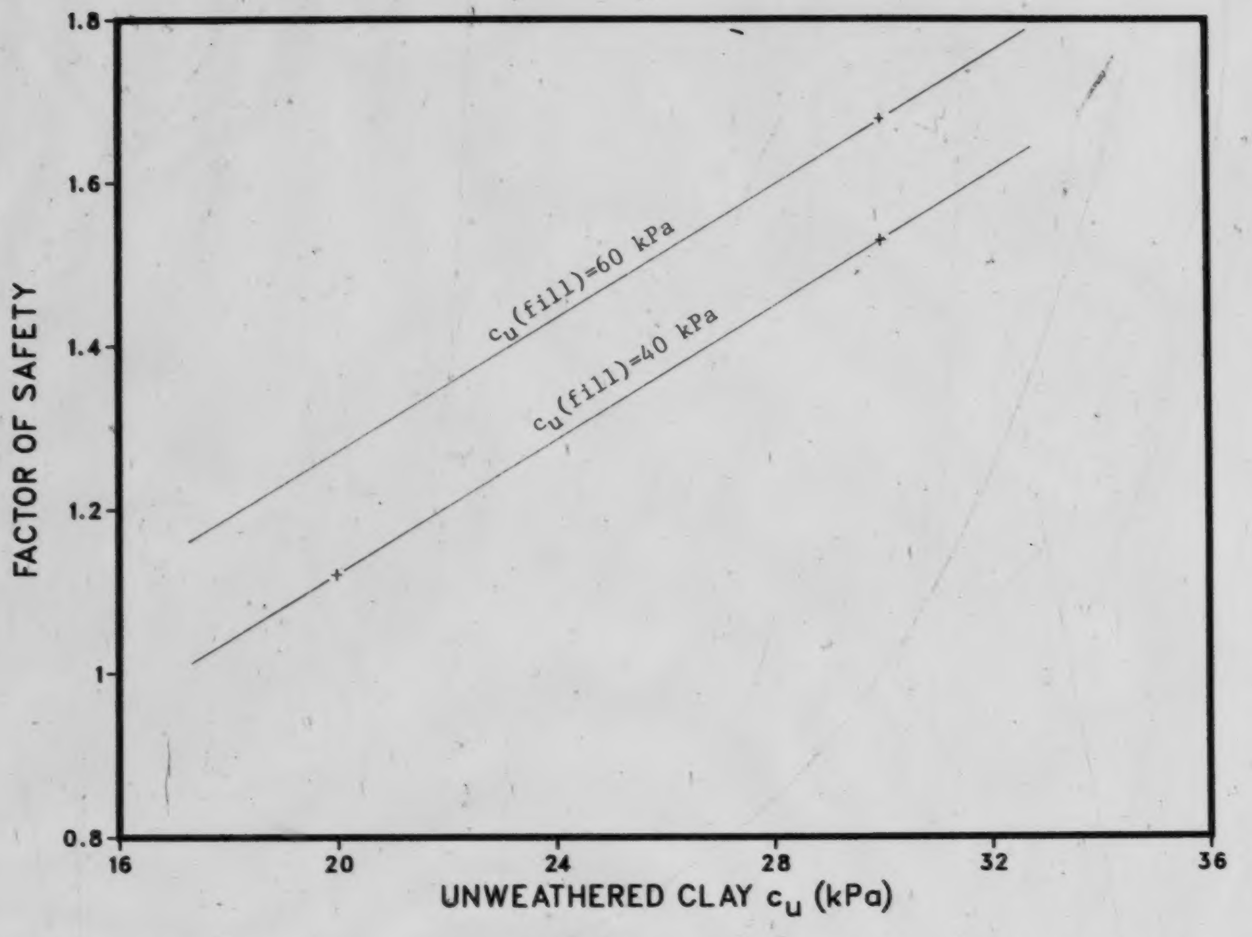

Figure 7.16 Total stress analysis results of high dyke.

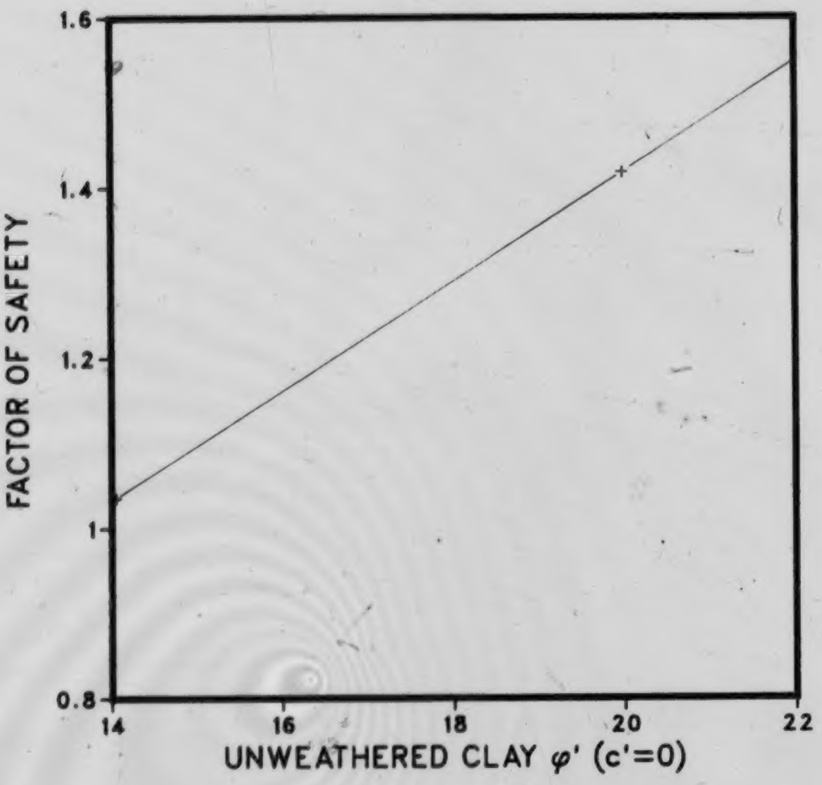

Figure 7.17 Effective stress analysis of high dyke.

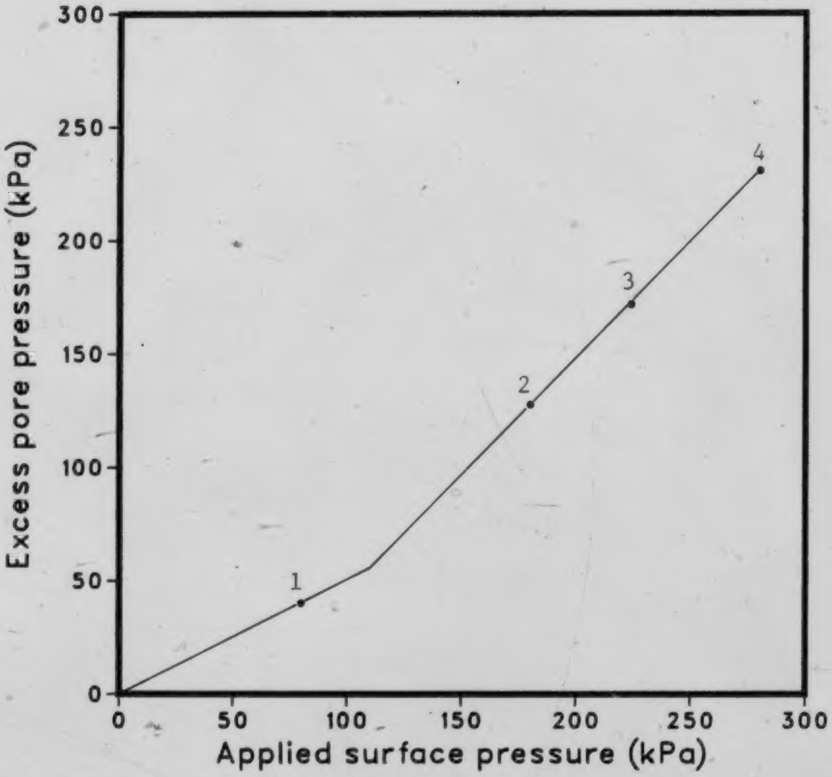

Figure 7.18 Observed excess pore pressure against applied surface pressure.

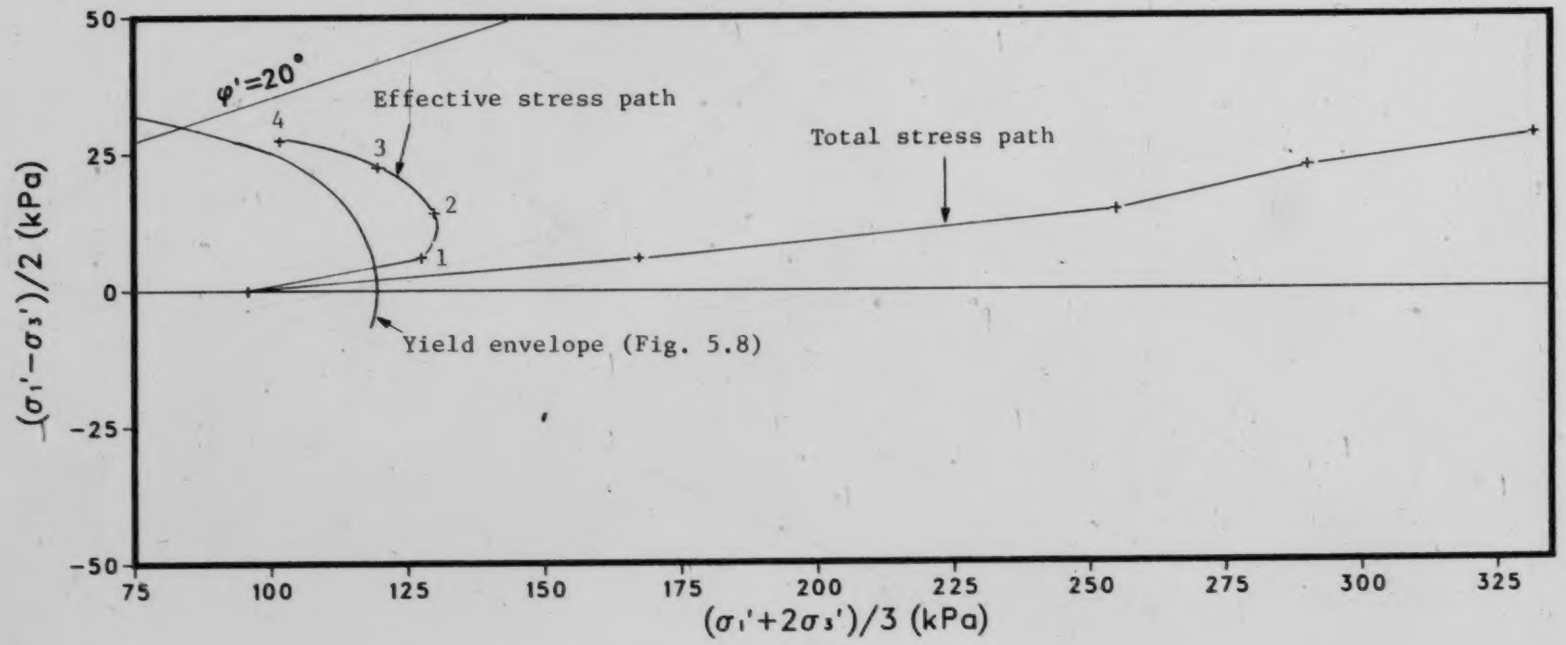

Figure 7.19 Stress paths at piezometer HDP23.

the previous chapter that the laboratory results seem to indicate that the clay would behave isotropically. Therefore, there is the possibility that some of the excess pore pressure could have dissipated during the first stage of dyke construction.

2. the yield envelope for the block sample need not represent the one for the soil at the level of piezometer HDP 23 as the position of the envelope is dependent on the past stress history. However, the shape of the envelope would be similar.
3. it is found that yielding started shortly after reaching point 1 (Fig. 7.18 and 7.19), that is, after the stress path reached the yield envelope. Therefore, the yield envelope for the soil at HDP 23 lies slightly beyond the one for the block sample. After yielding, high pore pressures were generated and it is of interest to note that the effective stress path followed the yield envelope or was close to it.
4. the soil under consideration had not reached failure which is represented by the large strain strength envelope in Fig. 7.19 although other zones of soil under the embankment might have been in a state of contained failure.
5. the high straining indicated by the slope indicator SI 5 represented the yielding or contained failure of the soil under the embankment.

The stress path followed by the clay closely resembled that found by Tavenas (1979) in studying the cases in Eastern Canadian clays. While the interpretation of yielding has been made from the observations of pore pressures in the present study, Clausen et al (1984) discussed other possible methods of identifying yielding such as from measurements of strain and observations of creep behaviour under the loading zone.

## 7.5 DISCUSSION

The main point of interest in this chapter is to determine the role of discontinuities within the Genesee Clay in controlling its field behaviour. The total stress analyses have shown that the mass undrained strength of the clay is between 22 and 28 kPa and the conventional correction factors of Bjerrum (1972) applied to the minimum field vane data are inadequate to predict these strengths. Therefore, these point to the fact that the operational strength is controlled by discontinuities and that field vane tests are not satisfactory in providing data for the stability analysis of fissured clays.

The most significant work in the effective stress analysis of structures built on soft fissured clays is the backanalysis of various failures by Rivard and Lu (1978). These authors subsequently recommended the use of $c' = 0$ and $\phi'$ obtained from tests within the normal consolidation stress range. On the other hand, Pilot et al (1982) recommended the use of the CIU or CAU large strain strength parameters on samples consolidated to the estimated overburden pressures although they were not working specifically with fissured soils. These two approaches approximate to the fully softened condition proposed by Skempton (1970). Backanalysis of the SR770 failure shows that the operational strength for the Genesee Clay is $c' = 0$ and $\phi' = 20^\circ$ which are also parameters given by the large strain tests on samples containing discontinuities; this implicitly confirms the role of discontinuities in controlling the field strength. It is interesting to note that within the normally consolidated range, $\phi'$ is also equal to 20°. Nevertheless, the fact that the operational strength is between the peak and residual envelopes and there is no evidence that the failures occurred along any plane of failure indicates that the mechanism of progressive failure might have existed in the cases studied.

The monitoring of pore pressures under the high dyke has been helpful in determining the behaviour of the Genesee Clay prior to failure. It was found that the soil started to yield shortly after the surface loading was applied as a result of the fact that the in-situ state of stress was close to the yield envelope; this is due to the clay being lightly overconsolidated and also the high value of $K_0$. After the stress path reached the yield envelope high pore pressures were generated as a result of the fact that the clay followed the yield envelope towards the failure line.

Therefore, the determination of the yield envelope is helpful in observing, at least qualitatively, the behaviour of the clay under loading.

# 8. CONCLUSIONS

This chapter has been divided into 3 parts in order to reflect the steps followed in the investigation of the Genesee clay. The first part is related to the geological characteristics of the clay; in the second part, conclusions concerning the methods of investigation are made and the third part deals with the field behaviour of the clay.

## 8.1 CHARACTERISTICS OF GENESEE CLAY

Genesee clay may be classified as a geotechnically complex material in the sense that geotechnical properties were observed to vary across a wide range within short distances of the order of less than 100 m. Although the clay was deposited in a complex fluctuating sedimentary environment, the genetic complexities do not dominate the present behaviour of the clay. The variations in properties occur not only in the strength of the intact material as determined by the vane shear tests but also in the distribution of the discontinuities. These variations are the results of a complex combination of epigenetic processes originating from deposition on a melt-out till which had a high ice content and of weathering processes. The post-depositional melting of the ice had two effects on the clay, namely:

1. the formation of slickensides and fissures as a result of internal stressing due to deformation at the bottom of the clay layer;

2. the spatial variation in the lateral stresses of the deposit which seems to be related to the topography. High $K_0$ were measured at the topographic highs and low $K_0$ at the topographic lows. However, the exact mechanism responsible for such a distribution is not known with certainty.

The presence of the slickensides has modified the behaviour of the clay into a strain-weakening material with the possibility of the discontinuities acting as stress concentrators. This behaviour is confirmed by both laboratory tests and backanalysis of the failures associated with construction of the Genesee Power Project. On the other hand, the spatial variation in the lateral stresses has resulted in a variation of the undrained strength across the site. Nevertheless, the present strength properties of the clay are dominated by the presence of the discontinuities.

## 8.2 FIELD AND LABORATORY INVESTIGATIONS

One of the special tests was the determination of the in-situ lateral stresses. In this respect, it was found that the total stress cells driven into the soil gave good prediction of the lateral stresses. Hydraulic fracture, although giving comparable results to the total stress cells in the zones where $K_0$ is less than unity, measured lateral stresses higher than the overburden pressures in zones of high lateral stress. Therefore, there is some doubt as to whether the hydraulic fracture tests measure the minor principal stress. The performance of the Marchetti flat plate dilatometer was variable so that further testing of this method is required before its acceptability can be judged.

For the estimation of $K_0$ in the laboratory, the suction method of Skempton (1961) was found satisfactory although this method requires good quality block samples. On the other hand, the tube samples seemed to have lost most of the suction through sampling disturbance.

The yield envelope determined in the laboratory by stressing the soil along different stress paths was found to be consistent with the field stress path followed by the clay which was yielding under the embankment loading.

## 8.3 FIELD BEHAVIOUR OF GENESEE CLAY

The field behaviour was determined from the instrumented structures for the Genesee Power Project. Backanalysis of a slope failure and an embankment failure indicates that the operational strength of the Genesee Clay is controlled by the randomly distributed discontinuities. It was found that, for this class of material, the total stress analysis based on strengths derived from empirical correlations is not a useful tool for design purposes. On the other hand, the effective stress analysis has shown that the operational strength of $c'=0$ and $\phi'=20°$ for the Genesee Clay could be found adequately from the large strain strength envelope determined from undrained triaxial tests with pore pressure measurements on samples consolidated to the in-situ stresses and tested to strains of about 15%.

In addition, because (1) the clay exhibited strain-weakening behaviour in laboratory tests, (2) there is no indication that failure occurred along a single plane of weakness and (3) the operational strength in the field is between the peak and residual envelopes, there is the likelihood that progressive failure mechanisms were operational in the cases studied.

# REFERENCES

Abdelhamid, M.S. and Krizek, R.J. 1976. At - rest lateral earth pressure of a consolidating clay. ASCE Journal of the Geotechnical Engineering Division, Vol. 102, GT 7, pp. 721 - 738.

Acton, D.F. and Fehrenbacher, J.B. 1976. Mineralogy and topography of glacial tills and their effect on soil formation in Saskatchewan. In: Glacial Till, ed. by R.F. Legget, Royal Society of Canada, Special Publication 12, pp. 170 - 185.

Al-Hussaini, M. 1981. Comparison of various methods of determining Ko. In: Laboratory shear strength of soil, ASTM STP 740, ed. by R.N. Yong and F.C. Townsend, ASTM, pp. 78 - 93.

Andersen, K.H., DiBiagio, E. and Bjerrum, L. 1972. Discussion. Proceedings, 5th European Conference on Soil Mechanics and Foundation Engineering, Madrid, Vol. 2, pp. 97 - 98.

Andriashek, L.D., Fenton, M.H. and Root, J.D. 1978. Surficial Geology, Wabamum Lake, 83G, Alberta Research Council.

Audibert, J.E. and Tavenas, F.A. 1975. Discussion on "Evaluation of stress cell performance ". ASCE Journal of the Geotechnical Engineering Division, Vol. 101, GT 7, pp. 705 - 707.

Baguelin, F., Jezequel, J.F., Lemee, E. and Le Mehaute, A. 1972. Expansion of cylindrical probes in cohesive soil. ASCE Journal of the Soil Mechanics and Foundations Division, Vol.98, SM 11, pp. 1129 - 1142.

Balkir, A. and Marsh, A.D. 1974. Triaxial tests on soils: corrections for effect of membrane and filter drain. Transport and Road Research Laboratory, Department of the Environment, U.K., Supplementary Report 90 UC.

Baracos, A. 1977. Compositional and structural anisotropy of Winnipeg soils - a study based on scanning electron microscopy and x-ray diffraction analyses. Canadian Geotechnical Journal, Vol. 14, pp. 125 - 137.

Baracos, A., Graham, J. and Domaschuk, L. 1980. Yielding and rupture of a lacustrine clay. Canadian Geotechnical Journal, Vol. 17, pp. 559 - 573.

Bayrock, L.A. and Hughes, G.M. 1962. Surficial geology of the Edmonton District, Alberta. Alberta Research

Council, Preliminary report 62-6.

Bishop, A.W. 1955. The use of the slip circle in the stability analysis of slopes. Geotechnique, Vol. 5, pp. 7 - 17.

Bishop, A.W. 1958. Test requirements for measuring the coefficient of earth pressure at rest. Proceedings, Conference on Earth Pressure Problems, Brussels, Vol. 1, pp. 2 - 14.

Bishop, A.W. and Henkel, D.J. 1962. The measurement of soil properties in the triaxial test. Edward Arnold, London.

Bishop, A.W. and Little, A.L. 1967. The influence of the size and orientation of the sample on the apparent strength of the London Clay at Maldon, Essex. Proceedings, Oslo Geotechnical Conference, Vol. 1, pp. 89 - 96.

Bishop, A.W., Webb, D.L. and Lewin, P.I. 1965. Undisturbed samples of London Clay from Ashford Common shaft: strength effective stress relationships. Geotechnique, Vol. 15, pp. 1 - 31.

Bishop, A.W. and Wesley, L.D. 1975. A hydraulic triaxial apparatus for controlled stress path testing.

Geotechnique, Vol. 25, No. 4, pp. 657 - 670.

Bjerrum, L. 1972. Embankments on soft ground. Proceedings, ASCE Specialty Conference on Performance of Earth and Earth - Supported Structures. Purdue University, Lafayette, Indiana, pp. 1 - 54.

Bjerrum, L. 1973. Problems of soil mechanics and construction on soft clays. State of the art report, Session 1V, 8th International Conference on Soil Mechanics and Foundation Engineering, Moscow, pp. 1 - 53.

Bjerrum, L. and Andersen, K.H. 1972. In-situ measurement of lateral pressures in clay. Proceedings, 5th European Conference on Soil Engineering and Foundation Engineering, Madrid, Vol. 1, pp. 11 - 20.

Bjerrum, L., Nash, J.K.T.L., Kennard, R.M. and Gibson, R.E. 1972. Hydraulic fracturing in field permeability testing. Geotechnique, Vol. 22, No. 2, pp. 319 - 332.

Boulton, G.S. 1968. Flow tills and related deposits on some Vestspitsbergen glaciers. Journal of Glaciology, Vol. 7, No. 51, pp. 391 - 412.

Bozozuk, M. 1974. Minor principal stress measurements in marine clay with hydraulic fracture tests. Proceedings, ASCE Specialty Conference on Subsurface Exploration for Underground Excavation and Heavy Construction, Henniker, pp. 333 - 349.

Brooker, E.W. and Ireland, H.O. 1965. Earth pressures at rest related to stress history. Canadian Geotechnical Journal, Vol. 2, No. 1, pp. 1 - 5.

Brumund, W.F., Jonas, E. and Ladd, C.C. 1976. Estimating in situ maximum past (preconsolidation) pressure of saturated clays from results of laboratory consolidometer tests. Special report 163, Transportation Research Board, Washington, D.C., pp. 4 - 12.

Burdick, J.L., Rice, E.F. and Phukan, A. 1978. Cold regions: descriptive and geotechnical aspects. In: Geotechnical Engineering for Cold Regions, ed. by O.B. Ansderland and D.M. Anderson, McGraw Hill, USA, pp. 1 - 29.

Burland, J.B. 1979. Discussion. 7th European Conference on Soil Mechanics and Foundation Engineering, Brighton, UK., Vol. 4 , p. 149.

Burland, J.B. and Maswoswe, J. 1982. Discussion on " In situ measurement of horizontal stress in overconsolidated clay using push-in spade-shaped pressure cells."

Geotechnique, Vol. 32, No. 3, pp. 285 - 286.

Campbell, C.V. 1967. Laminae, lamina set, bed and bedset. Sedimentology, Vol. 8, pp. 7 - 26.

Campanella, R.G. and Robertson, P.K. 1983. Flat plate dilatometer testing: research and development at UBC. Soil mechanics series no. 68. Department of Civil Engineering, UBC, Vancouver, B.C.

Carlson, V.A. 1970. Bedrock topography of the Wabamum Lake map area, 83G, Alberta. Alberta Research Council.

Chandler, R.J. 1966. The measurement of residual strength in triaxial compression. Geotechnique, Vol. 26, pp. 181 - 186.

Chandler, R.J. 1967. Discussion. Proceedings, Oslo Geotechnical Conference, Vol. 2, pp. 177 - 178.

Chandler, R.J. 1973. A study of structural discontinuities in stiff clays using a polarising microscope. Proceedings, International Symposium on Soil Structure, Gothenburg, Sweden, pp. 78 - 85.

Clausen, C.J.F., Graham, J. and Wood, D.M. 1984. Yielding in soft clay at Mastemyr, Norway. Geotechnique, Vol. 34, pp. 581 - 600.

Clayton, L. 1967. Stagnant glacier features of the Missouri Coteau in North Dakota. North Dakota Geological Survey, misc. series 30, pp. 25 - 46.

Clayton, L. and Cherry, J.A. 1967. Pleistocene superglacial and ice-walled lakes of west-central North America. North Dakota Geological Survey, misc. series 30, pp.1 - 24.

Clayton, L. and Moran, S.R. 1974. A glacial process-form model. In: Glacial geomorphorlogy, ed. by D.R. Coates, G. Allen and Unwin, London. pp. 89 - 119.

Clough, G.W. and Denby, G.M. 1980. Self-boring pressuremeter study of San Francisco Bay mud. ASCE Journal of the Geotechnical Engineering Division, Vol. 106, GT 1, pp. 45 - 63.

Collinson, J.D. and Thompson, D.B. 1982. Sedimentary structures. 1st edition, George Allen & Unwin, London, UK.

Crooks, J.H.A., Been, K., Mickleborough, B.W. and Dean, J.P. 1985. An embankment failure on soft fissured clay. Paper submitted to Canadian Geotechnical Journal.

Crooks, J.H.A. and Graham, J. 1976. Geotechnical properties of the Belfast estuarine deposits. Geotechnique, Vol. 26, pp. 293 - 315.

Denby, G.M. and Clough, G.W. 1980. Self-boring pressuremeter tests in clay. ASCE Journal of the Geotechnical Engineering Division, Vol. 106, GT 12, pp. 1369 - 1387.

Donaghe, R.T. and Townsend, F.C. 1978. Effects of anisotropic versus isotropic consolidation in consolidated-undrained triaxial compression tests of cohesive soils. ASTM Geotechnical Testing Journal, Vol. 1, No. 4, pp. 173 - 189.

Dreimanis, A. 1976. Tills: their origin and properties. In: Glacial till: an interdisciplinary study, ed. by R.F. Legget, Royal Society of Canada , Special Publication 12, pp. 1 - 49.

Duncan, J.M. and Seed, H.B. 1966a. Anisotropy and stress reorientation in clay. ASCE Journal of the Soil Mechanics and Foundations Division, Vol. 92, SM 5, pp. 21 - 50.

Duncan, J.M. and Seed, H.B. 1966b. Strength variation along failure surfaces in clay. ASCE Journal of the Soil

Mechanics and Foundations Division, Vol. 92, SM 6, pp. 81 - 104.

EBA Engineering. 1982. Geotechnical investigation for the Genesee Power Plant. Report submitted to Integ-International Engineering Ltd.

EBA Engineering. 1983. Geotechnical report for the coal handling plant at the Genesee Power Plant. Vol. 1. Report submitted to Integ - International Engineering.

Eden, W.J. and Mitchell, R.J. 1970. The mechanics of landslides in Leda clay. Canadian Geotechnical Journal, Vol. 7, pp. 285 - 296.

Eigenbrod, K.D. 1975. Analysis of the pore pressure changes following the excavation of a slope. Canadian Geotechnical Journal, Vol. 12, pp. 429 - 440.

Einsele, G., Overbeck, R., Schwarz, H.U. and Unsoeld, G. 1974. Mass physical properties, sliding and erodibility of experimentally deposited and differently consolidated clayey muds. Sedimentology, Vol. 21, pp. 339 - 372.

Esu, F. and Calabresi, G. 1969. Slope stability in an overconsolidated clay. Proceedings, 7th International Conference on Soil Mechanics and Foundation Engineering, Mexico, Vol. 2, pp. 555 - 564.

Fookes, P.G. 1965. Orientation of fissures in stiff overconsolidated clay of the Siwalik system. Geotechnique, Vol. 15, pp.195 - 206.

Fookes, P.G. and Denness, B. 1969. Observational studies on fissure patterns in Cretaceous sediments of South-East England. Geotechnique, Vol. 19, No. 4, pp. 453 - 477.

Gillott, J.E. 1969. Study of the fabric of fine-grained sediments with the scanning electron microscope. Journal of Sedimentary Petrology, Vol. 39, pp. 90 - 105.

Golder Associates (GA). 1982. Geotechnical investigation of north approach fill failure, SR770 relocation, Genesee Power Project. Report submitted to Stanley Associates Engineering Ltd.

Graham, J. 1985. Personal communication.

Graham, J. and Au, V.C.S. 1985. Effects of freeze-thaw and softening on a natural clay at low stresses. Canadian Geotechnical Journal, Vol. 22, pp. 69 - 78.

Gravenor, C.P. 1955. The origin and significance of prairie mounds. American Journal of Science, Vol. 253, pp. 475 -

481.

Gravenor, C.P. and Bayrock, L.A. 1956. Stream-trench systems in east-central Alberta. Research Council of Alberta, Preliminary Report 56-4, 11 pp.

Gravenor, C.P. and Bayrock, L.A. 1965. Glacial deposits of Alberta. In: Soils in Canada, ed. by R.F. Legget, Royal Society of Canada, Special Publications No. 3, Toronto, pp. 33 - 50.

Gravenor, C.P. and Kuspch, W.O. 1959. Ice-disintegration features in Western Canada. Journal of Geology, Vol. 67, pp. 48 - 67.

Handy, R.L., Remmes, B., Moldt, S., Lutenegger, A.J. and Trott, G. 1982. In situ stress determination by Iowa stepped blade. ASCE Journal of the Geotechnical Engineering Division, Vol. 108, GT 11, pp. 1405 - 1422.

Hansen, J.B. and Gibson, R.E. 1949. Undrained shear strengths of anisotropically consolidated clays. Geotechnique, Vol. 1, pp. 189 - 204.

Head, K.H. 1981. Manual of soil laboratory testing. Vol. 1 & 2. Pentech Press, London.

Henderson, E.P. 1952. Pleistocene geology of the Watino quadrangle, Alberta. Unpublished PhD thesis, Indiana University.

Henderson, E.P. 1967. Surficial geology of the St Lawrence River, Kingston to Prescott. Geology of parts of Eastern Ontario and Western Quebec, Kingston. Geological Association of Canada Guidebook, pp. 199 - 207.

Henkel, D.J. 1970. Geotechnical consideration of lateral stresses. Proceedings, ASCE Specialty Conference on Lateral Stresses in the Ground and Design of Earth-Retaining Structures, Cornell University, Vol. 1, pp.1 - 49.

Henkel, D.J. and Gilbert, G.D. 1952. The effect of the rubber membrane on the measured triaxial compression strength of clay samples. Geotechnique, Vol. 3, pp. 20 - 29.

Hight, D.W., Gens, A. and Jardine, R.J. 1985. Discussion on "The reaction of clays to sampling stress relief." Geotechnique, Vol. 35, pp. 86 - 88.

Hoppe, G. 1952. Hummocky moraine regions, with special reference to the interior of Norbotton. Geografiska Annaler, Vol. 34, pp. 1 - 71.

Irad Gage. 1982. Vibrating wire earth pressure cell model EPC. Instruction manual IM 82-17. Irad Gage, Etna Road, New Hampshire, USA.

Kathol, C.P. and McPherson, R.A. 1975. Urban geology of Edmonton. Alberta Research Council, Bulletin No. 32, pp. 1 - 61.

Kenney, T.C. 1967. Field measurements of in situ stresses in quick clays. Proceedings, Geotechnical Conference, Oslo, Vol. 1, pp. 49 - 55.

Kenney, T.C. 1976. Formation and geotechnical characteristics of glacial-lake varved soils. In: Laurits Bjerrum Memorial Volume, ed. by N. Janbu, F. Jorstad and B. Kjaernsli, Norwegian Geotechnical Institute, Oslo, pp. 15 - 35.

Kenney, T.C. and Folkes, D.J. 1979. Mechanical properties of soft soils. State of the Art Report, 32nd Canadian Geotechnical Conference, Quebec City, pp. 1 - 51.

Kirkpatrick, W.M. and Rennie, I.A.1975. Stress relief effects in deep sampling operations. Proceedings, Conference on Offshore Engineering, Cardiff.

Lacasse, S. and Lunne, T. 1982. In situ horizontal stress from pressuremeter tests. Proceedings, Symposium on Pressuremeter and its Marine Applications, Paris, pp. 187 - 208.

Lacasse, S. and Lunne, T. 1983. Dilatometer tests in two soft marine clays. Norwegian Geotachnical Institute, Publication No. 146, pp. 1 - 8.

Ladd, C.C. 1965. Stress-strain behaviour of anisotropically consolidated clays during undrained shear. Proceedings, 6th International Conference on Soil Mechanics and Foundation Engineering, Montreal, Vol. 1, pp. 282 - 286.

Ladd, C.C., Foott, R., Ishihara, K., Poulos, H.G. and Schlosser, F. 1977.Stress-defofmation and strength characteristics. Proceedings, 9th International Conference on Soil Mechanics and Foundation Engineering, Tokyo, Vol. 2, pp. 421 - 494.

LaRochelle, P. 1967. Membrane, drain and area correction in triaxial test on soil samples failing along a single shear plane. Proceedings, 3rd Panamerican Conference on Soil Mechanics and Foundation Engineering, Venezuela, Vol. 1, pp. 273 - 292.

Larsson, R. 1981. Drained behaviour of Swedish clays.

Swedish Geotechnical Institute, Report No. 12, 157 p.

Leckie, D.A. and McCann, S.B. 1981. Glacio-lacustrine sedimentation on low slope prograding delta. Proceedings, 6th Guelph Symposium on Geomorphology, pp. 261 - 278.

Lefebvre, G., Philibert, A., Bozozuk, M. and Pare, J.J. 1981. Fissuring from hydraulic fracture of clay soil. Proceedings, 10th International Conference on Soil Mechanics and Foundation Engineering, Stockholm, Vol. 2, pp. 513 - 518.

Lo, K.Y. 1965. Stability of slopes in anisotropic soils. ASCE Journal of Soil Mechanics and Foundations Division, Vol. 91, SM4, pp. 85 - 106.

Lo, K.Y. and Vallee, J. 1970. Strength anisotropy due to parallel planes of discontinuities in clays. 2nd South East Asian Regional Conference on Soil Engineering, pp. 245 - 263.

Marchetti, S. 1979. The in-situ determination of an 'extended' overconsolidation ratio. Proceedings, 7th European Conference on Soil Mechanics and Foundation Engineering, Brighton, England, Vol. 2, pp. 239 - 244.

Marchetti, S. 1980. In situ tests by flat dilatometer. ASCE Journal of Geotechnical Engineering Division, Vol. 106, GT 3, pp. 299 - 321.

Marchetti, S. and Crapps, D.K. 1981. Flat dilatometer manual. Geotechnical Equipment, 4509 N.W. 23rd. Avenue, Gainesville, Florida, 32601.

Marsland, A. 1972. The shear strength of fissured clay. In: Stress - strain behaviour of soils, Roscoe Memorial Symposium, UK., pp. 59 - 68.

Marsland, A., McGown, A. and Derbyshire, E. 1980. Soil profile mapping in relation to site evaluation for foundations and earthwork. International Association of Engineering Geology, Bulletin No. 21, pp. 139 - 155.

Marsland, A., Prince, A. and Love, M.A. 1982. The role of soil fabric studies in the evaluation of the engineering parameters of offshore deposits. Proceedings, 3rd International Conference on the Behaviour of Offshore Structures, Vol. 1, MIT, Cambridge, Mass., pp. 181 - 200.

Massarsch, K.R. 1975. New method for measurement of lateral earth pressure in cohesive soils. Canadian Geotechnical Journal, Vol. 12, No. 1, pp. 142 - 146.

Massarsch, K.R. 1978. New aspects of soil fracturing in clay. ASCE Journal of the Geotechnicl Engineering Division, Vol. 104, GT 8, pp. 1109 - 1123.

Massarsch, K.R. 1979. Lateral earth pressure in normally consolidated clay. Proceedings, 7th European Conference on Soil Mechanics and Foundation Engineering, Brighton, England, Vol. 2, pp. 245 - 249.

Massarsch, K.R. and Broms, B.B. 1976. Lateral earth pressure at rest in soft clay. ASCE Journal of the Geotechnical Engineering Division, Vol. 102, GT 10, pp. 1041 - 1047.

Massarsch, K.R., Holtz, R.D., Holm, B.G. and Fredriksson, A. 1975. Measurement of horizontal in situ stresses. Proceedings, ASCE Specialty Conference on In-situ Measurement of Soil Properties, Rayleigh N.C.1, pp. 266 - 286.

Mathews, W.H. 1963. Quarternary stratigraphy and geomorphology of the Fort St. John area, Northeastern B.C., Dept. Mines & Petroleum Resources, pp. 22.

May, R.W. and Thomson, S. 1978. The geology and geotechnical properties of till and related deposits in the Edmonton, Alberta, area. Canadian Geotechnical Journal, Vol. 15, pp. 362 - 370.

Mayne, P.W. and Kulhawy, F.H. 1982. Ko - OCR relationship in soil. ASCE Journal of the Geotechnical Engineering Division, Vol. 108, GT 6, pp. 851 - 872.

Mayne, P.W.and Kulhawy, F.H. 1983. Closure to discussion on ' Ko - OCR relationships in soils.' ASCE Journal of the Geotechnical Engineering Division, Vol. 109, GT 6 , pp. 867 - 869.

McDonald, B.C. and Shilts, W.W. 1973. Interpretation of faults in glaciofluvial sediments. In: Glaciofluvial and glaciolacustrine sedimentation, ed.by A.V. Jopling and B.C. McDonald, Society of Economic Paleontologists and Mineralogists, SP 23, Tulsa, Oklahoma, USA, pp. 123 - 131.

McGown, A., Marsland, A., Radwan, A.M. and Gabr, A.W.A. 1980. Recording and interpreting soil macrofabric data. Geotechnique, Vol. 30, No. 4, pp. 417 - 447.

McRoberts, E.C. and Morgenstern, N.R. 1974. The stability of thawing slopes. Canadian Geotechnical Journal, Vol. 11, pp. 447 - 469.

Mesri, G. 1975. Discussion. ASCE Journal of the Geotechnical

Engineering Division, Vol. 101, GT 4, pp. 409 - 412.

Meyboom, P. 1966. Unsteady groundwater flow near a willow ring in hummocky moraine. Journal of Hydrology, Vol. 4, pp. 38 - 62.

Mitchell, R.J. 1970. On yielding and mechanical strength of Leda clays. Canadian Geotechnical Journal, Vol. 7, pp. 297 - 312.

Mollard, J.D. 1983. The origin of reticulate and orbicular patterns on the floor of the Lake Agassz basin. In: Glacial Lake Agassiz,ed. by J.T. Teller and L. Clayton, Geological Association of Canada Special Paper 26, pp. 355 - 374.

Morgenstern, N.R. 1967a. Shear strength of stiff clay. Proceedings, Oslo Geotechnical Conference, Vol. 2, pp. 59 - 69.

Morgenstern, N.R. 1967b. Submarine slumping and the initiation of turbidity currents. In: Marine Geotechnique, ed. by A.F. Richards, pp. 189 - 220.

Morgenstern, N.R. 1977. Slopes and excavations in heavily overconsolidated clay. State of the art report, 9th International Conference on Soil Mechanics and

Foundation Engineering, Tokyo, pp. 567 - 581.

Morgenstern, N.R. and Cruden, D. 1979. Description and classification of geotechnical complexities. Proceedings, International Symposium on the Geotechnics of Structurally Complex Formations, Capri, Vol. 2, pp. 195 - 203.

Morgenstern, N.R. and Eisenstein, Z. 1970. Methods of estimating lateral loads and deformations. Proceedings, ASCE Specialty Conference on Lateral Stresses in the Ground and Design of Earth - Retaining Structures, Cornell University, Vol. 1, pp. 51 - 102.

Morgenstern, N.R. and Price, V.E. 1965. The analysis of the stability of general slip surfaces. Geotechnique, Vol. 15, pp. 79 - 93.

Morgenstern, N.R. and Tchalenko, J.S. 1967. Microstructural observations on shear zones from slips in natural clays. Proceedings, Oslo Geotechnical Conference, Vol. 1, pp. 147 - 152.

Mulder, D.C. 1981. Development of the Genesee Power Project. C.I.M. Bulletin, Vol. 74, No. 832, pp. 68 - 72.

O'Brien, N.R. 1968. Electron microscope study of black shale fabric. Naturwissenschaften, Vol. 55, pp. 490 - 491.

Odynsky, W. 1971. Mounds (humpies) in the Peace River area of Alberta. Canadian Journal of Soil Science, Vol. 51, pp. 132 - 135.

Parry, R.H.G. and Wroth, C.P. 1981. Shear stress-strain properties of soft clay. In: Soft clay engineering, Developments in geotechnical engineering, Vol. 20, Elsevier Scientific Publishing Company, Amsterdam, pp. 311 - 364.

Paul, M.A. 1983. The supraglacial landsystem. In: Glacial Geology - An introduction for engineers and earth scientists, ed. by N. Eyles, Pergamon Press, UK.

Pawluk, S. and Bayrock, L.A. 1969. Some characteristics and physical properties of Alberta tills. Research Council of Alberta, Bulletin No. 26, pp. 1 - 72.

Pender, M.J., Parry, R.H.G. and George, P.J. 1975. The response of a soft clay layer to embankment loading. Proceedings, 2nd Australian-New Zealand Conference on Geomechanics, Brisbane, pp. 169 - 173.

Penman, A.D.M. 1975. Earth pressures measured with hydraulic piezometers. Proceedings, ASCE Specialty Conference on

In-situ Measurements of Soil Properties, Raleigh, N.C., Vol. 2, pp. 361 - 381.

Pilot, G., Trak, B. and LaRochelle, P. 1982. Effective stress analysis of the stability of embankments on soft soils. Canadian Geotechnical Journal, Vol. 19, pp. 433 - 450.

Poulos, H.G. and Davis, E.H. 1972. Laboratory determination of in-situ horizontal stress in soil masses. Geotechnique, Vol. 22, pp. 177 - 182.

Poulos, H.G. and Davis, E.H. 1974. Elastic solutions for soil and rock mechanics. Wiley, New York, 411 pp.

Quigley, R.M. 1980. Geology, mineralogy, and geochemistry of Canadian soft soils : a geotechnical perspective. Canadian Geotechnical Journal, Vol. 17, pp. 261 - 285.

Quigley, R.M. and Ogunbadejo, T.A. 1972. Clay layer fabric and oedometer consolidation of a soft varved clay. Canadian Geotechnical Journal, Vol. 9, pp. 165 - 175.

Rivard, P.J. and Goodwin, T.E. 1978. Geotechnical characteristics of compacted clays for earth embankments in the Prairie provinces. Canadian Geotechnical Journal, Vol. 15, pp. 391 - 401.

Rivard, P.J. and Lu, Y. 1978. Shear strength of soft fissured clays. Canadian Geotechnical Journal, Vol. 15, pp. 382 - 390.

Roctest Ltd.1982. Instruction manual for the Nilcon vane borer. Roctest Ltd., St. Lambert, Montreal, Canada.

Rowe, P.W. 1972. The relevance of soil fabric to site investigation practice. Geotechnique, Vol. 22, pp. 193 - 300.

Sanford, A.R. 1959. Analytical and experimental study of simple geologic structures. Bulletin, Geological Society of America, Vol. 70, pp. 19 - 52.

Sangrey, D.A. 1970. Evidence of glacial readvance over soft-layered sediments near Kingston, Ontario. Canadian Journal of Earth Science, Vol. 7, pp. 1331 - 1339.

Schmertmann, J.H. 1975. Measurement of in situ shear strength. Proceedings, ASCE Specialty Conference on In-situ Measurements of Soil Properties, Raleigh NC, Vol. 2, pp. 57 - 138.

Schmertmann, J.H. 1983. A simple question about consolidation. ASCE Journal of the Geotechnical

Engineering Division, Vol. 109, GT 2, pp. 119 - 122.

Schmidt, B. 1966. Discussion on ' Earth pressures at rest related to stress history. ' Canadian Geotechnical Journal, Vol. 3, pp. 239 - 242.

Schmidt, B. 1983. Discussion on ' Ko - OCR relationships in soils. ' ASCE Journal of the Geotechnical Engineering Division, V0l. 109, GT 6, pp. 866 - 867.

Scott, J.S. 1976. Geology of Canadian tills. In: Glacial Till, ed. R.F. Legget, Royal Society of Canada, Special Publication, No. 12, pp. 50 - 66.

Shaw, J. 1982. Melt-out till in the Edmonton area, Alberta, Canada. Canadian Journal of Earth Science, Vol. 19, pp 1548 - 1569.

Skempton, A.W. 1954. The pore-pressure coefficients A and B. Geotechnique, Vol. 4, pp. 143 - 147.

Skempton, A.W. 1961. Horizontal stresses in an overconsolidated Eocene clay. Proceedings, 5th International Conference on Soil Mechanics and Foundation Engineering, Paris, Vol. 1, pp. 351 - 357.

Skempton, A.W. 1964. Long term stability of clay slopes.

Geotechnique, Vol. 14, pp. 77 - 102.

Skempton, A.W. 1966. Some observations on tectonic shear zones. Proceedings, 1st International Conference on Rock Mechanics, Lisbon, Vol. 1, pp. 329 - 335.

Skempton, A.W. 1970. First-time slides in over-consolidated clays. Geotechnique, Vol. 20, pp. 320 - 324.

Skempton, A.W. and Bishop, A.W. 1954. Building materials their elasticity and inelasticity. In: Soils, Chapter 10, North-Holland Publishing Co., Amsterdam, pp. 417 - 482.

Skempton, A.W. and Hutchinson, J. 1969. Stability of natural slopes and embankments foundations. State-of-the-art report, 7th International Conference on Soil Mechanics and Foundation Engineering, Mexico, pp. 291 - 340.

Skempton, A.W. and Northey, R.D. 1953. Sensitivity of clays. Geotechnique, Vol. 3, pp. 30 - 53.

Skempton, A.W. and Petley, D. 1967. The strength along structural discontinuities in stiff clays. Proceedings, Geotechnical Conference on Shear Strength of Natural Soils and Rocks, Oslo, Vol. 2, pp. 3 - 20.

Skempton, A.W., Shuster, R.L. and Petley, D.J. 1969. Joints and fissures in the London Clay at Wraysbury and Edgware. Geotechnique, Vol. 19, pp. 205 - 217.

Smith, N.D. 1978. Sedimentation processes and patterns in a glacier-fed lake with low sediment input. Canadian Journal of Earth Science, Vol. 15, pp. 741 - 756.

St. Onge, 1972. Sequence of glacial lakes in north central Alberta. Geological Survey of Canada, Bulletin 213, 16p.

Tavenas, F. 1979. The behaviour of embankments on clay foundations: a state of the art. 32nd Canadian Geotechnical Conference, Quebec City, pp. 1 - 32.

Tavenas, F.A., Blanchette, G., Leroueil, S., Roy, M., and LaRochelle, P. 1975. Difficulties in the in-situ determination of Ko in soft sensitive clays. Proceedinngs, ASCE Specialty Conference on In-situ Measurement of Soil Properties, Raleigh, N.C., Vol. 1, pp. 450 - 476.

Tavenas, F., Des Rosiers, J.P., Leroueil, S., LaRochelle,P. and Roy, M. 1979. The use of strain energy as a yield and creep criterion for lightly overconsolidated clays. Geotechnique, Vol. 29, pp. 285 - 303.

Tavenas, F. and Leroueil, S. 1979. Clay behaviour and the selection of design parameters. 7th European Conference on Soil Mechanics and Foundation Engineering, Brighton, England, Vol. 1, pp. 281 - 291.

Tedd, P. and Charles, J.A. 1981. In situ measurement of horizontal stress in overconsolidated clay using push-in spade-shaped pressure cells. Geotechnique, Vol. 31, No. 4, pp. 554 - 558.

Tedd, P. and Charles, J.A. 1983. Evaluation of push-in pressure cell results in stiff clay. Building Research Establishment, U.K.

Terzaghi, K. 1936. Stability of slopes of natural clay. Proceedings, 1st International Conference on Soil Mechanics, Cambridge, Mass., Vol. 1, pp. 161 - 165.

Terzaghi, K. and Peck, R.B. 1967. Soil Mechanics in Engineering Practice. 2nd edition, Wiley, New York, 729 pp.

Thurber Consultants. 1982a. Borrow investigation report, Genesee Power Project. Report submitted to Integ-International Engineering Ltd.

Thurber Consultants. 1982b. Geotechnical investigation for cooling pond dyke, river water pumphouse and makeup pipeline, Genesee Power Project. Report submitted to Integ-International Engineering Ltd.

Thurber Consultants. 1985. Cooling pond dyke, geotechnical instrumentation report and construction activity (August - December 1984), Genesee Power Project. Report submitted to Edmonton Power.

Tovey, N.K. and Wong, K.Y. 1973. The preparation of soils and other geological materials for the SEM. Proceedings, International Symposium on Soil Structure, Gothenburg, Sweden, pp. 59 - 67.

Tovey, N.K. and Wong, K.Y. 1977. Preparation, selection and interpretation problems in scanning electron microscope studies of sediments. In: Scanning Electron Microscopy in the Study of Sediments, ed. by W.B. Whalley, pp. 181 - 199.

Vaughan, P.R. 1971. The use of hydraulic fracturing tests to detect crack formation in embankment dam cores. Interim Report, Department of Civil Engineering, Imperial College, London, UK.

Vaughan, P.R. and Walbancke, H.J. 1973. Pore pressure changes and the delayed failure of cutting slopes in overconsolidated clay. Geotechnique, Vol. 23, pp. 531 - 539.

Wilkes, P.F. 1974. Permeability tests in alluvial deposits and the determination of $K_0$. Geotechnique, Vol. 24, No. 1, pp. 1 - 11.

Windle, D. and Wroth, C.P. 1977. In situ measurement of the properties of stiff clays. Proceedings, 9th International Conference on Soil Mechanics and Foundation Engineering, Tokyo, Vol. 1, pp. 347 - 352.

Wroth, C.P. 1975. In situ measurement of initial stresses and deformation characteristics. Proceedings, ASCE Conference on In Situ Measurements of Soil Properties, Raleigh, N.C., Vol. 2, pp. 181 - 230.

Wroth, C.P. 1984. The interpretation of in-situ soil tests. Geotechnique, Vol. 34, pp. 449 - 489.

Wroth, C.P. and Hughes, J.M.O. 1973. An instrument for the in-situ measurement of the properties of soft clays. Proceedings, 8th International Conference on Soil Mechanics and Foundation Engineering, Moscow, Vol. 1, pp. 487 - 494.

Zeevaert, L. 1953. Discussion. Proceedings, 3rd

International Conference on Soil Mechanics and Foundation Engineering, Switzerland, Vol. 3, pp. 113 - 114.

# APPENDIX A - CHARACTERISTICS OF TILL

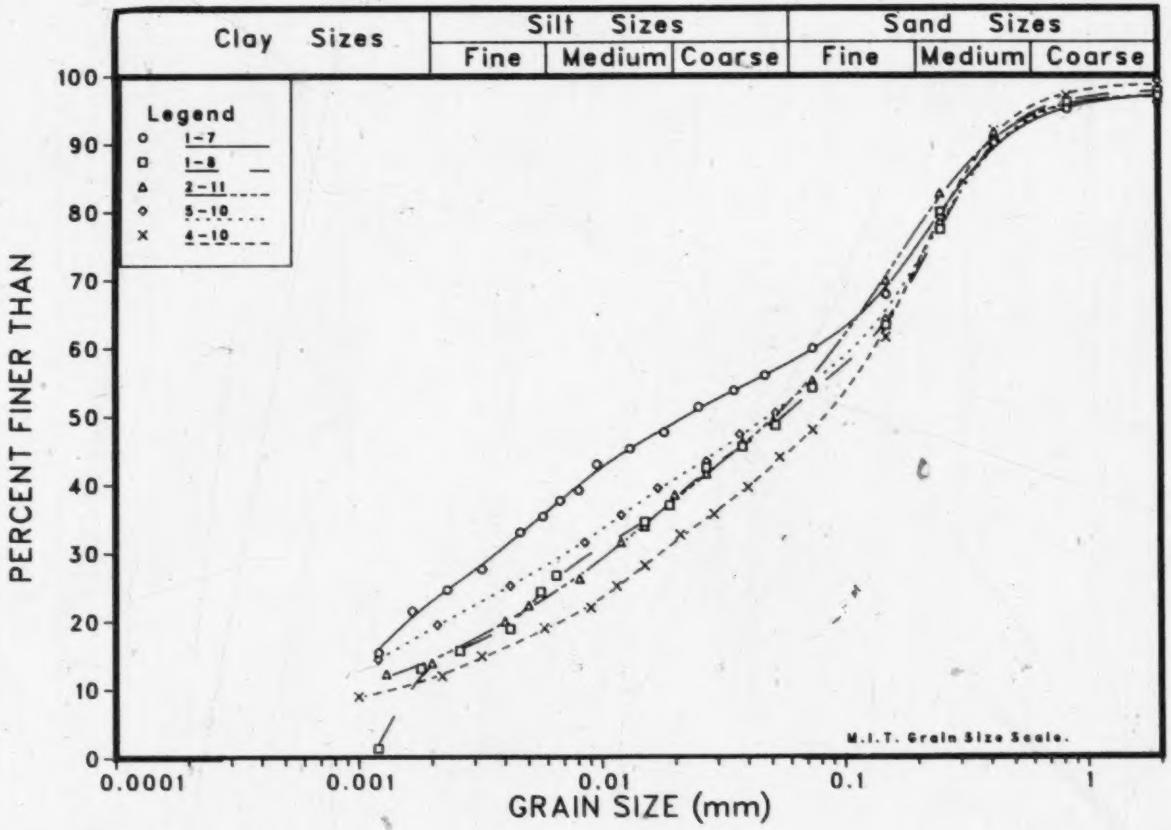

Figure A.1 Grain size analysis of till.

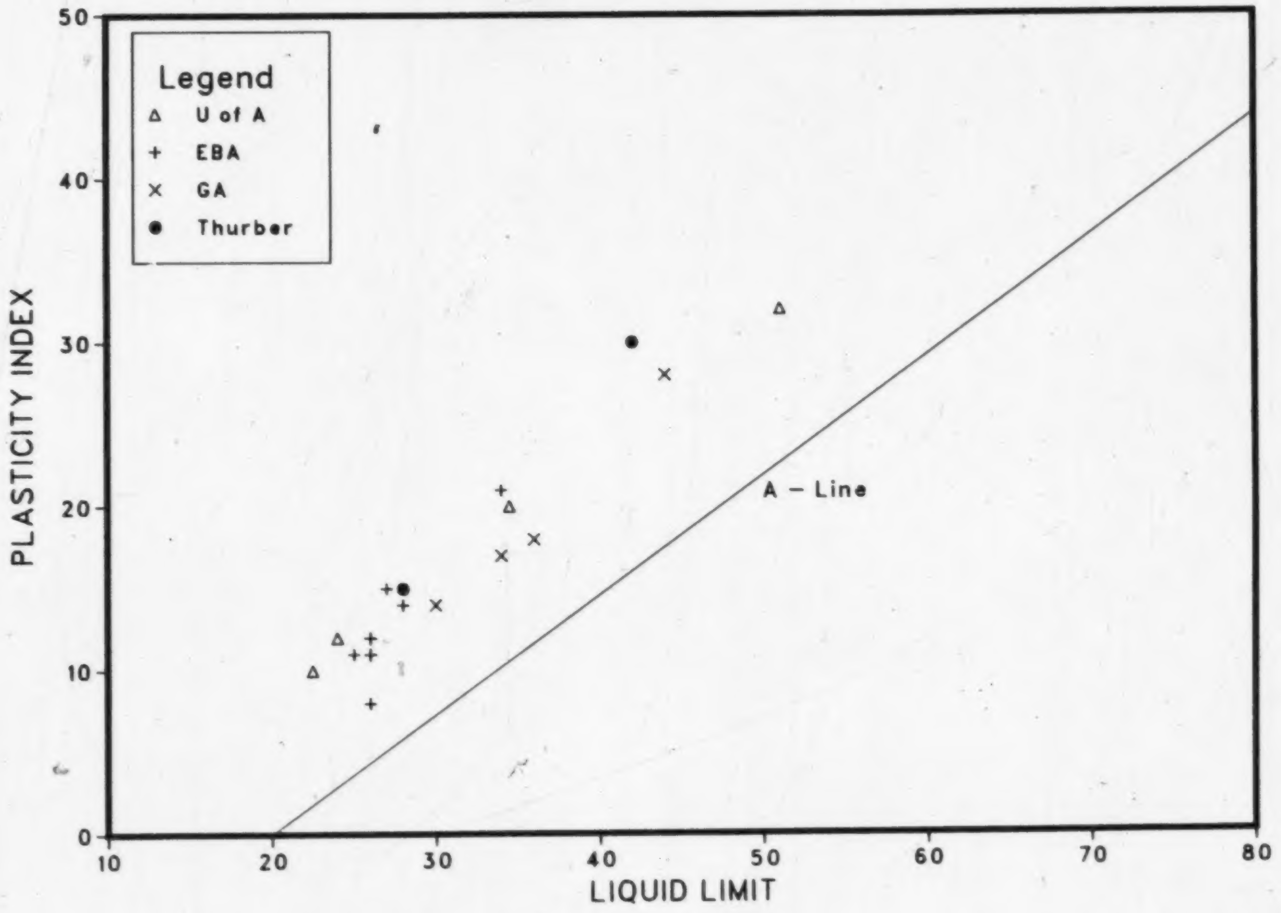

Figure A.2 Plasticity characteristics of till.

Plate A.1 Homogeneous structure of till.

# APPENDIX B - GRAIN SIZE ANALYSIS OF CLAY

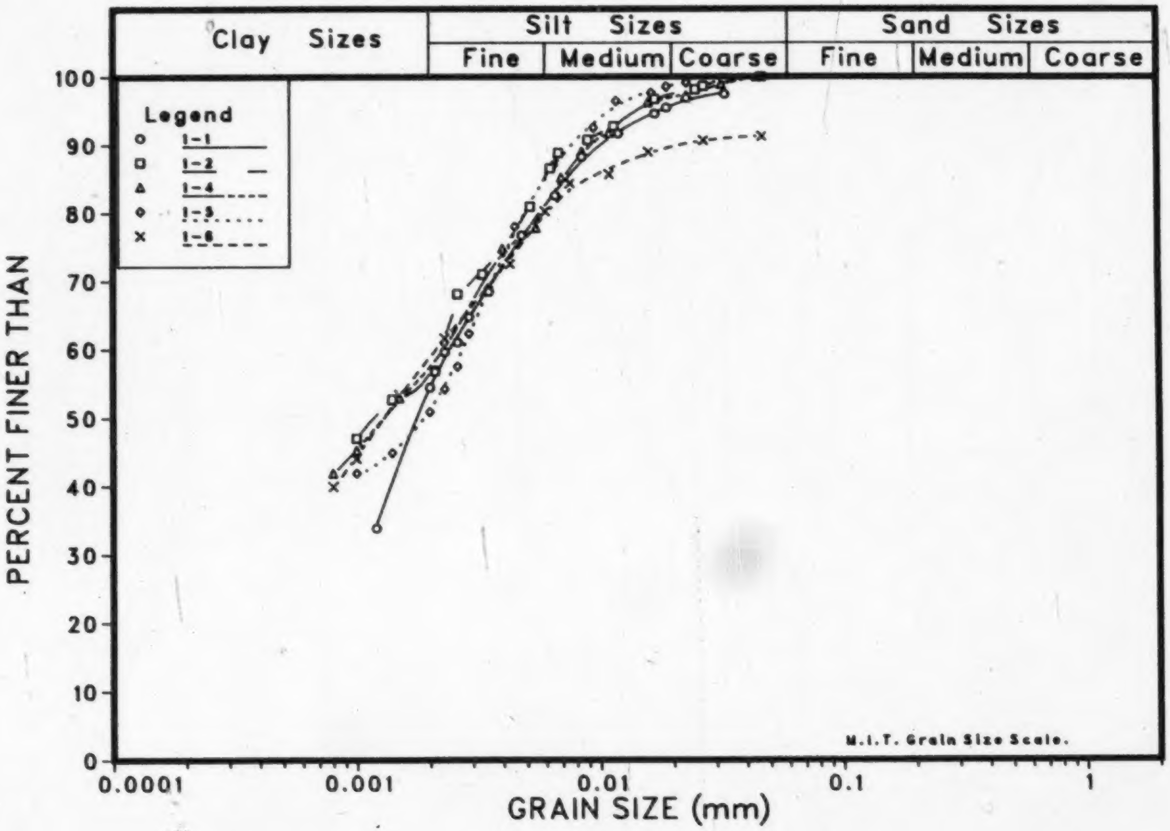

Figure B.1 Grain size analysis of UA1 clay samples.

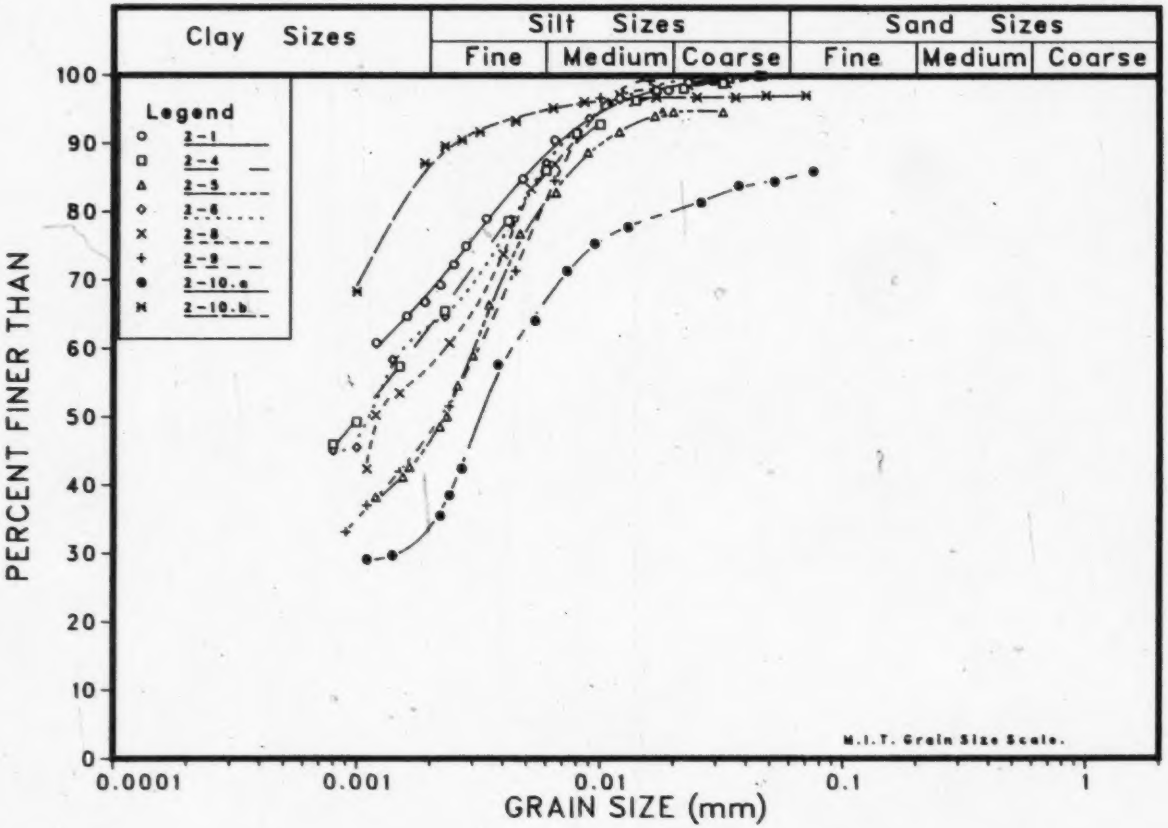

Figure B.2 Grain size analysis of UA2 clay samples.

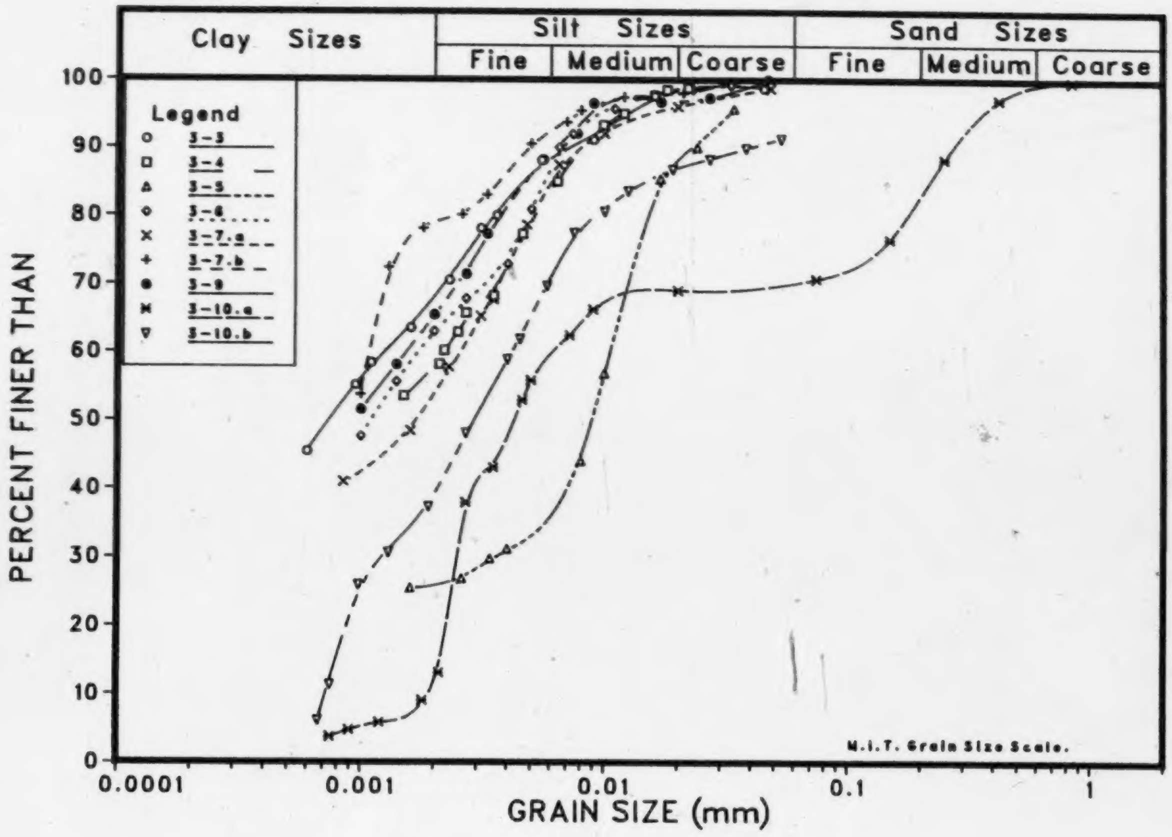

Figure B.3 Grain size analysis of UA3 clay samples.

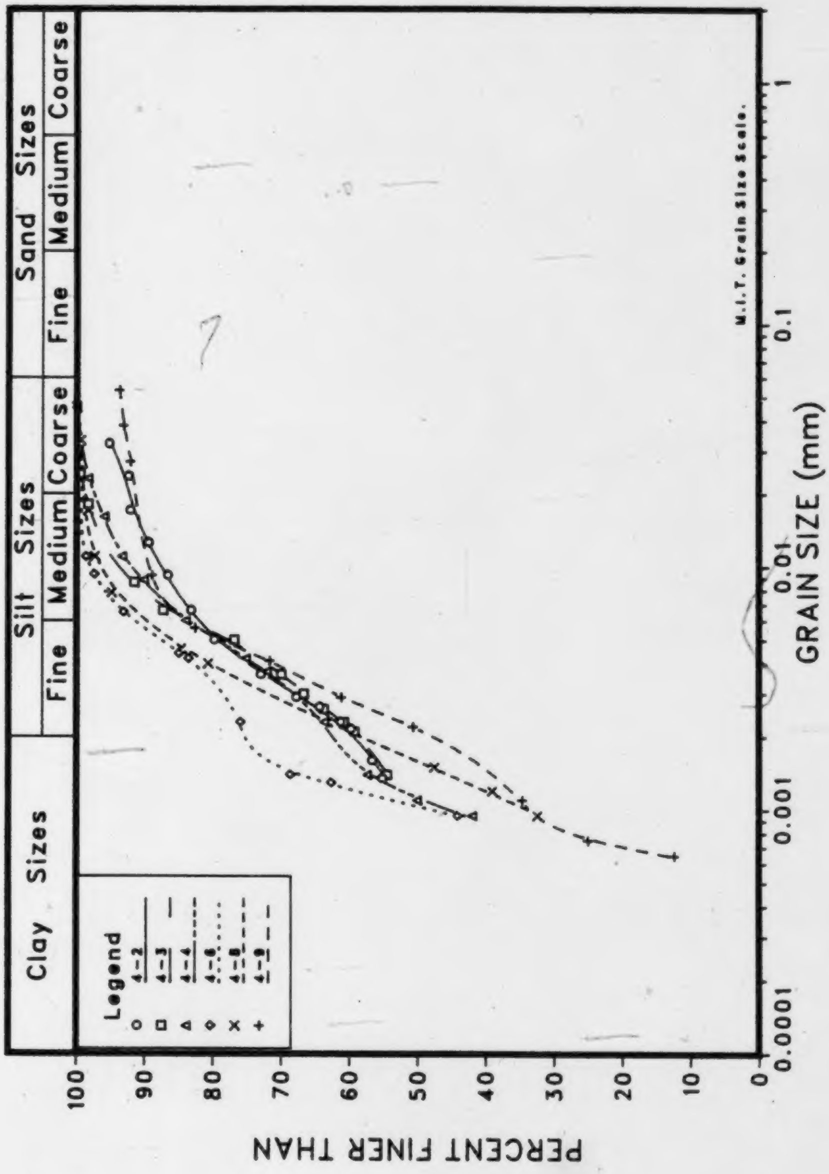

Figure B.4 Grain size analysis of UA4 clay samples.

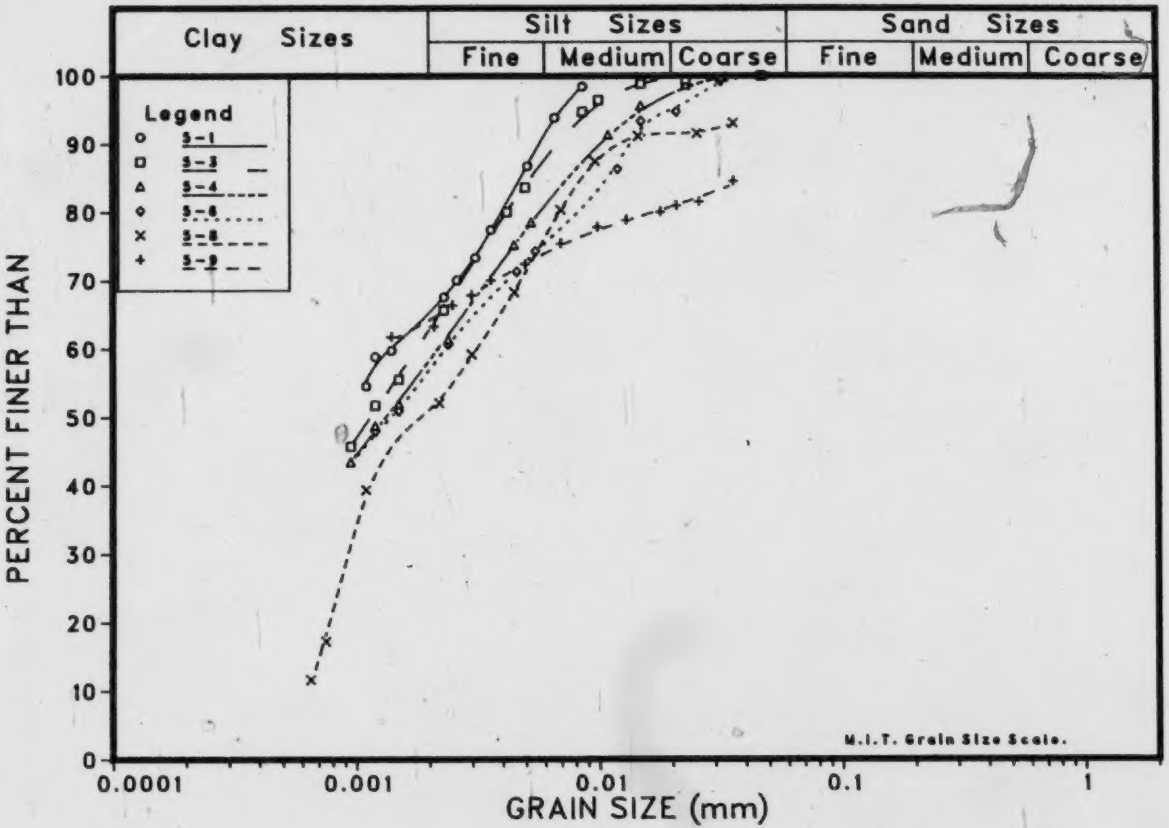

Figure B.5 Grain size analysis of UA5 clay samples.

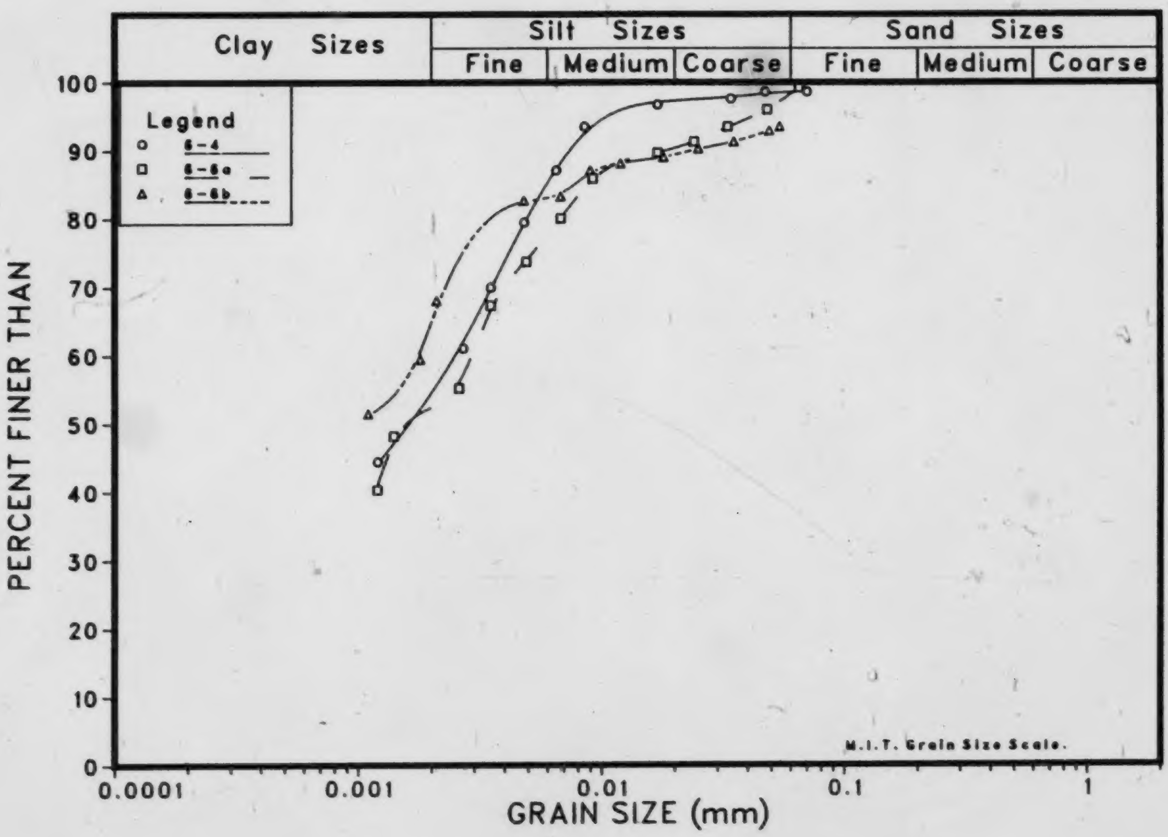

Figure B.6 Grain size analysis of UA6 clay samples.

# APPENDIX C - DETAILED BOREHOLE LOGGING

In the borehole log sheets that follow, the abbreviations or symbols that are used are explained below.

**Soil description**

MP - medium plastic

HP - highly plastic

**Depositional features**

These are assumed to be planar unless stated otherwise.

Bedding planes are represented by solid lines.

**Structural features**

slick - slickenside

Slickensides and fissures are represented by dashed lines.

**Test**

CAU - Anisotropically consolidated undrained triaxial test.

CIU - Isotropically consolidated undrained triaxial test.

Con - One dimensional consolidation test on vertical sample.

Hor. con - One dimensional consolidation test on horizontal sample.

Table C.1 Detailed borehole log for UA1.

| Depth(m) | Sample No | Material | Soil Description | Depositional Features | Structural Features | Water Content(%) | | | Test |
|---|---|---|---|---|---|---|---|---|---|
| | | | | | | w | $w_P$ | $w_L$ | |
| | | 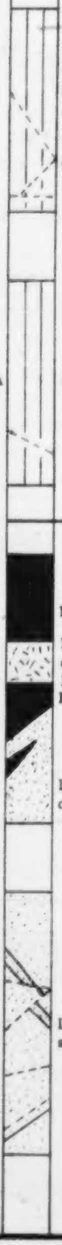 | | | | | | | |
| 5.6 | | | Brown grey clay, angular to sub-angular nuggets (3-5mm) with nodules (3mm)of dark grey clay, MP to HP. | Homogeneous, no visible bedding. | Minor vertical slick and fissures. | 41.8 | | | |
| | 1-1 | | | | Major slick,no striations, -45° dip | 42.3 | | | CIU |
| 5.7 | | | | | | | | | |
| | | | | | -60° dip -horizontal | 42.3 | 27 | 74 | Cons |
| 5.8 | | | | | | | | | |
| 7.6 | | | | | | | | | |
| | | | | | | 36.7 | | | CIU |
| 7.7 | | | | | | | | | |
| | 1-1A | | same as 1-1. | same as 1-1. | | 48.5 | 29 | 75 | Cons |
| 7.8 | | | | | | | | | |
| | | | | | Major slick,slight striations,20° dip. | | | | |
| 7.9 | | | | | | | | | |
| | | | Weathered Clay | | | | | | |
| 8.5 | | | | | | 57.8 | | | |
| 8.6 | | | Dark grey clay, HP. | Fine laminae, sub-horizontal. | Intense minor slick. | 59.3 | | | |
| | | | Light grey silty clay,coal chips and 12 mm pebbles. | | | 41.0 | | | |
| 8.7 | 1-2 | | Dark grey clay, HP. | Fine laminae, 15° dip. | Intense minor slick, | 60.0 | | | CIU |
| | | | | | Pull-apart and slump features (Plate 3.8). Randomly oriented minor slick. | | | | |
| 8.8 | | | | | | | | | |
| | | | Light brown grey clay, MP. | Homogeneous. | | 38.0 | 24 | 68 | Cons |
| 8.9 | | | | | | | | | |
| 10.0 | | | | | | | | | |
| | | | | Homogeneous. | | 43.2 | 26 | 63 | Cons |
| 10.1 | | | | | | | | | |
| | | | | 5mm lamina, 50° dip. | Major slick, slight striations, 30° dip (Plate 3.9). | 45.2 | | | CIU |
| 10.2 | 1-3 | | Light grey clay, soft, MP. | | | | | | |
| | | | | | Major slick,no striations,30° dip. | | | | |
| 10.3 | | | | 45° dip bedding plane. | | | | | |
| | | | | Contorted laminae. | Major slick,slight striations,40°dip. | | | | |
| 10.4 | | | | | | | | | |

Table C.2 Detailed borehole log for UA1 (continued).

| Depth(m) | Sample No | Material | Soil Description | Depositional Features | Structural Features | Water Content (%) | | | Test |
|---|---|---|---|---|---|---|---|---|---|
| | | | | | | $w$ | $w_P$ | $w_L$ | |
| 11.6 | | | Dark grey clay, HP. | Disturbed by drilling. | | 42.6 | 25 | 63 | Cons |
| 11.7 | | | | Cross-laminae, 20 to 50° dip. | | 41.9 | | | CIU |
| 11.8 | 1-4 | | | Contorted laminae. | | 40.3 | | | Hor. Cons |
| 11.9 | | | Light brown grey clay, MP. | Cross-laminae, 40° dip. | | 39.9 | | | |
| 12.0 | | | | Contorted laminae. | | 40.9 | | | |
| 12.1 | | | | | | | | | |
| 13.1 | | | | | | 39.7 | 22 | 55 | Hor. Cons |
| 13.2 | 1-5 | | Light grey clay, silty, soft, MP. | Contorted laminae. | | 38.5 | | | |
| 13.3 | | | | | | 45.0 | | | |
| 13.4 | | | | | | | | | |
| 14.6 | | | | | Major slick, highly striated, 60° dip (Plate 3.13). | 62.7 | | | |
| 14.7 | | | | | | | | | |
| 14.8 | 1-6 | | Light to dark grey clay, soft, MP. to HP. | Fine horizontal laminae. | | 45.1 | | | CIU |
| 14.9 | | | | | | 56.3 | | | CIU |
| 15.0 | | | | | Major slick, no striations, 30° dip. | 49.7 | 25 | 69 | Cons |
| 15.1 | | | | | | | | | |

Table C.3 Detailed borehole log for UA1 (continued).

| Depth(m) | Sample No | Material | Soil Description | Depositional Features | Structural Features | Water Content(%) | | | Test |
|---|---|---|---|---|---|---|---|---|---|
| | | | | | | w | $w_P$ | $w_L$ | |
| 16.2 | | | Light grey clayey sand(till),numerous pebbles (3-4mm). | Flow. | | 23.3 | | | |
| 16.3 | | | | | | | | | |
| 16.4 | 1-7 | | Light grey clayey sand and silt(till). | Interbeds(15mm) of lacustrine clay or silt at 100mm spacing. | | 30.8 | | | |
| 16.5 | | | | | | 23.4<br>36.7 | | | |
| 16.6 | | | | | | | | | |
| 17.8 | | | | | | | | | |
| 17.9 | 1-8 | | Dark grey clayey sand and silt(till), coal chips and pebbles. | Homogeneous. | | 17.2 | | | |
| 18.0 | | | | | | | | | |
| 18.1 | | | | | | | | | |

Table C.4 Detailed borehole log for UA2.

| Depth(m) | Sample No | Material | Soil Description | Depositional Features | Structural Features | Water Content(%) | | | Test |
|---|---|---|---|---|---|---|---|---|---|
| | | | | | | w | $w_P$ | $w_L$ | |
| 5.5 | | | | | | | | | |
| 5.6 | | | | | Major slick, no striations,<br>-35° and 55° dip<br>-vertical<br>-20° dip. | | | | |
| | 2-1 | | Mottled brown and grey clay,MP. | Homogeneous, no visible bedding. | | | | | |
| 5.7 | | | | | | | | | |
| 5.8 | | | | | | 41.7 | 27 | 69 | CIU |
| 8.5 | | | | | | | | | |
| 8.6 | | | | | Major slick, no striations, 70° dip. | 36.7 | 27 | 80 | |
| 8.7 | 2-2 | | Mottled brown and grey clay, MP. | Homogeneous. | | | | | |
| 8.8 | | | | | Minor slick,no striations,random orientations, mostly confined to grey clay. | 57.0 | 36 | 88 | |
| 8.9 | | | | | | | | | |
| | | | | Weathered Clay | | | | | |
| 10.1 | | | | | | | | | |
| | | | | | Major slick, highly striated,rust stains, 30° dip. | | | | |
| 10.2 | | | | | | | | | |
| 10.3 | 2-3 | | Light brown grey clay, MP with dark grey clay,HP, lenses (2-3 cm). | Homogeneous. | Major slick,no striations,matt,horizontal. | 39.2<br>54.3<br>35.4 | 24 | 65 | Cons |
| 10.4 | | | | | Major slick,no striations,undulated surface.<br>Clay above slick contains minor randomly oriented fissures with matt and smooth surface. | 34.9 | | | |
| 10.5 | | | | | | | | | |
| 11.6 | | | | | | | | | |
| 11.7 | | | | | | 41.9 | | | |
| 11.8 | 2-4 | | Light brown grey clay, MP. | Fine laminae, horizontal. | | 39.4 | | | CIU |
| 11.9 | | | | | Major slick,matt,smooth, 40° dip.<br>Intense minor vertical fissures (2-3cm) above slick. | 41.7 | 26 | 68 | Cons |
| 12.0 | | | | | | | | | |

Table C.5 Detailed borehole log for UA2 (continued).

| Depth(m) | Sample No | Material | Soil Description | Depositional Features | Structural Features | Water Content(%) w | Water Content(%) $w_P$ | Water Content(%) $w_L$ | Test |
|---|---|---|---|---|---|---|---|---|---|
| 13.1 | | 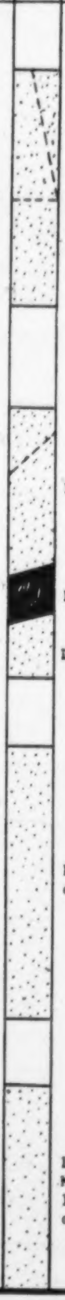 | | | | | | | |
| 13.2 | | | | | | 35.6 | | | |
| 13.3 | 2-5 | | Light brown grey clay, MP, with nodules of dark grey clay, HP, stiff. | Homogeneous. | Major slick, slight striations, sub-vertical. | 40.9 | | | |
| 13.4 | | | | | Major slick, slight striations, sub-horizontal. | 34.3 | 25 | 66 | Cons |
| 13.5 | | | | | | | | | |
| 14.6 | | | | | | | | | |
| 14.7 | | | Light grey clay, MP. | Homogeneous. | Major slick, slight striations, 40° dip. | 41.1 | | | CIU |
| 14.8 | 2-6 | | | | | | | | |
| 14.9 | | | Dark grey clay, HP. | | Intense minor slick. | 55.0 | | | |
| 15.0 | | | Light grey clay, MP. | Cross-laminae, 15° dip. | | 40.1 | 25 | 66 | Cons |
| 16.2 | | | | | | | | | |
| 16.3 | | | | | | | | | |
| 16.4 | 2-7 | | Light brown grey clay, MP. | Fine laminae, horizontal. | | | | | |
| 16.5 | | | | | | 36.6 | 25 | 66 | Cons |
| 16.6 | | | | | | | | | |
| 17.6 | | | | | | | | | Hor. Cons |
| 17.7 | 2-8 | | Light grey clay, silty, MP, with swirls of lighter grey silty clay. | Contorted laminae. | | 37.2 | 23 | 57 | Cons |
| 17.8 | | | | | | 38.5 | | | CIU |
| 17.9 | | | | | | 36.7 | | | CAU |

Table C.6 Detailed borehole log for UA2 (continued).

| Depth(m) | Sample No | Material | Soil Description | Depositional Features | Structural Features | Water Content (%) | | | Test |
|---|---|---|---|---|---|---|---|---|---|
| | | | | | | w | $w_P$ | $w_L$ | |
| 19.2 | | 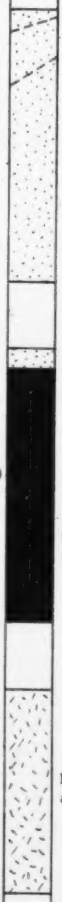 | | | | | | | |
| 19.3 | | | | | | 32.8 | | | |
| | | | | | Major slick, slight striations, 20° and 40° dip. Sheared deformation of bed above 20° slick (Plate 3.7). | 36.4 | | | |
| 19.4 | 2-9 | | Light grey clay, silty, MP, with swirls of dark grey clay. | Contorted laminae. | | 36.7 | | | |
| 19.5 | | | | | | 37.7<br>44.3 | | | [illegible] |
| | | | | | | 37.1 | 20 | 55 | [illegible] |
| 19.6 | | | | | | | | | |
| 20.7 | | | Light grey silty clay, LP. | | Intense minor slick, along bedding. | 41.0 | 24 | 49 | |
| 20.8 | | | | | | | | | |
| 20.9 | 2-10 | | | | | | | | |
| | | | Dark grey clay, HP, with occasional sand pockets. | Fine laminae, sub-horizontal, with silt partings. Laminae tend to be contorted towards bottom of sample. | 5 major slick, slight striations, across bedding, 20° to 40° dip. | 82.4 | | | CIU |
| 21.0 | | | | | | | | | |
| 21.1 | | | | | | 64.3 | 37 | 99 | |
| 22.3 | | | | | | | | | |
| 22.4 | 2-11 | | | | | | | | |
| | | | Dark grey clayey sand and silt (till), LP. | Homogeneous. | | 17.3 | | | |
| 22.5 | | | | | | | | | |
| 22.6 | | | | | | | | | |

Table C.7 Detailed borehole log for UA5.

| Depth(m) | Sample No | Material | Soil Description | Depositional Features | Structural Features | Water Content(%) | | | Test |
|---|---|---|---|---|---|---|---|---|---|
| | | | | | | w | $w_P$ | $w_L$ | |
| 5.5 | | | | | | | | | |
| 5.6 | 5-1 | | Brown clay,angular to subangular nuggets(3-5mm), MP. | Homogeneous. | Faint vertical fissures,3-4mm long. | 38.6 | | | CIU |
| 5.7 | | | | | | 37.5 | 27 | 70 | CIU |
| 5.8 | | | | | | | | | |
| 7.1 | | | | | | | | | |
| 7.2 | 5-2 | | Mottled brown and dark grey clay with occasional pebbles (2-3mm) and coal chips, MP. | Homogeneous. | | 37.0 | 26 | 67 | Cons |
| 7.3 | | | | | Major slick,25° dip. | 39.3 | | | CIU |
| 7.4 | | | | Weathered Clay | | | | | |
| 8.5 | | | | | | | | | |
| | | | | | | 34.1 | 24 | 65 | Cons |
| 8.6 | | | Light grey MP clay with mottles of dark grey HP clay (Plate 3-4). | No visible bedding. | | 60.0 | | | |
| 8.7 | 5-3 | | | | | 42.2 | | | |
| | | | Dark grey clay,HP. | Fine laminae. | Intense minor slick with silt partings. | 64.5 | | | |
| 8.8 | | | Light brown grey clay,MP becoming more silty at bottom. | Homogeneous. | | 45.8 | | | |
| | | | | | | 32.8 | | | |
| 8.9 | | | | | | | | | |
| 10.0 | | | | | | | | | |
| 10.1 | | | | | Minor slick,no striation ,60° dip, 70% of sample area. | 36.8 | | | CAU |
| | | | | | Major slick,slight striations,30° dip. | | | | |
| 10.2 | 5-4 | | Light grey clay, MP. | Homogeneous. | | | | | |
| 10.3 | | | | | Major slick,matt,no striations,curved. | 36.3 | | | CIU |
| 10.4 | | | | | Major slick,slight striations,60° dip. | 36.4 | 23 | 63 | Cons |

Table C.8 Detailed borehole log for UA5 (continued).

| Depth(m) | Sample No | Material | Soil Description | Depositional Features | Structural Features | Water Content (%) |  |  | Test |
|---|---|---|---|---|---|---|---|---|---|
|  |  |  |  |  |  | w | $w_P$ | $w_L$ |  |
| 11.6 |  |  |  |  |  |  |  |  |  |
| 11.7 |  |  |  |  |  |  |  |  |  |
| 11.8 | 5-5 |  | Light grey clay, MP. | Homogeneous. | 1 vertical fissure, matt,smooth,planar, 100% sample. | 36.0 |  |  | Hor Cons |
| 11.9 |  |  |  |  |  | 36.4 | 24 | 62 | Cons |
| 12.0 |  |  |  |  |  |  |  |  |  |
| 13.1 |  |  |  |  |  |  |  |  |  |
| 13.2 |  |  | Silt partings. |  |  | 36.8 | 20 | 62 | Cons |
| 13.3 | 5-6 |  | Light grey clay, MP. | Fine laminae, sub-horizontal. |  | 39.6 |  |  | CIU |
| 13.4 |  |  | Light grey clay,MP with swirls of white silt. | Inclined bedding plane,55° dip. |  | 38.2 |  |  | CIU |
| 13.5 |  |  |  | Contorted. |  | 41.7 |  |  |  |
| 14.6 |  |  |  |  |  |  |  |  |  |
| 14.7 |  |  |  |  |  | 39.3 |  |  | Hor Cons |
| 14.8 | 5-7 |  | Light grey clay, MP. | Fine (1-2mm) interbeds of light grey and darker grey clay. | Major slick,slight striations,45°dip, across bedding. |  |  |  |  |
| 14.9 |  |  |  |  |  | 38.4 | 21 | 59 | Cons |
| 15.0 |  |  |  |  |  |  |  |  |  |

Table C.9 Detailed borehole log for UA5 (continued).

| Depth(m) | Sample No | Material | Soil Description | Depositional Features | Structural Features | Water Content(%) w | $w_P$ | $w_L$ | Test |
|---|---|---|---|---|---|---|---|---|---|
| 16.1 | | | | | | | | | |
| 16.2 | | | 3mm silt lamina. | | | | | | |
| 16.3 | S-8 | | | | | 40.0 | 23 | 65 | CIU |
| | | | Light grey clay,MP with swirls of darker grey clay. | Contorted. | | | | | |
| 16.4 | | | | | | 34.0 | | | |
| 16.5 | | | | | | | | | |
| 17.6 | | | | | | | | | |
| | | | Dark grey clay,MP to HP,some coal chips. | Homogeneous. | | 46.8 | 21 | 53 | CIU |
| 17.7 | | | | | | 59.7 | | | |
| | | | Light grey clayey silt(till),MP. | Homogeneous. | | 23.6 | | | |
| 17.8 | | | Dark grey clay,HP. | Fine laminae,25°dip. | Intense minor slick, slight striations. | 43.7 | | | |
| | S-9 | | Light grey silty clay,MP. | | | 40.1<br>30.8 | | | |
| 17.9 | | | Light grey clayey silt(till),LP. | Fine laminae,15°dip. | Faint vertical crack matt,smooth,planar, 100% sample. | 41.2 | | | |
| | | | Light grey silty clay,MP to HP. | Homogeneous. | | 20.3 | | | |
| 18.0 | | | | 2-3mm laminae. | | | | | |
| | | | Grey clayey sand (till),LP. | Flow or slump. | | | | | |
| 18.1 | | | | | | | | | |
| 19.2 | | | | | | | | | |
| 19.3 | | | | | | | | | |
| 19.4 | S-10 | | Grey clayey sand (till),LP. | Interbeds (15mm) of lacustrine silty clay. | | 18.2 | 12 | 24 | Cons |
| 19.5 | | | | | | | | | |
| 19.6 | | | | | | | | | |

Table C.10 Detailed borehole log for UA3.

| Depth(m) | Sample No | Material | Soil Description | Depositional Features | Structural Features | Water Content(%) | | | Test |
|---|---|---|---|---|---|---|---|---|---|
| | | | | | | $w$ | $w_P$ | $w_L$ | |
| 2.4 | | | | | | | | | |
| 2.5 | 3-1 | ▨ | Brown silty clay, MP (fill) | | | 34.2 | | | |
| 2.6 | | | | | | | | | |
| 4.0 | | | | | | | | | |
| 4.1 | | ▥ | | | | | | | |
| 4.2 | 3-2 | ▥ | Mottled brown and grey clay with organics and roots, MP. | | | 39.9 | | | |
| 4.3 | | ▥ | | | | | | | |
| 4.4 | | | | | | | | | |
| 5.5 | | | | | | | | | |
| 5.6 | | ▥ | | | | 40.6 | 30 | 76 | Cons |
| 5.7 | 3-3 | ▥ | Mottled brown and grey clay, sub-angular nuggets (5mm), MP, some roots | Homogeneous, no visible bedding | Major slick, slight striations, 8° dip<br>Major slick, no striation, 60° dip | 36.0 | | | |
| 5.8 | | ▥ | | | | | | | |
| 5.9 | | | | | | | | | |
| 7.0 | | | | | | | | | |
| 7.1 | | ▥ | | | | 37.4 | 25 | 66 | CIU |
| 7.2 | 3-4 | ▥ | Mottled brown and grey clay, angular to sub-angular nuggets (3-5mm), MP. | Homogeneous | Randomly oriented minor slick (2-3 cm long) | 33.3 | | | Cons |
| 7.3 | | ▥ | | | | | | | |
| 7.4 | | | | | | | | | |
| | | | | Weathered Clay | | | | | |

Table C.11 Detailed borehole log for UA3 (continued).

| Depth(m) | Sample No | Material | Soil Description | Depositional Features | Structural Features | Water Content(%) | | | Test |
|---|---|---|---|---|---|---|---|---|---|
| | | | | | | w | $w_P$ | $w_L$ | |
| 8.5 | | 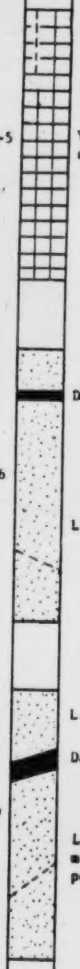 | | | About 10cm long sub-vertical fissure | 33.1 | | | |
| 8.6 | | | | | | | | | |
| 8.7 | 3-5 | | Yellowish brown silt,LP | Cross laminated, 30 to 50° dip | | | | | |
| 8.8 | | | | | | 30.0 | 18 | 40 | |
| 8.9 | | | | | | | | | |
| 10.0 | | | | | | | | | |
| 10.1 | | | Dark grey clay,HP | Fine laminae, sub-horizontal | Intense minor slick parallel to bedding and major slick, no striation along lower bedding plane | | | | |
| 10.2 | 3-6 | | | | Intense minor faint fissures(2-3cm long), random orientation, varies from matt smooth to rough | 45.2 | 20 | 79 | Hor cons<br>Cons |
| 10.3 | | | Light grey clay,MP | Homogeneous | | | | | |
| 10.4 | | | | | Minor slick(80% sample area),slight striations, undulated surface,20°dip | 38.0 | | | |
| 11.6 | | | | | | | | | |
| | | | Light grey clay,MP | Fine laminae, sub-horizontal | | 40.6 | 26 | 58 | |
| 11.7 | | | Dark grey clay,HP | Fine laminae, 20° dip,parallel to bedding plane | Major slick,slight striations,30° dip | 56.1 | 36 | 110 | Cons |
| 11.8 | 3-7 | | | | | 37.5 | | | Hor cons |
| 11.9 | | | Light grey clay,MP, minute(2-3mm) silt pockets. | Fine laminae, sub-horizontal | Major slick,no striation,45°dip | | | | |
| | | | | | | 38.4 | 32 | 100 | CIU |
| 12.0 | | | | | | | | | |

Table C.12 Detailed borehole log for UA3 (continued).

| Depth(m) | Sample No | Material | Soil Description | Depositional Features | Structural Features | Water Content(%) |  |  | Test |
|---|---|---|---|---|---|---|---|---|---|
|  |  |  |  |  |  | w | $w_P$ | $w_L$ |  |
| 13.1 |  |  |  |  |  |  |  |  |  |
|  |  |  | Light grey clay,MP | Homogeneous |  | 40.9 |  |  |  |
| 13.2 |  |  | Darker grey clay,MP | Fine laminae,some silt partings | Intense minor slick | 47.3 |  |  |  |
| 13.3 | 3-8 |  |  |  | Major slick,no striation,40° and 50° dip | 34.7 |  |  | Hor cons |
| 13.4 |  |  | Light grey clay,MP with some silt pockets (10mm) and occasional coal chips | Homogeneous |  | 36.1 |  |  | CIU |
| 13.5 |  |  |  |  |  | 40.2 | 27 | 72 | Cons |
| 14.6 |  |  |  |  |  |  |  |  |  |
|  |  |  |  |  |  | 31.5 |  |  |  |
| 14.7 |  |  | Light grey clay,MP siltier towards top of sample |  | Fissure,matt,smooth, no indication of movement,45° dip |  |  |  |  |
|  |  |  |  |  |  | 37.8 |  |  |  |
| 14.8 | 3-9 |  |  |  |  | 51.7 |  |  |  |
| 14.9 |  |  | Dark grey clay, MP to HP | Fine laminae, horizontal | Intense randomly oriented minor slick, polished,no striation, 2-3 cm long | 53.0 |  |  | CIU |
| 15.0 |  |  | Light grey clay,MP |  |  | 44.1 | 30 | 76 | Cons |
| 16.2 |  |  |  |  |  |  |  |  |  |
|  |  |  | Light grey silty clay,LP |  |  | 32.0 | 14 | 34 |  |
| 16.3 |  |  |  |  |  | 37.3 | 19 | 51 | Cons |
| 16.4 | 3-10 |  | Light grey clay,MP some silt lenses (1-2mm) | Homogeneous |  |  |  |  |  |
|  |  |  |  |  |  | 38.5 |  |  |  |
| 16.5 |  |  |  |  |  |  |  |  |  |
| 16.6 |  |  | Loose silty sand, some pebbles and coal chips,LP | Flow or slump |  | 16.6 |  |  |  |

Table C.13 Detailed borehole log for UA4.

| Depth(m) | Sample No | Material | Soil Description | Depositional Features | Structural Features | Water Content (%) | | | Test |
|---|---|---|---|---|---|---|---|---|---|
| | | | | | | $w$ | $w_P$ | $w_L$ | |
| 4.0 | | | | | | | | | |
| 4.1 | 4-1 | | Mottled brown and grey clay with organics and roots, MP. | | | 32.2 | | | |
| 4.2 | | | | | | | | | |
| 4.3 | | | | | | | | | |
| 5.5 | | | | | | | | | |
| 5.6 | 4-2 | | Mottled brown and grey clay, angular to subangular nuggets (2-3mm), MP. | Homogeneous, no visible bedding. | | 32.9 | 28 | 65 | |
| 5.7 | | | | | | | | | |
| 5.8 | | | | | | | | | |
| 7.0 | | | | | | | | | |
| 7.1 | 4-3 | | Brown clay, silty, LP, angular to subangular nuggets (2-3mm). | Homogeneous. | | 38.0 | | | |
| 7.2 | | | | | | | | | |
| 7.3 | | | | | | | | | |
| 7.8 | | | | | | | | | |
| 7.9 | 4-3A | | Brown clay, angular to subangular nuggets (1-3mm), MP. | Homogeneous. | | 30.0 | 26 | 67 | DST |
| 8.0 | | | | | | | | | |
| 8.1 | | | | Weathered Clay. | | | | | |

Table C.14 Detailed borehole log for UA4 (continued).

| Depth(m) | Sample No | Material | Soil Description | Depositional Features | Structural Features | Water Content (%) w | $w_P$ | $w_L$ | Test |
|---|---|---|---|---|---|---|---|---|---|
| 8.5 | | | | | | | | | |
| | | ░ | | | | 32.7 | 25 | 66 | Cons |
| 8.6 | | ░ | | | | | | | |
| 8.7 | 4-4 | ░ | Light brown grey clay,MP. | Homogeneous. | Randomly oriented faint fissures,unsheared,opening up by manual manipulation. | 33.4 | | | CIU |
| 8.8 | | ░ | | | | 35.1 | | | |
| 8.9 | | | | | | | | | |
| 10.1 | | ░ | | | | | | | |
| 10.2 | | ░ | | | | | | | |
| 10.3 | 4-5 | ░ | Light brown grey clay with swirls of silty grey clay,MP. | Contorted. | Intense faint vertical fissures. | 35.6 | 24 | 62 | |
| 10.4 | | ░ | | | | | | | |
| 10.5 | | | | | | | | | |
| 11.6 | | ■ | | | | | | | |
| | | ■ | Dark grey clay,HP. | Fine laminae with silt partings,subhorizontal. | Intense minor slick along bedding. | 56.9 | 33 | 101 | Cons |
| 11.7 | 4-6 | ■ | | | Major slick,no striation,30° dip. | | | | |
| 11.8 | | ░ | Light grey clay,MP. | Inclined laminae, 60° dip. | | 39.1 | | | CIU |
| 11.9 | | | | | | | | | |
| 13.1 | | ■ | | | | | | | |
| 13.2 | | ■ | Dark grey clay,MP to HP. | No visible lamination.[1] | Major slick,matt,smooth,40° dip. | 54.5 | | | CIU |
| 13.3 | 4-7 | ░ | 2mm silt parting. | | Randomly oriented minor slick,no striation. | 55.2 | 28 | 73 | Cons |
| 13.4 | | ░ | Light grey clay with some silt pockets (2-3mm), MP. | Homogeneous. | Faint fissures,1-2 cm long,difficult to separate. | 37.9 | | | CAU |
| 13.5 | | ░ | | | | | | | |

Table C.15 Detailed borehole log for UA4 (continued).

| Depth(m) | Sample No | Material | Soil Description | Depositional Features | Structural Features | Water Content(%) | | | Test |
|---|---|---|---|---|---|---|---|---|---|
| | | | | | | w | $w_P$ | $w_L$ | |
| 14.6 | | | | | | | | | |
| | | | | | | 63.8 | | | |
| 14.7 | | | | | Major slick,matt, subhorizontal. | 56.3 | | | |
| 14.8 | 4-8 | | Light grey clay,MP. | Fine laminae, sub-horizontal. | Randomly oriented faint fissures,1-2 cm long,difficult to separate. | 46.7 | | | CAU |
| 14.9 | | | | | | 49.0 | | | CIU |
| 15.0 | | | Light grey clay with sand pockets (3-4mm),HP. | Homogeneous. | | 41.1 | 25 | 63 | Cons |
| 16.2 | | | | | | | | | |
| 16.3 | | | Light brown grey clay with silt pockets (3-4mm), MP. | | Possible slick, based on failure mode of CIU test, 50° dip. | 37.1 | 25 | 62 | CIU |
| 16.4 | 4-9 | | Dark grey clay,HP. | Fine laminae with silt partings. | Intense minor slick along bedding. | 56.9 | 28 | 95 | Cons |
| 16.5 | | | See Plate 3.2 for details. | | | | | | |
| 16.6 | | | | | | | | | |
| 17.7 | | | | | | 20.2 | | | |
| 17.8 | | | | | | | | | |
| 17.9 | 4-10 | | Dark grey clayey sand (till),stiff but softer near top of sample, LP. | Homogeneous with possible flow at top of sample. | | 17.3 | | | |
| 18.0 | | | | | | | | | |
| 18.1 | | | | | | 17.9 | | | |

Table C.16 Detailed borehole log for UA6.

| Depth(m) | Sample No | Material | Soil Description | Depositional Features | Structural Features | Water Content (%) | | | Test |
|---|---|---|---|---|---|---|---|---|---|
| | | | | | | w | $w_P$ | $w_L$ | |
| 7.0 | | | | | | | | | |
| 7.1 | 6-1 | | Mottled brown and grey clay, angular to subangular nuggets (2-3mm), some roots, MP. | | | 34.4 | 24 | 65 | |
| 7.2 | | | | | | | | | |
| 8.5 | | | | | | | | | |
| 8.6 | | | | | Major slick, slight striations, 65° dip. | 37.8 | | | |
| | 6-2 | | Brown clay, MP. | Homogeneous, no visible bedding. | | | | | |
| 8.7 | | | | | | | | | |
| 8.8 | | | | | | 39.1 | 26 | 64 | |
| | | | Weathered Clay | | | | | | |
| 10.1 | | | | | | | | | |
| | | | | | Major slick, no striation, horizontal. | 40.0 | | | |
| 10.2 | | | | | | | | | |
| | 6-3 | | Light brown clay, MP. | Homogeneous. | Randomly oriented intense minor fissures, 1-4 cm long, matt, smooth.<br>Fissures divide clay into angular blocks (about 1cm cube). | | | | |
| 10.3 | | | | | | 37.8 | | | |
| 10.4 | | | | | | | | | |
| 11.6 | | | | | | | | | |
| 11.7 | | | | | | 47.0 | | | |
| | 6-4 | | Light grey clay, MP with sparse dark grey, MP, lenses. | Homogeneous. | Few minor slick (1-2cm) shiny, no striation, randomly oriented. | | | | |
| 11.8 | | | | | | 43.7 | 24 | 74 | Cons |
| 11.9 | | | | | | | | | |

Table C.17 Detailed borehole log for UA6 (continued).

| Depth(m) | Sample No | Material | Soil Description | Depositional Features | Structural Features | Water Content(%) |  |  | Test |
|---|---|---|---|---|---|---|---|---|---|
|  |  |  |  |  |  | w | $w_P$ | $w_L$ |  |
| 13.1 |  |  | Light brown grey clay,MP. | Homogeneous. | Few minor fissures (1-2cm), matt, vertical. | 35.8 |  |  |  |
| 13.2 |  |  | Light brown grey clay,silty, LP. | Homogeneous. |  | 31.4 |  |  |  |
| 13.3 | 6-5 |  | light grey silty clay,occasional pebbles(3-10mm), till-like,LP. | Appears to be of lacustrine origin. |  | 31.8 |  |  |  |
| 13.4 |  |  | Dark grey clay, MP to HP, some sand pockets (5-10mm) | Fine laminae, subhorizontal. | Intense minor slick, along bedding. | 59.3 |  |  |  |
| 14.6 |  |  |  |  |  |  |  |  |  |
| 14.7 |  |  |  |  |  |  |  |  |  |
| 14.8 | 6-6 |  | See Plate 3.3. |  |  |  |  |  |  |
| 14.9 |  |  |  |  |  |  |  |  |  |
| 15.0 |  |  |  |  |  |  |  |  |  |
| 16.2 |  |  |  |  |  |  |  |  |  |
| 16.3 | 6-7 |  | Dark grey clayey sand(till), LP. | Homogeneous. |  | 18.4 |  |  |  |
| 16.4 |  |  |  |  |  |  |  |  |  |
| 16.5 |  |  |  |  |  |  |  |  |  |

# APPENDIX D - FIELD INVESTIGATION RESULTS

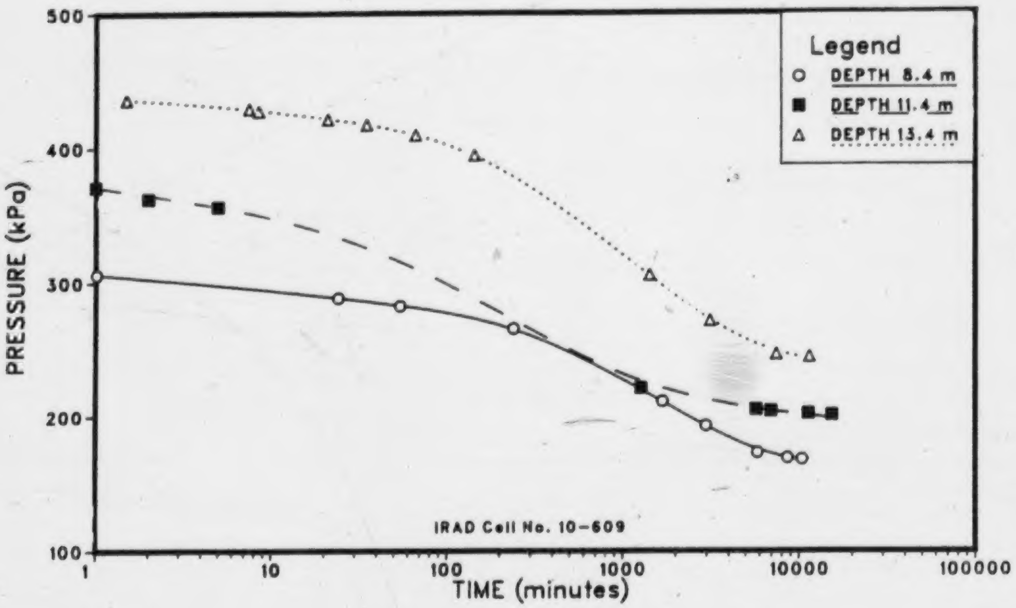

Figure D.1 TSC results at UA1 with cell in North-South direction.

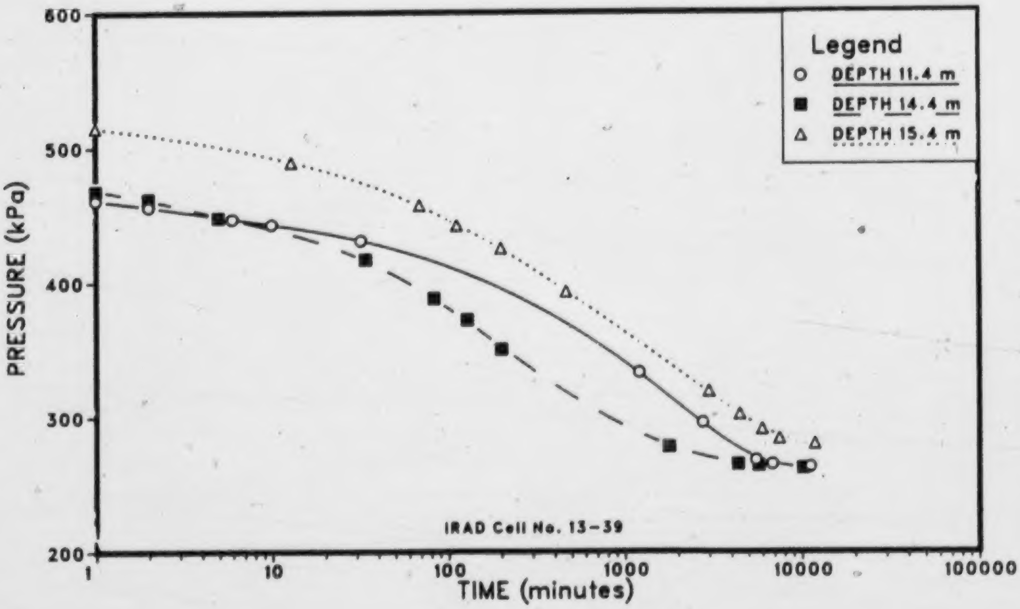

Figure D.2 TSC results at UA1 with cell in East-West direction.

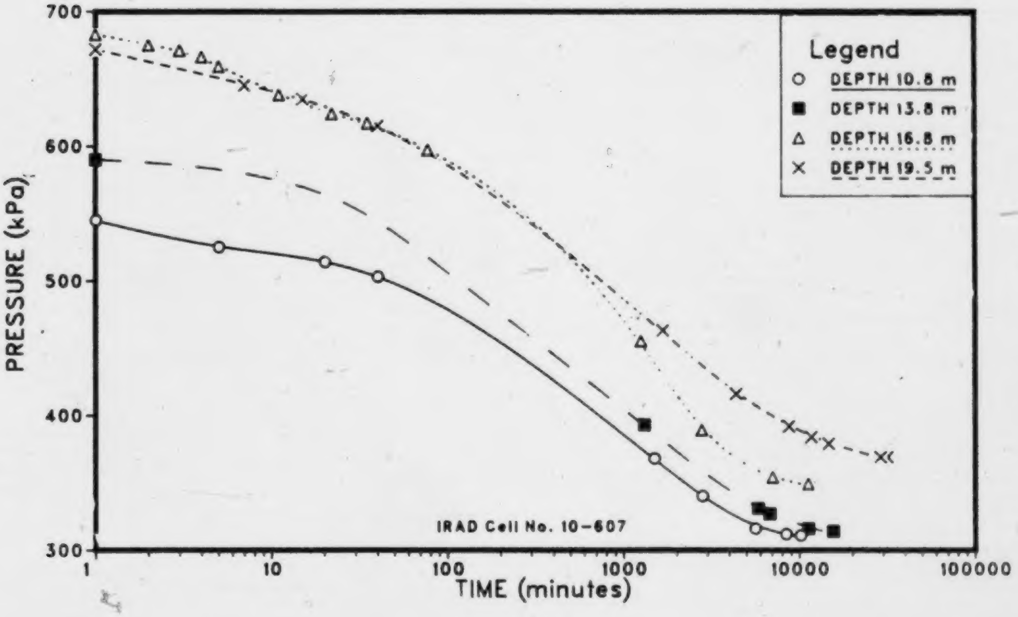

Figure D.3 TSC results at UA2 with cell in North-South direction.

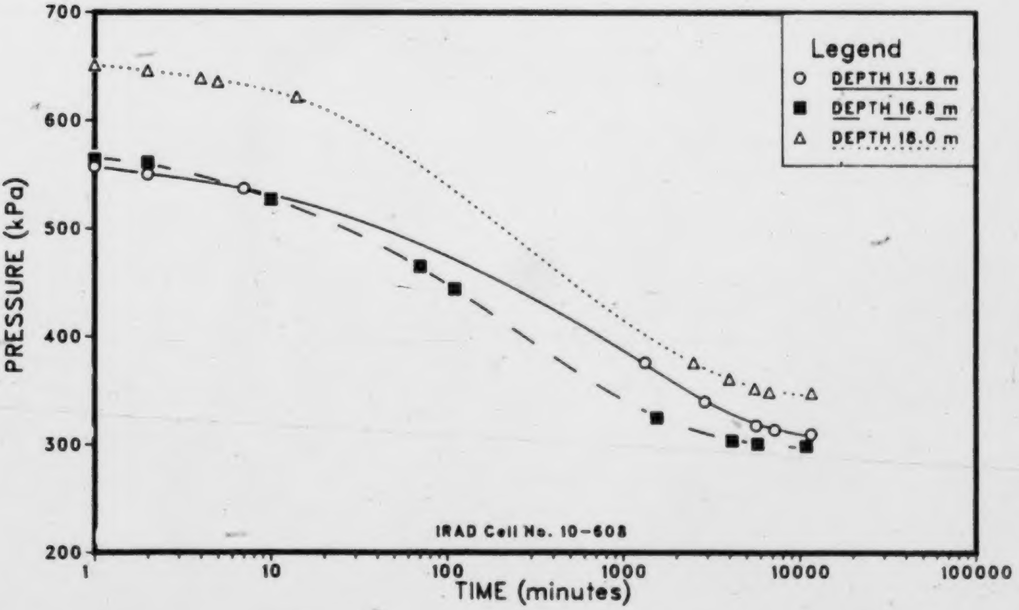

Figure D.4 TSC results at UA2 with cell in East-West direction.

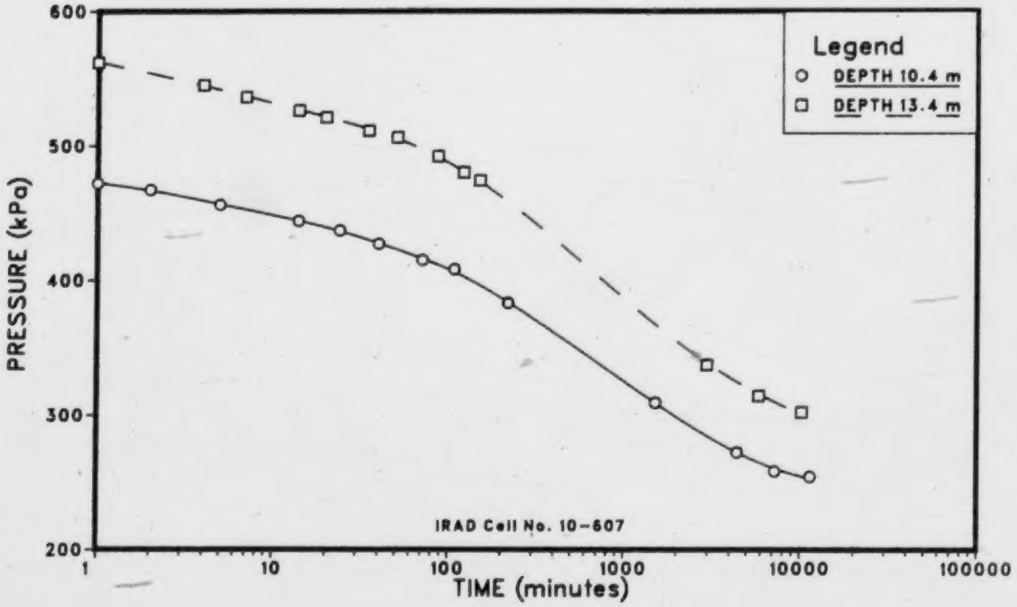

Figure D.5 TSC results at UA5 with cell in North-South direction.

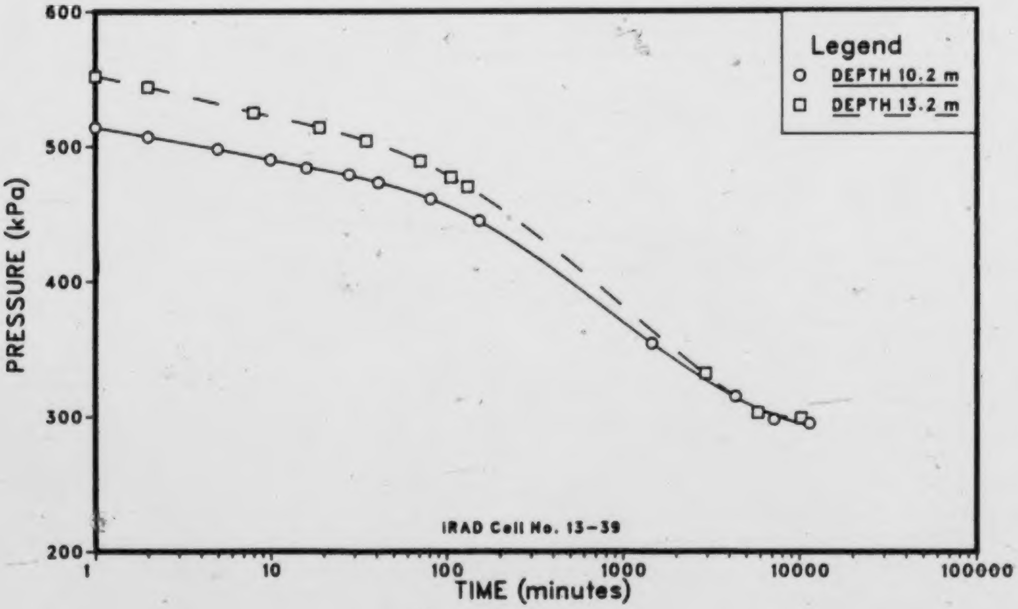

Figure D.6 TSC results at UA5 with cell in East-West direction.

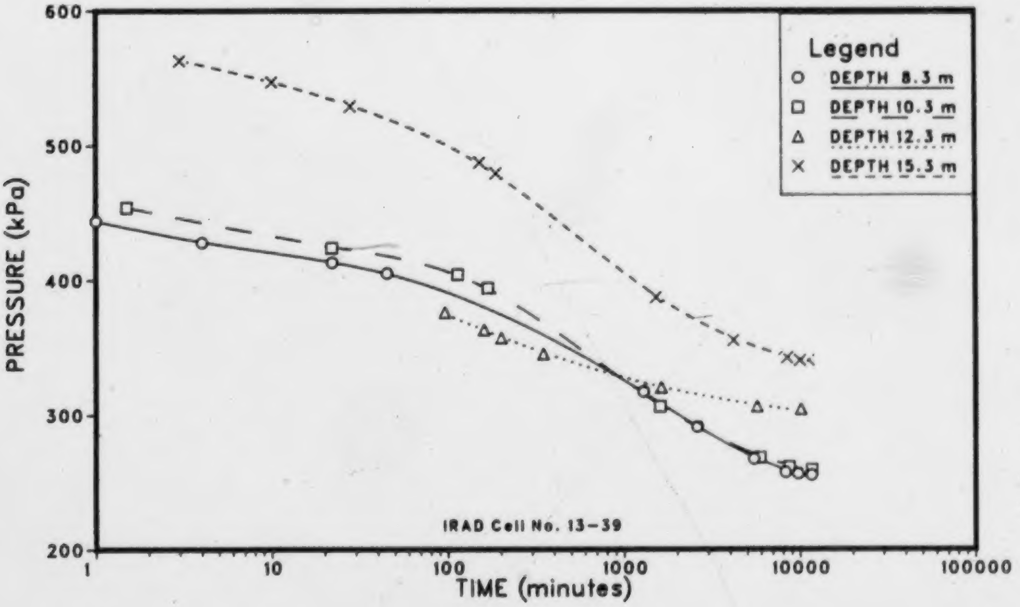

Figure D.7 TSC results at UA3 with cell in North-South direction.

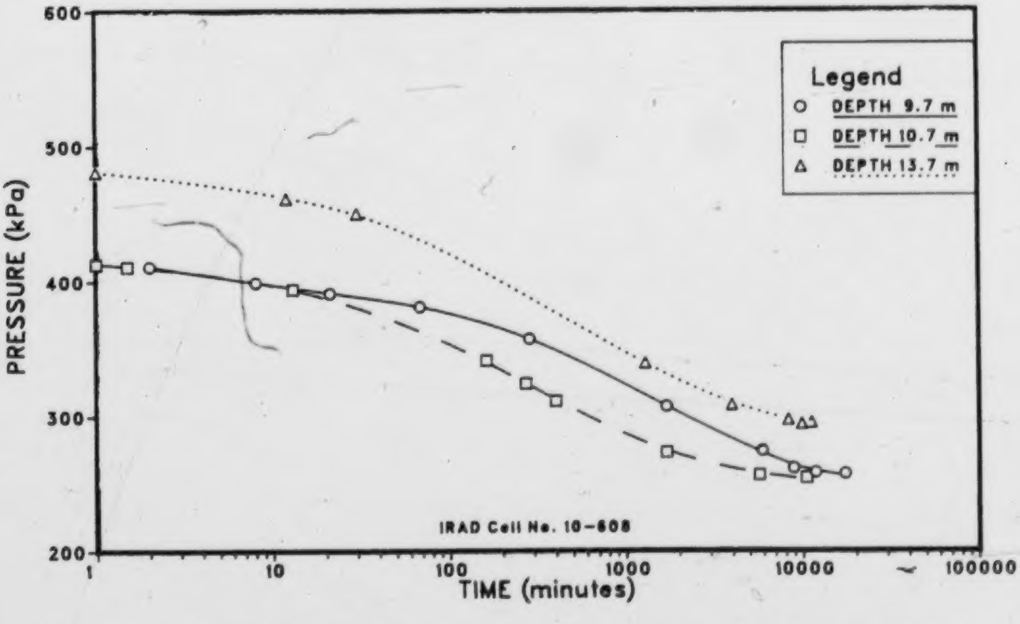

Figure D.8 TSC results at UA4 with cell in North-South direction.

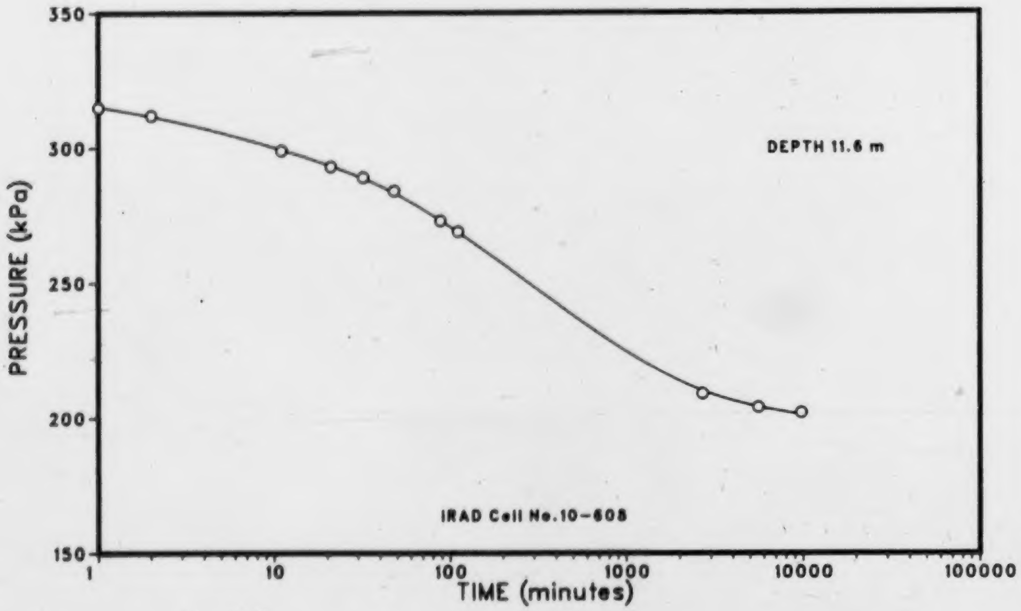

Figure D.9 TSC results at UA6 with cell in North-South direction.

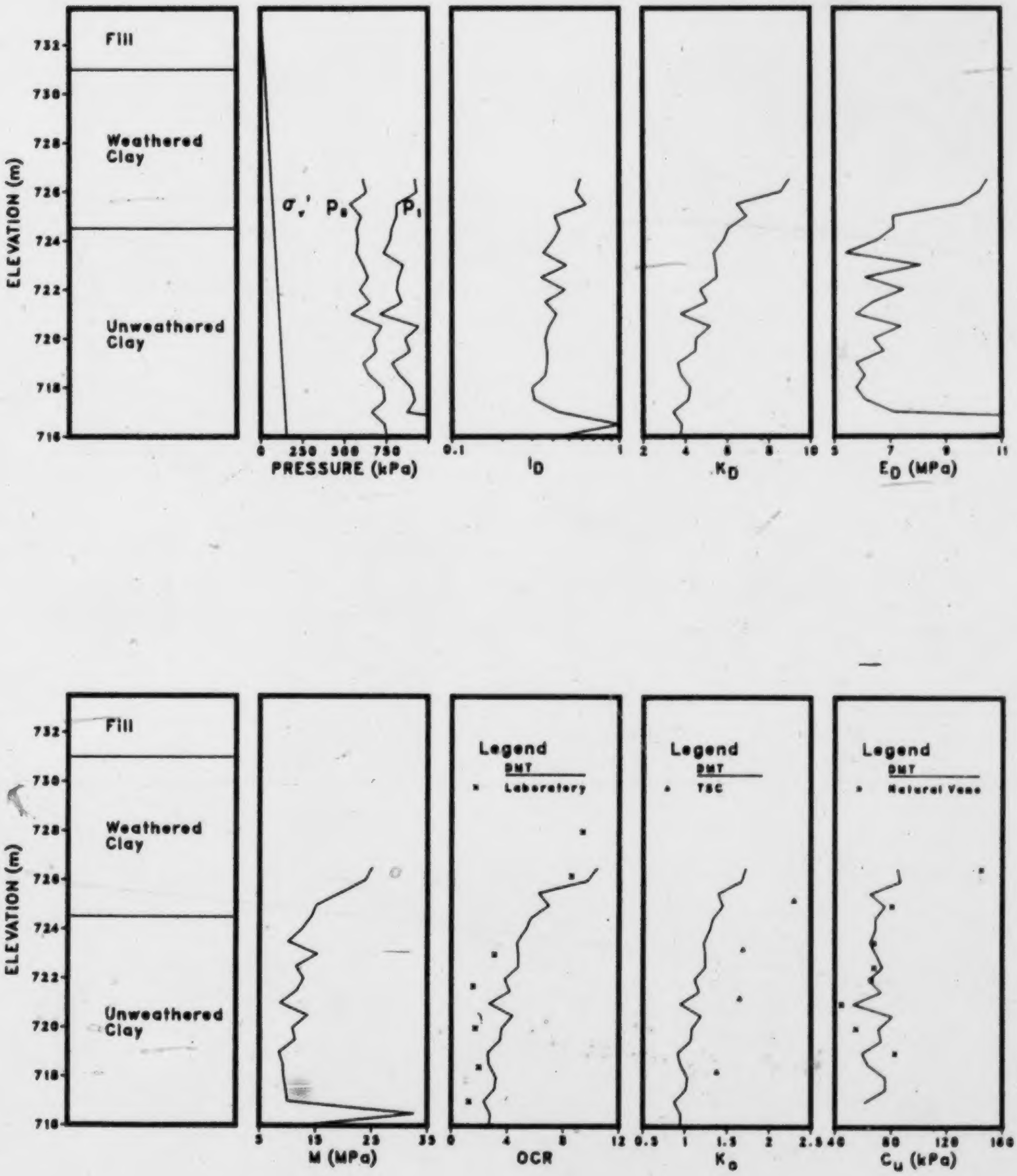

Figure D.10 Dilatometer test results at UA3.

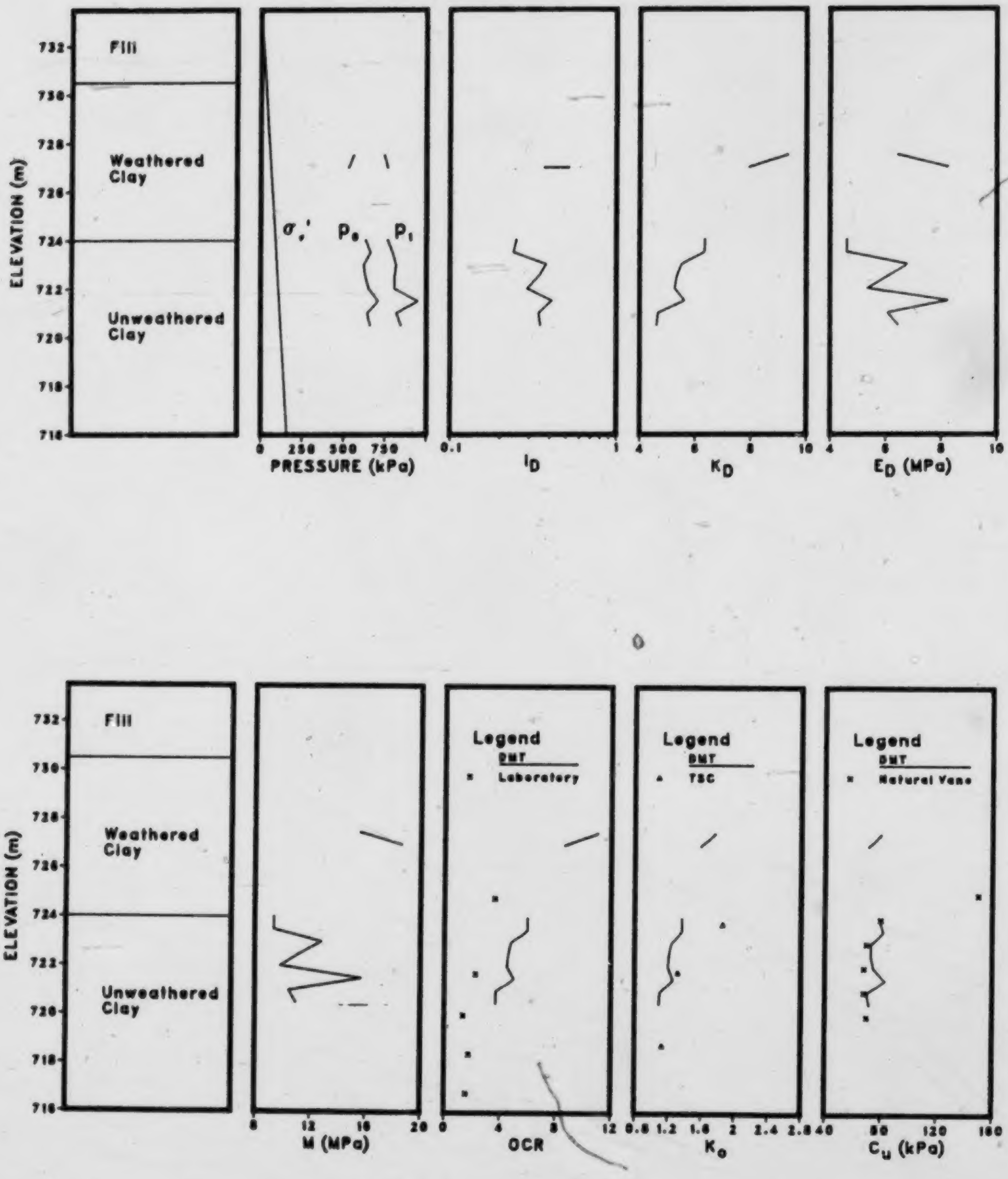

Figure D.11 Dilatometer test results at UA4.

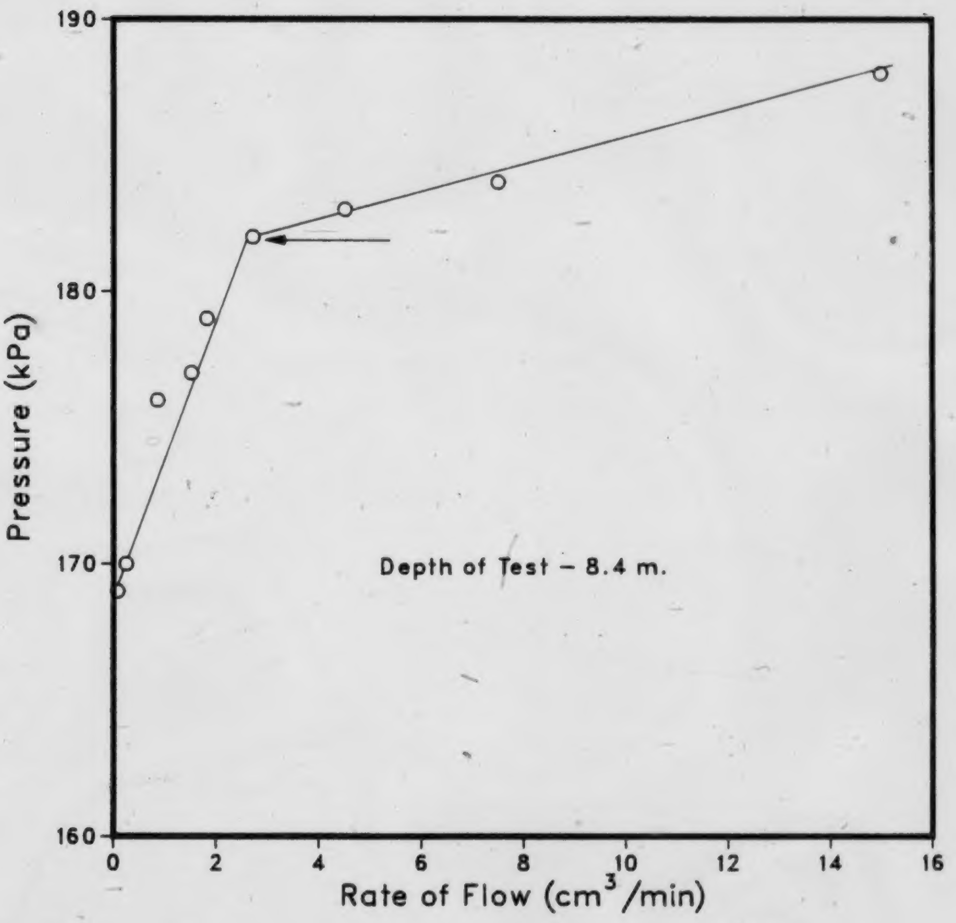

Figure D.12 Hydraulic fracture at UA1 at depth of 8.4 m.

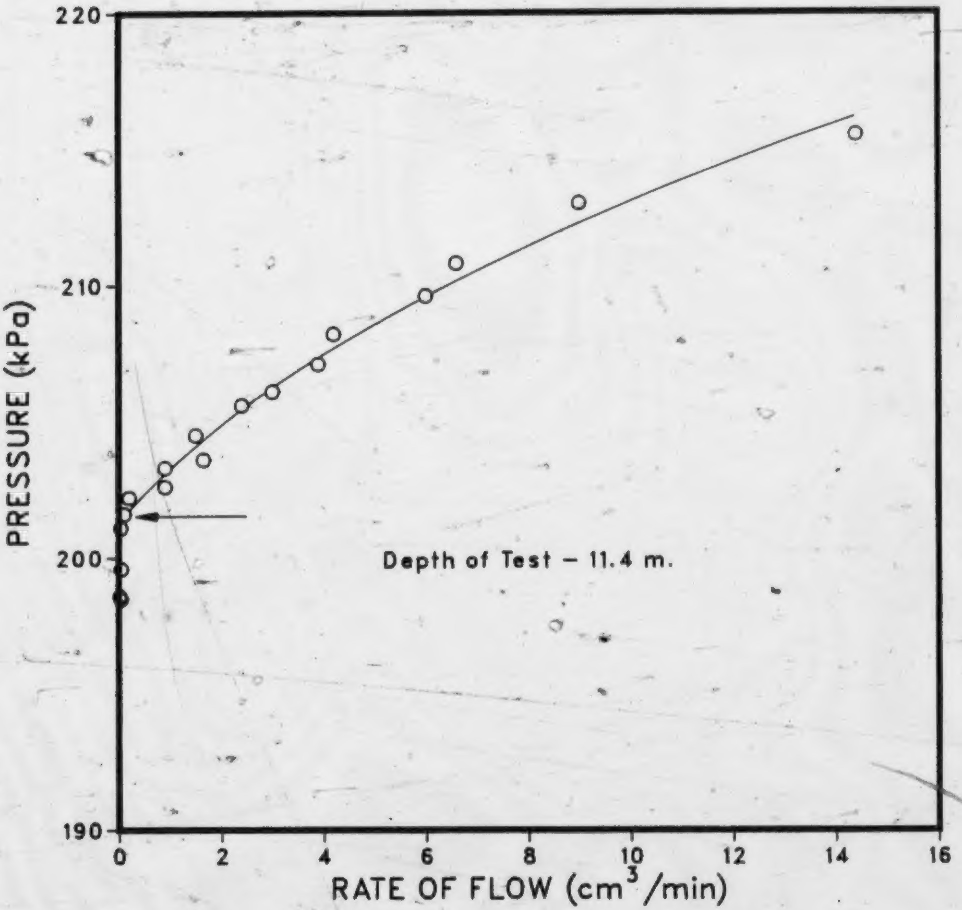

Figure D.13 Hydraulic fracture at UA1 at depth of 11.4 m.

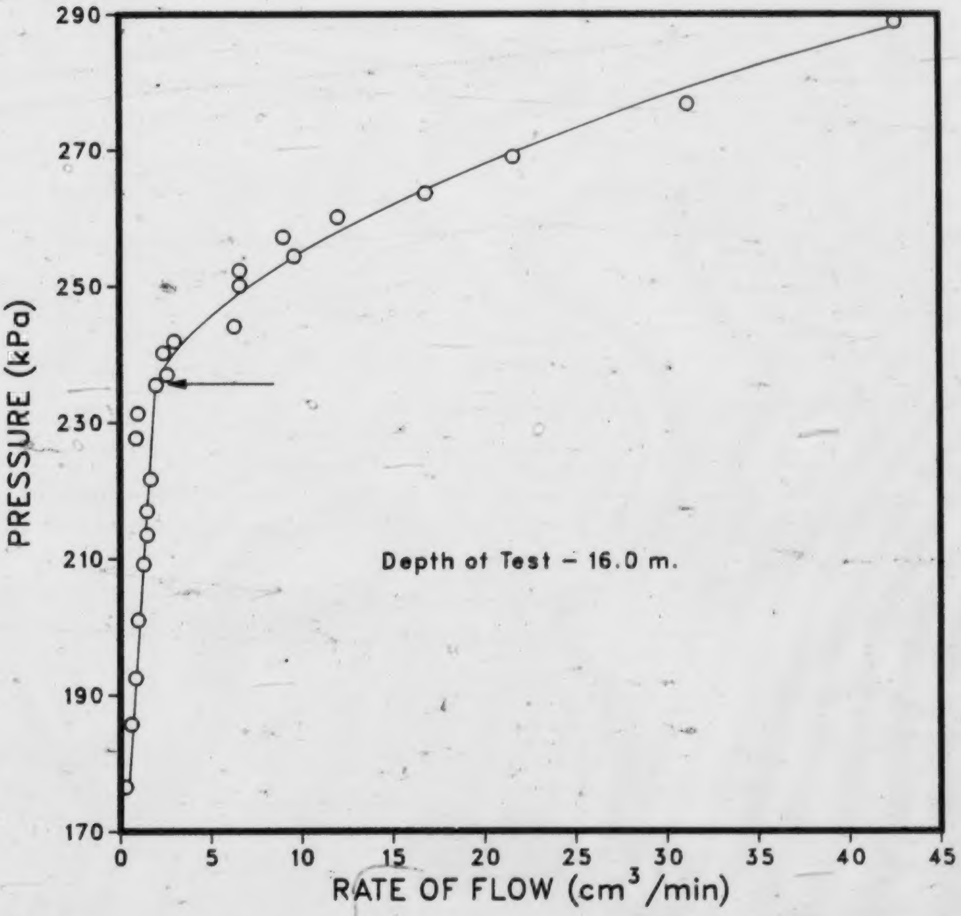

Figure D.14 Hydraulic fracture at UA1 at depth of 16.0 m.

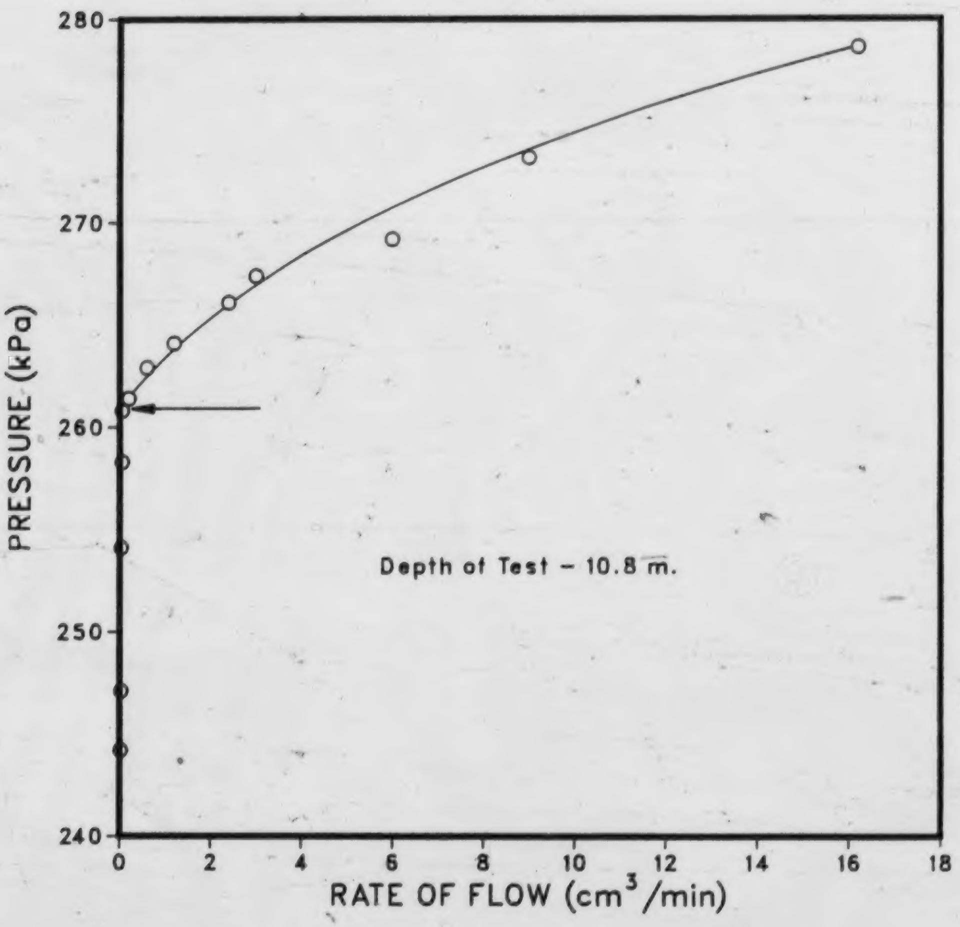

Figure D.15 Hydraulic fracture at UA2 at depth of 10.8 m.

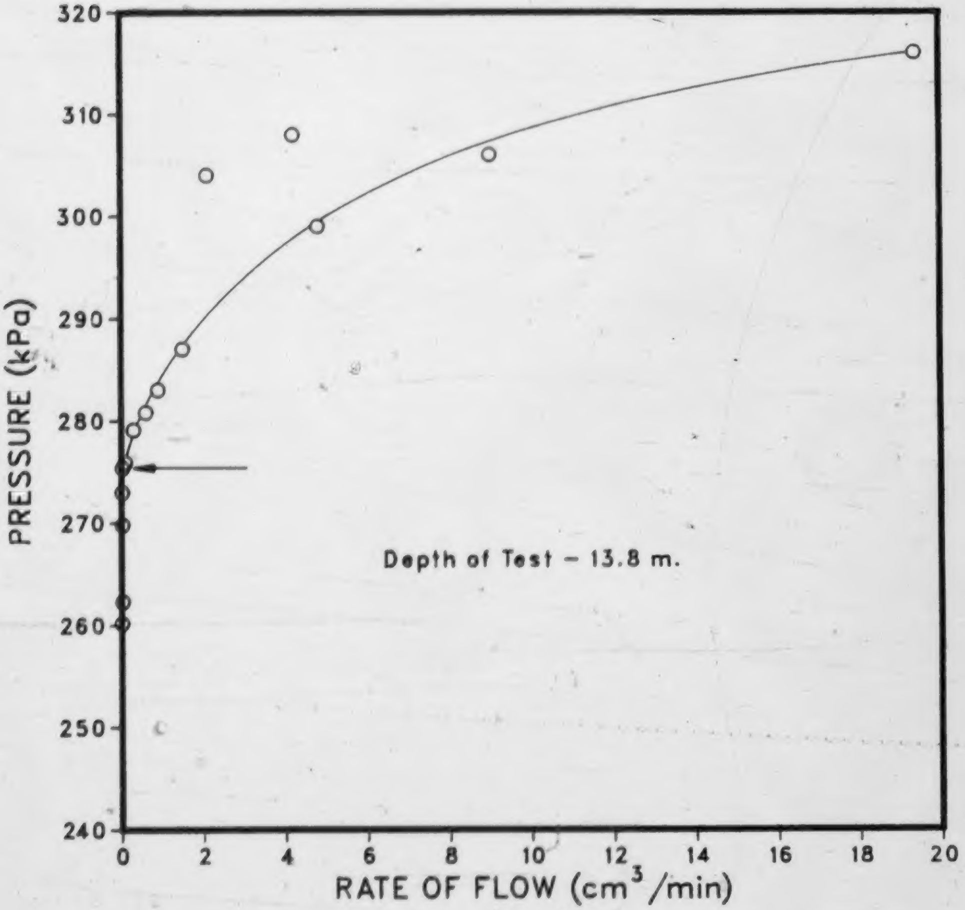

Figure D.16 Hydraulic fracture at UA2 at depth of 13.8 m.

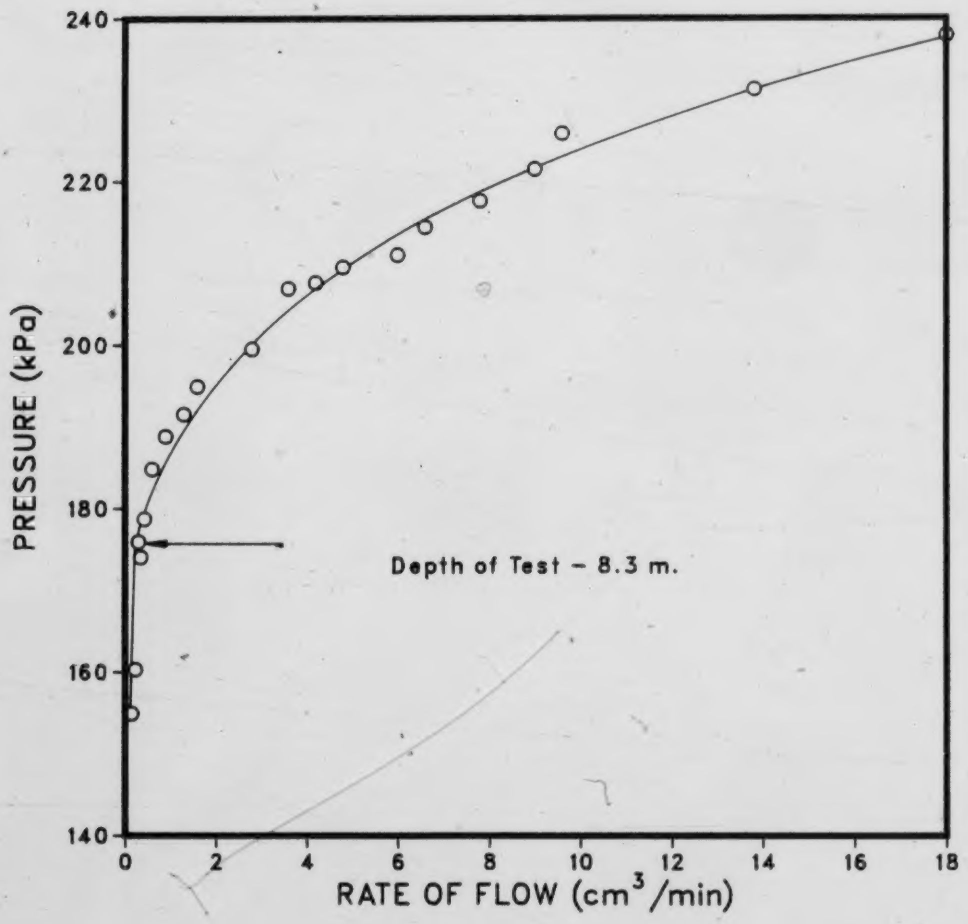

Figure D.17 Hydraulic fracture at UA3 at depth of 8.3 m.

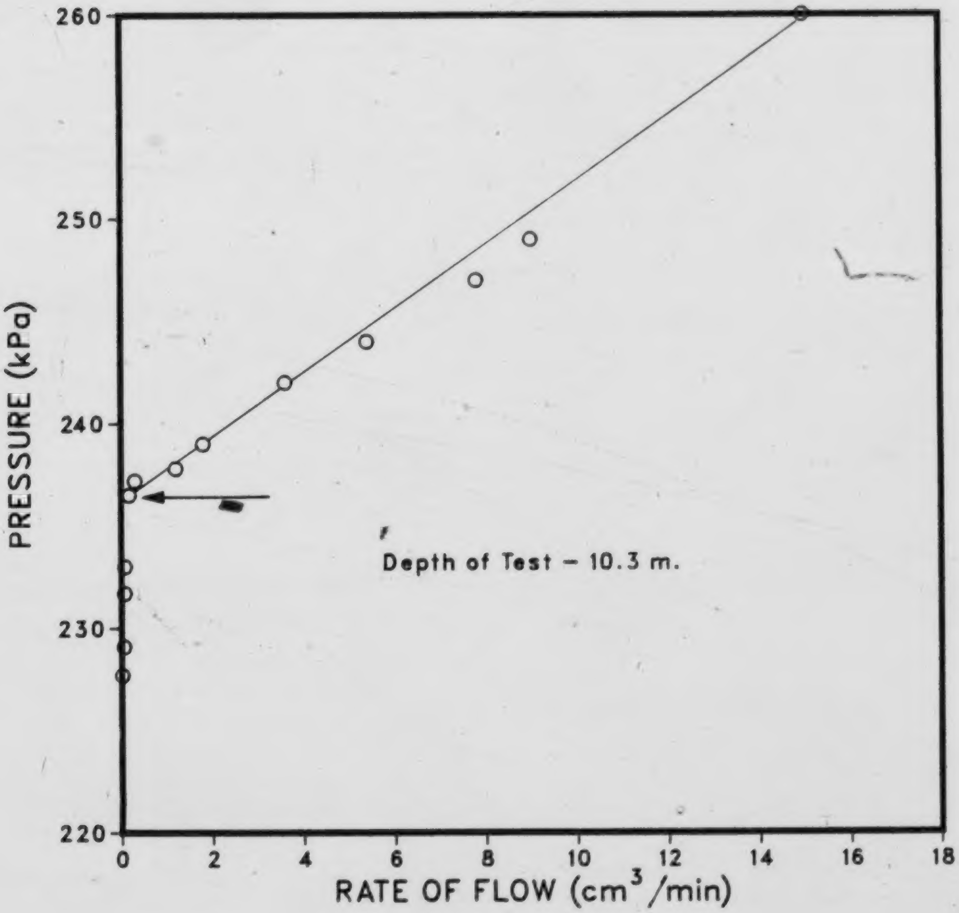

Figure D.18 Hydraulic fracture at UA3 at depth of 10.3 m.

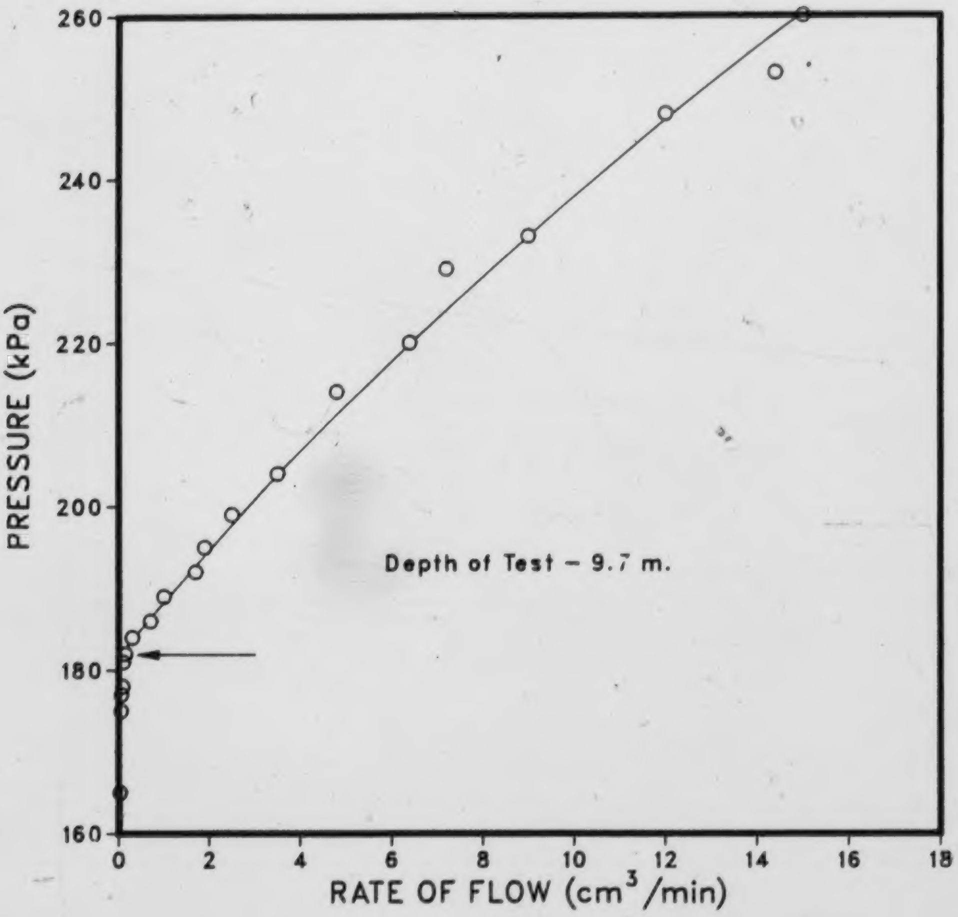

Figure D.19 Hydraulic fracture at UA4 at depth of 9.7 m.

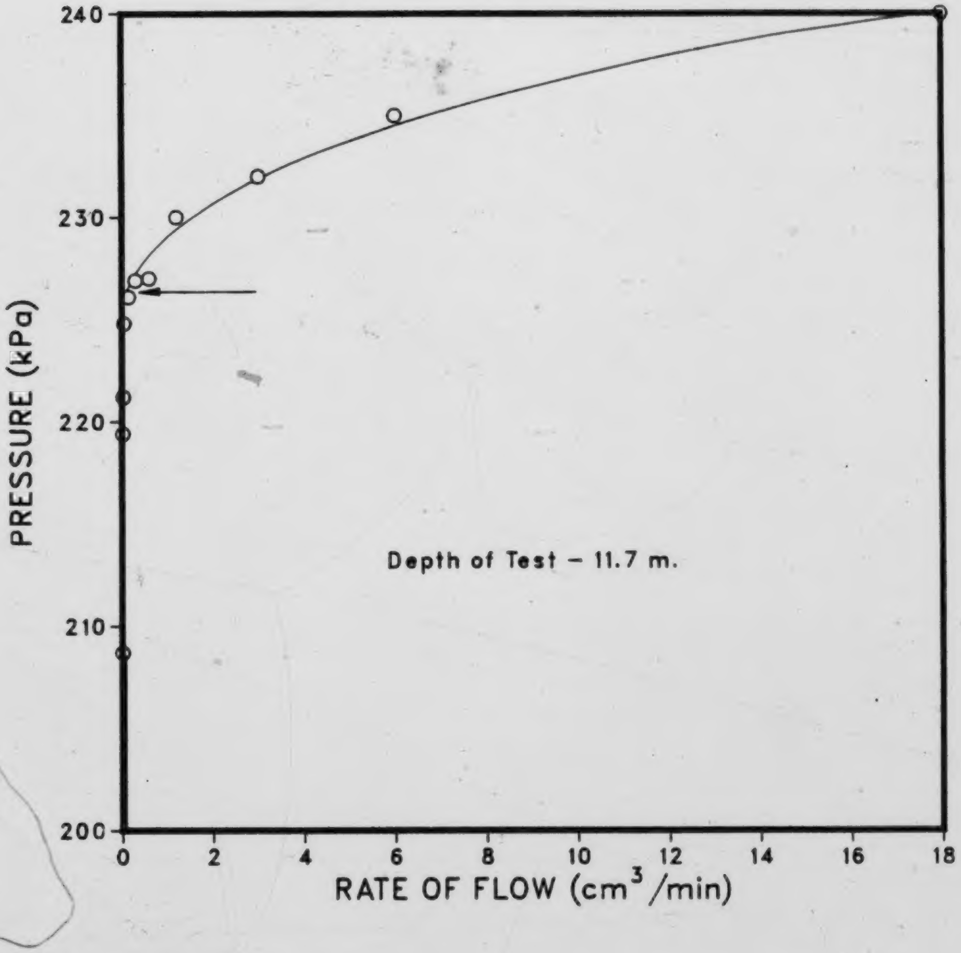

Figure D.20 Hydraulic fracture at UA4 at depth of 11.7 m.

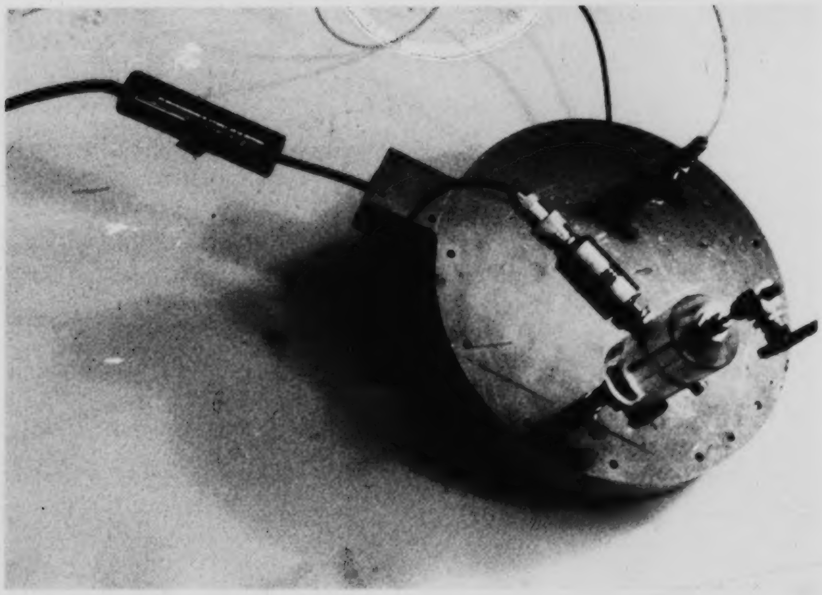

Plate D.1 Calibration chamber for total stress cell.

# APPENDIX E - LABORATORY INVESTIGATION RESULTS

Table E.1 Summary of consolidation test data.

| Sample No | Depth (m) | $w$ (%) | $w_L$ (%) | $w_P$ (%) | $I_P$ (%) | $I_L$ (%) | $\rho$ $Mg/m^3$ | $e_0$ |
|---|---|---|---|---|---|---|---|---|
| B1 | 6.0 | 39.2 | 58 | 21 | 37 | 0.51 | 1.77 | 1.10 |
| 1-1 | 5.7 | 42.3 | 74 | 27 | 47 | 0.33 | 1.81 | 1.13 |
| 1-1A | 7.8 | 48.5 | 75 | 29 | 46 | 0.43 | 1.77 | 1.27 |
| 1-2 | 8.9 | 41.5 | 68 | 24 | 44 | 0.40 | 1.84 | 1.08 |
| 1-3 | 10.1 | 43.2 | 63 | 26 | 37 | 0.46 | 1.81 | 1.13 |
| 1-4 | 11.7 | 42.4 | 63 | 25 | 38 | 0.46 | 1.80 | 1.14 |
| 1-6 | 15.0 | 49.7 | 69 | 25 | 44 | 0.56 | 1.64 | 1.46 |
| 2-3 | 10.3 | 39.2 | 65 | 24 | 41 | 0.37 | 1.84 | 1.04 |
| 2-4 | 11.9 | 41.7 | 68 | 26 | 42 | 0.37 | 1.80 | 1.12 |
| 2-5 | 13.4 | 34.3 | 66 | 25 | 41 | 0.23 | 1.90 | 0.91 |
| 2-6 | 15.0 | 40.1 | 66 | 25 | 41 | 0.37 | 1.83 | 1.06 |
| 2-7 | 16.5 | 36.6 | 66 | 25 | 41 | 0.28 | 1.86 | 0.99 |
| 2-8 | 17.7 | 37.2 | 57 | 23 | 34 | 0.42 | 1.84 | 1.01 |
| 2-9 | 19.6 | 37.1 | 55 | 20 | 35 | 0.49 | 1.85 | 1.01 |
| 2-10 | 21.1 | 64.3 | 99 | 37 | 62 | 0.44 | 1.61 | 1.76 |
| 5-2 | 7.3 | 37.0 | 67 | 26 | 41 | 0.27 | 1.86 | 0.99 |
| 5-3 | 8.6 | 34.1 | 65 | 24 | 41 | 0.25 | 1.88 | 0.92 |
| 5-4 | 10.4 | 36.1 | 63 | 23 | 40 | 0.33 | 1.86 | 0.97 |
| 5-5 | 12.0 | 36.4 | 62 | 24 | 38 | 0.33 | 1.86 | 0.98 |
| 5-6 | 13.2 | 36.8 | 62 | 20 | 42 | 0.40 | 1.85 | 0.99 |
| 5-7 | 14.9 | 38.4 | 59 | 21 | 38 | 0.46 | 1.84 | 1.03 |
| 5-10 | 19.4 | 18.2 | 24 | 12 | 12 | 0.52 | 2.09 | 0.53 |
| 3-3 | 5.6 | 40.6 | 76 | 30 | 46 | 0.23 | 1.78 | 1.13 |
| 3-4 | 7.3 | 33.3 | ** | ** | ** | **** | 1.92 | 0.88 |
| 3-6 | 10.2 | 45.2 | 79 | 20 | 59 | 0.43 | 1.77 | 1.22 |
| 3-7 | 11.7 | 48.5 | 110 | 36 | 74 | 0.17 | 1.75 | 1.29 |
| 3-8 | 13.5 | 40.2 | 72 | 27 | 45 | 0.29 | 1.81 | 1.09 |
| 3-9 | 15.0 | 44.1 | 76 | 30 | 46 | 0.31 | 1.76 | 1.21 |
| 3-10 | 16.3 | 37.3 | 51 | 19 | 32 | 0.57 | 1.84 | 1.01 |
| 4-4 | 8.6 | 32.7 | 66 | 25 | 41 | 0.19 | 1.91 | 0.88 |
| 4-6 | 11.7 | 56.9 | 101 | 33 | 68 | 0.35 | 1.71 | 1.48 |
| 4-7 | 13.3 | 55.2 | 73 | 28 | 45 | 0.60 | 1.71 | 1.45 |
| 4-8 | 15.0 | 41.1 | 63 | 25 | 38 | 0.42 | 1.78 | 1.15 |
| 4-9 | 16.4 | 56.9 | 95 | 28 | 67 | 0.43 | 1.70 | 1.49 |
| 6-4 | 11.8 | 43.7 | 74 | 24 | 50 | 0.39 | 1.79 | 1.17 |

Table E.2 Summary of consolidation test data (continued).

| Sample No | $\sigma'_{vo}$ (kPa) | Swell Press (kPa) | $\sigma'_p$ (kPa) | OCR | $c_v$ (m²/yr) $\sigma'_{vo}-\sigma'_p$ | $m_v$ (m²/MN) $\sigma'_{vo}-\sigma'_p$ | $C_c$ | C, |
|---|---|---|---|---|---|---|---|---|
| B1 | 60 | 22 | 120 | 2.0 | 0.35-0.26 | .80-.38 | .32 | .05 |
| 1-1 | 63 | 26 | 190 | 3.0 | 0.86-0.60 | .31-.25 | .37 | .12 |
| 1-1A | 83 | 33 | 180 | 2.2 | 0.96-0.51 | .35-.32 | .45 | .12 |
| 1-2 | 95 | 16 | 200 | 2.1 | 1.10-0.54 | .30-.25 | .40 | .09 |
| 1-3 | 105 | 20 | 210 | 2.0 | 0.93-0.65 | .34-.26 | .44 | .10 |
| 1-4 | 119 | 12 | 140 | 1.2 | 1.32-0.85 | .39-.37 | .43 | .09 |
| 1-6 | 147 | 18 | 160 | 1.1 | 0.32-0.37 | .44-.49 | .91 | .17 |
| 2-3 | 151 | 32 | 340 | 2.3 | 3.25-1.52 | .18-.19 | .53 | .10 |
| 2-4 | 166 | 21 | 205 | 1.2 | 1.00-0.82 | .29-.27 | .44 | .09 |
| 2-5 | 177 | 35 | 620 | 3.5 | 2.95-1.32 | 0.10 | .43 | .09 |
| 2-6 | 190 | 25 | 270 | 1.4 | 1.61-0.81 | .17-.19 | .46 | .10 |
| 2-7 | 206 | 33 | 330 | 1.6 | 1.15-0.89 | .17-.19 | .44 | .11 |
| 2-8 | 220 | 19 | 310 | 1.4 | 1.54-0.75 | 0.18 | .39 | .09 |
| 2-9 | 234 | 19 | 240 | 1.0 | 4.50 | 0.16 | .36 | .08 |
| 2-10 | 244 | 35 | 225 | 0.9 | 0.52 | 0.25 | .98 | .23 |
| 5-2 | 101 | 29 | 380 | 3.8 | 2.51-2.19 | 0.16 | .45 | .09 |
| 5-3 | 113 | 22 | 425 | 3.8 | 2.70-1.92 | .17-.12 | .40 | .08 |
| 5-4 | 126 | 24 | 305 | 2.4 | 1.16-1.20 | .20-.15 | .40 | .10 |
| 5-5 | 140 | 26 | 310 | 2.2 | 2.00-2.65 | 0.20 | .44 | .08 |
| 5-6 | 152 | 24 | 275 | 1.8 | 0.84-0.75 | .27-.19 | .43 | .10 |
| 5-7 | 165 | 24 | 255 | 1.6 | 2.28-1.56 | .15-.17 | .44 | .09 |
| 5-10 | 212 | 0 | 200 | 1.0 | 1.56 | 0.14 | .13 | .01 |
| 3-3 | 32 | 23 | 500 | 15.4 | 1.70-0.87 | .14-.13 | .45 | .12 |
| 3-4 | 49 | 25 | 600 | 12.3 | 4.15-1.82 | .13-.09 | .38 | .09 |
| 3-6 | 78 | 22 | 300 | 3.9 | 1.60-0.88 | .25-.18 | .47 | .13 |
| 3-7 | 91 | 29 | 175 | 1.9 | 0.88-0.51 | .32-.26 | .44 | .15 |
| 3-8 | 104 | 37 | 215 | 2.1 | 0.46-0.22 | .27-.26 | .45 | .15 |
| 3-9 | 118 | 35 | 275 | 2.3 | 0.68-0.44 | .24-.21 | .62 | .16 |
| 3-10 | 130 | 0 | 190 | 1.5 | 0.71-0.29 | .37-.28 | .37 | .11 |
| 4-4 | 58 | 24 | 300 | 5.1 | 1.06-1.13 | .22-.15 | .40 | .07 |
| 4-6 | 85 | 25 | 245 | 2.9 | 1.56-1.10 | .27-.25 | .63 | .18 |
| 4-7 | 100 | 24 | 170 | 1.7 | 0.51-0.40 | .35-.34 | .56 | .18 |
| 4-8 | 114 | 22 | 245 | 2.1 | 7.10-2.20 | .17-.21 | .43 | .11 |
| 4-9 | 126 | 28 | 235 | 1.9 | 0.81-0.55 | .23-.21 | .48 | .16 |
| 6-4 | 77 | 12.5 | 160 | 2.1 | 2.60-1.90 | .35-.31 | .42 | .10 |

Table E.3 Summary of direct shear tests on clay samples.

| Sample No | Depth (m) | Initial Conditions | | | | |
|---|---|---|---|---|---|---|
| | | Width (mm) | Ht (mm) | $\rho$ Mg/m$^3$ | w (%) | $e_o$ |
| Grey Clay | | | | | | |
| 2-10 | 20.8 | 63.2 | 25.0 | 1.81 | 40.4 | 1.09 |
| B3.1 | 6.0 | 60.3 | 25.4 | 1.86 | 34.8 | 0.96 |
| B3.2 | 6.0 | 63.5 | 25.0 | 1.88 | 37.0 | 0.97 |
| B3.3 | 6.0 | 63.5 | 25.0 | 1.90 | 35.7 | 0.93 |
| B3.4 | 6.0 | 60.3 | 25.4 | 1.87 | 34.6 | 0.94 |
| Brown Clay | | | | | | |
| 4.1 | 7.9 | 60.3 | 25.4 | 1.93 | 30.4 | 0.82 |
| 4.2 | 7.9 | 60.3 | 25.4 | 1.95 | 29.7 | 0.80 |
| 4.3 | 7.9 | 60.3 | 25.4 | 1.93 | 30.4 | 0.82 |
| 4.4 | 7.9 | 60.3 | 25.4 | 1.89 | 32.1 | 0.89 |

| Sample No | Final w.c (%) | Cons. Press (kPa) | $C_v$ (m$^2$/yr) | Shear Rate (cm/hr) | $\tau_p$ (kPa) | $\tau_r$ (kPa) |
|---|---|---|---|---|---|---|
| 2-10 | 35.5 | 240.2 | 1.37 | 0.012 | 95 | 76 |
| B3.1 | 33.5 | 100.0 | 0.86 | 0.012 | 61 | 29 |
| B3.2 | 31.4 | 200.0 | 0.90 | 0.012 | 96 | 58 |
| B3.3 | 29.3 | 300.0 | 0.69 | 0.012 | 125 | 70 |
| B3.4 | 26.5 | 500.0 | 1.37 | 0.012 | 231 | 132 |
| 4.1 | 31.5 | 100.0 | 3.34 | 0.020 | 72 | 25 |
| 4.2 | 28.6 | 300.0 | 1.84 | 0.020 | 172 | 75 |
| 4.3 | 27.4 | 700.0 | 1.25 | 0.020 | 300 | 145 |
| 4.4 | 28.0 | 500.0 | 1.64 | 0.020 | 235 | 80 |

Table E.4 Summary of triaxial tests on UA1 grey clay samples.

| Sample No | Depth (m) | Initial Conditions | | | | | |
|---|---|---|---|---|---|---|---|
| | | Ht (mm) | Dia (mm) | $\rho$ Mg/m$^3$ | w (%) | $e_o$ | $\Delta V$ (cm$^3$) |
| 1-2 | 8.7 | 77.4 | 38.4 | 1.65 | 52.0 | 1.49 | +1.40 |
| 1-3 | 10.2 | 77.5 | 38.2 | 1.77 | 45.2 | 1.21 | -1.00 |
| 1-4 | 11.8 | 77.6 | 38.6 | 1.81 | 41.9 | 1.12 | ** |
| 1-6a | 14.8 | 77.5 | 38.7 | 1.72 | 45.1 | 1.23 | +1.60 |
| 1-6b | 14.9 | 77.1 | 38.4 | 1.72 | 56.3 | 1.45 | +2.30 |

| Sample No | Final w.c (%) | $\sigma_1c'$ (kPa) | Init. $\frac{\sigma_3'}{\sigma_1'}$ | At max. $(\sigma_1-\sigma_3)$ | | | |
|---|---|---|---|---|---|---|---|
| | | | | $\frac{\sigma_1-\sigma_3}{2}$ (kPa) | $\frac{\sigma_1'+\sigma_3'}{2}$ (kPa) | Axial $\epsilon$ (%) | A |
| 1-2 | 62.8 | 95. | 1.0 | 27.6 | 91.8 | 10.37 | 0.55 |
| 1-3 | 45.5 | 105. | 1.0 | 49.7 | 123.1 | 4.38 | 0.32 |
| 1-4 | 39.9 | 120. | 1.0 | 53.3 | 117.6 | 10.50 | 0.52 |
| 1-6a | 50.2 | 140. | 1.0 | 50.4 | 121.0 | 7.20 | 0.69 |
| 1-6b | 47.1 | 300. | 1.0 | 76.4 | 226.5 | 8.05 | 1.06 |

| Sample No | At max. $\sigma_1'/\sigma_3'$ | | | Failure Mode & Angle To Horizontal |
|---|---|---|---|---|
| | $\frac{\sigma_1'}{\sigma_3'}$ | Axial $\epsilon$ (%) | A | |
| 1-2 | 1.86 | 10.37 | 0.55 | Shear - 50°(slickenside) |
| 1-3 | 2.35 | 4.38 | 0.32 | Multiple shear - 35 to 55° |
| 1-4 | 2.66 | 10.50 | 0.52 | Shear - 65° |
| 1-6a | 2.51 | 11.04 | 0.77 | Plastic failure |
| 1-6b | 2.09 | 9.11 | 1.24 | Shear - 55° |

Table E.5 Summary of triaxial tests on UA2 grey clay samples.

| Sample No | Depth (m) | Initial Conditions | | | | | $\Delta V$ (cm$^3$) |
|---|---|---|---|---|---|---|---|
| | | Ht (mm) | Dia (mm) | $\rho$ Mg/m$^3$ | w (%) | $e_0$ | |
| 2-4 | 11.8 | 77.2 | 38.3 | 1.84 | 41.2 | 1.07 | +3.00 |
| 2-6 | 14.6 | 77.5 | 38.5 | 1.81 | 44.3 | 0.99 | +1.60 |
| 2-8a | 17.8 | 77.3 | 38.1 | 1.83 | 38.5 | 1.04 | +0.33 |
| 2-8b | 17.9 | 77.2 | 38.0 | 1.86 | 36.7 | 0.98 | +2.15 |
| 2-9 | 19.6 | 77.5 | 38.7 | 1.81 | 37.7 | 1.05 | +0.90 |
| 2-10 | 21.0 | 77.3 | 38.0 | 1.62 | 82.4 | 3.03 | +4.50 |

| Sample No | Final w.c (%) | $\sigma_1 c'$ (kPa) | Init. $\frac{\sigma_3'}{\sigma_1'}$ | At max. $(\sigma_1-\sigma_3)$ | | | |
|---|---|---|---|---|---|---|---|
| | | | | $\frac{\sigma_1-\sigma_3}{2}$ (kPa) | $\frac{\sigma_1'+\sigma_3'}{2}$ (kPa) | Axial $\epsilon$ (%) | A |
| 2-4 | 39.4 | 160. | 1.0 | 82.1 | 159.1 | 10.86 | 0.45 |
| 2-6 | 41.1 | 188. | 1.0 | 88.2 | 187.5 | 8.02 | 0.45 |
| 2-8a | 39.3 | 205. | 0.6 | 92.0 | 178.3 | 3.05 | 0.37 |
| 2-8b | 36.1 | 221. | 1.0 | 103.3 | 209.4 | 7.40 | 0.56 |
| 2-9 | 37.7 | 230. | 0.64 | 77.8 | 193.0 | 1.77 | 0.44 |
| 2-10 | 59.4 | 240. | 1.0 | 59.0 | 221.1 | 3.20 | 0.58 |

| Sample No | At max. $\sigma_1'/\sigma_3'$ | | | Failure Mode & Angle To Horizontal |
|---|---|---|---|---|
| | $\frac{\sigma_1'}{\sigma_3'}$ | Axial $\epsilon$ (%) | A | |
| 2-4 | 3.14 | 9.70 | 0.45 | Plastic failure |
| 2-6 | 2.78 | 8.02 | 0.45 | Shear - 45° |
| 2-8a | 3.16 | 3.05 | 0.37 | Shear - 50° |
| 2-8b | 2.94 | 7.40 | 0.56 | Shear - 55° |
| 2-9 | 2.37 | 2.73 | 0.50 | Shear - 45° along dark grey clay lamination |
| 2-10 | 1.73 | 3.20 | 0.58 | Shear - 55°(slickenside) |

Table E.6 Summary of triaxial tests on UA5 grey clay samples.

| Sample No | Depth (m) | Initial Conditions | | | | | $\Delta V$ (cm³) |
|---|---|---|---|---|---|---|---|
| | | Ht (mm) | Dia (mm) | $\rho$ Mg/m³ | w (%) | $e_0$ | |
| 5-4a | 10.3 | 77.6 | 38.0 | 1.86 | 36.3 | 0.98 | +0.85 |
| 5-4b | 10.1 | 77.7 | 38.1 | 1.86 | 36.7 | 0.98 | +0.99 |
| 5-6b | 13.4 | 77.7 | 38.0 | 1.87 | 38.2 | 1.00 | +0.20 |
| 5-6a | 13.4 | 78.0 | 38.1 | 1.84 | 39.6 | 1.05 | +1.98 |
| 5-8 | 16.2 | 78.1 | 38.0 | 1.82 | 40.0 | 1.08 | +2.50 |
| 5-9 | 17.7 | 78.4 | 38.3 | 1.73 | 46.8 | 1.29 | +4.90 |

| Sample No | Final w.c (%) | $\sigma_1c'$ (kPa) | Init. $\frac{\sigma_3'}{\sigma_1'}$ | At max. $(\sigma_1-\sigma_3)$ | | | |
|---|---|---|---|---|---|---|---|
| | | | | $\frac{\sigma_1-\sigma_3}{2}$ (kPa) | $\frac{\sigma_1'+\sigma_3'}{2}$ (kPa) | Axial $\epsilon$ (%) | A |
| 5-4a | 37.1 | 130. | 1.0 | 62.8 | 146.1 | 5.54 | 0.37 |
| 5-4b | 35.4 | 130. | 1.5 | 84.1 | 188.9 | 11.2 | 0.39 |
| 5-6b | 36.9 | 165. | 1.0 | 80.2 | 175.2 | 8.77 | 0.44 |
| 5-6a | 38.7 | 160. | 1.0 | 75.3 | 170.4 | 6.58 | 0.43 |
| 5-8 | 38.4 | 195. | 1.0 | 87.1 | 181.7 | 8.07 | 0.58 |
| 5-9 | 43.9 | 210. | 1.0 | 60.0 | 179.9 | 4.10 | 0.75 |

| Sample No | At max. $\sigma_1'/\sigma_3'$ | | | Failure Mode & Angle To Horizontal |
|---|---|---|---|---|
| | $\frac{\sigma_1'}{\sigma_3'}$ | Axial $\epsilon$ (%) | A | |
| 5-4a | 2.51 | 5.54 | 0.37 | Shear - 62° |
| 5-4b | 2.60 | 11.2 | 0.39 | Plastic failure |
| 5-6b | 2.74 | 7.12 | 0.46 | Plastic failure |
| 5-6a | 2.52 | 6.58 | 0.43 | Shear - 55°(bedding plane) |
| 5-8 | 2.84 | 8.07 | 0.58 | Shear - 55° |
| 5-9 | 2.06 | 6.45 | 0.85 | Shear - 55° |

Table E.7 Summary of triaxial tests on UA3 grey clay samples.

| Sample No | Depth (m) | Initial Conditions | | | | | $\Delta V$ (cm³) |
|---|---|---|---|---|---|---|---|
| | | Ht (mm) | Dia (mm) | $\rho$ Mg/m³ | w (%) | $e_0$ | |
| 3-7 | 12.0 | 78.8 | 37.8 | 1.83 | 38.4 | 1.04 | -1.35 |
| 3-8 | 13.4 | 77.1 | 38.0 | 1.85 | 36.1 | 1.08 | +1.05 |
| 3-9 | 14.9 | 77.3 | 38.6 | 1.72 | 53.0 | 1.40 | +0.70 |

| Sample No | Final w.c (%) | $\sigma_1 c'$ (kPa) | Init. $\frac{\sigma_3'}{\sigma_1'}$ | At max. $(\sigma_1-\sigma_3)$ | | | |
|---|---|---|---|---|---|---|---|
| | | | | $\frac{\sigma_1-\sigma_3}{2}$ (kPa) | $\frac{\sigma_1'+\sigma_3'}{2}$ (kPa) | Axial $\epsilon$ (%) | A |
| 3-7 | 39.7 | 100. | 1.0 | 56.9 | 115.0 | 2.85 | 0.37 |
| 3-8 | 37.8 | 110. | 1.0 | 69.0 | 131.1 | 3.29 | 0.35 |
| 3-9 | 51.9 | 125. | 1.0 | 66.5 | 117.4 | 3.45 | 0.56 |

| Sample No | At max. $\sigma_1'/\sigma_3'$ | | | Failure Mode & Angle To Horizontal |
|---|---|---|---|---|
| | $\frac{\sigma_1'}{\sigma_3'}$ | Axial $\epsilon$ (%) | A | |
| 3-7 | 3.00 | 2.61 | 0.38 | Shear - 45°(slickenside) |
| 3-8 | 3.22 | 3.29 | 0.35 | Shear - 55° |
| 3-9 | 3.61 | 3.45 | 0.56 | Multiple shear - mainly 55° |

Table E.8 Summary of triaxial tests on UA4 grey clay samples.

| Sample No | Depth (m) | Initial Conditions | | | | | $\Delta V$ ($cm^3$) |
|---|---|---|---|---|---|---|---|
| | | Ht (mm) | Dia (mm) | $\rho$ $Mg/m^3$ | w (%) | $e_0$ | |
| 4-4 | 8.7 | 77.9 | 38.0 | 1.87 | 33.4 | 0.93 | -0.40 |
| 4-6 | 11.9 | 78.3 | 37.9 | 1.82 | 39.1 | 1.06 | +0.28 |
| 4-7a | 13.2 | 78.1 | 38.8 | 1.72 | 54.5 | 1.42 | +1.62 |
| 4-7b | 13.5 | 77.0 | 37.9 | 1.83 | 37.9 | 1.03 | +3.09 |
| 4-8a | 14.9 | 77.7 | 38.7 | 1.77 | 49.0 | 1.27 | +1.50 |
| 4-8b | 14.8 | 77.3 | 38.1 | 1.75 | 46.7 | 1.26 | +3.49 |
| 4-9 | 16.3 | 77.9 | 38.8 | 1.73 | 37.1 | 1.14 | +2.30 |

| Sample No | Final w.c (%) | $\sigma_1 c'$ (kPa) | Init. $\frac{\sigma_3'}{\sigma_1'}$ | At max. $(\sigma_1-\sigma_3)$ | | | |
|---|---|---|---|---|---|---|---|
| | | | | $\frac{\sigma_1-\sigma_3}{2}$ (kPa) | $\frac{\sigma_1'+\sigma_3'}{2}$ (kPa) | Axial $\epsilon$ (%) | A |
| 4-4 | 34.5 | 75. | 1.0 | 66.0 | 111.3 | 5.09 | 0.23 |
| 4-6 | 40.3 | 100. | 1.0 | 82.4 | 158.0 | 6.23 | 0.15 |
| 4-7a | 52.5 | 115. | 1.0 | 43.7 | 117.9 | 2.00 | 0.47 |
| 4-7b | 40.6 | 112. | 1.4 | 75.6 | 148.0 | 9.39 | 0.43 |
| 4-8a | 46.2 | 125. | 1.0 | 77.0 | 143.2 | 4.22 | 0.38 |
| 4-8b | 48.5 | 126. | 1.3 | 67.2 | 142.4 | 6.99 | 0.51 |
| 4-9 | 32.0 | 140. | 1.0 | 61.6 | 138.0 | 3.28 | 0.52 |

| Sample No | At max. $\sigma_1'/\sigma_3'$ | | | Failure Mode & Angle To Horizontal |
|---|---|---|---|---|
| | $\frac{\sigma_1'}{\sigma_3'}$ | Axial $\epsilon$ (%) | A | |
| 4-4 | 3.91 | 5.09 | 0.23 | Multiple shear - mainly 62° |
| 4-6 | 3.31 | 4.24 | 0.19 | Plastic failure |
| 4-7a | 2.18 | 2.00 | 0.47 | Multiple shear - 35 to 55° |
| 4-7b | 3.09 | 9.39 | 0.43 | Shear - 50° |
| 4-8a | 3.37 | 3.71 | 0.40 | Shear - 50° |
| 4-8b | 2.79 | 6.99 | 0.51 | Multiple shear - mainly 50° |
| 4-9 | 2.61 | 3.28 | 0.52 | Shear - 50°(slickenside) |

Table E.9 Summary of CIU tests on weathered brown clay.

| Sample No | Depth (m) | Initial Conditions | | | | | $\Delta V$ (cm$^3$) |
|---|---|---|---|---|---|---|---|
| | | Ht (mm) | Dia (mm) | $\rho$ Mg/m$^3$ | w (%) | $e_0$ | |
| 1-1 | 5.6 | 77.2 | 37.9 | 1.82 | 42.3 | 1.11 | +10.70 |
| 1-1A | 7.6 | 77.6 | 38.3 | 1.87 | 36.7 | 0.97 | +1.80 |
| 2-1 | 5.7 | 77.3 | 38.0 | 1.78 | 41.7 | 1.15 | -1.75 |
| 5-1a | 5.7 | 77.0 | 38.0 | 1.84 | 37.7 | 1.02 | +1.05 |
| 5-1b | 5.7 | 77.2 | 38.2 | 1.78 | 41.2 | 1.14 | +5.75 |
| 5-2 | 7.4 | 77.3 | 38.0 | 1.82 | 39.3 | 1.07 | ** |
| 3-4 | 7.1 | 77.5 | 38.0 | 1.83 | 37.4 | 1.03 | -2.60 |

| Sample No | Final w.c (%) | $\sigma_1 c'$ (kPa) | Init. $\frac{\sigma_3'}{\sigma_1'}$ | At max. $(\sigma_1 - \sigma_3)$ | | | |
|---|---|---|---|---|---|---|---|
| | | | | $\frac{\sigma_1 - \sigma_3}{2}$ (kPa) | $\frac{\sigma_1' + \sigma_3'}{2}$ (kPa) | Axial $\epsilon$ (%) | A |
| 1-1 | 34.4 | 600. | 1.0 | 125.0 | 517.1 | 6.68 | 0.83 |
| 1-1A | 32.6 | 80. | 1.0 | 52.7 | 98.2 | 4.55 | 0.34 |
| 2-1 | 44.6 | 90. | 1.0 | 52.8 | 111.3 | 2.33 | 0.30 |
| 5-1a | 38.6 | 250. | 1.0 | 126.1 | 277.3 | 4.80 | 0.39 |
| 5-1b | 37.5 | 600. | 1.0 | 191.0 | 551.6 | 4.14 | 0.63 |
| 5-2 | 38.3 | 105. | 1.0 | 80.5 | 150.2 | 3.86 | 0.22 |
| 3-4 | 40.0 | 60. | 1.0 | 52.9 | 99.1 | 4.92 | 0.13 |

| Sample No | At max. $\sigma_1'/\sigma_3'$ | | | Failure Mode & Angle To Horizontal |
|---|---|---|---|---|
| | $\frac{\sigma_1'}{\sigma_3'}$ | Axial $\epsilon$ (%) | A | |
| 1-1 | 1.64 | 6.68 | 0.83 | Shear - 52° |
| 1-1A | 3.80 | 4.55 | 0.34 | Shear - 55° |
| 2-1 | 2.86 | 1.84 | 0.32 | Shear - 35°(slickenside) |
| 5-1a | 3.51 | 5.19 | 0.40 | Multiple shear - 40 to 60° (fissures) |
| 5-1b | 2.06 | 4.14 | 0.63 | Shear - 52° |
| 5-2 | 3.37 | 3.32 | 0.24 | Shear - 25°(slickenside) |
| 3-4 | 3.70 | 2.54 | 0.21 | Multiple shear - 40 to 70° (fissures) |

Table E.10 Summary of CIU tests on grey clay block samples - vertical specimens.

| Sample No | Depth (m) | Initial Conditions |  |  |  |  | $\Delta V$ ($cm^3$) |
|---|---|---|---|---|---|---|---|
|  |  | Ht (mm) | Dia (mm) | $\rho$ $Mg/m^3$ | w (%) | $e_0$ |  |
| B2-1V | 6.0 | 76.1 | 38.5 | 1.88 | 36.1 | 0.95 | -2.10 |
| B3-2V | 6.0 | 76.8 | 38.6 | 1.89 | 35.2 | 0.93 | -1.95 |
| B2-3V | 6.0 | 77.6 | 38.8 | 1.88 | 35.0 | 0.94 | +0.25 |
| B1-4V | 6.0 | 77.5 | 38.7 | 1.86 | 37.7 | 1.00 | +4.54 |
| B3-5V | 6.0 | 77.3 | 38.0 | 1.90 | 34.4 | 0.91 | +4.15 |
| B2-6V | 6.0 | 77.4 | 38.2 | 1.86 | 34.3 | 0.95 | +3.85 |
| B2-7V | 6.0 | 77.0 | 38.5 | 1.88 | 36.3 | 0.96 | +7.80 |

| Sample No | Final w.c (%) | $\sigma_1 c'$ (kPa) | Init. $\frac{\sigma_3'}{\sigma_1'}$ | At max. $(\sigma_1-\sigma_3)$ |  |  |  |
|---|---|---|---|---|---|---|---|
|  |  |  |  | $\frac{\sigma_1-\sigma_3}{2}$ (kPa) | $\frac{\sigma_1'+\sigma_3'}{2}$ (kPa) | Axial $\epsilon$ (%) | A |
| B2-1V | 38.7 | 0 | 1.0 | 29.7 | 39.7 | 13.00 | -0.17 |
| B3-2V | 36.2 | 30. | 1.0 | 34.5 | 51.2 | 6.55 | 0.19 |
| B2-3V | 36.1 | 60. | 1.0 | 45.8 | 90.4 | 4.30 | 0.17 |
| B1-4V | 34.6 | 120. | 1.0 | 74.2 | 125.9 | 7.34 | 0.46 |
| B3-5V | 30.0 | 200. | 1.0 | 103.4 | 222.7 | 9.24 | 0.39 |
| B2-6V | 31.1 | 250. | 1.0 | 119.1 | 239.7 | 8.05 | 0.54 |
| B2-7V | 29.2 | 450. | 1.0 | 155.3 | 376.6 | 8.84 | 0.74 |

| Sample No | At max. $\sigma_1'/\sigma_3'$ |  |  | Failure Mode & Angle To Horizontal |
|---|---|---|---|---|
|  | $\frac{\sigma_1'}{\sigma_3'}$ | Axial $\epsilon$ (%) | A |  |
| B2-1V | 6.94 | 13.00 | 0.17 | Shear - 45° |
| B3-2V | 5.86 | 3.72 | 0.30 | Shear - 65° |
| B3-3V | 3.05 | 4.30 | 0.17 | Shear - 55° |
| B1-4V | 4.26 | 5.89 | 0.51 | Shear - 55° |
| B1-5V | 2.76 | 6.62 | 0.43 | Shear - 65° |
| B2-6V | 3.12 | 5.77 | 0.61 | Shear - 55° |
| B2-7V | 2.40 | 8.84 | 0.74 | Shear - 55° |

Table E.11 Summary of CIU tests on grey clay block samples - horizontal specimens.

| Sample No | Depth (m) | Initial Conditions | | | | | $\Delta V$ ($cm^3$) |
|---|---|---|---|---|---|---|---|
| | | Ht (mm) | Dia (mm) | $\rho$ $Mg/m^3$ | w (%) | $e_0$ | |
| B2-1H | 6.0 | 77.4 | 38.3 | 1.87 | 37.5 | 0.99 | -1.85 |
| B1-2H | 6.0 | 77.0 | 38.4 | 1.88 | 37.6 | 0.98 | -0.20 |
| B2-3H | 6.0 | 77.2 | 38.5 | 1.88 | 37.6 | 0.98 | +1.70 |
| B1-4H | 6.0 | 77.0 | 38.5 | 1.83 | 36.7 | 1.02 | +6.60 |
| B2-5H | 6.0 | 77.1 | 38.5 | 1.86 | 38.5 | 1.01 | +6.05 |
| B1-6H | 6.0 | 77.2 | 38.3 | 1.86 | 37.2 | 0.99 | +9.35 |

| Sample No | Final w.c (%) | $\sigma_1c'$ (kPa) | Init. $\frac{\sigma_3'}{\sigma_1'}$ | At max. $(\sigma_1-\sigma_3)$ | | | |
|---|---|---|---|---|---|---|---|
| | | | | $\frac{\sigma_1-\sigma_3}{2}$ (kPa) | $\frac{\sigma_1'+\sigma_3'}{2}$ (kPa) | Axial $\epsilon$ (%) | A |
| B2-1H | 37.4 | 30. | 1.0 | 32.8 | 49.0 | 5.46 | 0.21 |
| B1-2H | 35.3 | 60. | 1.0 | 37.0 | 79.6 | 7.73 | 0.24 |
| B2-3H | 35.1 | 90. | 1.0 | 66.1 | 116.3 | 7.96 | 0.30 |
| B1-4H | 35.4 | 200. | 1.0 | 83.2 | 169.8 | 7.15 | 0.68 |
| B2-5H | 32.8 | 250. | 1.0 | 114.8 | 241.1 | 8.87 | 0.54 |
| B1-6H | 30.6 | 400. | 1.0 | 149.2 | 338.0 | 8.64 | 0.71 |

| Sample No | At max. $\sigma_1'/\sigma_3'$ | | | Failure Mode & Angle To Horizontal |
|---|---|---|---|---|
| | $\frac{\sigma_1'}{\sigma_3'}$ | Axial $\epsilon$ (%) | A | |
| B2-1H | 5.26 | 5.93 | 0.22 | Shear - 55° |
| B1-2H | 2.78 | 10.50 | 0.25 | Shear - 55° |
| B2-3H | 3.73 | 6.08 | 0.33 | Shear - 55° |
| B1-4H | 2.92 | 7.15 | 0.68 | Shear - 55° |
| B2-5H | 2.82 | 8.87 | 0.54 | Shear - 55° |
| B1-6H | 2.58 | 8.64 | 0.71 | Shear - 55° |

Table E.12 Summary of data on samples for yield tests.

| Sample No | Depth (m) | Initial Conditions | | | | Final | |
|---|---|---|---|---|---|---|---|
| | | Ht (mm) | Dia (mm) | $\rho$ Mg/m³ | w (%) | w.c (%) | $\frac{\sigma_3'}{\sigma_1'}$ |
| B1-Y1 | 6.0 | 77.0 | 38.7 | 1.86 | 36.9 | 32.6 | 0.5 |
| B1-Y2 | 6.0 | 77.3 | 38.7 | 1.86 | 37.2 | 33.7 | 0.6 |
| B2-Y3 | 6.0 | 77.0 | 38.4 | 1.89 | 38.0 | 35.8 | 0.7 |
| B1-Y4 | 6.0 | 77.8 | 38.6 | 1.84 | 39.9 | 34.9 | 1.0 |
| B3-Y5 | 6.0 | 77.5 | 38.1 | 1.89 | 35.5 | 31.2 | 1.2 |
| B3-Y6 | 6.0 | 78.0 | 38.0 | 1.88 | 36.8 | 33.1 | 1.8 |

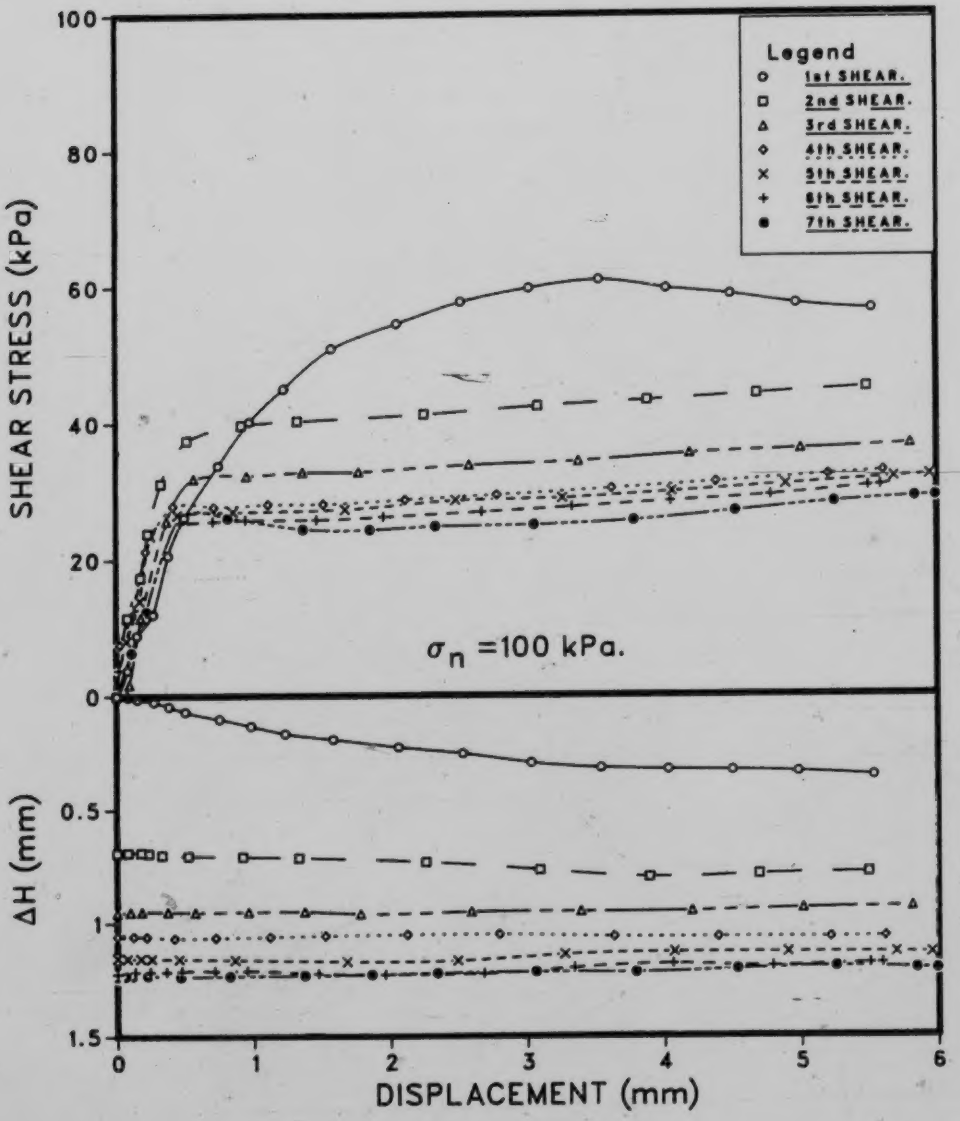

Figure E.1 Direct shear test on grey clay - sample DST.B3.1.

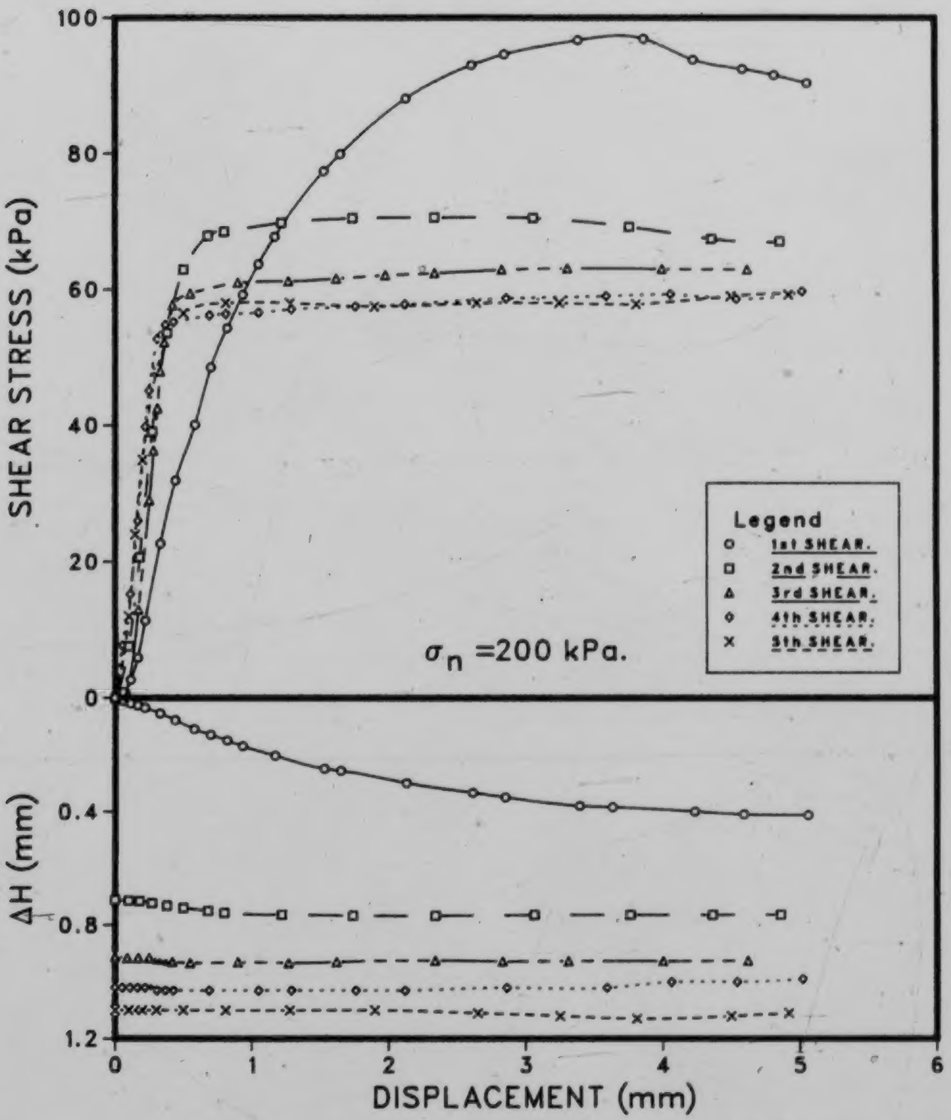

Figure E.2 Direct shear test on grey clay - sample DST.B3.2.

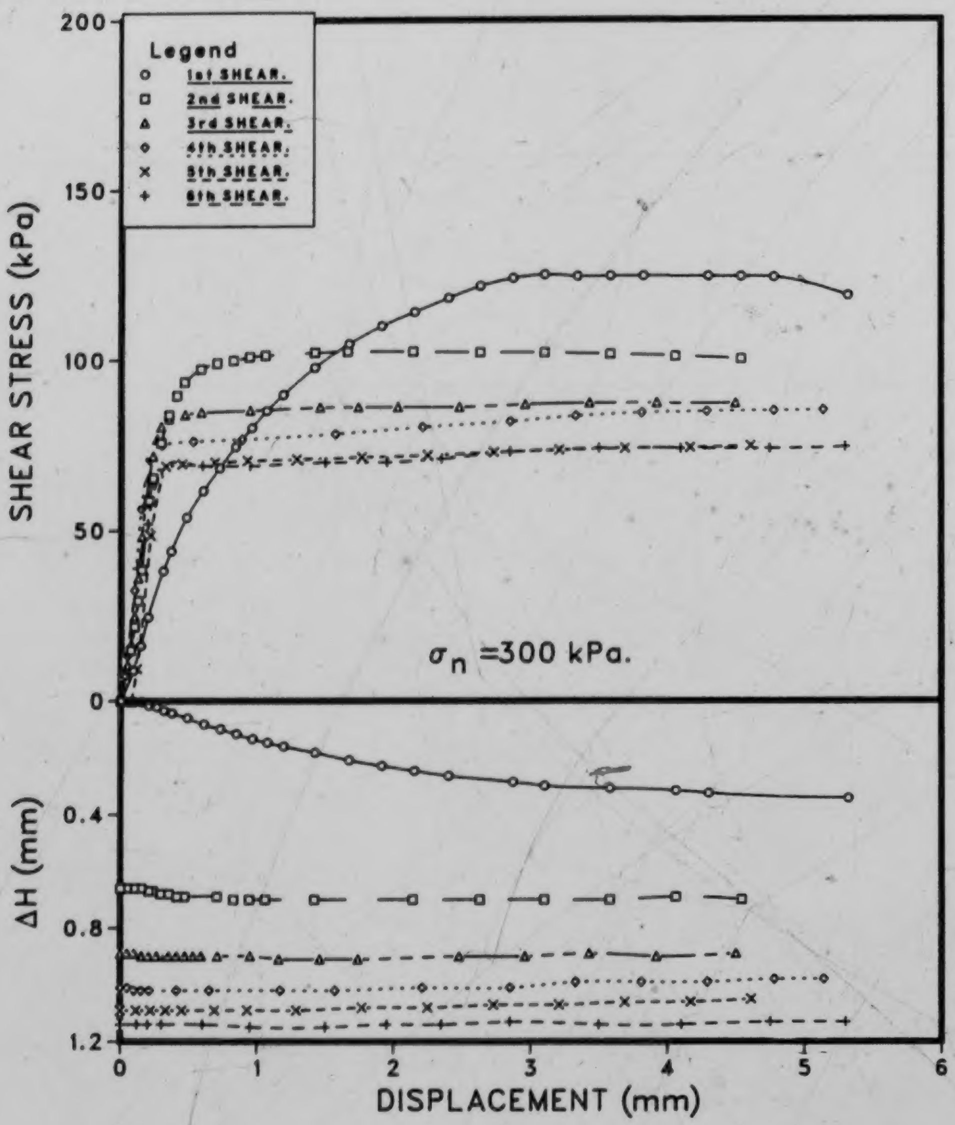

Figure E.3 Direct shear test on grey clay - sample DST.B3.3.

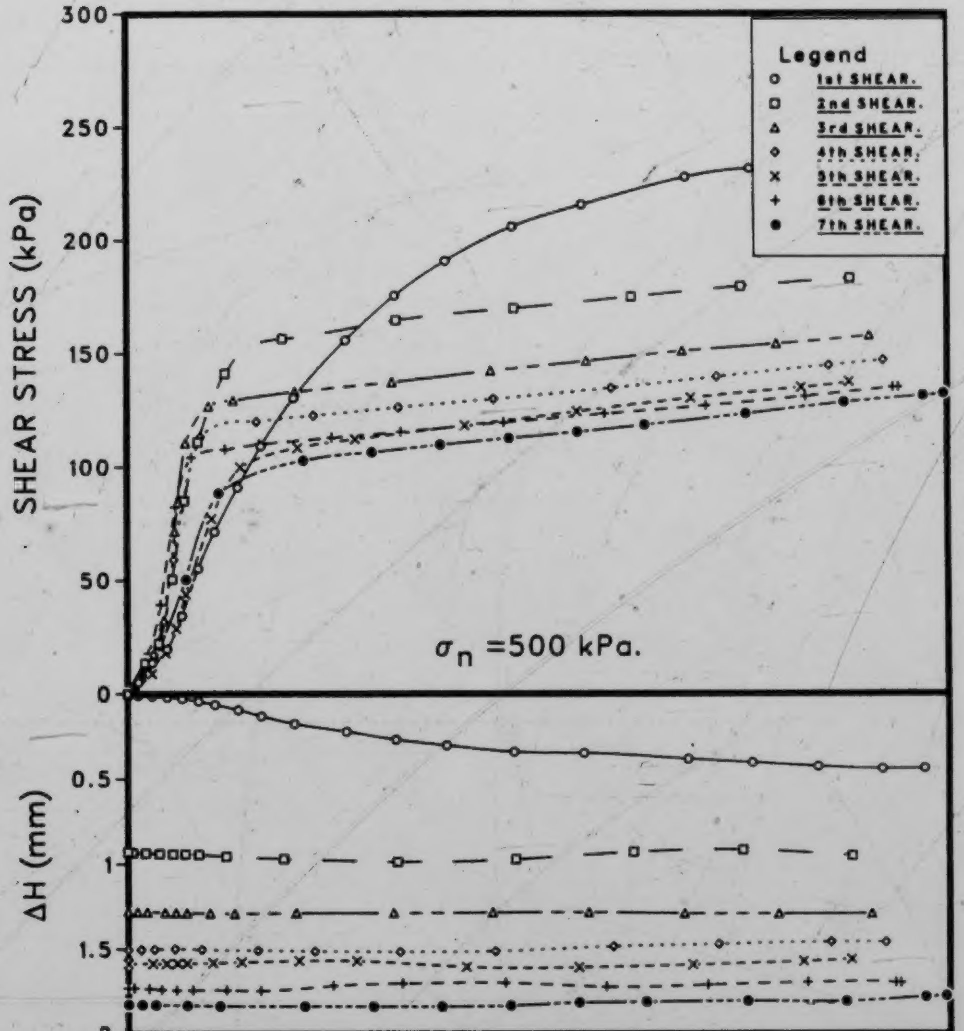

Figure E.4 Direct shear test on grey clay - sample DST.B3.4.

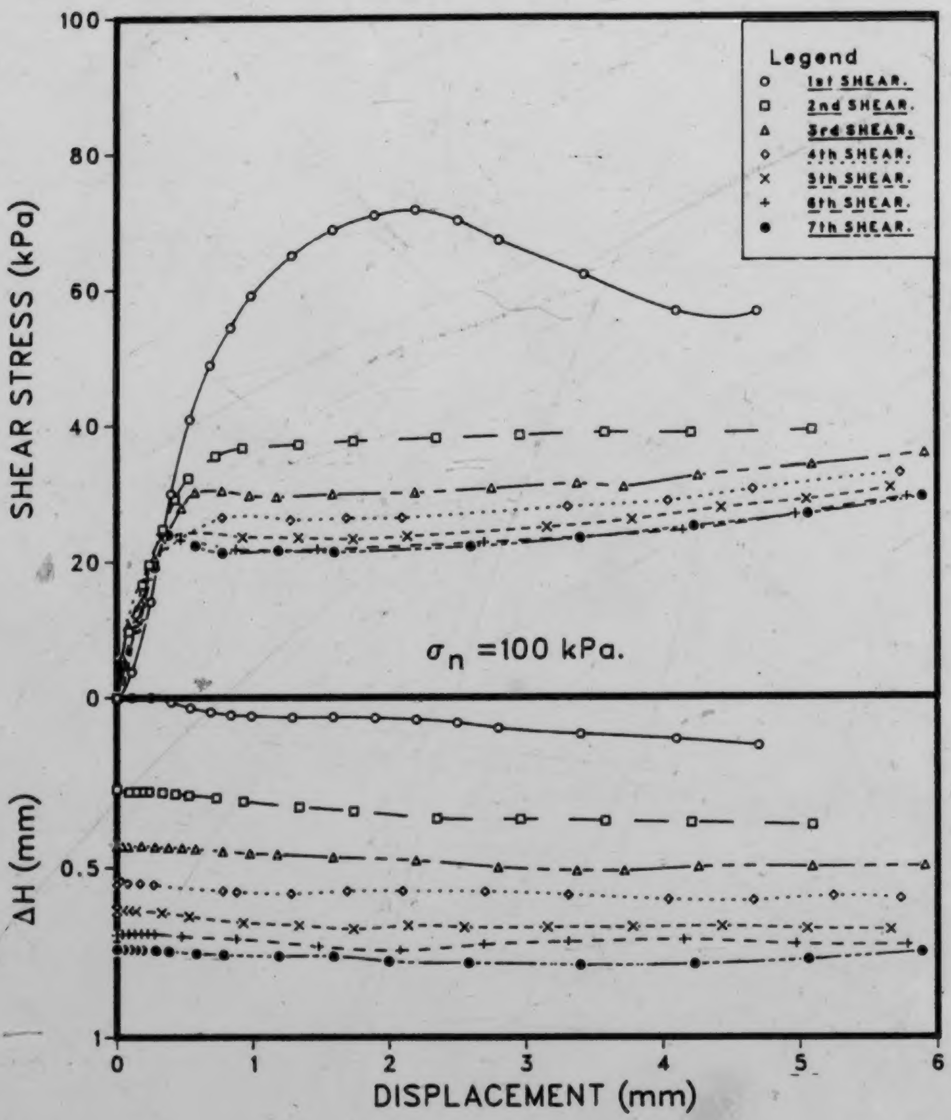

Figure E.5 Direct shear test on brown clay - sample DST.4.1.

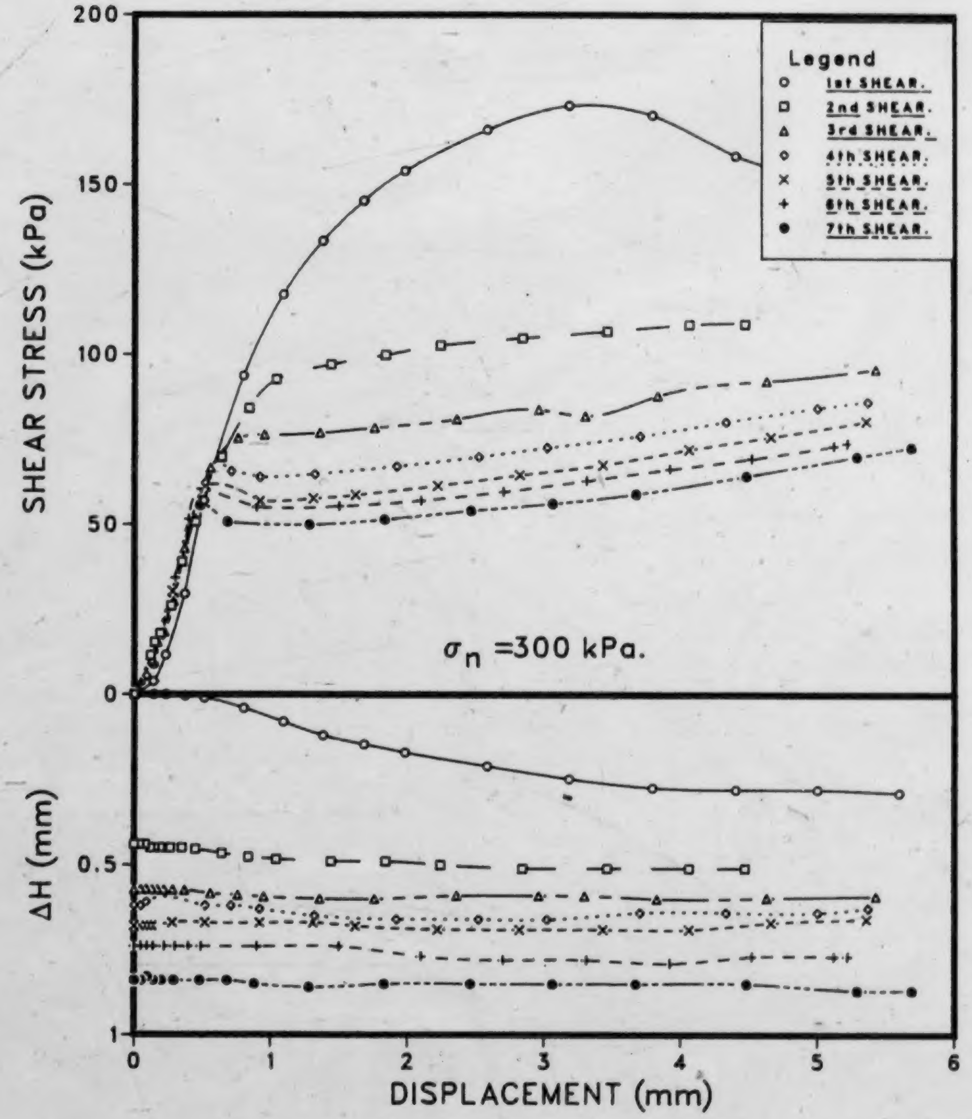

Figure E.6 Direct shear test on brown clay - sample DST.4.2.

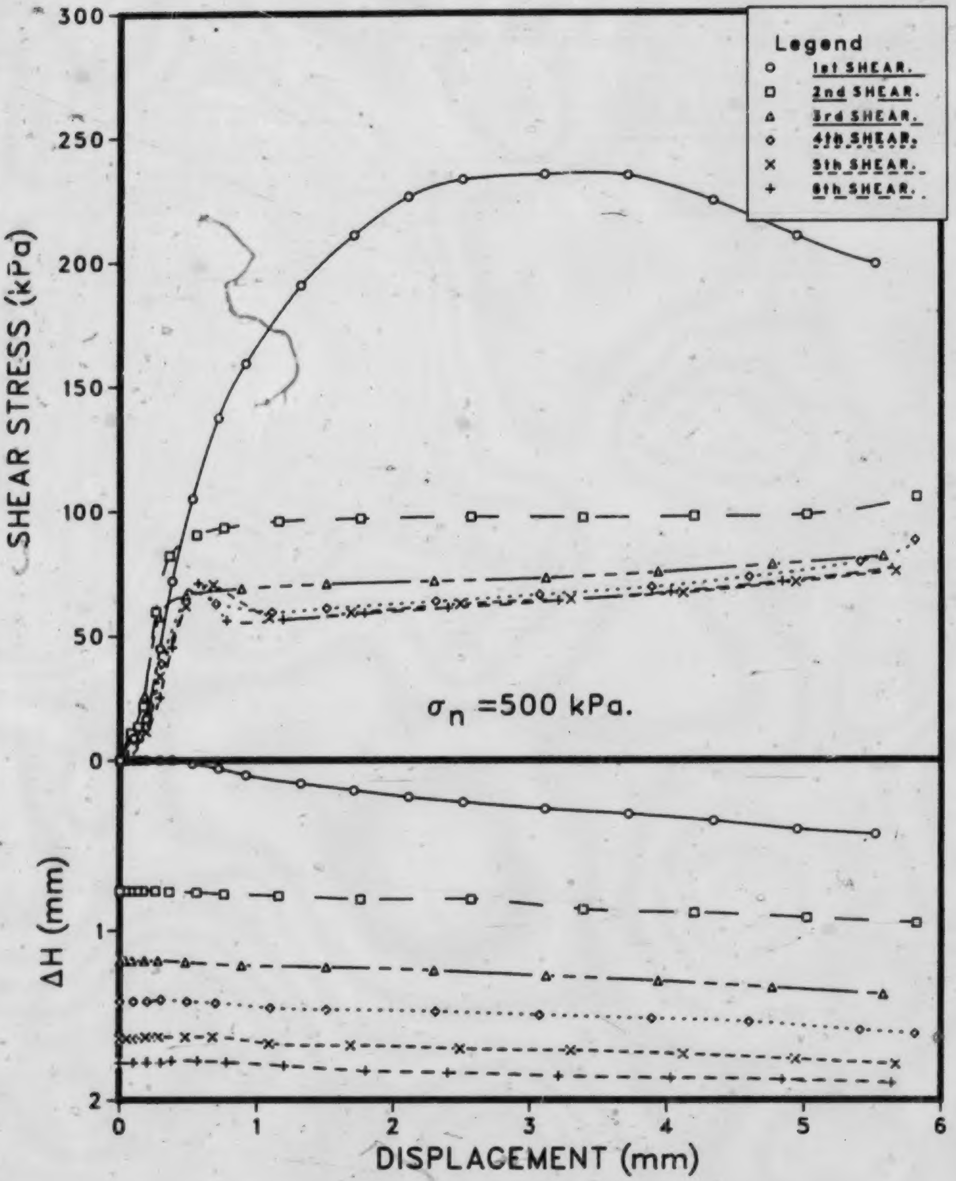

Figure E.7 Direct shear test on brown clay - sample DST.4.3.

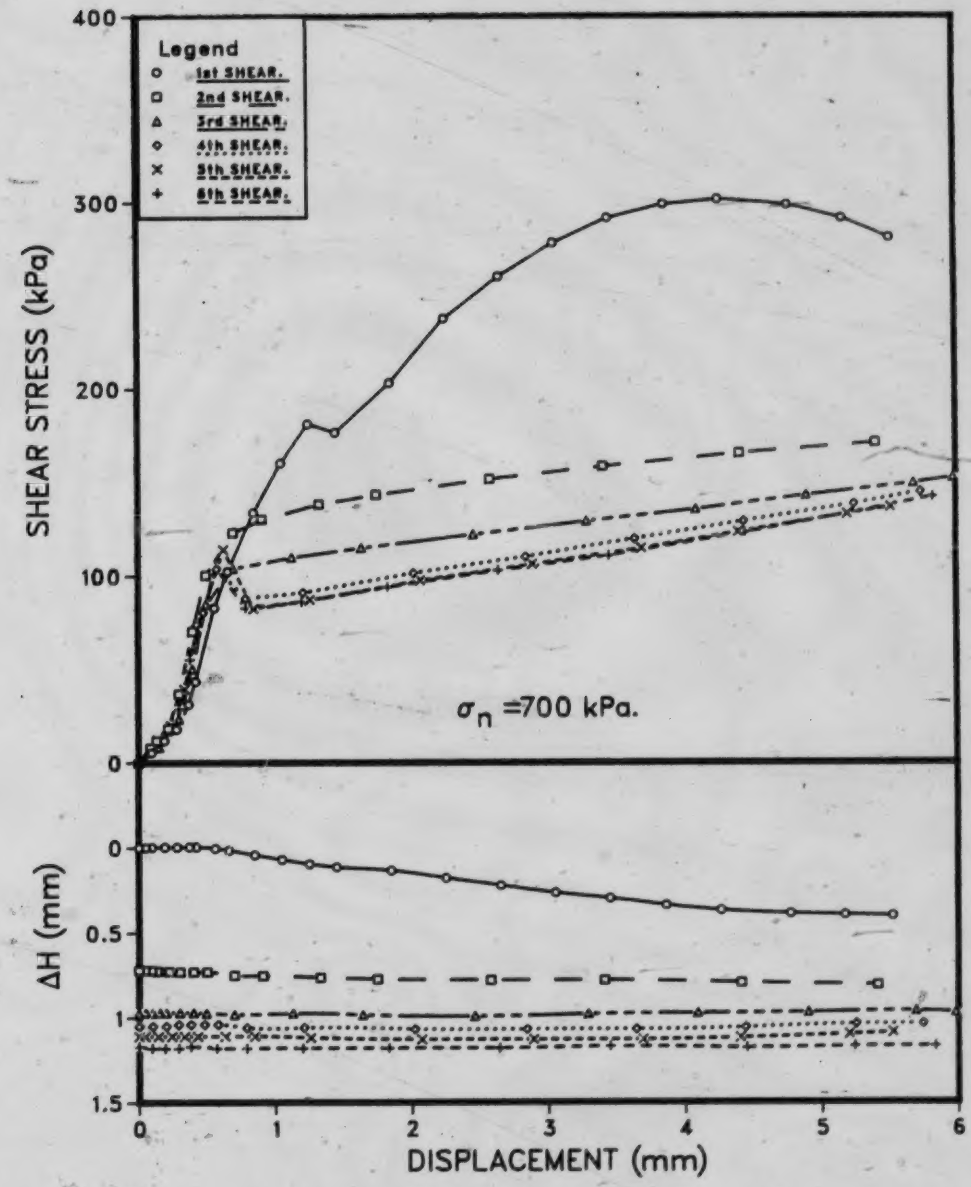

Figure E.8 Direct shear test on brown clay - sample DST.4.4.

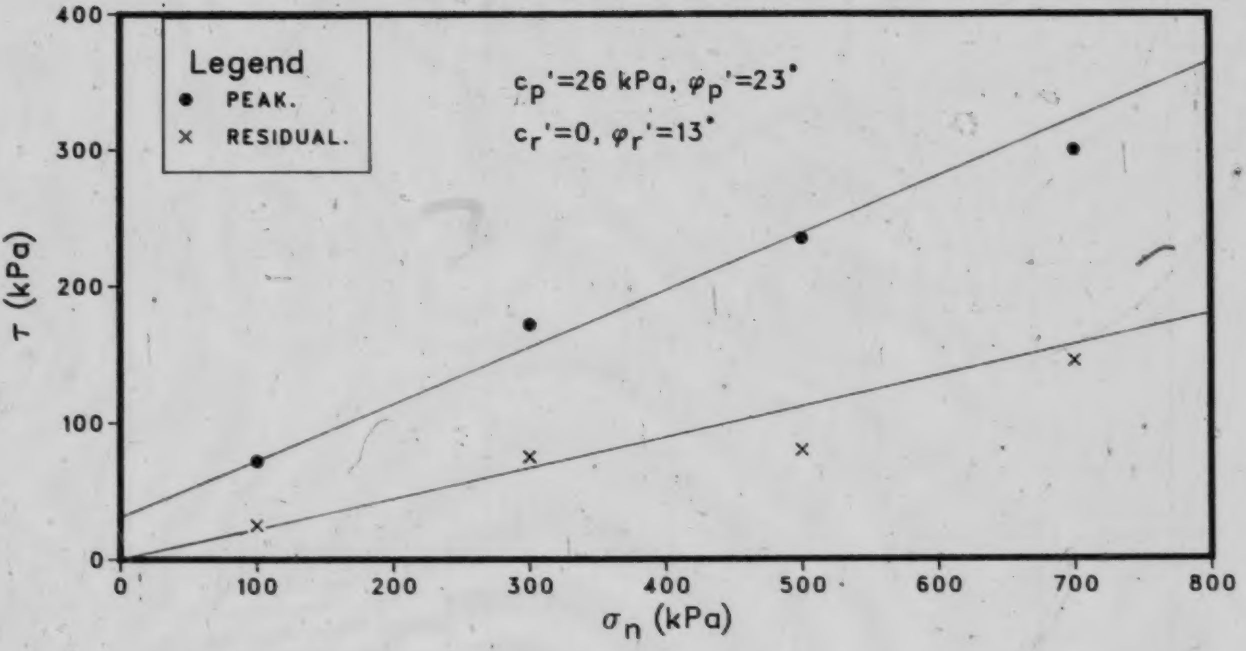

Figure E.9 Direct shear test strength parameters for brown clay.

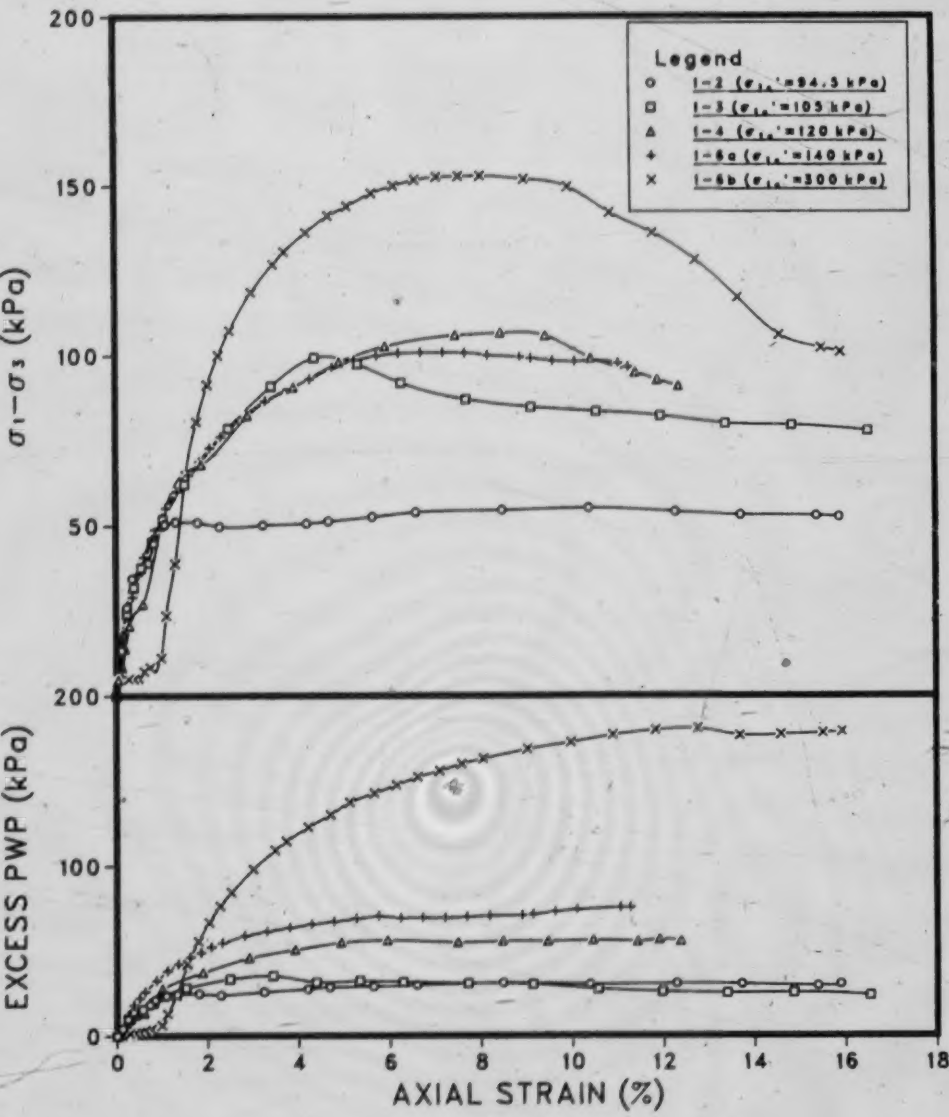

Figure E.10 Triaxial test results on UA1 grey clay.

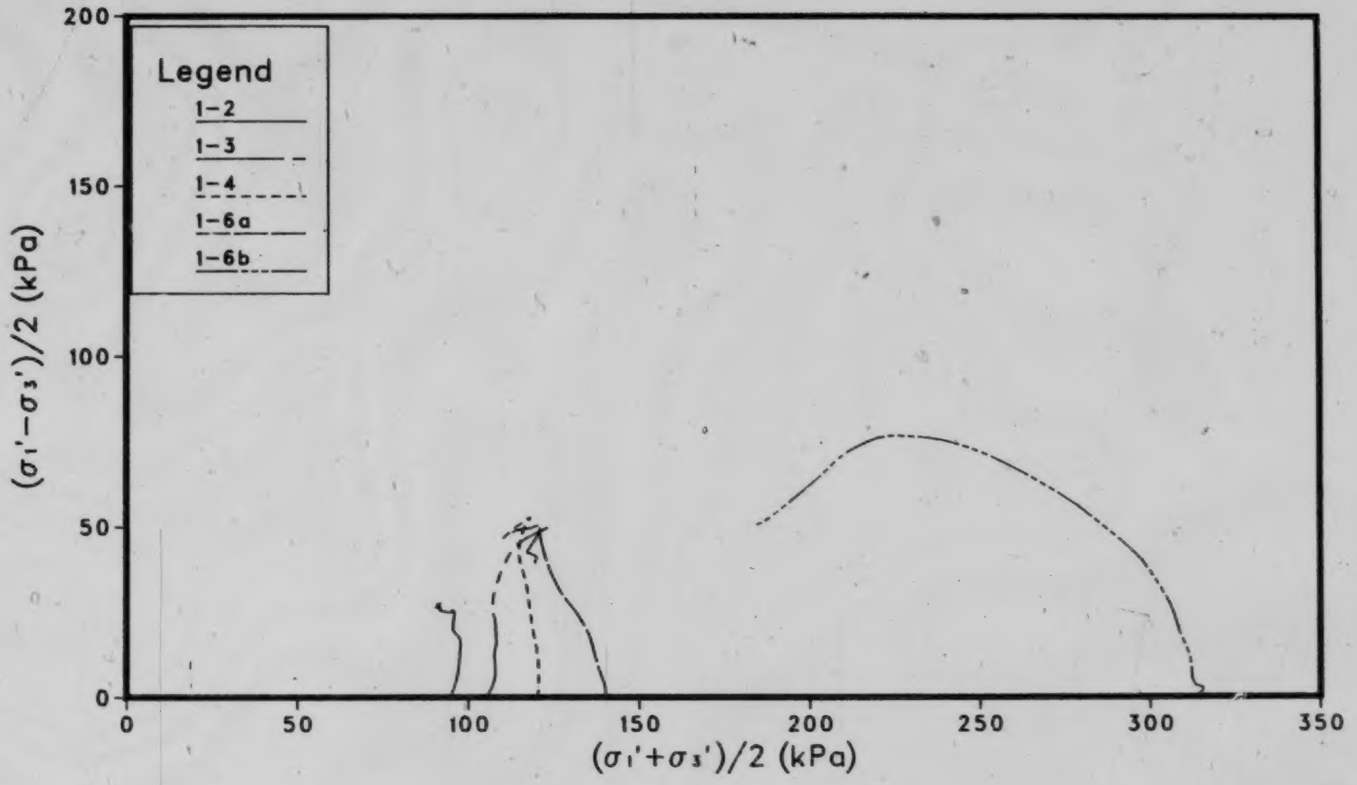

Figure E.11 Triaxial stress paths for UA1 grey clay.

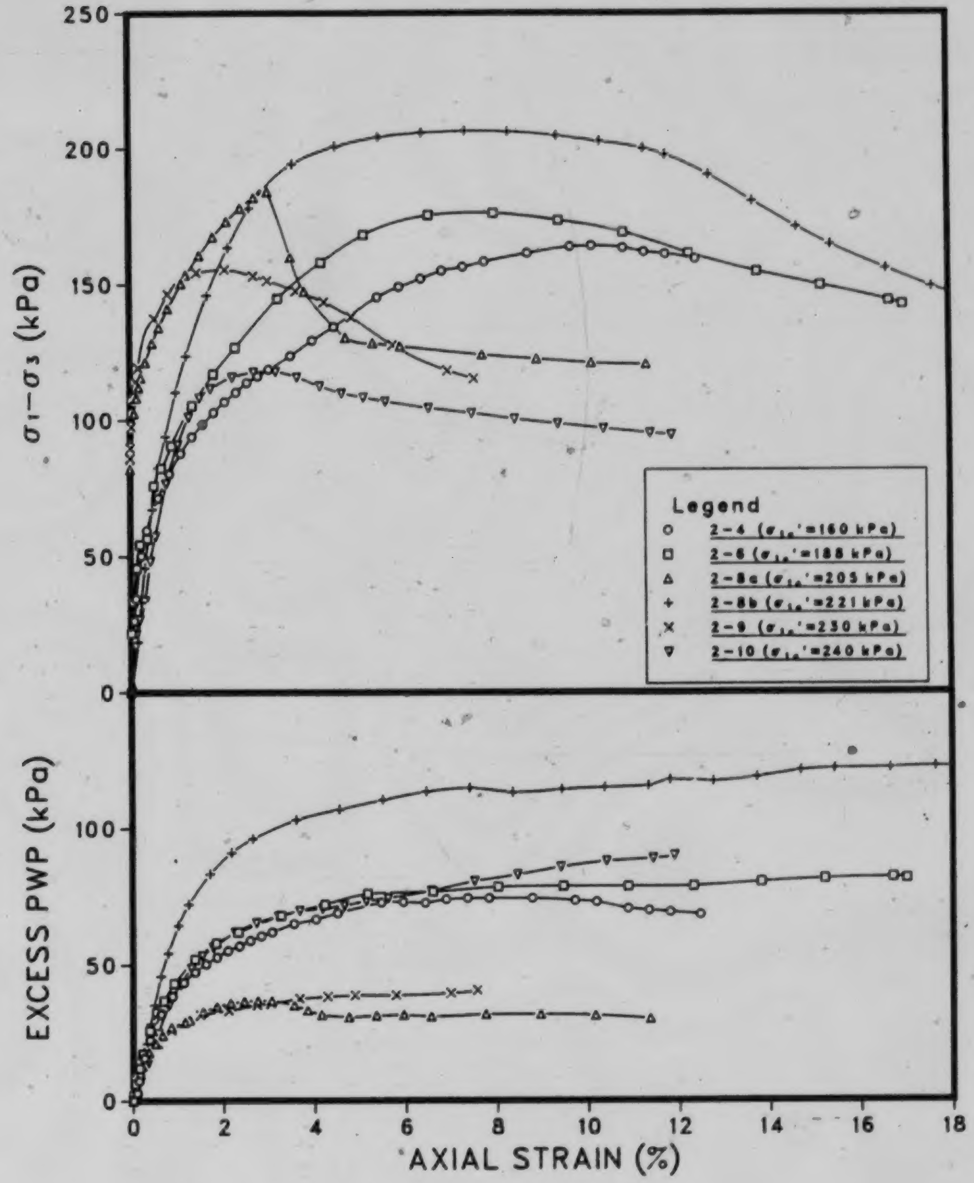

Figure E.12 Triaxial test results on UA2 grey clay.

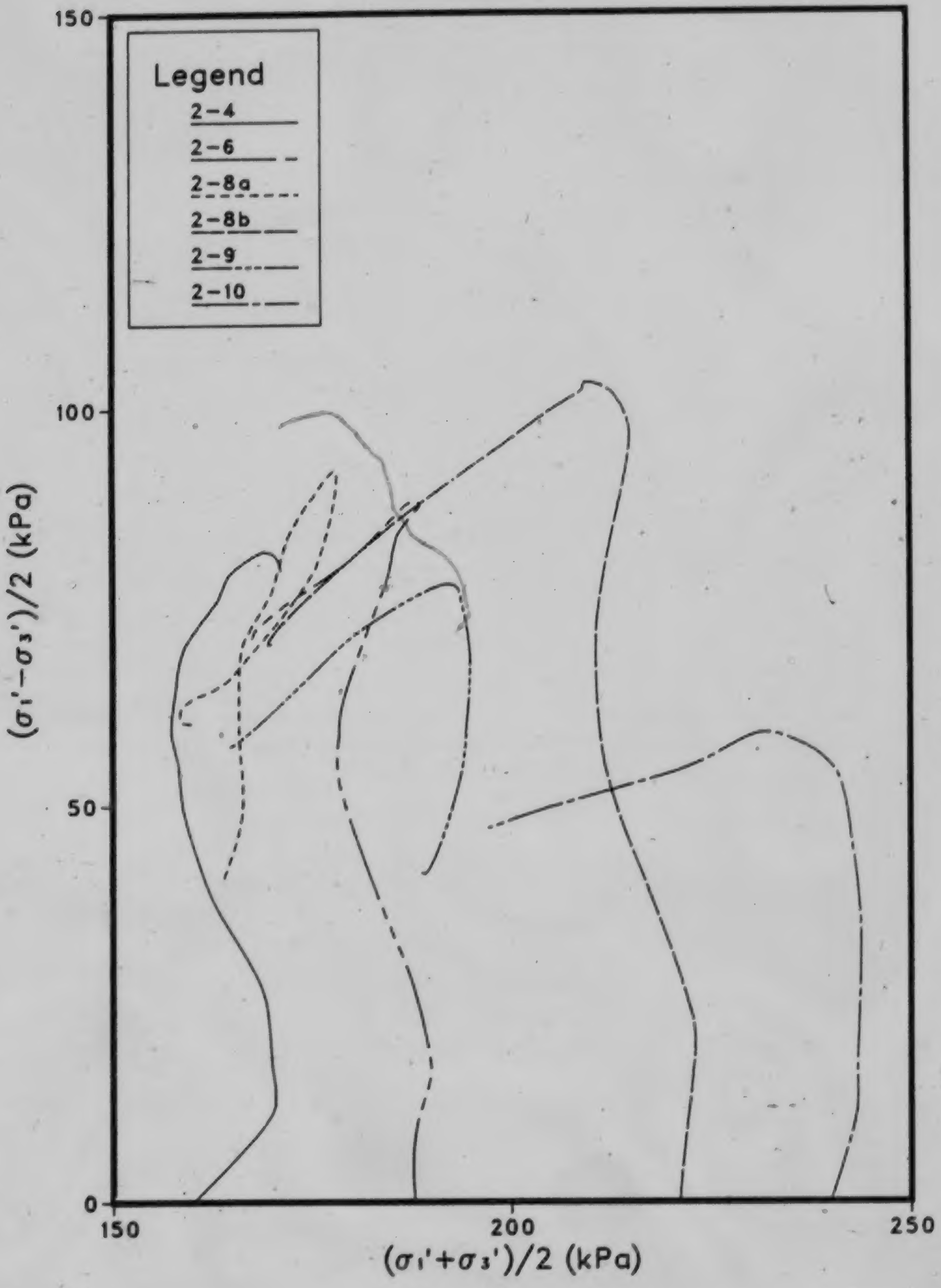

Figure E.13 Triaxial test stress paths for UA2 grey clay.

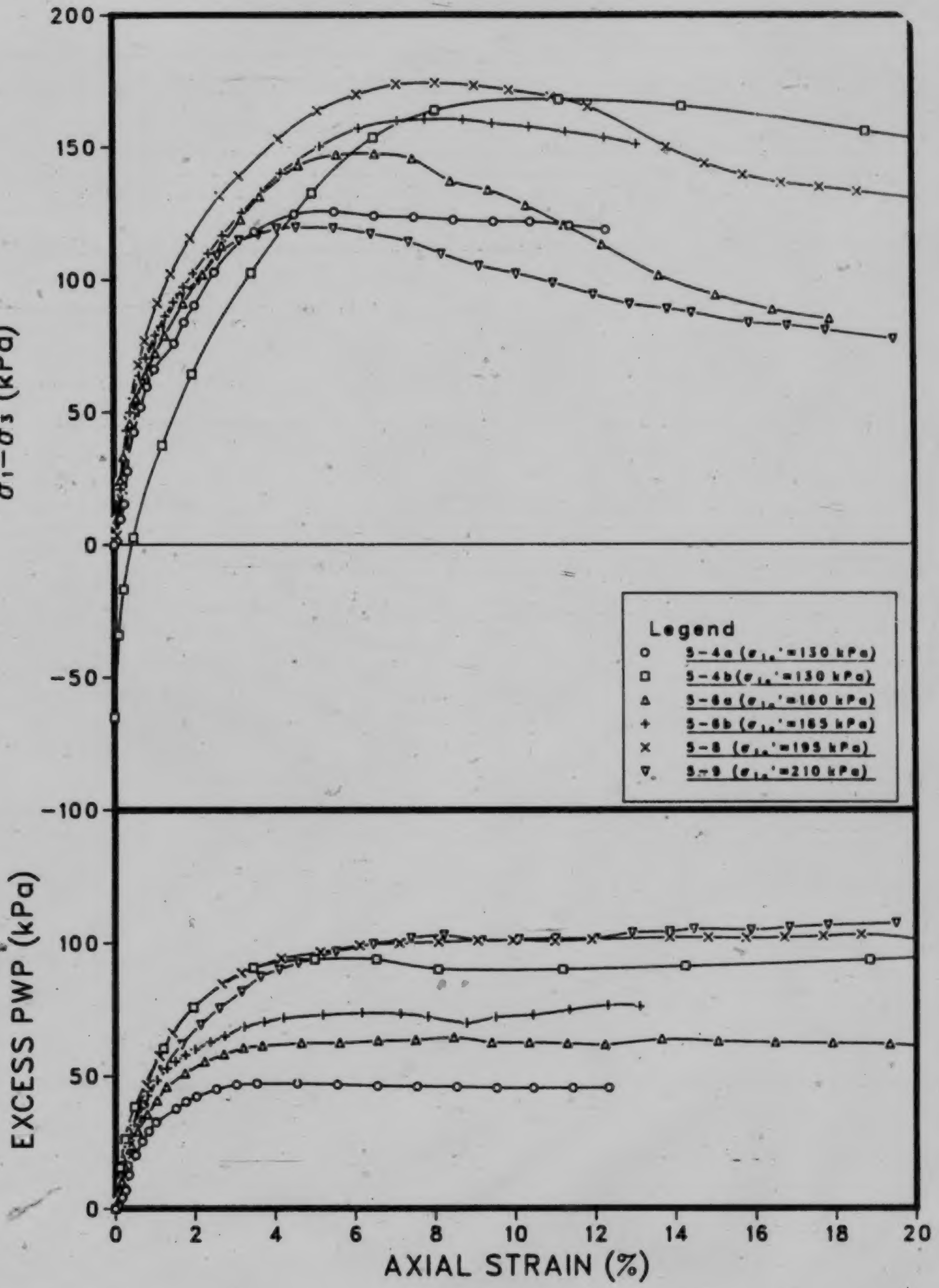

Figure E.14 Triaxial test results on UA5 grey clay.

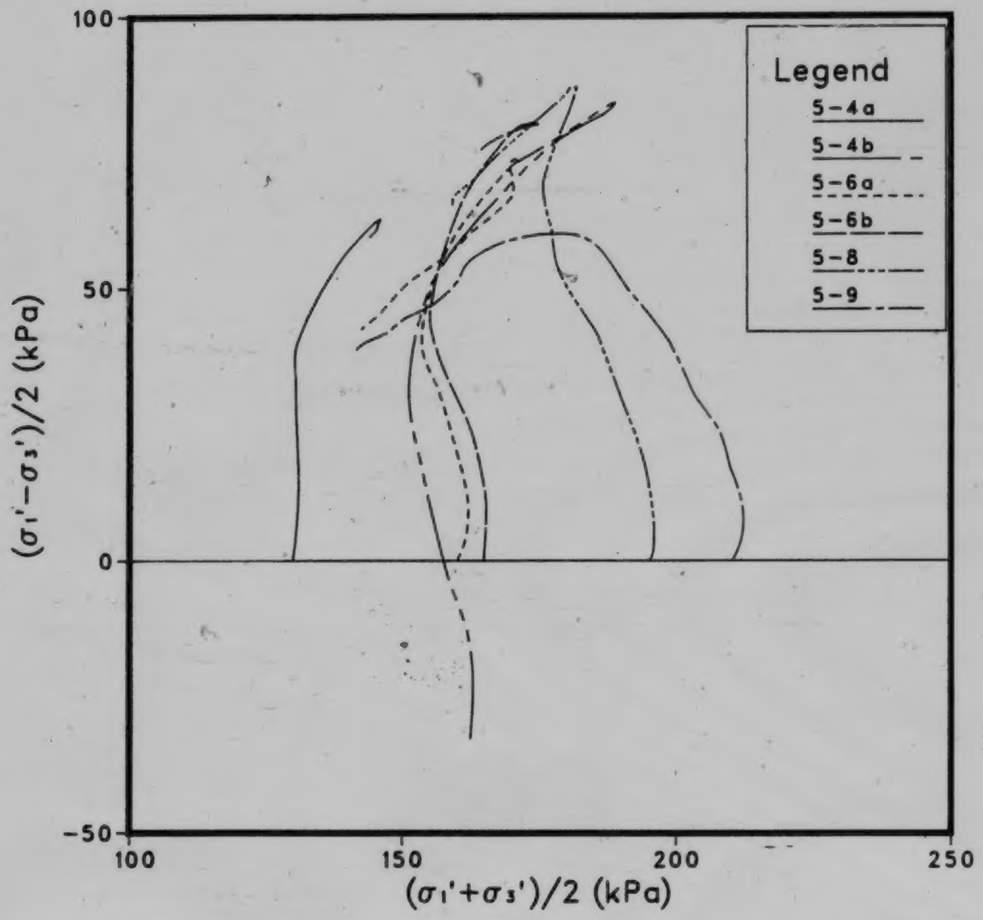

Figure E.15 Triaxial test stress paths for UA5 grey clay.

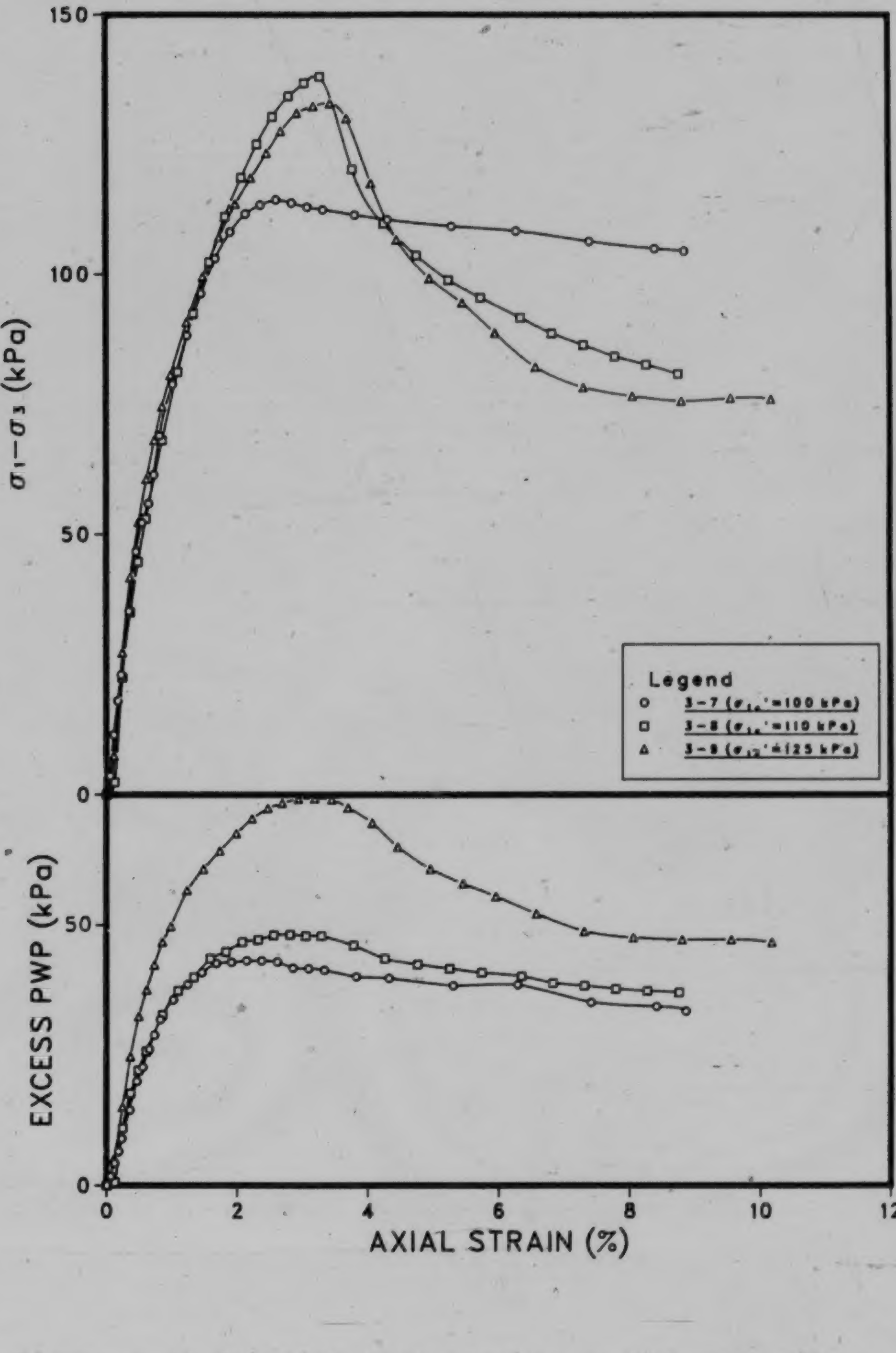

Figure E.16 Triaxial test results on UA3 grey clay.

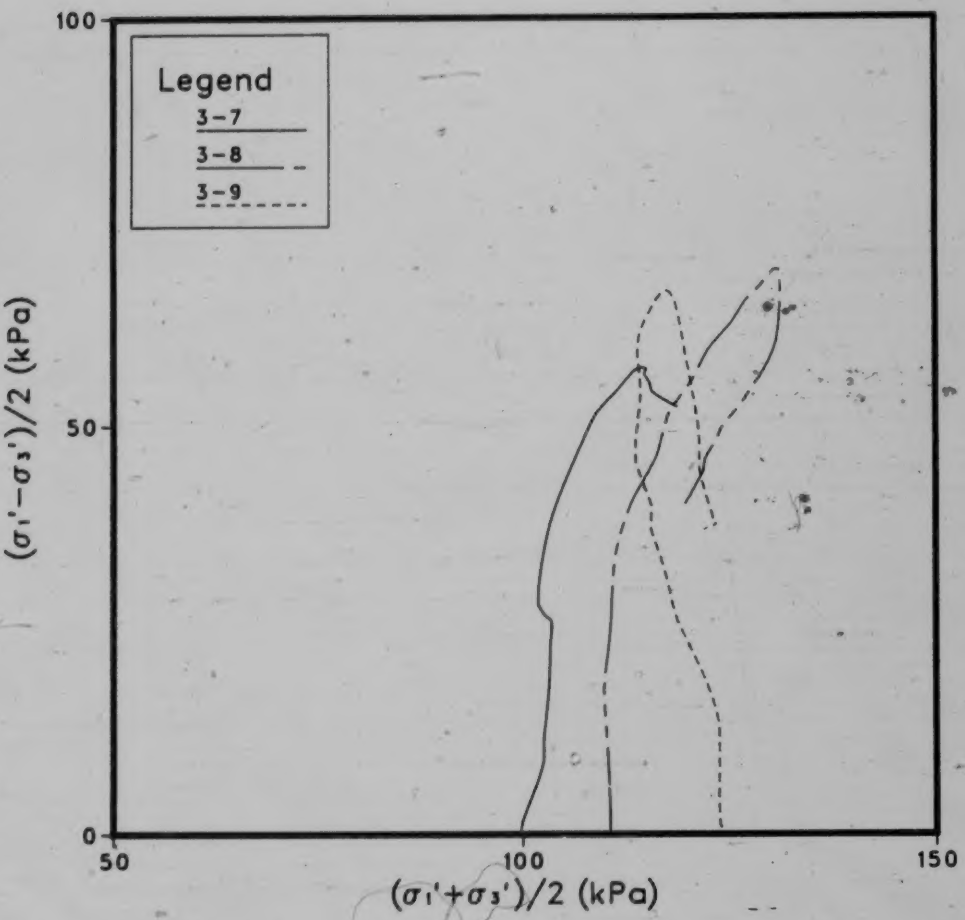

Figure E.17 Triaxial test stress paths for UA3 grey clay.

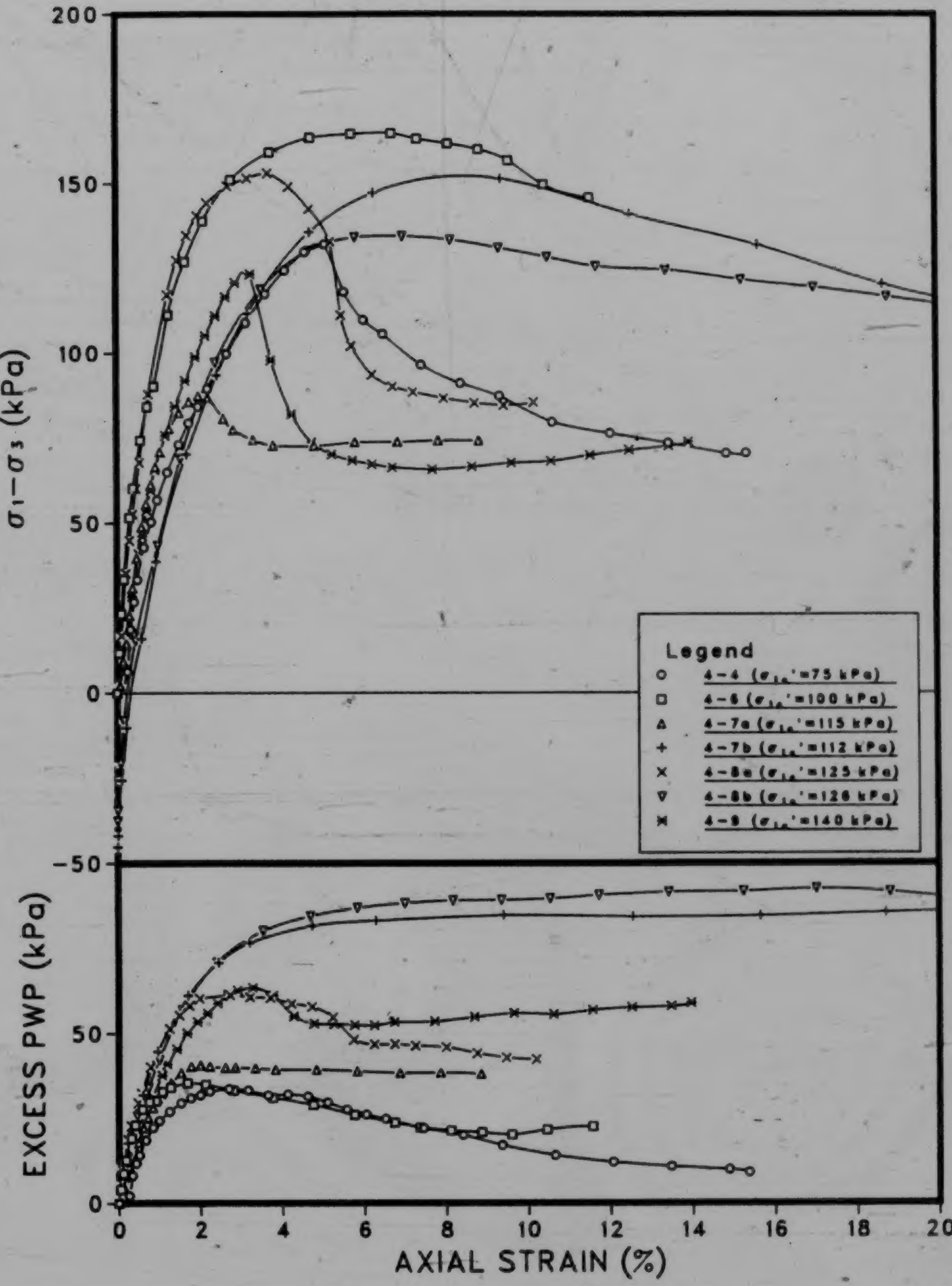

Figure E.18 Triaxial test results on UA4 grey clay.

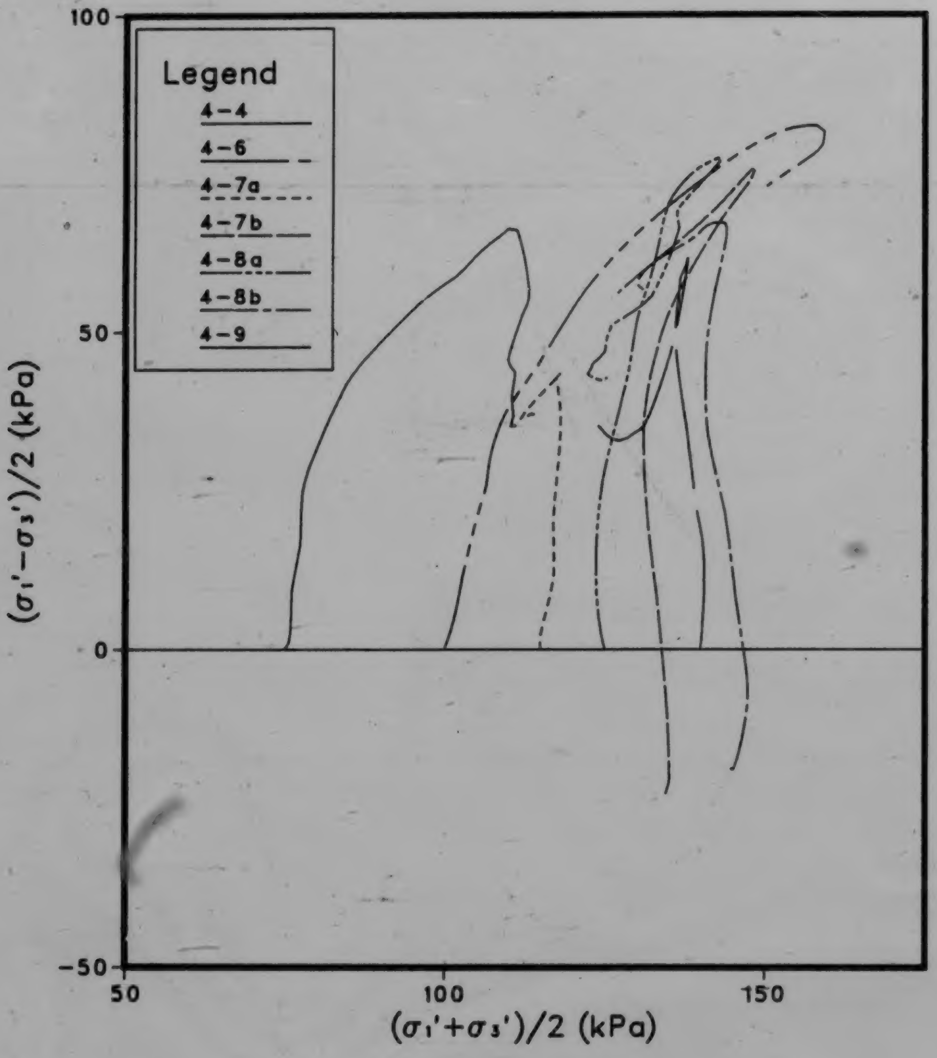

Figure E.19 Triaxial test stress paths for UA4 grey clay.

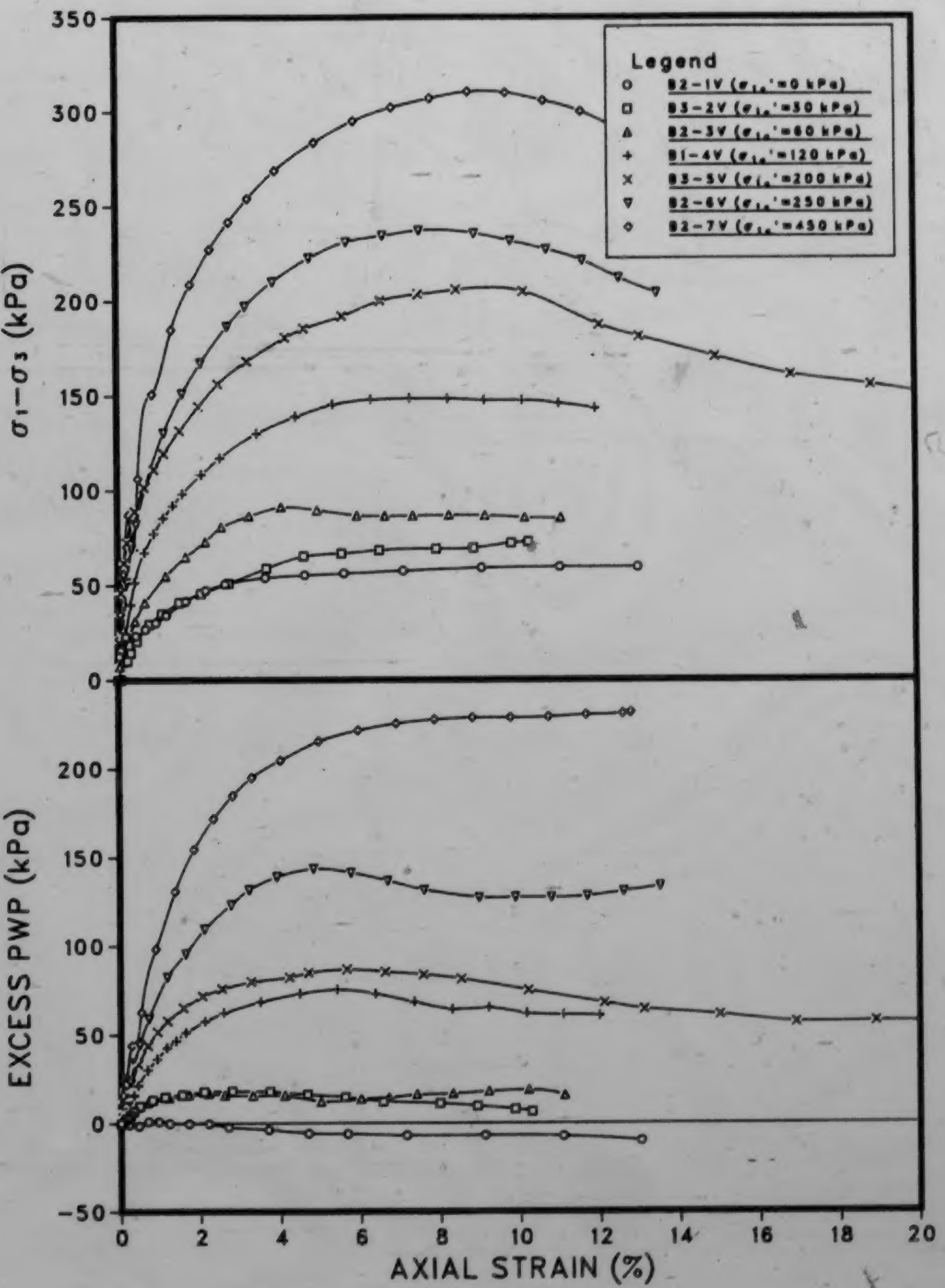

Figure E.20 Triaxial test results on grey clay block samples(V).

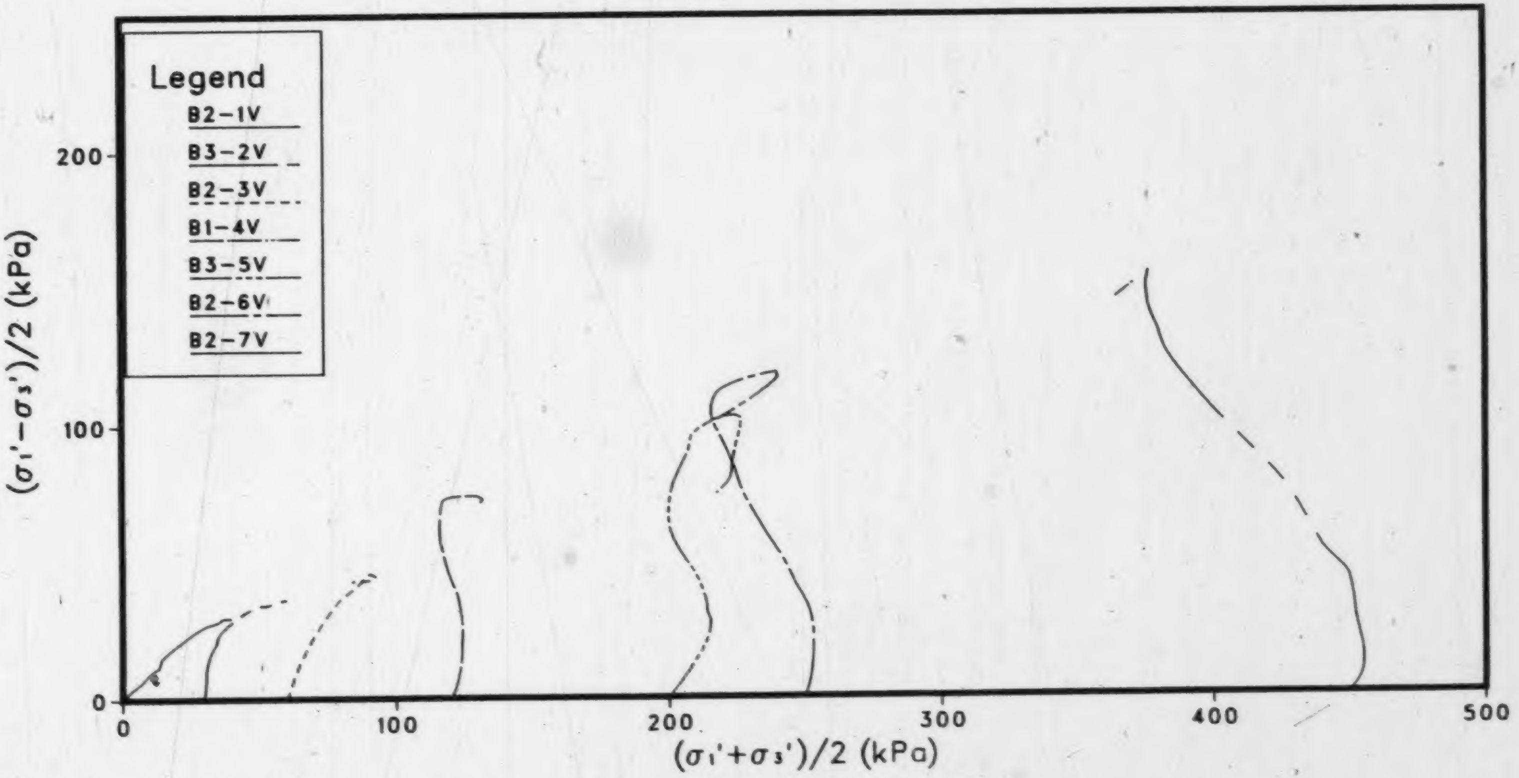

Figure E.21 Triaxial test stress path for grey clay block samples(V).

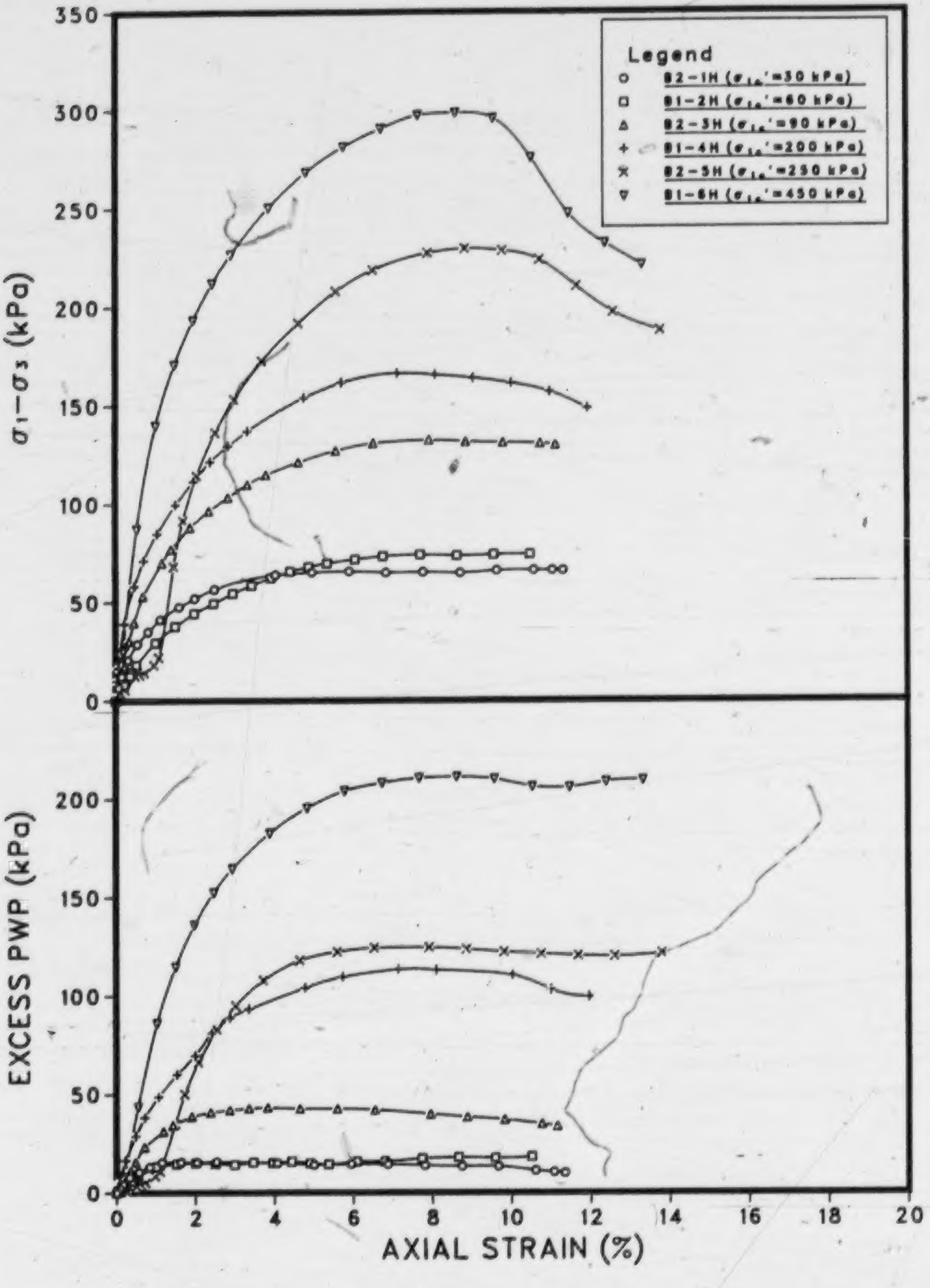

Figure E.22 Triaxial test results on grey clay block samples(H).

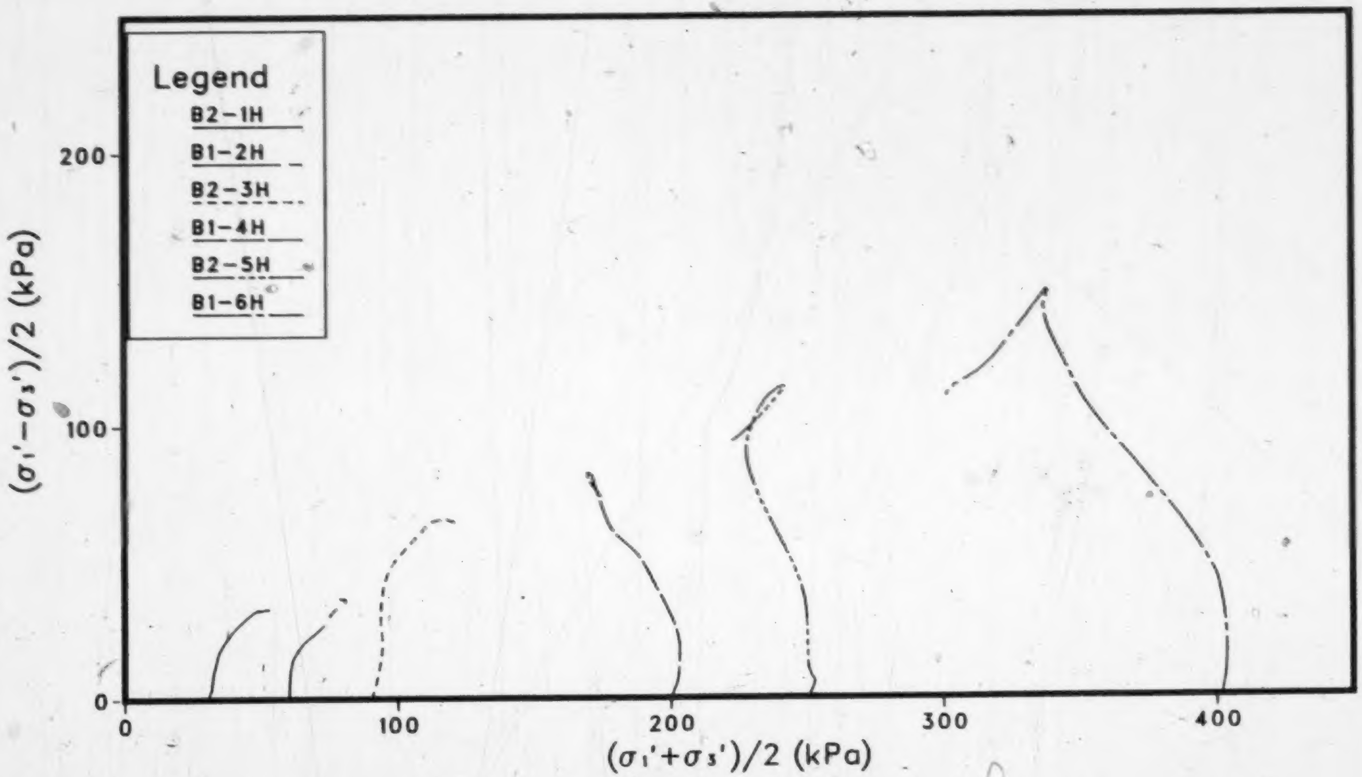

Figure E.20 Triaxial test stress path for grey clay block samples(H).

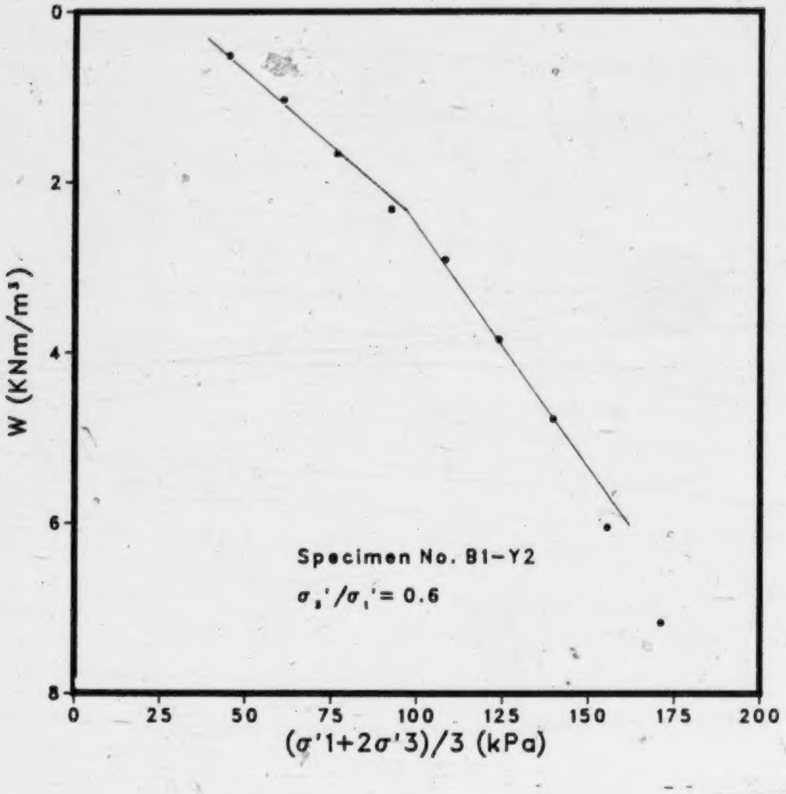

Figure E.24 Yielding in Genesee Clay with $\sigma_3'/\sigma_1'$=0.6.

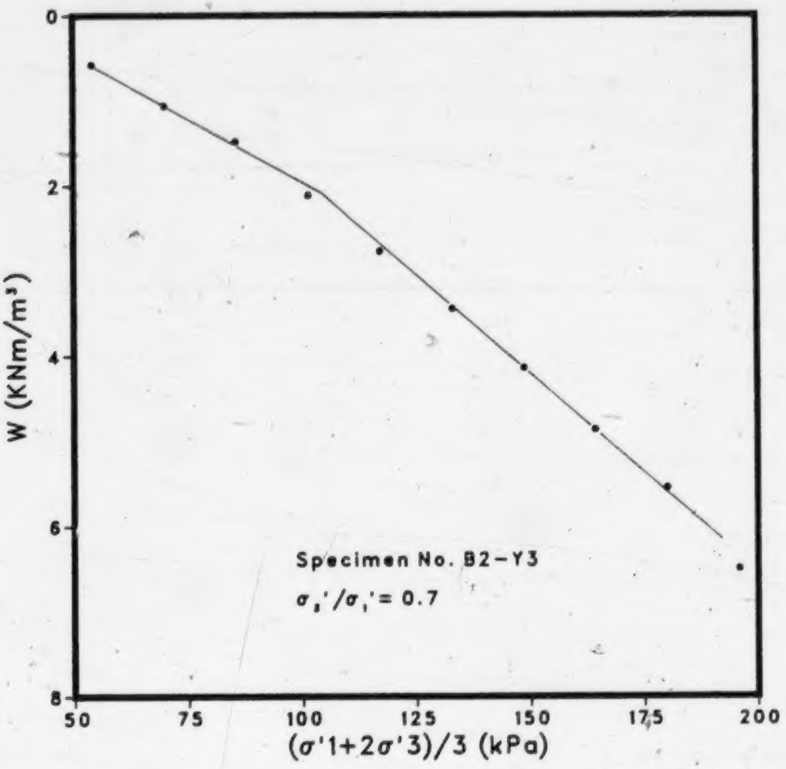

Figure E.25 Yielding in Genesee Clay with $\sigma_3'/\sigma_1'$=0.7.

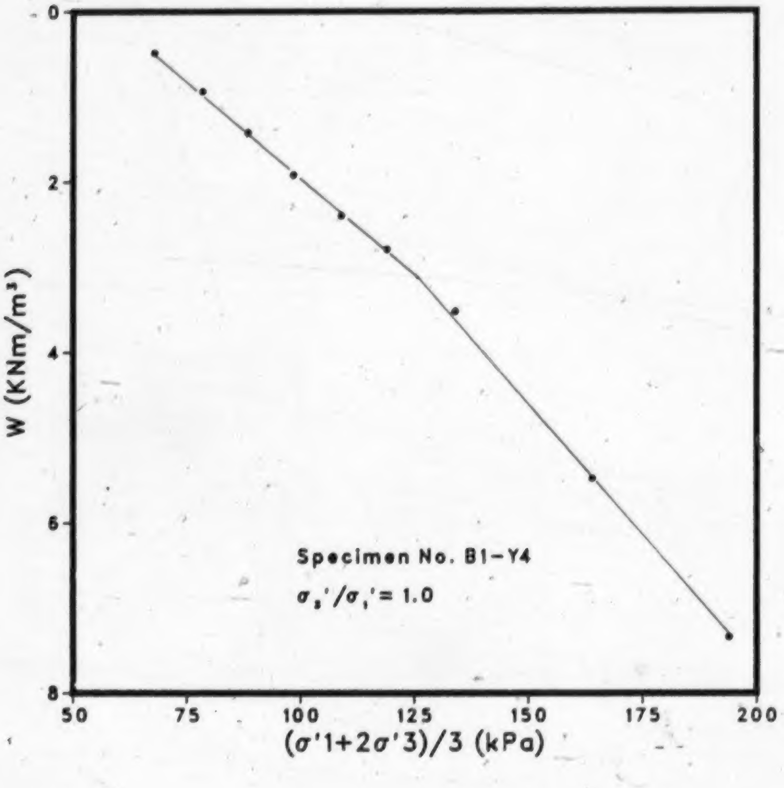

Figure E.26 Yielding in Genesee Clay with $\sigma_3'/\sigma_1'$=1.0.

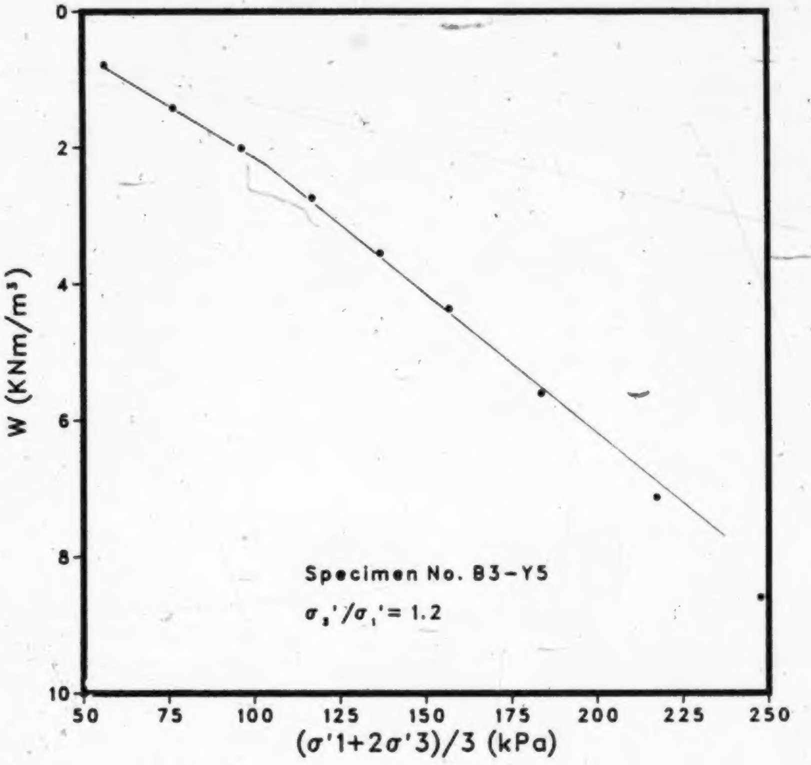

Figure E.27 Yielding in Genesee Clay with $\sigma_3'/\sigma_1'=1.2$.

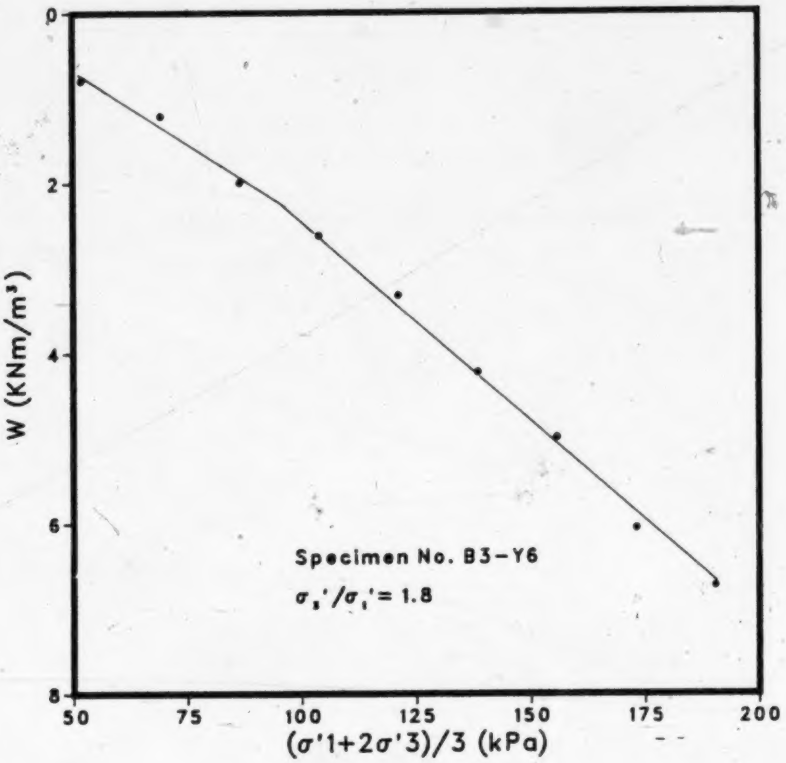

Figure E.28 Yielding in Genesee Clay with $\sigma_3'/\sigma_1'=1.8$.

# APPENDIX F - AUTOMATIC CONTROLLER FOR THE BISHOP AND WESLEY TRIAXIAL CELL

The hydraulic triaxial cell is described in detail by Bishop and Wesley (1975) from which a layout of the equipment is reproduced in Fig. F.1. A photograph of the cell for 38mm diameter samples is shown in Plate F.1.

An automatic controller,B, for the hydraulic cell was designed and built by the Civil Engineering Electronic Shop, University of Alberta to operate a stepping motor,C, which is in turn connected to a Bishop ram,D (see Plate F.2). The development of the controller is intended for stress path tests requiring the independent control of the axial stress, cell pressure and pore pressure. The system shown in Plate F.2 controls the axial stress through the electrical transducer, A, in Plate F.1 whereas the cell and back pressures are supplied by conventional methods. The University of Alberta controller has the ability to perform both stress and strain controlled tests through instructions coded from a keyboard,E (Plate F.2).

At present, the controller can operate at a minimum rate of strain of $6.2 \times 10^{-5}$ mm/sec and a maximum rate of $4.3 \times 10^{-2}$ mm/sec. In stress control mode, the minimum rate is 1 kPa every 15 minutes and the maximum rate is 1 kPa every second.

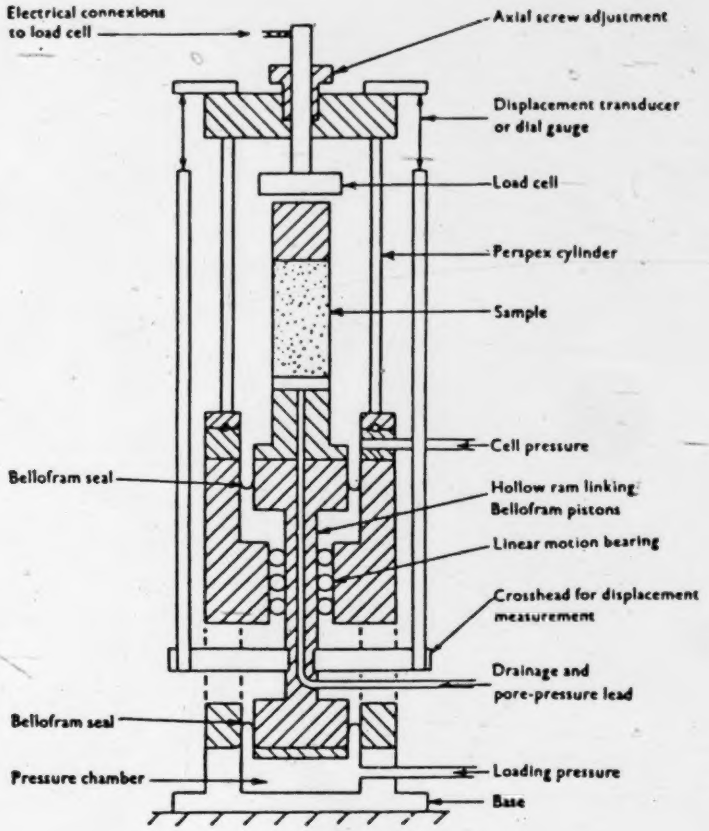
Electrical connexions to load cell
Axial screw adjustment
Displacement transducer or dial gauge
Load cell
Perspex cylinder
Sample
Cell pressure
Bellofram seal
Hollow ram linking Bellofram pistons
Linear motion bearing
Crosshead for displacement measurement
Drainage and pore-pressure lead
Bellofram seal
Loading pressure
Pressure chamber
Base

Figure F.1 Diagrammatic layout of Bishop and Wesley cell.

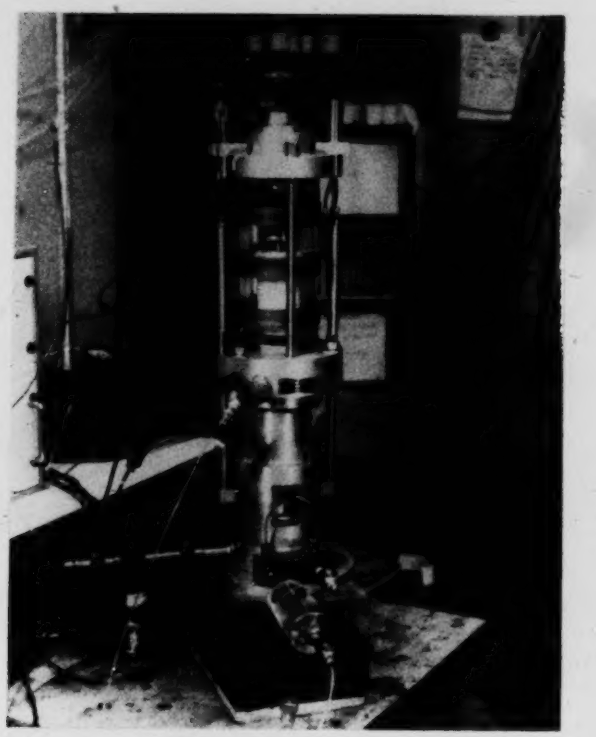

Plate F.1 Bishop and Wesley cell.

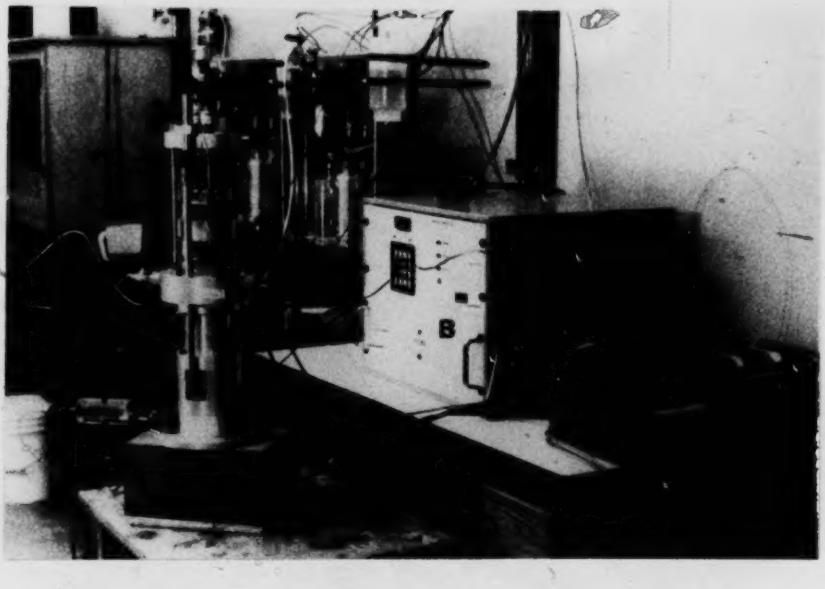

Plate F.2 Automatic controller.